Preface

Over the past nine months I have been working on my master thesis project. This report presents the results of my work. The subject of my thesis is to determine the effects of storm-erosion on sea dikes. The work has mainly been carried out at the 'RIKZ' Dutch National Institute for Coastal and Marine Management in The Hague.

First of all I would like to express my gratitude to the members of my thesis committee. Their support and advice have been very helpful. I would also like to thank T. Zitman of Delft University of Technology for his contribution during the start of my thesis.

The contact with all members of the OSFG and OSFM group has been very pleasant. Especially I would like to thank F. den Heijer and R. Spanhoff for the opportunities and possibilities that they gave me at the RIKZ. Furthermore I would like to thank my colleagues that I shared a room with during my flexible stay starting with A.C. de Kruif, C.G. Israel, J. van de Kreeke, J.J. Jacobse, J.H. and Andorka Gal.

I would like to thank M. Boers of RIKZ and D. Walstra of WL| Delft hydraulics for their support and patience with my problems using the computer model UNIBEST-TC. Finally I would like to thank all fellow-students, friends and relatives who have enthusiastically supported me over the past months.

Michiel van Baak
The Hague, October 2002

Summary (in Dutch)

Onderzoek
Tijdens mijn afstudeeronderzoek heb ik een studie verricht naar de invloed van morfologische ontwikkelingen voor de Pettemer zeewering tijdens stormcondities. Het onderzoek heeft zich voornamelijk gericht op de effecten van stormerosie van de vooroever op het doordringen van golven tot aan de zeewering.

Momenteel worden morfologische veranderingen op korte termijn niet meegenomen in de toetsing van harde kustconstructies, aangezien de effecten moeilijk te voorspellen zijn. Deze studie heeft dan ook als doel het belang van deze morfologische veranderingen alsmede de dominante parameters vast te stellen. Aangezien dijken worden getoetst aan de hand van veiligheidscriteria is het praktisch het effect van morfologische veranderingen uit te drukken in overschrijdingsfrequenties van golfoploop dan wel benodigde kruinhoogte. Vervolgens kunnen de huidige ontwerp- en toetsrandvoorwaarden worden vergeleken met de randvoorwaarden die volgen uit de toepassing waarin wel rekening wordt gehouden met morfologische veranderingen. Als studie locatie is de meetsite bij Petten gekozen.

Locatie
De anderhalve kilometer lange Pettemer zeewering vormt het noordelijke deel van de ca. 5.5 km lange zeewering. De Hondsbossche zeewering vormt het zuidelijke deel van de aan de Noord-Hollandse kust gelegen zeewering. De zeewering wordt beschermd met kribben tegen erosie tengevolge van langstransport. De kribben hebben een onderlinge afstand van 120m en zijn 80m lang. Ongeveer 350m uit de kust op een diepte variërend tussen NAP -3m en NAP -5m ligt een zanderige brekerbank. Deze bank vertoonde over de afgelopen periode van 35 jaar een stabiel karakter. Langs de Nederlandse kust vertonen de zandbanken over het algemeen een veel dynamischer karakter waarbij er veelal zeewaarts gerichte verplaatsing in de tijd optreedt.

Op een afstand van ongeveer drie kilometer van de Pettemer zeewering ligt een ondiep gedeelte variërend tussen de NAP -6m en NAP -7m. Dit gedeelte blijkt praktisch niet te eroderen en wordt de Pettemer polder genoemd. De Pettemer polder onderbreekt de NAP -10m lijn die nagenoeg parallel aan de Nederlandse kust loopt. Deze onderbreking zorgt voor enige contractie van het langsstroomprofiel. De contractie wordt versterkt door het feit dat de Pettemer zeewering de locale kust 100m zeewaarts van de omliggende kustlijn heeft gefixeerd. Het gevolg is dat langstransporten belangrijker worden in vergelijking tot andere locaties langs de Nederlandse kust.

Meetgegevens van Petten
Er is gestart met het verzamelen en het analyseren van meetdata verkregen voor de kust van de Pettemer zeewering. De bodemgegevens bestaan uit een 35 jarige reeks van zomers gemeten bodem lodingen, de zogenaamde JARKUS profielen en een reeks van 20 lodingen gemeten gedurende het gehele jaar over de afgelopen 5 jaar. Naast de bodemprofielen zijn er op verschillende dieptes bij Petten zowel golf- als waterstandgegevens gemeten tijdens stormcondities.

Effect van storm op de morfologie
Aangezien er geen meetgegevens van bodemprofielen tijdens stormen beschikbaar zijn, (momenteel zijn er alleen bodemprofielen van enkele weken voor de storm beschikbaar) is het niet mogelijk de morfologische processen volledig aan de hand van metingen te onderzoeken. Desondanks is er geprobeerd het effect van morfologische ontwikkelingen te onderzoeken. Twee methodieken zijn toegepast:

1. Allereerst is er geprobeerd de jaarlijkse veranderingen in de gemeten bodemprofielen te verklaren aan de hand van stormintensiteit en individuele stormkracht.
2. Vervolgens is er voor een aantal stormen waarvan de hydrodynamische condities zijn gemeten geprobeerd de ontwikkeling van de bodemhoogte gedurende een stormperiode te simuleren op een vast punt.

Effect van storm op de jaarlijkse veranderingen van de gemeten bodemprofielen
Tijdens het analyseren van profielveranderingen is er gebruik gemaakt van de profielen ter hoogte van raai 20.830. Het zandvolume van de gemeten profielen is onderling vergeleken en de verschillen in volume zijn vergeleken met gesommeerde stormuren en individuele stormintensiteiten uit de tussenliggende perioden.

Het profiel gemeten in het jaar 1990 bleek aanzienlijk minder zand te bevatten dan voorgaande profielen. De gemeten verdieping van het profiel vergeleken met het voorgaande jaar gemiddeld over een lengte van 700m betrof een halve meter. Deze profielverandering vond redelijk verdeeld over het profiel plaats. De verlaging bleek echter niet aantoonbaar door storm invloeden te zijn veroorzaakt, ondanks dat de winter van 1990 werd gekenmerkt door een aantal zeer krachtige en langdurige stormen. Dergelijke stormen werden namelijk reeds eerder waargenomen in de jaren ‘70 zonder noemenswaardige gevolgen. Tijdens de analyse is geen rekening gehouden met waterstanden en windrichting, terwijl beide factoren wel degelijk een rol spelen in de het doorwerken van de hydrodynamische belasting.

Waarschijnlijk worden de jaarlijks gemeten profielveranderingen veroorzaakt door verschillen in golfcondities over een langere periode en spelen momentane processen geen grote rol.

Ontwikkeling van de bodemligging tijdens storm
Met behulp van golfmetingen tijdens storm op ondiep water is geprobeerd om inzicht in de bodemontwikkeling op korte termijn te krijgen. Tijdens stormomstandigheden is gebleken dat praktisch alle golven ter hoogte van het gebruikte meetpunt breken. Er kan dus worden aangenomen dat de waterdiepte bepalend is voor de gemeten golfhoogte.

Tijdens deze analyse is er uitgegaan van een lineaire constante relatie tussen locale waterdiepte en locale golfhoogte. De constante wordt ook wel brekerindex genoemd en in praktijk blijkt dat de waarde van deze brekerindex varieert tussen de 0,5 en 0,6 wanneer men de golfhoogten beschrijft met de significante golfhoogte.

De bodemontwikkeling is aldus voor 6 verschillende stormen nagegaan en blijkt nogal te variëren. Stormen gemeten in 1995 bleken praktisch geen verandering in het profiel teweeg te brengen, terwijl stormen van soortgelijke kracht in 1999 voor aanzienlijke bodemdalingen zorgden, in de orde van een halve tot anderhalve meter.

De voorspelde bodemontwikkeling blijkt redelijk gevoelig voor de aangenomen brekerindex constante. Tijdens de simulatie is er uitgegaan van een constante brekerindex van 0.55. Helaas, valt het te betwijfelen of de brekerindex tijdens storm constant blijft. Vermoedelijk is de waarde sterk afhankelijk van de golfperiode en bodemhelling. Desalniettemin kan hiermee een indicatie van de erosie worden verkregen. De bodemhoogte voorafgaand aan een storm lijkt eveneens van groot belang voor de erosiediepte.

Analyse van bodemontwikkelingen en de effecten met UNIBEST-TC
Vervolgens is de invloed van golfhoogte, golfperiode, waterstand en bodemhoogte op de morfologische ontwikkeling en de golfhoogte nabij de teen van de dijk geanalyseerd met het model UNIBEST-TC. UNIBEST-TC veronderstelt de volgende condities:

- Uniforme kust in langsrichting.
- Behoud van zandvolume over het bodemprofiel, wanneer er sprake is van ‘cross-shore’ transport.

Het blijkt dat vooral de hoogte van de vooroeverbodem (gebied tussen de kribvakken) bepalend is voor het doordringen van golven tot aan de zeewering; de kruinhoogte van zandbanken is ondergeschikt. De hoogte van zandbanken beïnvloedt wel degelijk de golfhoogte en golfbelasting van de golven op de vooroever, en daarmee ook de erosiesnelheid van de vooroever, maar niet de daadwerkelijke golfhoogte aan de voet van de zeewering. Daarnaast blijkt het verhogen van de waterstand in hogere mate bij te dragen aan hogere golven dan het verhogen van de golfhoogte op diepwater. Geconcludeerd kan worden dat de stormimpact voornamelijk door de waterstand of waterdiepte wordt veroorzaakt.

Tijdens constant veronderstelde extreme diepwater-randvoorwaarden (waterstand van NAP +5m en 'root-mean-square' golfhoogte op diepwater van H_{rms} = 5m) blijkt dat de vooroever direct voor de dijk zeer snel erodeert; orde van grote 1m per dag. Toch blijkt de golfhoogte niet direct toe te nemen, ondanks het toenemen van de locale waterdiepte. Dit is te wijten aan het feit dat het zand zeewaarts wordt verplaatst. Hierdoor wordt er meer golfenergie zeewaarts gedissipeerd. Bovendien neemt de golfgroepsnelheid af als gevolg van de toenemende waterdiepte door erosie voor de zeewering waardoor de golfhoogte reduceert bij een gelijkblijvende golfenergieflux.

Op lange termijn, meer dan een dag, is er sprake van golfgroei aan de teen van de zeewering tengevolge van een aanhoudend zeewaarts transport van zand naar dieper gelegen water. Blijkbaar worden de processen die de initiële golfafname veroorzaken bij voldoende zandverplaatsing ondergeschikt. Ondanks de ondergeschikte rol bij aanhoudende simulaties heeft deze initiële golfafname aanzienlijke gevolgen voor de berekende impact van stormerosie. Het verdient dan ook de aanbeveling om uit te zoeken of deze afname reëel is, wanneer blijkt dat de stormerosie van belang is.

Probabilistische analyse
Er is gebruik gemaakt van een probabilistische benadering om uiteindelijk de resultaten van het UNIBEST-TC model, dat is toegepast op extreme condities, te vertalen naar overschrijdingsfrequentie van golfoploop en de bijbehorende benodigde kruinhoogte. Mede met behulp van de probabilistische analyse kunnen de effecten van de bodemveranderingen worden vertaald naar ontwerpgrootheden met inachtneming van onzekerheden.

De daadwerkelijke bezwijkkans wordt vastgesteld met behulp van het faalmechanisme ‘golfoverslag’. Naast dit faalmechanisme bestaan er nog andere faalmechanismen die een rol kunnen spelen, zoals stabiliteitsverlies door ontgronding of door falen van de taludbescherming, maar deze mechanismen worden gedurende deze analyse verwaarloosd. Tijdens de gebruikte probabilistische methode om de faalkans te bepalen zijn slechts de twee belangrijkste parameters, diepwater golfhoogte en waterniveau, stochastisch benaderd. De andere parameters zijn deterministisch beschreven.

Het blijkt dat ondanks de aanzienlijke morfologische verandering die er volgens de UNIBEST-TC simulaties optreden, er aanvankelijk vrijwel geen sprake is van een toename van de golfhoogte. Pas na ongeveer 12 tot 24 uur begint de golfhoogte met enkele centimeters toe te nemen. Vanuit de verandering in faalkans door lokale stormerosie kan eveneens worden geconcludeerd dat de effecten van stormerosie verwaarloosd kunnen worden bij zowel het ontwerpen als het toetsen van zeeweringen. Hierbij moet wel worden opgemerkt dat de uitkomsten zijn verkregen zonder 3 dimensionale effecten mee te nemen.

Conclusies
Het blijkt dat de initiële ligging van de vooroever van groter belang is voor de golfhoogte nabij de teen van de zeewering dan de ontwikkeling van de locale diepte ter plaatse van de teen van de zeewering tijdens storm. Eveneens blijkt uit metingen dat het bodemniveau met ongeveer 2.5m kan variëren waardoor er een aanzienlijke onzekerheid over het aanwezige bodemniveau bestaat. Het verdient dan ook de aanbeveling om verder onderzoek te concentreren op het profiel dat bij aanvang van een storm aanwezig kan zijn en niet direct op de morfologische veranderingen tijdens een periode van storm, aangezien deze veranderingen gering zijn. In het bijzonder zijn de veranderingen van de vooroever van belang bij het bepalen van een 'maatgevend' bodemprofiel bij aanvang van storm. Een stochastische beschrijving van de bodemhoogte gebaseerd op metingen kan hiervoor in aanmerking komen.

Summary

Research topic
For my final degree project, I have investigated the influence of morphological change during storms on the sea defence in Petten. The research focuses mainly on the effects of erosion due to storms on the near-shore area where the waves reach the sea defence.

At present, short-term morphological change is not taken into account during the design and evaluation of sea defences because its effect is difficult to predict. This project aims to assess the importance of short-term morphological change and to determine the dominant parameters.

The evaluation of dikes is subject to strict safety criteria. It is, therefore, sensible to discuss the effects of morphological change in terms of probability of failure or crest height being exceeded rather than in terms of erosion depth. The actual evaluation of the dike and the safety parameters can then be compared with those that result from a model in which morphological change is incorporated. For this study data gathered at the Pettemer site has been assessed.

Location
The 1½ km long sea defence at Petten forms the most northern part of the sea defence structure on the coast of the province of Noord-Holland. The Hondsbossche sea defence forms the 4km southern part. The Pettemer sea defence is protected from erosion due to longshore currents by 80m long groynes at intervals of 120m. About 350m out to sea, at a depth, which varies between NAP - 3m and NAP - 5m, lays a sandy bar where the waves break. This bar has remained in a stable position during the last 35 years although sand banks along the Dutch coast generally tend to shift in a seaward direction. Three km from the sea defence at Petten lays a shallow area where the water depth varies between NAP - 6m and NAP - 7m. This area, called the Pettemer polder, appears not to be affected by erosion.

This area interrupts the NAP -10m line, which runs more or less parallel to the Dutch coast. The Pettemer polder causes an irregularity of the alongshore profile, that results in some contraction in flow profile. Together with the protruding Pettemer sea defence (100m) this results in longshore transport becoming more important here than in other locations along the Dutch coast.

Measurement data from Petten
A start has been made with the collection and analysis of measurements taken in front of the sea defence at Petten. The seabed data consists of a series of 35 bottom soundings taken annually each summer. These are the so-called JARKUS profiles. In addition, a series of 20 soundings has been taken over the last five years at intervals during the entire year. Data has also been obtained at Petten of wave and water level heights at a number of locations of varying depth.

The effects of storm on the morphology
At present, seabed profiles for storms are only available for a few weeks, making it impossible to investigate morphological change through measurement data alone. To try to investigate the effect of morphological change despite this limitation, two methods have been used:

1. Firstly, an attempt has been made to explain the alterations in the bed profile over the year through storm force and duration.
2. Secondly, as there are a number of storms for which hydrodynamic conditions have been measured, an attempt has been made to simulate the changes that occur in the seabed height during a storm period for a specific point.

The influence of storms on changes to the measured seabed profiles over the years.
For the analysis of profile changes, the bed profiles obtained at cross-section 20.830 have been used. The sand volumes of the measured profiles have been compared to each other, while the differences between them have been related to total storm hours and intensity occurring in the intervening period between the measurements.

The 1990-profile turned out to contain significantly less sand than the earlier profiles. The measured profile averaged over a distance of 700m was half a meter lower than the previous year. The change was more or less constant over the whole length of the profile. This decrease cannot, however, be proven to be the result of storm action, even though the winter of 1990 was marked by a number of lengthy and intense storms. A similar storm pattern was also observed in the seventies without causing notable change in the profile. In the analysis, water level and wind direction have not been taken into consideration although they certainly contribute to the effects of hydrodynamic load.

The changes in the annual profiles are probably caused by wave changes over a long period, while short-term factors do not play a major part.

Seabed developments during storms
An attempt has been made to understand short-term changes in the seabed by taking wave measurements. It appeared that during storms nearly all the waves broke at the depth where the measurements were taken. This suggests that the depth of the water determines wave height.

In this analysis, a constant linear relation between local water depth and wave height has been assumed. This constant is called the 'breaker index' and experience has taught that it varies between 0.5 and 0.6 for significant wave heights.

The seabed developments have been studied for six different storms and show considerable variation. Storms measured in 1995 caused little or no change in the seabed profile, while storms of a similar strength in 1999 lowered the seabed considerably up to 1½ m. The predicted seabed erosion has been determined using a breaker index of 0.55. Regrettably, it is doubtful whether the breaker index remains constant during storms and its value depends very much on the wave period and the steepness of the seabed. Nevertheless, it is possible to obtain an idea of the level of erosion through this method.

Analysis of seabed change and its effects with UNIBEST-TC
Next, the effects of wave height, wave period, water level, the seabed height on morphological change and the wave height at the toe of the dike has been analysed using the UNIBEST-TC model.

UNIBEST-TC assumes the following conditions:

- The coastline is uniform in longshore direction.
- When 'cross-shore' transport occurs, the volume of sand across the seabed profile remains constant.

It appears that the height of the seabed at the nearshore (the area between the groynes) is particularly important in determining how far the waves penetrate towards the sea defence; the crest height of the sandbars is of only minor significance. However, the height of the sandbars does affect the wave height and impact of waves on the nearshore area and, consequently, the speed of erosion in that area; but not the actual wave height at the toe of the sea dike. A rise in the water level proves more significant in creating higher waves in shallow water than an increase of the wave height in deep-water. Storm impact is therefore mainly depending on the water level or water depth.

With extreme deep-water parameters (a water level of NAP + 5m and a root-mean-square wave height in deep-water of H_{rms} = 5m) assumed to be constant, it appears that the nearshore immediately in front of the dike suffers from rapid erosion during extreme conditions; in the order of magnitude of 1m per day. Even so, the wave height does not increase despite the rise in local water depth. This is because sand is shifted seawards resulting in greater wave energy dissipation seaward.

Over the long-term, the wave height increases at the toe of the sea defence as a result of continuous seaward-directed sediment transports to deeper water. Apparently the processes that cause the initial wave height reduction become secondary when sufficient quantities of sand have been transported seaward. Despite of the process becoming secondary after some time it has considerable effects on the calculated impact of storm-erosion.

Probabilistic analysis

A probabilistic approach has been applied to express the results generate by UNIBEST-TC, that has been used to simulate extreme conditions, in crest height and probability of failure. Considering the probabilistic analysis it is possible to determine the design parameters taking into account the uncertainties.

The actual probability of failure is determined by means of the failure mechanism ‘wave run-up’, however, other failure mechanisms also are of influence like loss of stability due to the loss of sand or failure of the revetment protection. The influence of these failure mechanisms has not been considered during the probabilistic analysis. The applied probabilistic method to determine the probability of failure considers only two random variables; deep-water wave height and water level. All other parameters are taken into account deterministic.

Apparently, despite the rather significant morphological changes that occur according to the UNIBEST-TC simulations, little initial wave height growth has been generated by these seabed changes. After about 12 to 24 hours the local wave height increases with a few centimetres. Also the variation in probability of failure due to local storm-erosion suggests a similar small effect. Consequently the effects of storm-erosion can be neglected during the design, however, 3D effects are not considered during this analysis.

Conclusions

It appears that the pre-storm level of the nearshore area is of greater significance than the wave height development at the sea defence toe during storm. According to survey data the averaged level of the nearshore area varies with 2.5m causing a significant uncertainty in the seabed level that is present at the beginning of a storm. Therefore it is recommended to concentrate future research on the pre-storm seabed level instead of the seabed development during a storm. Especially the nearshore bed level variations are of considerable importance for the determination of the normative seabed profile. It would be favourable to incorporate the seabed level stochastically in future probabilistic analyses that are used for the design and testing purposes.

Contents

1. Introduction

1.1 General problem

It appears to be problematic to match the design boundary conditions of coastal defensive structures, like dunes and dikes, with the enforced safety conditions. The Dutch government, represented by 'Rijkswaterstaat', a governmental institute that is responsible for the observations of the safety demands, is responsible by law for the hydraulic boundary conditions of all coastal defences. To be able to design and test the coastal defences, a set of local boundary conditions based upon extreme conditions with a certain probability of exceedance has to be available. The water level and the deep-water wave height are identified as main parameters.

For deep-water conditions (offshore) the boundary conditions are reasonably known and have a more general occurrence, while in order to determine the local boundary conditions the local influences have to be taken into account. To do so, Rijkswaterstaat plans to use a wave simulation model called SWAN, to simulate the process of energy dissipation from the deep-water wave height to the local shallow water wave height. In a first validation study [JACOBSE, 2000] it appeared that the measured wave heights near the Pettemer sea defence where higher than the maximum possible wave heights that could be simulated. It appeared that the difference in wave height had been caused by seabed variation over time.

Furthermore, SWAN requires representative seabed geometry to determine the local hydrodynamic conditions that can be used as boundary conditions. A current problem is the formulation of the representative seabed geometry. The difficulty in finding the required geometry is caused by two problems according to the following literature [VLEDDER VAN, 2001; TONIS AND VEEN, 2001]:

- The pre-storm seabed level that exists simultaneously with the occurrence of an extreme event is uncertain.
- The behaviour of the seabed profile during extreme events is also uncertain.

In this thesis the seabed behaviour during an extreme event is the point of focus. This study is triggered by recent research that showed that higher waves were measured than that could exist according to model computations.

1.2 Objectives

The main objective is to increase the understanding of the processes and involved parameters that affect the behaviour of seabed profiles during storm situation. At present little is known about the exact seabed behaviour during storms. The main research question has therefore been defined as follows:

What is the contribution of short-term morphological variations (local erosion) due to storm events on the coastal safety conditions stated by 'Rijkswaterstaat' at the Pettemer sea defence?

The main research question has been divided into two more specified research questions:

1. What are the most important parameters that affect the local storm-erosion process?
2. What is the effect of a storm on the local seabed variation?
3. What are the consequences of seabed variation on wave and crest height or probability of failure?

1.3 Research approach

To tackle these three sub-research questions several analyses have been used. The first question has been approached with a literature study on sediment transport in general and a study on the design of coastal defences and the decision-making process involved. The possible mechanisms of failure are examined as well as the methods used by the government to determine whether a sea defence is 'safe'.

Data analysis
Because the effects of extreme storm events are largely determined by local conditions the effects of storm-erosion are examined more closely at the Pettemer sea defence. First of all, the understanding of storm effects has been gained by data analyses. The data analyses consist of:

- A comparison of annual seabed sand volumes.
- A comparison of annual seabed volume variations and storm intensities.
- A hindcast analysis of local bed variation using local wave height measurements.

The first analysis gives an indication of measured seabed variations, which can be compared with individual storm effects. Furthermore these variations in cross-section volumes are compared with the occurrence of storm intensities, because it is expected that fair-weather conditions result in a higher seabed level than rough conditions do. Finally the contribution of a single storm to the bed level variation in front of the sea defence is examined. This has been done with a hindcast analysis that uses measured wave data at a specified location in the surf zone to determine the variation in bed level. Wave data has been used because the seabed has not been measured during a storm conditions.

Model simulations
Another method to gain understanding of the effects of a single storm is by means of model simulations. During this thesis a morphological model called UNIBEST-TC has been used. This model is capable of computing sediment transports due to waves and currents based on physical relations. These simulations contribute greatly in gaining perception of the parameters involved. Furthermore, it is possible to examine extreme scenarios that have never been observed in reality. This is important because these extreme events are responsible for inundation.

Probabilistic analysis
Whenever the storm-erosion has to be expressed in terms of safety, the approaches, that are used by the government, to determine these effects have to be followed. At present, the use of a probabilistic approach is necessary because safety is expressed in probability of failure. The probabilistic approach that has been applied during this thesis uses the UNIBEST-TC simulations to determine the probability of failure at the Pettemer sea defence.

Whenever the seabed alterations are expressed in terms of probability of failure it is possible to determine the contribution of these alterations on the actual safety, answering the final question: 'What is the contribution of storm-erosion on the safety conditions at the Pettemer sea defence?'

1.4 Report outline

The first part of this thesis is dedicated to increase the perception of the seabed behaviour during storm by means of data analysis and literature studies. Chapter 2 is the result of a literature study dealing with the framework. To study and analyse the behaviour of the seabed cross-sections during storm situations, data from the Pettemer field site has been used. Chapter 3 is concerned with the Pettemer area and the available measurements for the data analysis. The actual data analysis is described in Chapter 4. Furthermore, the model simulations are discussed in Chapter 5, resulting in an overview of the parameters involved. Chapter 6 treats the probabilistic analysis that has been used to determine the actual contribution of the storm-erosion on the safety. Chapter 7 deals with the discussion. Also the effect of individual parameters has been considered resulting in the final conclusions and recommendations described in Chapter 8.

2. Framework

2.1 General

Erosion effects are not taken into account during the formulation of the boundary conditions for fixed coastal structures like ‘dikes’. These boundary conditions are derived from the safety requirements. However, to determine the effect of erosion, consideration of the development over time of the boundary conditions is essential.

Furthermore, the development of new methods for the evaluation of coastal structures is taking place. Hence, it seems useful to incorporate recently developed methods and to use them to determine the effect of erosion caused by storms on evaluation conditions. In the Netherlands, structures that function as defences are evaluated every 5 years in order to check whether they satisfy the requirements. If the structure does not function adequately, the structure must be improved. This results in different boundary conditions for design and evaluation.

This chapter considers the developments of the boundary conditions for evaluation purposes. The following Paragraph 2.2 describes the safety philosophy, the process of policy decision-making and the available approaches and methods that are used for the formulation of required boundary conditions. A description of the recent developments in the field of implementing morphological aspects into the boundary conditions will be given in Paragraph 2.3. The final Paragraph 2.4 deals with the conclusions and recommendations.

2.2 From safety to boundary conditions

2.2.1 Safety philosophy

Frequent inundations are unacceptable because the consequences are potentially serious. The effect of the flooding of 1953 and the more recent high river discharges of 1993 and 1995 are examples of extreme floodings. This has not always been the case. In the early days people adjusted themselves to the situation that existed: people settled on higher parts and built artificial hills to keep dry. In those days the consequences of flooding were minor. Besides, flooding brought a lot of fertile silt and sand, increasing the level of land at the same pace as the sea level rise.

The pressure of a fast expanding population leads to the use of lower lying land. To protect agricultural activity and increase production, facilities for water regulation were constructed. The result was a lowering of the level of the land. The impact of inundations increased and people started to build defence structures like ‘dikes’ for protection.

At present the low-lying land is densely populated and the water level in these areas is artificially kept low. Again the result is a decrease in the level of the land, while the level of the sea continuously rises. It can be concluded that the present situation has significantly deteriorated; compared to the past: the consequences of inundation have increased with time, more lives are at stake and the size of possible damage is greater. Therefore it is important that the safety of the people is guaranteed to an agreed level.

2.2.2 Safety policy

To 'guarantee' a certain level of safety, the Law on Water Defensive Structures became operative in 1996. This Law has major consequences for the Dutch government system. The Law dictates that sea defence structures have to be maintained by the local government institutes called 'Waterschappen' or water boards. The water boards are also responsible for the design of sea defences in their region. To discover whether maintenance is necessary, water boards evaluate if their sea defences still satisfy the requirements. These evaluations are done every 5 years under the control of the provincial government. The national government acts as the supreme supervisor and is responsible for planning the safety policy.

Risk
In principle absolute protection against the effects of flooding would be nice. However, it can never be achieved for the full 100%. Natural phenomena that lead to inundations are unpredictable. The maximum possible extent of a natural phenomenon is unknown, as is the moment when it will occur. Natural phenomena are therefore often described by probability distribution functions. Safety approaches that use a distribution of probability are frequently quantified in terms of risk. In the case of sea defences, risk is defined as the probability multiplied by the consequences of inundations:

Risk = Consequences * Probability

Whenever a certain level of risk is accepted, an increase in the possible consequences has to be compensated for by decreasing the probability of them occurring.

Consequences
The consequences of inundation are difficult to determine. Besides the costs, non-quantifiable subjective aspects also play a part, like emotional distress and the loss of lives. The considerable amounts of money provided by the government involved in the improvement, maintenance and construction of sea defences make it important to determine the consequences as precisely as possible.

The consequences mainly depend on the following aspects [TAW, 1998]:
- Polder dimensions (A small polder fills up faster, decreasing the needed evacuation time).
- Polder level (Low levelled polders will suffer a higher level of flooding).
- Population density and investments.
- The degree of preparations for a flooding (emergency evacuation plans).
- Fresh water or salt-water inundation.

Probability
Expressed by a frequency of exceedance a year or a return period, the distribution of probability of failure is the other factor that influences the risk. Probability of failure is described as the probability a defensive structure fails. Failure means that the structure is incapable of fulfilling its function, which will be discussed further on in this chapter. The probability of failure is based on the fact that although the exact parameter values are unknown, a certain range of occurrence can be determined.

History of safety policy
Before 1953 (the year of the flooding in the south western part of the Netherlands) risk estimates were based on intuition and experience. The highest recorded water level, together with a safety margin, was used as reference for the construction height of sea defences. In 1960, the 'Delta Commission' tried to express the level of safety into a return period. The safety level based on frequencies of exceedance has been integrated in the 'Delta Wet'. In the process, the consequences were examined, and the loss of all capital goods in an inundated region was included. However, the loss of lives was neglected because the commission was unable to quantify these losses in an ethical manner.

After 1992 it became possible to translate the determined return period into boundary conditions for the design of fixed sea defence structures. Important failure mechanisms were neglected. Hence a different approach was chosen. Water levels with a frequency exceeding 1/1250 up to 1/10000 a year, depending on the value of the area, had to be withstood to be 'completely safe'. These frequency figures are given by a cost-benefit-analysis for the region 'Central Holland' number 14 in Figure 2.1.

'Completely safe' appears to be the case when 2% of the run-up induced by waves during the design water level exceeds the structure height. It is necessary to note that the failure problem is hereby reduced to only one failure mechanism 'wave run-up'. If the water level for which the structure is designed to cope with, has been reached, the structures won't collapse immediately, because built in safety margins provide a structure stronger than that is absolutely necessary to withstand the water level it was designed for.

According to the [TAW, 2000], the previously described method has to be mainly improved on three ways:

- The transition of a dike section approach to dike-ring-approach. Instead of a dike section a dike-ring, composed of dikes, dunes and structures, is used to determine the strength.
- Different failure mechanisms have to be taken into account, instead of the present method that is dominated by the failure mechanism 'wave run-up'.
- Systematically and verifiably all uncertainties in the calculation of the inundation probability have to be taken into account. Currently these uncertainties are taken into account at the end of the approach by using additional safety margins.

2.2.3 Safety approaches

The government is supported by the TAW 'Technische Adviescommissie voor de Waterkeringen' in their decision making process. The TAW has defined 4 approaches to determine the inundation risk based on the following factors:

1. Maximum load per dike-section (uniform properties).
2. Maximum load per dike-ring.
3. Inundation probability.
4. Inundation risk.

At present the first approach is policy, as described in Paragraph 2.2.2. The other approaches are optional and lead to a more sophisticated and detailed approach. Slowly the evaluation develops to the direction of the fourth approach as more information becomes available and the perception of failure increases.

The first approach is easiest to cope with. It is based on only one failure mechanism (e.g. the 2% run-up criterion as explained above) and the probability of the boundary conditions, which lead to exceeding this. Although it appears this approach reckons with just one failure mechanism, other potential failure mechanisms have to be taken into account. They are treated separately and are not allowed to exceed corresponding deterministic norms. Since the response of the structure during overflow conditions is not exactly known, the structure is declared 'unsafe' for a certain amount of wave run-up whereas this does not necessarily mean that the structure will collapse immediately.

The second method is an extension of the first. This method deals with the failure of a dike-ring that encloses a region. The weakest section in a dike-ring determines to a large extent the probability of failure of the total dike-ring. The safety of the dike-ring-area, the area enclosed by a dike-ring, is based on the probability of failure of the total dike-ring. The sections within a dike-ring consist of dikes, dunes and beaches, dams, and so forth. Figure 2.1 shows the division of the Netherlands into dike-rings. Different probabilities of failure are accepted for different regions according to the value and population of the protected region.

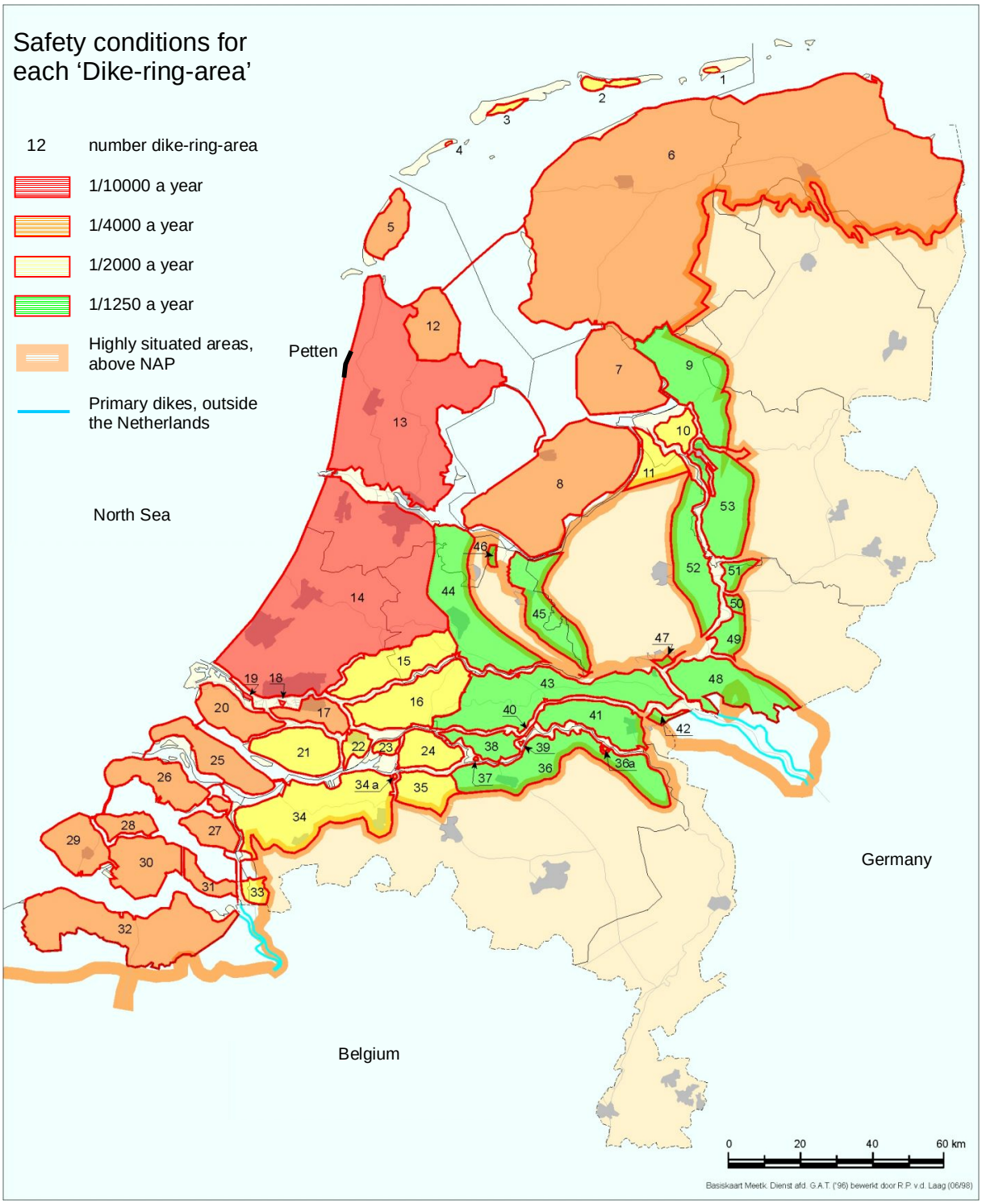

Figure 2.1: Dike-ring-areas and norms according to 'Wet op waterkeringen'. A dike-ring consists of several different sections like: dikes, dunes and beaches, dams and etcetera. [TAW, 2000A]

The third approach is based on the probability a dike-ring fails, taking into account all the possible failure mechanisms. Failure equals the summation of all possible failure mechanisms leading to water inconvenience or inundation.

The fourth approach is the most complete method. Risk is expressed in the magnitude of damage and number of victims within a dike-ring. This approach uses risk to determine the level of safety. The advantage of this approach is that the construction height can be related to the consequences of failure.

2.2.4 Safety methods to calculate safety loads

The different safety approaches are put into a useable format for the evaluation of coastal defence structures. This results in several methods of which three evaluation methods are listed:

1. Deterministic method.
2. Probabilistic method.
3. Delta Commission method.

Deterministic method
The deterministic method is based on assumptions about strength and safety. Sometimes the uncertainties are explicitly taken into account by a safety factor however more often they are implicitly taken into account. These safety assumptions are determined partly by experience and partly by intuition. A deterministic method can result in a proper design, however often the safety measurements and incorporated uncertainties are difficult to trace.

Probabilistic method
The probabilistic method is based on the probability of failure and the always-present uncertainties in the strength and load variables. It is essential to recognise the different failure mechanisms and to determine the correlation between the variables.

Delta Commission method or semi probabilistic method
The Delta Commission method is also a probabilistic approach that limits itself to one failure mechanism with one type of load; water overflow including wave run-up. The strength parameters are determined with the deterministic approach.

Of the three methods the probabilistic method is preferred, because it results in construction dimensions taking into account the uncertainties explicitly. However the deterministic method is the easiest to cope with. It uses averaged values in combination with sets of safety factors. However, the deterministic method is incapable of showing the uncertainty of the outcome. The Delta Commission method is positioned in-between both methods. A probabilistic output is realised with a minimum of effort because it is only partially based on probabilistic determined variables.

Most of the coastal structures are already built and used. However, after a certain period structures have to be improved. It is in the public interest to ensure a safe environment, but improvements are expensive. Small improvements that are relatively expensive have to be especially avoided. They are relatively expensive, because the mobilisation costs form a large share of the total costs. The boundary conditions for evaluation are used to determine whether improvements are necessary. To exclude minor improvements, the boundary conditions for evaluation are less severe than for the actual design conditions.

The National Institute for Coastal and Marine Management 'RIKZ' is responsible for providing criteria necessary for the five-yearly evaluation of the coastal defences. Therefore this thesis focuses on the evaluation aspects. The design aspects are rather similar however the responsible water board determines these criteria.

2.2.5 Evaluation process

In the Netherlands most defence structures are already built and have to be maintained. To determine whether maintenance is needed structures are evaluated. Local governments have to evaluate all structures every 5 years. For these evaluations, parameter settings are used that result in a minimum load that has to be withstood.

In future evaluations, it is preferable to use the inundation risk approach as a standard. The average probability of exceeding the limits has to be reduced as the consequences of flooding increase to maintain a similar level of safety. Over a period of 5 years the consequences of failure in a dike-ring-area are expected to increase significantly, because the population density as well as the investment values are expected to rise. To maintain an equal level of risk within a situation of increasing consequences, a decrease in probability is the only option. Consequently more severe evaluation conditions have to be applied, resulting in more frequent or more expensive improvements. A solution to this problem has to be found before the implementation of the inundation risk approach is acceptable. The outcome of this political problem greatly depends on the existing political climate and the occurrence of recent inundation incidents.

Furthermore the evaluation process is subjected to continuous improvements that take into account the most recent developments. This is the main reason why several different approaches are simultaneously used and combined. The introduction of the probabilistic method in the evaluation process has only recently been accepted. The precise applications of the probabilistic method are still under discussion by experts.

According to the TAW report [TAW, 2000B], it is already possible to calculate the probability of inundation of an area enclosed by dikes and dunes, a dike-ring-area. For a few dike-ring-areas the calculations have been completed and calculations for other areas will follow within the next two years. The recent calculations for the evaluation of most coastal improvements try to incorporate the probability of inundation of the total dike-ring-area, a summation of the probability of failure of each dike-ring-section.

The total dike-ring has to be evaluated as well as the different sections within this dike-ring. The evaluation of these individual sections is based on several failure mechanisms. In Figure 2.2, the main failure mechanisms for sea defences and dikes are shown. Furthermore other failure mechanisms exist, like: mirco-instability, settling, drifting ice and collision. To satisfy the desire for a probabilistic approach, the variables and the boundary conditions have to be defined by a distribution function, an average value and a standard deviation.

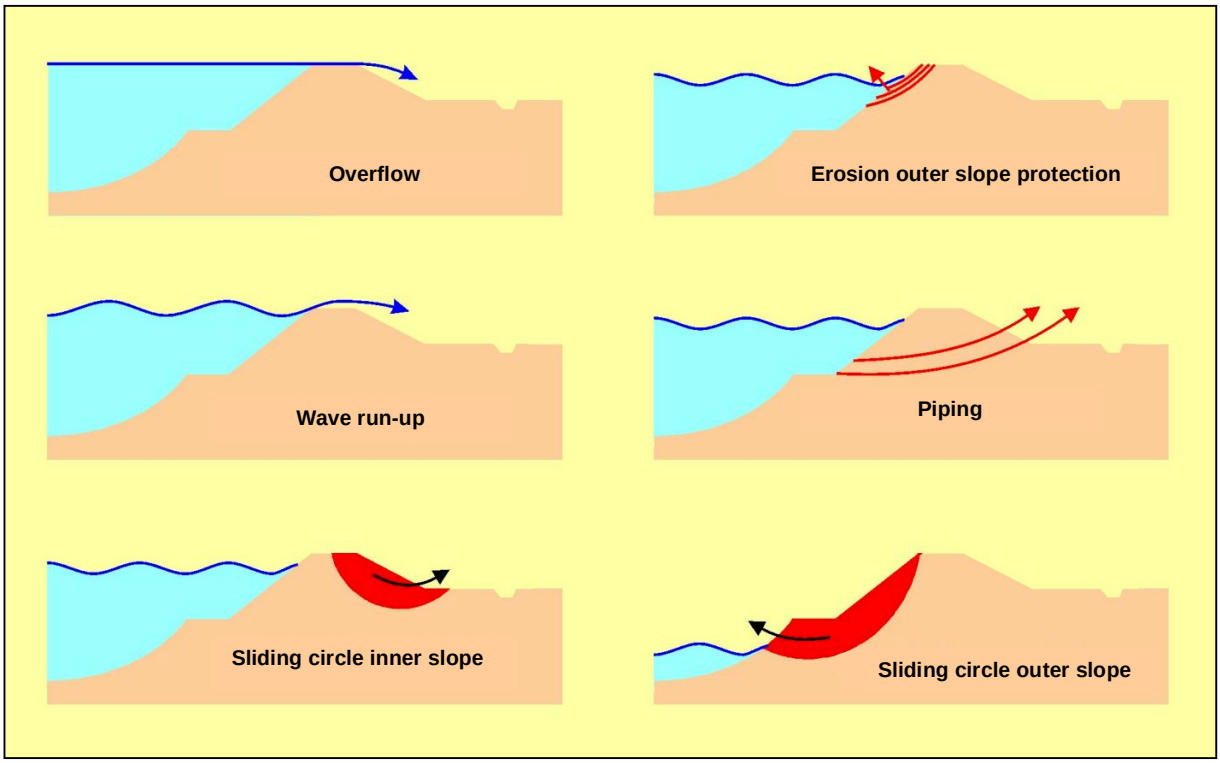

Figure 2.2: Failure mechanisms for dikes, [TAW, 2000B].

Within the evaluation it is necessary to reckon with failure and collapse. Failure occurs when the requirements for one or more failure mechanisms are not met. Collapsing is defined as the loss of coherence or the occurrence of significant geometrical deformations. A structure can fail and not collapse as well as collapse and not fail. As is described above, evaluation conditions are based on failure instead of collapse, resulting in an additional built in safety margin that still exists, just as in the deterministic approach.

2.2.6 Hydrodynamic boundary conditions

The National Institute for Coastal and Marine Management 'RIKZ' is involved in the process of evaluating the Dutch coastal defences and is responsible for supplying the required boundary conditions.

Knowledge of local water levels and local wave characteristics is necessary for the evaluation. To determine the local wave characteristics, deep-water wave data is used. With the aid of models that simulate wave dissipation the local wave height, period, angle and length are determined. However, in order to assess the local hydrodynamic conditions a representative seabed is required.

Seabed variation becomes important when local hydrodynamic boundary conditions are determined with the aid of models and the general hydrodynamic conditions on deep-water. The seabed varies annually and incidentally, for instance during storms. The changes in, and the behaviour of the seabed that take place during storm conditions are uncertain. These aspects are only recently being investigated and the background will be discussed in the next Paragraph (2.3).

Furthermore, the numerical instability of models increases towards the landward boundary. Therefore the error of the output increases, as the distance towards the shoreline decreases; the shoreline is often used as model boundary. To reduce this numerical error, wave characteristics simulated at the toe of a structure are often used. At Petten, the toe of the sea defence is approximately located at the RSP reference line.

Before the waves at the toe can be used, their relationship to the actual waves that hit the structure has to be found. According to experts at the 'RIKZ', the surveyed waves at ca. 60m offshore are similar to the waves that hit the dike. However several aspects are affecting this relationship. First of all the water depth decreases towards the coastline, resulting in lower possible waves. On the other hand the water depth is positively increased by wave and wind setup in the shoreward direction. Wave and wind setup increase with decreasing depths. Wave reflection increases the wave heights that hit the structures. This process is likely to have a significant effect, especially in situations dominated by long periodic waves in the nearshore area (shallow water depth).

Besides the fact that the models neglect wave reflection, and the effects, positive or negative, of the complex wave-current interaction, other 3D processes that are active in the breaker zone are neglected. Models will therefore always differ from reality, because certain processes are neglected. After a calibration of the model, a model factor can be determined. A model factor represents the accuracy of the model output.

2.3 Recent developments

Recently the problem of taking the geometry of the sea-bottom into consideration was raised as a result of the study for the validation of the SWAN-model at the Pettemer sea defence [JACOBSE, 2000]. SWAN, a model for wave simulation, has been used to determine the local hydrodynamic boundary conditions for evaluation purposes. SWAN uses deep-water conditions together with wind data as input to determine the local conditions at the shoreline.

During the SWAN validation study the simulation of wave dissipation from deep to shallow water has been examined. A 3D sea-bottom geometry constructed of cross-sections surveyed in 1994 was used for validation. This sea-bottom profile has also been used to determine the hydrodynamic boundary conditions for 1995.

According to this study executed by Jacobse, SWAN significantly underestimates the local wave height 60m in front of the Pettemer sea defence. The deviation is in the order of magnitude of 20 to 30% [JACOBSE, 2000]. The results of the SWAN model were compared with measured storm data from 1995. The comparisons lead to the conclusion that the wave heights measured in 1995 are physically impossible above the seabed geometry of 1994 that was used as input. Since the measured data are validated, a lower seabed level during the time of survey seems the only logical explanation if the model output can be trusted. According to [JACOBSE, 2000] the uncertainties in the SWAN model are caused by the following aspects:

- Long periodic waves.
- Wave development limit.
- Wave-current interaction.
- Wave breaking.
- Wave reflection.
- **Seabed behaviour during storm.**

One of the logical next steps would be to survey the seabed during storm situations. Unfortunately this is not possible with the current measuring techniques. Nowadays the seabed profile has been surveyed five or six times per year. The minimum period between two consecutive surveys is about one month, the maximum about four months. Due to the absence of survey data that encompass an actual storm period it is difficult to assess the morphological variations during a storm.

From a policy perspective it is interesting to examine the effect of seabed variation and the scale on which it occurs. However, it is not essential to comprehend the cause of seabed variation. From a technical point of view, it is understandable that effort is put into clarifying the processes that affect the behaviour of the seabed during storm.

The interests of policy perspectives have triggered the following studies:

1 A study on the normative seabed profile based on the JARKUS data set [VLEDDER VAN, 2001].
2 A study on the minimum profile at Petten [TÖNIS AND VEEN, 2001].

Van Vledder attempted to develop a normative sea-bottom geometry. A 3D bottom profile has been constructed with different cross-sections from the JARKUS data set. These ultimate profiles were selected on the basis of two criteria:

- The main criterion was based on the penetration of the load towards the nearshore area. The load was defined as the peak period (T_p) multiplied by the significant wave height (H_s). This criterion generated a top five of heavy-load cross-sections for a specified location.
- To ensure a realistic 3D-geometry, the second criterion was based on the minimisation of the period between two adjoining profiles. From the profile top five, the cross-sections were chosen with a minimum consecutive period.

The second criterion was necessary to maintain a realistic 3D barred geometry. Whenever this criterion would have been neglected the joint geometry would show a discontinue breaker bar due to the breaker bar migration over time.

Finally the significant wave height that corresponds with the 3D-geometry constructed according to the above criteria has been determined with the model SWAN. These wave heights have been compared with the wave height that correspond with the 1994-profile used for the boundary condition guidelines. At some locations the wave heights of the constructed geometric profile double the normative wave heights of the 1994-profile.

The second study also defines a minimum profile using the penetration of the load as a criterion. The minimum profile is defined as the profile that allows a maximum wave height at the toe of the Pettemer sea defence. Furthermore, two models were used to describe the morphological variation: UNIBEST-TC and DUROSTA. Only for DUROSTA results were obtained, UNIBEST-TC showed unrealistic results. According to this second study the minimum profile is difficult to determine and more measurements are necessary.

Both studies failed to obtain a seabed profile that was accepted by all experts. Several morphologists rejected the normative profile created by van Vledder because it did not represent a realistic profile. The study of Tönis and Veen did not result in a minimum seabed profile. The characteristics of the seabed still have to be determined in order to use a model to calculate the local boundary conditions.

2.4 Evaluation

This chapter has introduced the available methods for evaluation. Furthermore, the safety approaches that form the basis for evaluation conditions have been described. Several methods for evaluation are available and applied because the formulation of the boundary conditions is improving continuously. However, the currently proposed process for evaluation by the RIKZ has been shown in following diagram, Figure 2.3. This figure also shows the additional aspect that is discussed, 'taking into account seabed variation'.

In reality different sets of boundary conditions are used for evaluation and design. The boundaries for evaluations are determined by the central government. These evaluation boundary conditions are solely used to determine whether improvements are necessary. Each water board is responsible for the level of the design of their improvements. The design dimensions can be chosen by each water board individually for as long as they exceed the safety norm (level of evaluation).

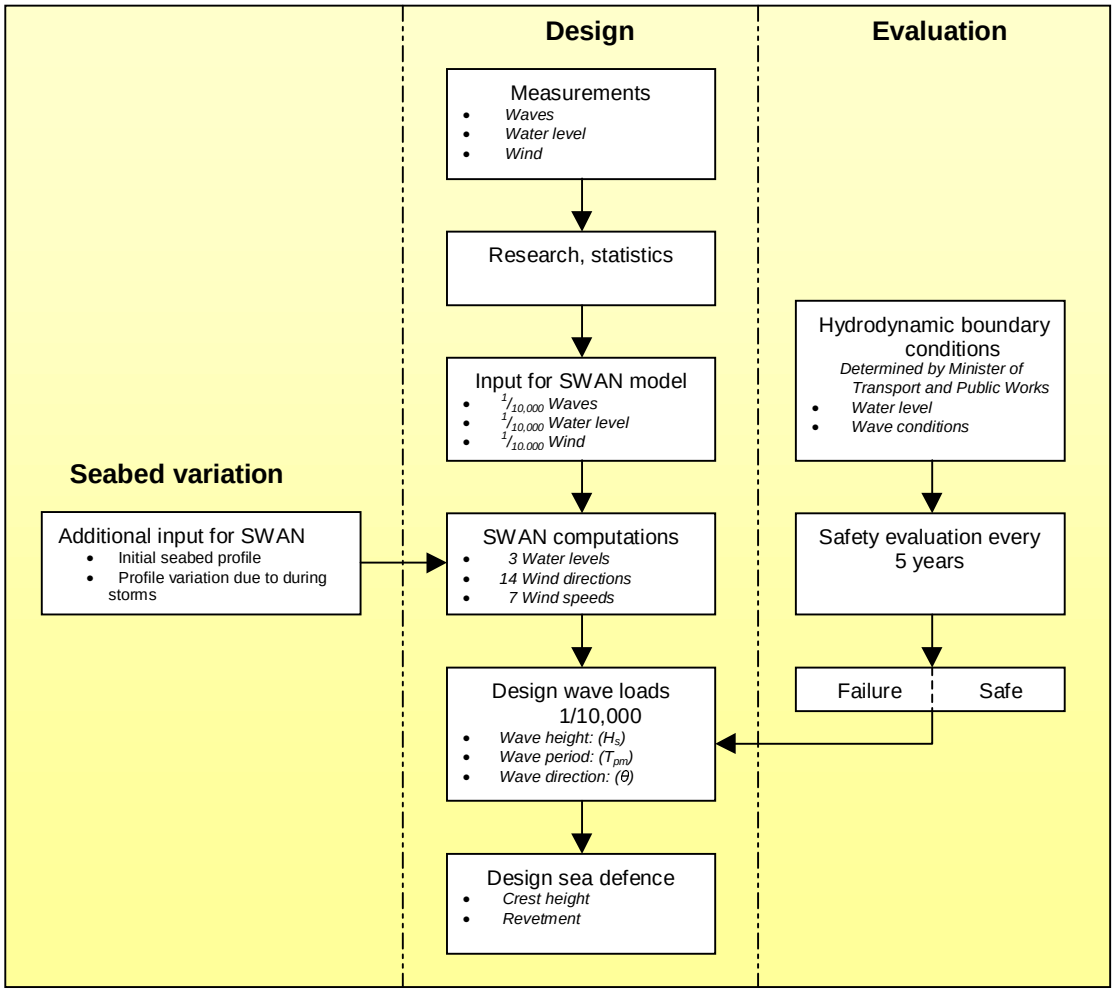

Figure 2.3: Diagram of the proposed design and evaluation, as well as the seabed variation aspect.

Politicians decide at what level the evaluation and minimum design boundaries are set and experts only advise the decision makers with their know-how. However, before politicians accept the proposed boundary conditions most experts have to agree on them. Technical considerations, as well as benefits and costs have a great influence on the final decision that often depends on the existing political climate as well as recent inundation incidents.

Recently wave propagation models have been used to determine the local wave conditions. Knowledge of these local wave conditions is necessary to determine the required boundary conditions. However, the resulting models do not have an overall support of experts. An ever-returning discussion on subjects of model accuracy, reliability and proper input is inevitable. At present, the output error band of the wave prediction models used is about 20% [VLEDDER VAN, 2001], while no morphological processes are taken into account. If the sea-bottom profile is morphologically determined, it is expected that the acceptance of morphologists will increase. Furthermore, the model output will incorporate a more realistic sea-bottom, which should decrease the error band on the model result.

The fact that experts disagree on the 'proper' seabed profile has resulted in further research on how the seabed behaves. A significant percentage of the uncertainties is caused by the lack of knowledge of how the seabed behaves; especially during storms conditions. No measurements of seabed profiles during storms are available along the Dutch coastline, because the measuring equipment is not operative during storm. Research has to be done before a convincing morphological seabed profile can be determined that can be used for model input. The main questions are:

1. How should the general initial seabed profile be determined and which processes mainly affect the profile contours?
2. What is the most plausible seabed profile under extreme storm conditions and where and in what magnitude does the seabed profile vary?

This thesis will focus on erosion due to storm waves or, more specifically, short-term cross-shore wave induced erosion of the area in front of a sea defence. The erosion of the area in front of a sea defence is expected to have the most effect on the penetration of wave energy up to the sea defence. This erosion effects the following failure mechanisms used for the design:

- Wave run-up due to increased wave loads.
- Instability due to erosion.
- Revetment failure due to increased wave loads.

This thesis focuses on the first failure mechanism ‘wave run-up’. Wave run-up appears to have no direct relation with the deepening of the area in front of the sea defence. However, it is expected that higher waves can penetrate up to defensive structures, leading to higher loads under conditions that are accepted as the maximum possible. The contribution of storm erosion was neglected during the formulation of previous boundary conditions. Whether this is unacceptable depends on the contribution of erosion on the increased probability of failure.

3. Site description

3.1 General

This chapter introduces the local situation at Petten and examines the survey data used during this thesis. The location and orientation of the project area will be discussed in Paragraph 3.2 followed by a description of the Pettemer sea defence. The seabed geometry is dealt with in Paragraph 3.3 by means of 3 characterising elements:

- The terrestrial zone.
- The bank and trough.
- The 'Pettemer polder' bank.

Although complex, the 3D geometry will be described by only one cross-section. This is an important assumption. In Paragraph 3.4 most of the 3D processes in the nearshore area are described. The nearshore area is one of the focus points for this thesis.

Paragraph 3.5, examines the hydrodynamic conditions at Petten where a distinction is made into wind, waves and tidal characteristics. The available seabed survey data has been treated in Paragraph 3.6 and the hydrodynamic data sets in Paragraph 3.7. The seabed data consist of three different sources that date back to 1964. The local hydrodynamic data set is based on data from several points along the cross-section 20.830. The locations of the measuring points as well as the equipment are discussed.

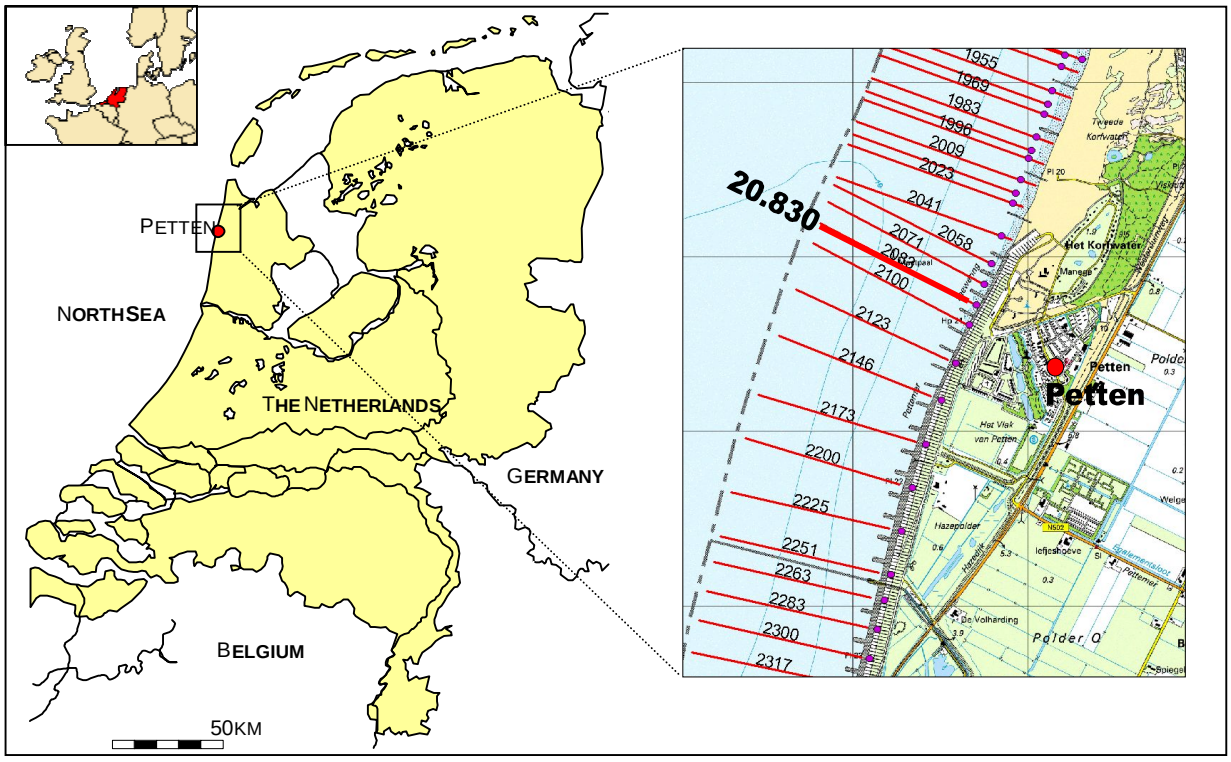

Figure 3.1: Location of the Pettemer field site.

3.2 Location

The Dutch coastline
The Holland coastline, a so-called closed part of the Dutch coastline, is a sandy coast with a morphology that is dominated by waves. The length of the coastal stretch is about 120 kilometres and the orientation of the slightly curved coastline is to the NNE-SSW. This coastline is part of the southern side of the North Sea basin. To the north the North Sea basin is wide open to the Atlantic Ocean while to the south a narrow strait connects it to the Atlantic Ocean, see Figure 3.1.

For the monitoring of coastal development along the full length of the Dutch coast a line of beach poles with an alongshore spacing of 250m serves as reference. The beach poles are numbered according to their distance from Den Helder southwards. In Dutch the series of beach poles is referred to as ‘Rijks Strand Palen lijn’ abbreviated as 'RSP Reference Line'.

The Pettemer site
The 1.5 km long Pettemer sea defence forms the northern part of the 5.5 km long sea defence. The southern part, the Hondsbossche sea defence, stretches from RSP 22 in the north to RSP 26 in the south over a distance of 4.0 km. The Pettemer sea defence lies between the RSP 20.5 and the 22. Dunes enclose the fixed defensive structure on both sides and in front the nearshore area has been protected against longshore erosion by groynes. The groynes in front of the Pettemer sea defence have an alongshore spacing of about 120m and stretch 80m into the sea.

The survey campaign at the Pettemer site started during the fall of 1995. Instruments are situated along the cross-shore 20.830 perpendicular to the coastline at cross-section 20.83. This cross-shore passes through the middle of a groyne section, shown in Figure 3.2c.

Figure 3.2a: The surveyed groyne section, photographed from the dike along the cross-section 20.830

Figure 3.2b: The Pettemer sea defence (right upper corner).

Figure 3.2c: Overview of the Pettemer sea defence with the orientation of the cross-section 20.830 (left lower corner).

The Pettemer sea defence

Human intervention in the development of the Dutch coastline dates almost back to the Middle Ages. In the 16th century the first sea defence was built near Petten. Before 1823 the sea defence was relocated several times because of ongoing erosion, caused by the 'sand hunger' of the Wadden Sea. Erosion still continues north and south of the Hondsbossche sea defence and nowadays the defensive structure protrudes into the sea [WIJNBERG, 1995]. In Appendix 1 the location of the Hondsbossche and Pettemer sea defence is compared to the location of the Dutch coastal line.

The latest improvement of the Pettemer sea defence took place in 1994 when the sea defence was raised to NAP +12.95m. In Figure 3.3 the profiles measured before and after the improvement are shown. From the backside (land side) to the top, the sea defence is covered with grass and a clay layer of 0.8m. On the seaward side, the sea defence has different slopes and types of protection. The upper part has a slope of 1:3 and is protected with basalt, just as the lower 1:4 slope. Between both slopes, at a height of NAP +5m (design water level height) a more or less horizontal section (berm) is protected with asphalt. The asphalt part can also be used as a road.

As can be seen in Figure 3.3, below NAP the level of both profiles differs significantly. The presence of sand results in a significant variation of the local profile height from the RSP line seaward. The toe itself is fixed with basalt blocks and asphalt. The base just in front of the toe is protected against scour by pouring asphalt. However, the exact region that is protected against scour is undefined. According to the surveys, the area from RSP –10m varies in height and is therefore probably unprotected.

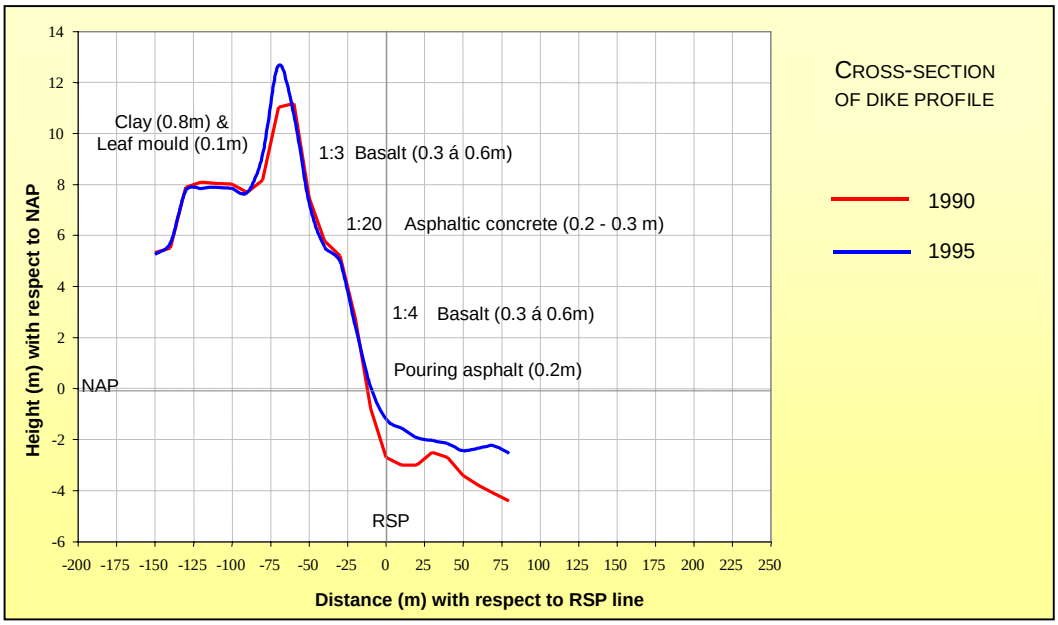

Figure 3.3: The profile including the types of protection of the Pettemer sea defence before and after improvement.

3.3 Seabed *geometry*

Bathymetry
Although the coastline along the fixed sea defence is virtually straight, the bottom bathymetry shows a more complex geometry according to Figure 3.4. This complexity has two causes: firstly the fixed 'Pettemer polder' bank; a shallow zone with a minimum depth of NAP -6m, that is located at 2 to 3 kilometres northwest of Petten. The Pettemer polder bank interrupts the depth contours of the surroundings. Secondly, a system of dynamic banks that are affected by the hydrodynamic conditions causes a rapidly changing bottom geometry near the coast.

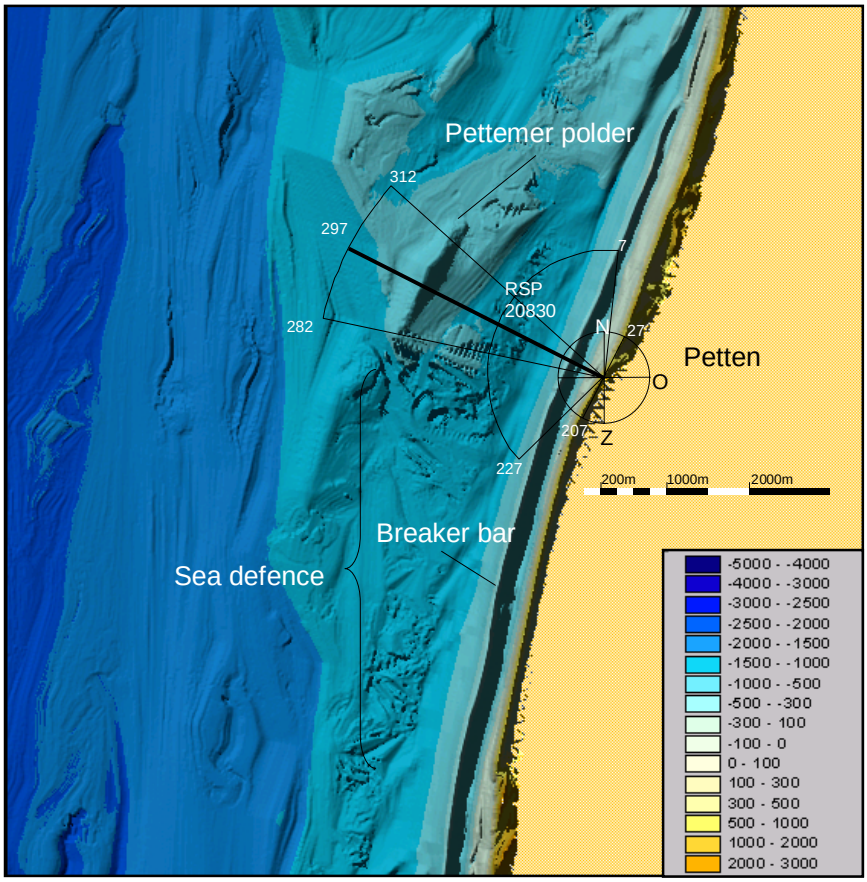

Figure 3.4: Seabed profile at Petten, [GIS map based on sounding data from 'Rijkswaterstaat' edition 1988], depth in decimeters. The orientation of the coastline as well as the orientation

The bottom geometry is represented by the cross-section at RSP line 20.830 shown in Figure 3.4. The representation of the seabed by this line 20.830 is reasonably valid between the 282º and 312º because this section includes the 'Pettemer polder' bank. Between a range of 227º to 7º waves are expected to attack the shoreline, waves that approach the shoreline under an angle of 20º or less (orientation between 207º and 227º or 7º and 27º) are blocked or significantly affected by the groynes.

A morphological process that influences the overall bottom profile in the long-term, is the sand attraction of the Wadden Sea. The accumulation of sand in the Wadden Sea is caused by the rise in sea level. The landward moving shoreline is the result of this process [ALLERSMA, 1988]. In this thesis short-term erosion processes are of most interest, and therefore the sand shortage of the Wadden Sea will not be taken into account.

Sediment
Most of the sediment along the coast of Holland is fine to medium range sand. At Petten the grain size lies within the 250-500μm class [STOLK, 1989]. The sand contains small amounts of clay and silt.

Description

To describe the seabed geometry at Petten, only the cross-section at RSP 20.830 has been used. The complexity of the Pettemer bed geometry is hereby reduced to a 2D instead of a 3D bed. This implies that the seabed variations in longshore direction are not covered. It is expected that cross-shore transport processes cause the short-term erosion under examination. If this is the case, a 2D approach should be sufficient to study the short-term erosion. Figure 3.5 shows the outline of the 2D profile at Petten, divided into three characteristic sections:

- The terrestrial zone.
- The bar and trough.
- The 'Pettemer polder' bank.

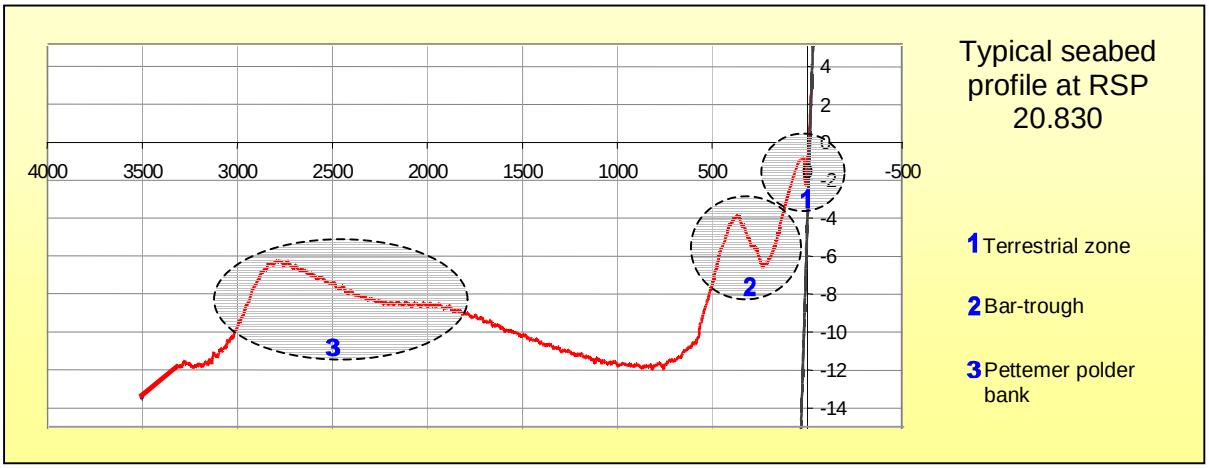

Figure 3.5: General 2D seabed profile in cross-section 20.830.

Terrestrial zone

This is the shallow zone between the groynes from the waterline to a depth of about NAP -2m. The bed geometry adjusts rapidly to the prevailing wave direction. Sometimes channels are formed during a period that is dominated by north or southwest winds. The process is shown in Figure 3.6.

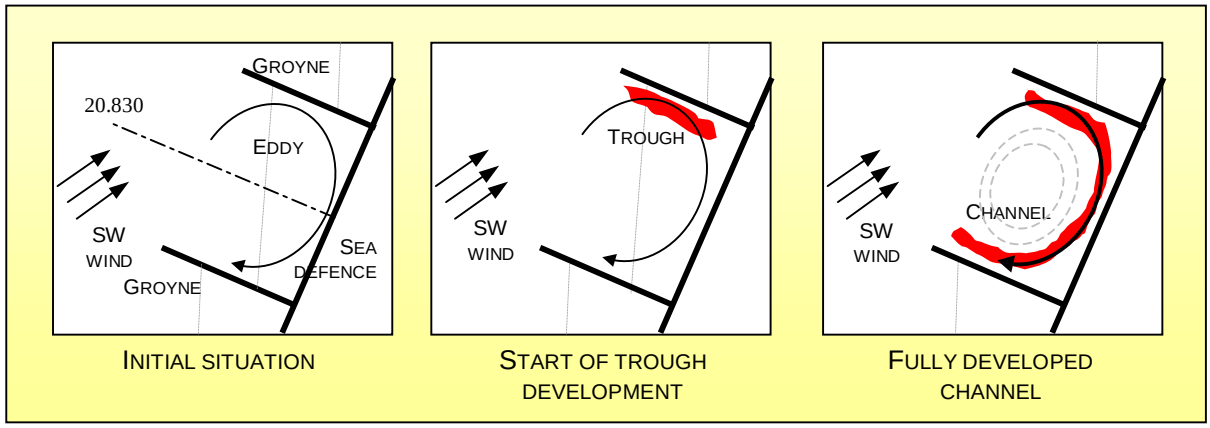

Figure 3.6: The process of channel development in a groyne section.

An eddy develops and a channel starts along the side of the groynes and grows in the direction of the shoreline, where the channels curve away along the shoreline. After a sufficient period an island develops during ebb tide in the middle of a groyne section. Consequently, the cross-section 20.830 shows a trough directly in front of the sea defence with steep slopes between 1:10 and 1:20. In Appendix 3 Figure A3.4 several surveyed cross-section of the seabed between the groynes are shown, including this so-called trough.

Furthermore, waves are reflected by the structure and possibly oscillate between the groynes. The bottom protection that consists of basalt rocks further increases the complex morphological predictions in this shallow water zone. Together, all these non-linear processes create a situation that cannot be simulated accurately, especially not on a short time scale.

Bar and trough

A trough is situated within the profile at cross-section 20.830 between the terrestrial zone and the bank with maximum depth of about NAP -8m. The bar is situated 350 to 450m offshore with a minimum depth of NAP -4m. According to the JARKUS profiles that will be discussed in Paragraph 3.6 the bar shows little variation in horizontal direction. The bar that ends a few hundred meters to the north of the Pettemer sea defence seems to be fixed. However, its southern part in front of the Hondsbossche sea defence slowly migrates in offshore direction.

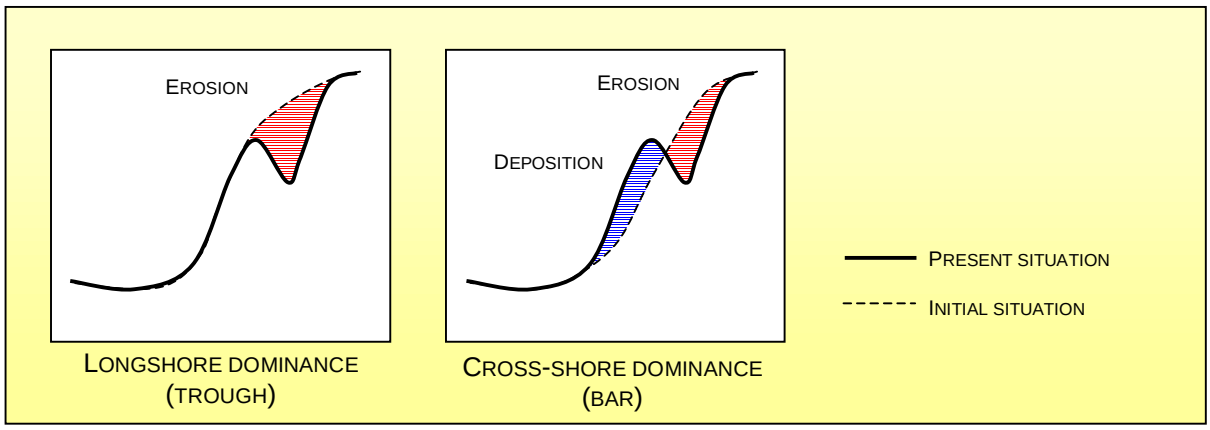

Figure 3.7: The differences in a longshore or cross-shore developed coast.

There are two possible explanations for the steady behaviour of the bar-trough-system in front of the Pettemer sea defence:

- Due to the constriction of the tidal current by the combination of the Pettemer polder and the protruding sea defence, an erosion channel has developed in the nearshore bed (left in Figure 3.7). Sand has been transported in a longshore direction.
- Due the relocation of sand by waves in the cross-shore profile, a bar-trough-system has been established (right in Figure 3.7). Sand has been relocated in a cross-shore direction.

Along the Dutch coast the waves dominate the sediment transport processes in the nearshore area. However, due to the constriction of the longshore directed tidal current at Petten the impact of longshore currents on the sediment transport processes has increased. According to the analysis of Allersma [ALLERSMA, 1988] this increased tidal dominance could be the main reason for the steady behaviour of the bar-trough-system.

Pettemer polder bank

The ‘Pettemer polder’ bank is another fixed bank, located at about 2800 meter offshore from the Pettemer sea defence, with a minimum depth of NAP -6m. Although the soundings show that the crest varies in height, the fact that the offshore bank has been given a name indicates its fixed position. During the last couple of years the variation in height has been in the order of magnitude of one meter. The precise location of the boundary between the fixed layer and the sandy layer is undetermined. It is important to note that the ‘Pettemer polder' bank has a local peak that crosses the cross-section 20.830 at about 2800m seaward of the sea defence. The use of the available cross-sections at RSP 20.830 could result in less wave penetration and an under-estimation of the local wave height conditions.

3.4 Coastal processes

The nearshore zone is characterised by a wide variety of interacting coastal processes. The middle and lower shoreface (depths that exceed 15m) are typically dominated by tide and wind induced currents, with the waves acting as a stirring mechanism, for example in turbulence and orbital motion. The net transport rates are mainly the result of the mean and residual currents. Close to the surf zone (the zone where wave breaking takes place), wave driven and current driven processes become equally important (between the 10m and the 7m depth contours). In and beyond the surf zone wave induced currents and other wave related processes like shoaling, breaking and dissipation become dominant. [ALLERSMA, 1989]

During fair conditions, low non-breaking waves and swell cause onshore directed sediment transport processes related to wave-asymmetry and wave-induced streaming that result in an accretion process. During storm conditions, high-energy waves heavily attack the coast, usually resulting in an erosion process. The sediment is carried in an offshore direction by undertow driven currents. Furthermore, longshore currents that feed the cross-shore directed rip currents can increase this offshore-directed transport process. These processes proceed relatively fast, according to the considerable short-term variations that have been surveyed in the nearshore area and at breaker bars. [RIJN VAN, 1998]

The explanation for morphological changes is found in the existence of gradients in the sediment transport, that are due to either a convergence or to a divergence of sediment transport rates; the nearshore zone results in either accretion or erosion. Thus, hydrodynamic conditions and morphological response are indisputably coupled. The morphological response depends heavily on the energy level of incoming waves and currents and the initial bed geometry at the start of the process.

3.5 Hydrodynamic conditions

Wind

The Dutch wind climate is largely determined by W-E tracking. Seasonal variations in atmospheric behaviour cause variations in wind speed. Most storms occur during the winter months, November to January, between April and August the weather is fair, the periods in between (Feb-Mar and Sep-Oct) are transitional periods. When the wind force exceeds Beaufort 8 for an averaged period of 10 minutes, it is called a storm. The duration is also of interest for this study, because waves have to adapt to the prevailing wind conditions. In Appendix 2, the results of the storm analysis are shown. [WIJNBERG, 1995]

The reports [AUGUSTIJN ET AL., 1990] and [AUGUSTIJN AND ZWART, 1997] provides a 32-year data set of storm occurrences along the Dutch coast. The annual number of storms in this data set varies between 13 and 48 with an average of 35 storms per year. During summer the number of storms varies between the 0 and 10 and during winter between the 10 and 43. The duration differs per storm and per season. During summer the average is about 5 hours as compared with 15 hours for winter conditions. The maximum duration observed is 50 hours for summer conditions as compared with 96 hours for winter conditions.

Waves
The wave climate is controlled by the wind climate and the geometry of the North Sea basin. The yearly mean wave height (H_{m0}) is 1.2m, the corresponding wave period (T_{m01}) is about 5s [ROSKAM, 1988]. Waves mainly approach the coastline from a southwest and north-northwest direction. It seems that the average wave height is correlated to the wave direction:
$H_s < 1.0$m often approach from the northwest direction (315°),
$1.5 < H_s < 3.5$m often approach from the southwest direction (225°) and
$H_s > 4.5$m often approach from the northwest direction (315°).

Tide
The tide along the Dutch coastline is asymmetric and semi-diurnal. The mean tidal range decreases from south to north; near IJmuiden it is about 1.65m, near Petten 1.55m and near Den Helder 1.37m [ALLERSMA, 1988]. The tidal range at Petten varies between the 1.75m and the 1.25m for spring and neap tide.

The peak tidal current velocities do not exceed 1m/s. During HW the tidal current flows in northward direction while during LW the tidal current flows southward. The result is a net flow in deep-water in the order of magnitude of 0.05 m/s in northward direction. Where the water is shallow the tidal flow decreases in velocity.

3.6 Seabed measurements

At Petten several seabed profiles are measured in time. Besides the available JARKUS profiles, treated in Appendix 5, additional surveys are executed; soundings and terrestrial zone surveys. The additional measured seabed profiles are based on soundings and surveys executed with rods in the shallow water zone. Both methods will be further explained in Appendices 3 and 4. The accuracy and the usefulness of these three methods of measuring the available cross-shore profiles, are discussed below.

JARKUS
Since 1964 profiles from the annually surveyed JARKUS data set are available. These JARKUS profiles are surveyed perpendicular to the coastline along the Holland coast at fixed locations about 250m apart. The distance along the cross-sections varies between 750 and 1200. The JARKUS profiles make use of the RSP reference line. For the cross-section 20.830 at Petten the base point is situated just in front of the sea defence. This location will be referred to as the toe of the sea defence during this thesis (shown in Figure 3.3).

The profiles are usually surveyed between early April and late September. This implies that the time interval between two successive profiles varies between 0.5 to 1.5 year. Further it implies that the profiles have a seasonal bias. Little is know about the seasonal changes along the Dutch coast. Generally the weather is less stormy in spring and summer compared to autumn and winter [WIJNBERG, 1995]. Nevertheless, hardly any seasonal variation was observed for the mean profile near Egmond over a period of 17 years [KROON, 1994].

The sounding accuracy of depth values is about 5cm to15cm. The accuracy decreases to about 15cm to 25cm when ship dependent errors are included. To compare depth differences within one profile an accuracy of 10cm is applied, whereas for a comparison of two different profiles an accuracy of 20cm is recommended. [WIJNBERG, 1995; TÖNIS AND VEEN, 2001]

Terrestrial surveys
Since the fall of 1997 surveys are executed for the terrestrial zone at the cross-section 20.830 near the Pettemer sea defence. In the fall of 1998 the survey frequency has been increased to 5 times a year. 7 cross-sections are surveyed with a rod in one groyne section at a distance of 15m apart. The length of the profile is dependent on the water depth. The maximum water depth that can be surveyed is about NAP -2m.

The accuracy of surveys is difficult to determine, because they are executed on foot. As can be seen in Figure A3.2 in Appendix 3, the actual survey line often deviates from the cross-section. Therefore the error depends on the accuracy of the survey method as well as on the quality of the work of the surveyor together with the variation in bottom level. An accuracy of 20cm is recommended. [TÖNIS AND VEEN, 2001]

Soundings
Since March 1999 soundings of the same cross-sections as the terrestrial survey are available. However, the soundings are not carried out at the same day. The sounding surveys start at about 80m and go up to a distance of 3500m from the sea defence along the cross-section. The accuracy of the soundings is more reliable than that of the terrestrial surveys. The applied sounding accuracy is 15cm. Several measured profiles are discussed in Appendix 4.

3.7 Hydrodynamic measurements

The Pettemer site
Besides survey profiles, hydraulic data is required. In the cross-section no. 20.830 at the Pettemer site several measuring points are available. Previously the hydrodynamic data was only measured for a period of 24 hours during storm conditions, but since the fall of 1999 hydrodynamic data is collected continuously. In the Figure 3.8 the different measure locations are shown. Tide, local wave height, period and direction, wind speed and wind direction are all measured at several locations with different instruments.

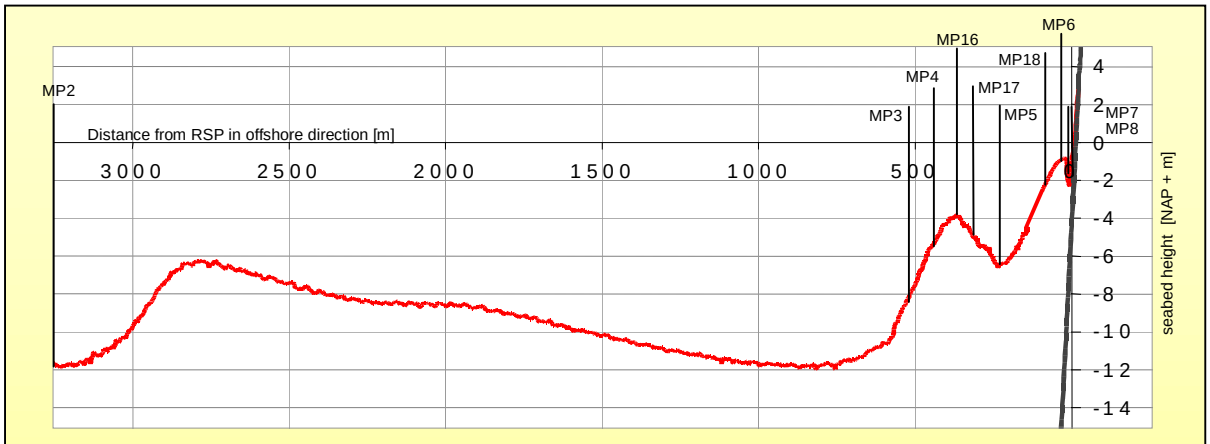

Description	Location	Type of equipment
MP1	7909m	Wave rider (not shown)
MP2	3434m	Wave rider
MP3	547m	Wave level meter
MP4	464m	Wave rider
MP5	239m	Wave rider, wave direction
MP6	60m	Rader-level meter, pressure sensor, wind vane and anemometer
MP7	12m	Pressure sensor
MP8	-7m	Pressure sensor
MP16	376m	Pressure sensor
MP17	329m	Pressure sensor, velocity meter
MP18	111m	Pressure sensor

Figure 3.8: Location and type of survey equipment.

4. Data analysis

4.1 General

A data analysis has been executed to obtain a better perception of the seabed developments in time during storms as well as during normal conditions. However, the developments during storm conditions are of special interest. It is important to establish a better understanding of local seabed variation as well as the dominant variables and processes, especially in the nearshore area during a single storm. The bed level of the nearshore area determines the maximum wave height that penetrates up to the sea dike toe and beyond.

The most obvious method to get a better understanding of the effects of storms on the bed level is by surveying the seabed several times during a large number of storms. The variation of the seabed level during a single storm can than be derived. However, up to now, this has never been done along the Dutch coastline, because the measuring equipment and instruments during severe storm conditions were unavailable.

Another option is to survey the seabed just before and directly after a period of storm. An approximation of the net effect on the bed profile of a single storm would then be obtained, though nothing could be said about the actual physical processes that dominate erosion during storms. However, it would give a first impression of the amount and location of the erosion. Unfortunately this information is unavailable as well.

Therefore this chapter deals with two methods that are used to increase our understanding of the seabed variation as well as storm erosion, based on available data. Both executed data analyses are extensively elaborated in several appendices. The results of both analyses will be discussed:

1. The comparison of profile volumes and the effect of storm intensity.
2. A hindcast analysis based on a constant breaker index.

The first analysis compares the geometry and volume of annually measured profiles. In particular, the developments of consecutive profiles showing a significant decrease in volume are examined. The variations in profile volume and height are compared with the intensity of the weather during the period between the consecutive surveys. It is assumed that the weather intensity is, most of all, determined by the hours of storm. During this analysis the annually surveyed JARKUS cross-sections are used for cross-section 20.830. It is expected that the results will increase our understanding of the effects of stormy conditions on the long term as well as the seabed variation in general.

A perception of the degree of erosion caused by one single storm is achieved by using a hindcast analysis based on a constant breaker index. It is expected that the wave heights measured 60m in front of the Pettemer sea defence contain a significant share of breaking waves. Knowing that the local water depth limits the maximum wave height of breaking waves, it is expected that the measured wave height accompanied by the water level can result in some information about the development of the local seabed level during the period of a single storm. This method is easy to apply, but the results are difficult to interpret, because a constant breaker index is hardly ever seen in reality.

The results of both analyses are examined and the complications discussed. After these analyses the variables that affect the short-term erosion process during storm are dealt with, including their correlation. The chapter finishes with the conclusions that follow from the executed analyses.

4.2 Erosion due to storm

A frequently used method to determine the amount of erosion caused by storms is to compare profile volumes, or as in case of this thesis, the amount of sand in a defined 2D area. Data presented in the Appendices 2, 3, 4 and 5 are used as sources of information throughout this analysis.

Boundaries settings
Assuming that only cross-shore transport conditions are operative, the choice of the locations of the offshore and shoreward boundaries affects the result. Whenever the offshore boundary has been chosen in deep-water and the shoreward boundary has been chosen on the dike the difference in volume between two consecutive volumes reduces to nil. Therefore the analysis results depend greatly on the boundaries chosen.

During this analysis it is assumed that the annual variation in the profiles is the result of net cross-shore transport. The existing longshore currents are significantly greater than the cross-shore currents, while their effects are negligible. Although the assumption is supported by literature, it should be used with caution. [VAN RIJN, 2000]

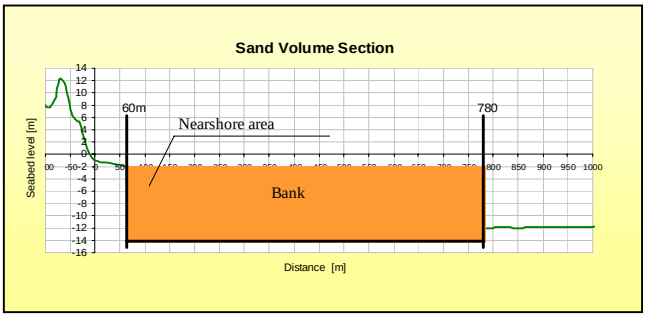

Figure 4.1: Averaged seabed profile including the compared region and the boundaries for the outer profile.

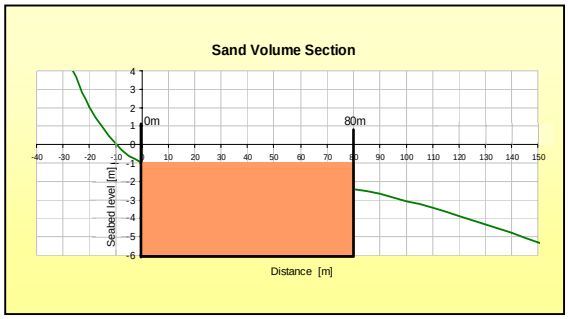

Figure 4.2: Boundaries for the nearshore area between the groynes used in the volume comparison.

Two areas are examined based on data from the JARKUS data set:

1. The outer profile; a section from 60 to 780m.
2. The nearshore area between the groynes from 0 to 80m.

The seabed level in the latter section (0 to 80m) is the most important, because of the dominant effect on the local wave height. The JARKUS data set used for the analysis of the nearshore area contains many gaps that have to be guessed at. This data manipulation significantly decreases the accuracy of the analysis. At the end of Appendix 5 the manipulation table A5.16 has been shown. The boundaries of the outer profile section are chosen in such a manner that all profiles available have been taken into account during the analysis without manipulation necessary.

The examination of both sections consists of a comparison of the annual sand volume (m^3/m), followed by an analysis of the effect of annual storm intensity on the variation in sand volume. According to the storm data set described in Appendix 2 [AUGUSTIJN ET AL., 1990, AGUSTIJN AND ZWART, 1997], all storms that exceed Beaufort 8 are taken into account.

4.2.1 Volume comparison

According to the available JARKUS data, an area with a length of 720m between the 60m and the 780m to RSP includes all profiles; the third boundary is the NAP -14m line, that encloses all profiles as is shown in Figure 4.1. Most attention is given to the area between the most shoreward boundary and the dike. (Figure 4.2)

The results of the volume comparison (Figure 4.3) show a more or less constant course up to 1989, the average amount of sand varies between the 4800 m^3/m and 5200 m^3/m. In 1990 it suddenly collapses to a minimum of 4350 m^3/m and thereafter, within a decade, climbs back to 5000 m^3/m. The fact that the volume of sand decreases to a minimum in the year 1990 could be caused by stormy weather conditions. Compared with the previous year (1989), an averaged decrease in the seabed level of about 0.6m over the entire length (720m) has been found (Figure 4.4).

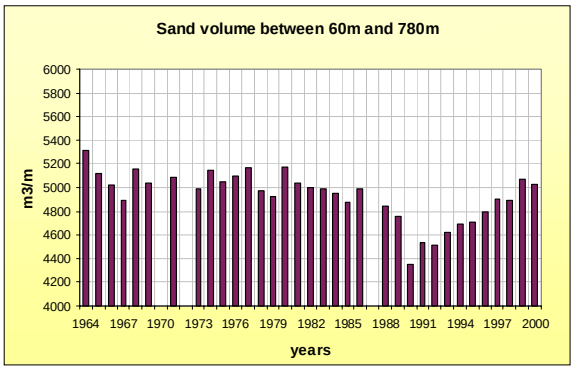

Figure 4.3: Annual sand volume (m^3/m).

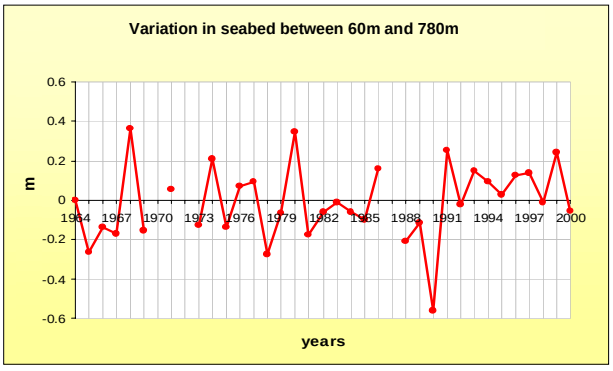

Figure 4.4: Difference in averaged seabed level variation (m) between two consecutive profiles.

For the area between the groynes (0 to 80m) the gaps in the data set are filled by data determined at the previous surveyed point. The profile of the gap is assumed to be horizontal from the previous surveyed point to the 0m point. In Appendix 5 Table A5.16, the profile manipulations are shown. To compare the different profiles with each other, the average level of the area between the groynes is used. The level of this area varies a lot and has an average level at -1.5m NAP. In general the variation patterns of the profile level between the groynes is similar to that of the profile outside the groynes. In 1990 the average bed level shows a decrease similar to that of the total profile (60 to 780m), Figure 4.5.

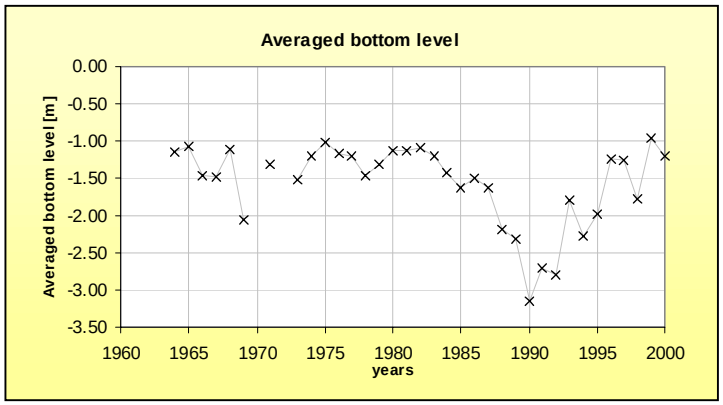

Figure 4.5: Variation in averaged seabed level of the area between the groynes (from 0 to 80m).

According to Appendix 2, the winter of 1989-1990 is marked by several storms. However, other years, like 1974 and 1983, show an even higher number of storm hours without a decrease of profile volume of the same magnitude.

The fact that the recovery of the profile after the year 1990 takes about a decade rules out a survey error. During the recovery period an averaged amount of sand (about 72 m3/m a year) settles on the profile. The outer slope of the sand bank recovers first, followed by the seaward slope of the nearshore area. This could be the result of sediment transport in shoreward direction. If that is the case, it is reasonable to assume that during storm conditions the sediment is transported in an offshore direction outside the chosen offshore boundary.

After further and more detailed analyses, it appears that most of the erosion took place on both seaward facing slopes; the nearshore area slope, and at the slope of the bar located about 400m from the sea dike toe. This could be explained by the fact that breaking occurs on both slopes and during wave breaking energy is dissipated by the bed. The outer slope of the bank shows similar regression to that which is found over the entire profile, while the decrease at the nearshore area slope exceeds the 1.0m over a distance of 160m, but the inner slope of the bank hardly erodes at all. According to the JARKUS data the breaker bar migrates in shoreward direction. In literature bars it had been found that bars tend to move in offshore direction during storm conditions [RIJN VAN, ET AL., 2002].

4.2.2 Profile changes versus storm hours

It is suspected that the reduction in volume of the profile surveyed in 1990 has been caused by storms. In order to determine whether storm induced processes contribute to variation of the bed, the storm data set of Augustijn and the JARKUS profile surveyed at the RSP number 20.830 at Petten are compared. The following comparisons are studied:

- Annual profile variation versus the number of storm hours.
- Annual profile variation versus the number of summer storm hours.
- Annual profile variation versus the number of winter storm hours.
- The effect of a high averaged bed profile of the previous year on the annual profile variation.
- The effect of the period between the survey date and the storm date.
- The effect of surveying in different months.

The results of these comparisons are shown in scatter plots that are dealt with in Appendix 6. These scatter plots show the bed variation between two consecutive years and the amount of storm hours for annual, winter and summer conditions. According to these scatter diagrams hardly any correlation between storm hours and profile changes has been found. Storms were expected to have but little effect on the seabed level variation for the area outside the groynes (from 60 to 780m), due to the precence of longshore currents. Furthermore the relatively large water depths decrease the influence of waves on the seabed as well.

For the nearshore area (from 0 to 80m) a correlation between storms and bed level variation was expected. Groynes protect this area from longshore currents and consequently the effect of cross-shore wave induced currents should be greater. The scatter plots show a pattern similar to that of the profile section situated outside the groyne section (60 to 780m). According to a linear trend line that is plotted in all scatter diagrams an increase in storm intensity of about 200 hours results in an average decrease of seabed level of about 0.25m. In Appendix 3 Figure A3.5 it appeared that the averaged bed level between the groynes varies between summer and winter. During winter the bed level is situated 0.50m lower, which has probably been caused be the increase of wave impact.

4.2.3 Evaluation

After analysing the annual variation of the profile at RSP 20.830 it can be concluded that variation in the surveyed bed profiles cannot be attributed to the presence of storms alone. The scatter plots for that part of the profile that is protected by groynes appear to show some correlation between the annual period of storm and the deepening of the bed. However, other aspects are also significant.

Complications of the method
First of all, the accuracy of the data is questionable, because the JARKUS profiles used are surveyed during summer instead of winter. The geometry of the profile has had some recovery time, because summer conditions are less severe than winter conditions. The averaged bed level for the nearshore area shows a significant difference in bed profile height between winter and summer survey profiles. The level of the averaged winter-surveyed profile lies about 0.5m lower compared to the average of summer-surveyed profiles. In Figure A3.5 in Appendix 3 shows the difference in the profile between the groynes.

Other factors that affect the accuracy negatively are the limited amount of measured profiles (only 35 profiles) in the data set and the fact that the period between two surveyed profiles varies between the 0.5 and the 1.5 years.

Hydrodynamic data instead of astronomical data
During the analysis the effect of annual storm hours has been examined as well as the duration of wind speed for individual storms. However, the effects of water level, wind direction and actual wave height, period and direction have not been taken into account. The analysis could have been more useful if wave data had been used, however wind and wave data are closely related.

Storm direction and North Sea geometry
Individual storms differ greatly and the development of a storm affects the resulting impact. The impact of a storm that, for instance, starts from the north and slowly turns to the northwest results in more setup due to the North Sea geometry. More setup allows higher waves to penetrate further shoreward. The impact of such a storm is expected to be significantly greater than a storm that comes solely from the north or northwest, with less accompanying setup.

Storm surges
The impact of a storm surge depends on a storm and a spring tide coinciding. Another important factor that influences the storm impact is the number of storms over a specified period. Studies that examined the cause of dune regression found that wind speed and water level are mainly responsible for dune regression. The water level allows the waves to reach the dunes, while high wind speed generates wave growth.

However, in case of a submerged seabed, as is the case with the terrestrial zone in front of the Pettemer sea defence, water level contributes solely to the penetration of larger waves. However, high water levels also reduce the load of a wave on the bed, because the distance between wave and bed has increased. Consequently, the importance of the water level reduces compared to the considerable impact storm surges have on the erosion of dunes.

The 1990 seabed profile

The question whether a storm has caused the decrease in volume of the 1990-profile remains unanswered. The surveyed data appear to be justified because of the slowly increasing bed level over the years. A survey error can therefore be ruled out. If the regression has been caused by storms it has to be a special event because more severe storm periods result in less regression.

An explanation for the fact that the process responsible for the erosion in 1990 is still storm driven can be found in the distribution of storm hours over the wind direction. According to Appendix 2 the storms between 1989 and 1990 are mainly southwest orientated. The wind direction could also have a significant affect on the storm impact, especially whenever it coincides with the direction of the tidal current. Contrary to the conditions of 1990 storms are normally reasonably well divided over the direction per year.

Another explanation for the regression of the 1990-profile could be a difference in the general weather conditions rather than the result of a storm or multiple storms. It is recommended that the cause of the sudden regression of the 1990-profile be further investigated to increase the understanding of sediment transport processes.

Nourishments

Nearby located nourishments could also affect the variation in bed level. In table 4.6 the location, date and quantities of the nourishments are shown. The exact effect of the nourishments is difficult to determine, because the impact is largely determined by wind-produced currents, the quantity and the location of the nourishment. Qualitatively the southern nourishments have more effect on the bed variations, because of net northward-directed transport. After 1990 the intensity and quantity of the nourishments has increased and the 'profile recovery' could also be partly caused by these nourishments.

Table 4.6: Selection of the nourishment database [WWW.MARIS.NL/KIK/SUPPLETIE, JULY 2002].

Start date	Finish date	Location	Start point	End point	m^3/m	Type of nourishment	Nourishment volume [m^3] south side	Nourishment volume [m^3] north side
041987	121987	Zwanenwater	14.70	17.84	54	Dune reinforcement		169.560
051990	061990	***Bergen aan Zee***	32.25	33.75	257	Beach Nourishment	385.500	
051990	061990	Bergen aan Zee	32.25	33.75	40	Other	60.000	
091991	101991	*Petten*	18.00	20.18	170	Beach Nourishment		370.600
051992	111992	Egmond-Camperduin	26.20	38.50	120	Beach Nourishment		1476000
061994	061994	Bergen aan Zee	32.90	33.50	168	Beach Nourishment	100.800	
051995	051995	Bergen aan Zee	32.62	33.62	306	Beach Nourishment	306.000	
091995	101995	Zwanenwater	16.24	17.60	226	Beach Nourishment		307.360
091995	101995	**Petten**	18.80	20.40	226	Beach Nourishment		361.600
061997	061997	*Schoorl*	26.00	30.05	346	Beach Nourishment	1.401.300	
061997	061997	Bergen aan Zee	30.05	31.05	133	Other	133.000	
041999	051999	Bergen aan Zee	32.50	33.75	165	Beach Nourishment	206.250	
012000	122000	Zwanenwater	16.26	16.88	194	Beach Nourishment		120.280
012000	122000	Bergen aan Zee	32.75	33.25	400	Beach Nourishment	200.000	
012000	122000	Bergen aan Zee	32.00	34.00	500	Submerged nourishment	1.000.000	

Little can be said about the actual contribution of one single storm to the profile geometry and the actual volume of sediment that is transported. Therefore the following analysis attempts to look on a smaller time scale.

4.3 Breaker index analysis

4.3.1 Method

Understanding of the seabed variation and in particular understanding of erosion during storms is desirable. However, precise bed profile data during storms are unavailable. Locally surveyed hydrodynamic conditions during storm are available at several nearshore locations at Petten. At these locations the wave height and water level is surveyed continuously during storm conditions. In the literature maximum wave heights during breaking conditions depend on the water depth. The ratio is called relative wave height or breaker index (γ). With the aid of a hindcast analysis the bed profile variation during storm can be simulated with hydrodynamic data alone and an assumed breaker index.

It is expected that during a storm at the nearshore erosion takes place, leading to a situation that allows higher waves on that location. Battjes and Janssen empirically found a more or less constant relation between wave height and water depth during wave breaking:

$$\gamma = \frac{H}{h} \qquad 0.5 \le \gamma \le 0.6 \tag{4.1}$$

The maximum wave height water depth ratio, or breaker index (γ) describes the limitation of the maximum wave height (H) on a specific water depth (h). The water depth is defined as the difference between the bed level and the water level surface, in other words water depths that include tide and wind setup. The bed level is hereby determined by the local hydrodynamic conditions. This results in the following equation:

$$h_{seabed} = -\frac{H_s}{\gamma_s} + h_{tide+setup} \tag{4.2}$$

This means that the possible sea-bottom level (h_{seabed}) with respect to NAP equals the local significant wave height (H_s) divided by the significant breaker index (γ_s) and added to the water surface including tide and setup ($h_{tide\ +setup}$).

The breaker index equation only calculates the seabed level during breaking conditions. If the hydrodynamic data set contains wave heights of non-breaking waves an incorrect seabed level will be calculated.

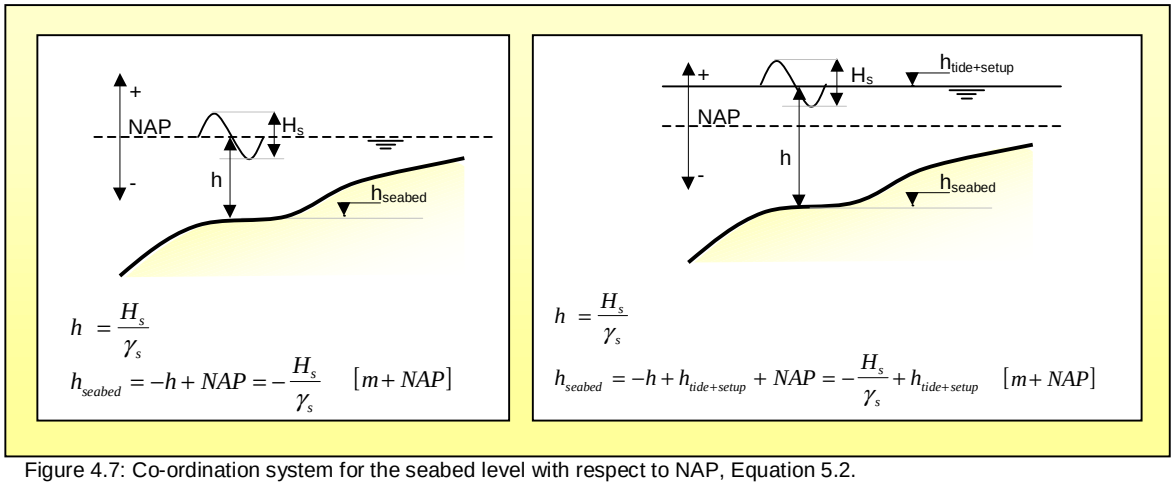

Figure 4.7: Co-ordination system for the seabed level with respect to NAP, Equation 5.2.

Trends
It is impossible to check whether the actual seabed corresponds with the calculated bed level described in Figure 4.7. The possibility exists that the actual seabed level lies even below the predicted bed level. Higher seabed levels are less likely because the surveyed waves could not exist. The prediction could only lead to a higher bed level if the breaker index has been under-estimated. The trend, found in the predicted bed level, describes the bed level variation or local erosion due to waves.

The breaker index affects the erosion depth negatively. Whenever the breaker index is increased the predicted bed level height increases too; higher waves are possible in more shallow water (green line in Figure 4.8). The amount of erosion that follows from the trend is also affected by the chosen constant of the breaker index. For instance, if the breaker index is 1, the difference in wave heights and tide are equally important. If the breaker index is reduced, for instance 0,5 the wave height variation is twice as important as the tidal variation.

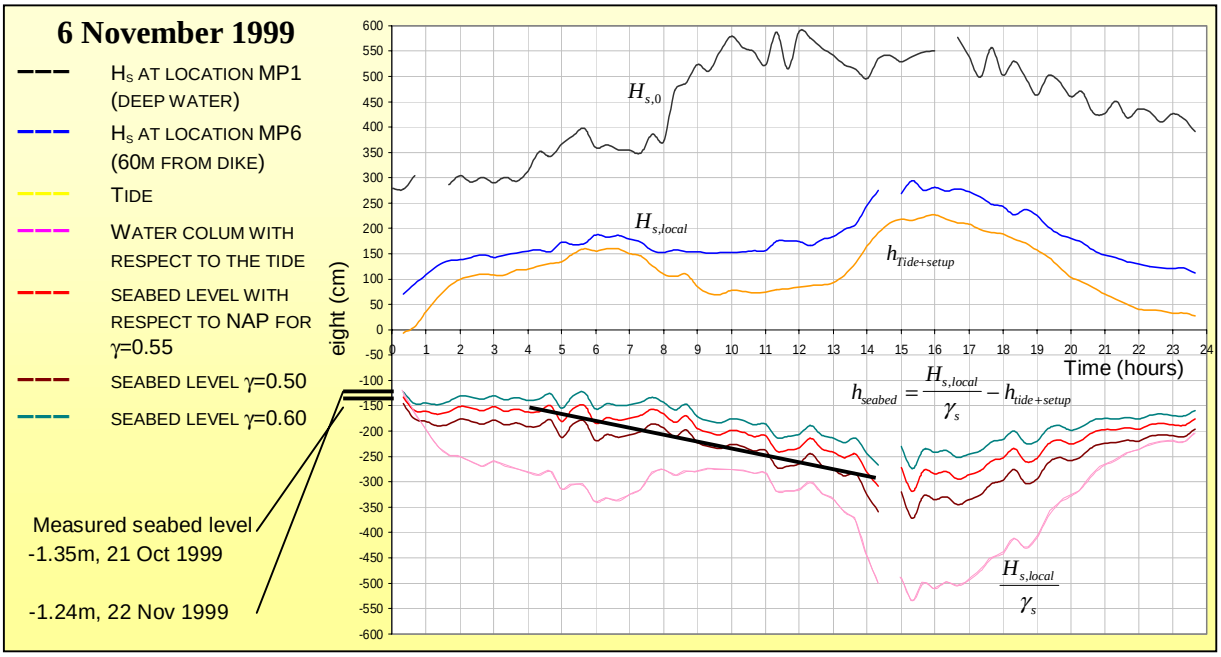

Figure 4.8: Result of the breaker index analysis of the storm of 6 November 1999.

4.3.2 Validation

The Battjes-Janssen equation can only be applied during wave breaking. In Appendix 7 a sequence of wave data is shown over a period of about two months. According to this sequence the wave height (H_{rms}) at measuring point 6 (MP6) in shallow waters appears to follow the tidal motion if the deep-water wave height (MP1) exceeds the 2m. Consequently, during storms conditions with waves heights that exceed the 3m, the water depth limits the significant wave height measured at MP6 at a distance of 60m from the RSP line of reference. The breaker index equation should be 'valid' during these conditions.

The measured significant wave height is averaged over a period of 10 minutes and includes all waves that pass during that 10 minutes. During the 10-minutes-period, breaking waves that already reached a maximum wave height, as well as non-breaking waves that are not yet limited by the water depth occur. This means that if Figure 4.8 shows an upward trend in the maximum seabed profile, it does not mean that the actual bed level increases and sedimentation takes place. It is the result of a decrease in wave height. Lower wave heights or a bigger share of non-breaking waves also result in an increase of the calculated bed level height.

The value of the constant breaker index has a significant effect on the calculated bed decrease. Different values of the breaker index are used in the literature and in practice. The value of the breaker index that should be valid at Petten according to the equations of Battjes [1978] and Battjes-Stive [1985] lies in the magnitude of 0.7 to 0.9 for maximum wave heights. The breaker index for significant wave heights (H_s) varies in theory between the 0.5 and 0.6 for mild bed slopes (<1:100). For steeper bed slopes (like Petten) limiting wave heights are strongly influenced by the relative wave steepness (s).

As well as the theoretical references, the breaker index is also measured at a site near Egmond, 20km south of Petten. According to these measurements, shown in Appendix 8 Figure A8.2, the breaker index depends on the wave steepness, just like in the empirically determined equation of Battjes-Stive [1985], and the average value varies between the 0.4 and 0.65, with a constant standard deviation of 0.075 for significant wave heights.

Although the measured breaker indices are not measured during storm conditions, they appear to be in agreement with the theory. During the hindcast analysis the breaker index is kept independent of the deep-water wave steepness. The wave steepness (s_{rms}) at Petten varies within a range from 1% to 3% that is similar to the measured wave steepness range at Egmond.

During the storm of 6 November 1999 the wave steepness (H_s/T_{m02}) varied between 0.021 and 0.028 with a mean value of 0.024. The measured wave steepness differs a factor (0.95 = 1.35/1.41) with the expression of the wave steepness (H_{rms}/T_p) used to determine the wave steepness at Egmond [DE RONDE, ET AL., 1995]. According to the Figure A8.3 in Appendix 8 a breaker index between the 0.55 and 0.65 is valid for Egmond. For the hindcast analysis a constant breaker index of 0.55 is used to calculate the bed level height.

Complications

Some complications arise when the results of this hindcast analysis are interpreted. First of all, the empirical Battjes-Janssen equation is not entirely valid because it has not been evaluated for coasts with sand bars and reasonable steep slopes (like the coast at Pettemer). Waves cannot react instantly to the changing water depth as they move shoreward. Some time is required before they actually break. Consequently, it is possible higher waves reach a lower water depth. The result is a higher value for the breaker index on relatively steep slopes

Secondly, the deep-water wave steepness ($s_{rms,0}$) affects the breaker index as can be seen in Figure A8.2. The deep-water wave steepness is defined as the significant wave height divided by the wavelength on deep water. Battjes and Stive [1985] improved the breaker index equation for the effect of wave steepness empirically. At a coast with sand bars, the local wave steepness appears to become important instead of normally used deep-water wave steepness. Waves with long wavelengths result in higher breaker indices. This effect is not taken into account during this hindcast analysis.

Recent research indicates that the tide also affects the breaker index value. The tidal effect has been studied at Egmond, about 20 kilometres south of Petten. According to [KLEINHOUT, 2000] the tide or water level height affects the breaker index height on a coast with sandy breaker bars. During low water conditions or neap tide more waves break on the furthest offshore located bar, resulting in a higher percentage of breaking waves, this results in a different wave height distribution. The percentage of broken wave affects the breaker index too.

4.3.3 Evaluation

The hindcast analysis has been completed for six storms; the input data is shown in Table 4.9. The corresponding graphs are shown in Appendix 8. The maximum deep-water wave height and the water level are shown to indicate the impact of a storm. All six storms came from the northwest. Only for these storm the hydrodynamic data was available for a period of 24 hours.

Table 4.9: Data used for the hindcast analysis.

Date hydrodynamic measurements	Max water level Tide + setup	Max deep-water wave height (H_S)	Date of previous Surveyed seabed level	Date of next Surveyed seabed level
1 January 1995	NAP + 2.35m	5.75m	JARKUS 1994	JARKUS 1995
2 January 1995	NAP + 2.30m	6.05m	JARKUS 1994	JARKUS 1995
10 January 1995	NAP + 1.65m	5.65m	JARKUS 1994	JARKUS 1995
29 October 1996	NAP + 2.15m	5.75m	JARKUS 1996	JARKUS 1997
5 February 1999	NAP + 2.40m	5.75m	2 December 1998	9 March 1999
6 November 1999	NAP + 2.25m	5.95m	21 October 1999	22 November 1999

Table 4.10: Results of the hindcast analysis.

Date storm	Max water level Tide + setup	Max deep-water wave height (H_S)	Previous seabed level	Next seabed level	Start seabed level*	End seabed level*	Erosion speed (m/hr)*
1 and 2 January 1995	NAP + 2.35m	6.05m	-2.60 NAP	-2.33 NAP	-2.00m NAP	-2.50m NAP	0.048
10 January 1995	NAP + 1.65m	5.65m	-2.60 NAP	-2.33 NAP	-2.35m NAP	-2.45m NAP	0.014
29 October 1996	NAP + 2.15m	5.75m	-1.48 NAP	-1.76 NAP	-1.70m NAP	-2.10m NAP	0.053
5 February 1999	NAP + 2.40m	5.75m	-1.68 NAP	-1.40 NAP	-2.20m NAP	-3.00m NAP	0.107
6 November 1999	NAP + 2.25m	5.95m	-1.35 NAP	-1.24 NAP	-1.70m NAP	-3.20m NAP	0.143

*For the results shown in Table 5.10 a breaker index of 0.55 is used.

In Table 4.10 the erosion depths for the storms of January 1st and 2nd are combined. During all three of the storms that occurred in 1995 little seabed variation has been predicted. This is probably due to the fact that the initial seabed level height was low (-2.60m below NAP). The 2-day storm of 1995 resulted in a predicted decrease of 0.50m in bed height, whereas the initial seabed level height lies in the same magnitude as the predicted bed level height after the storm. For the two storms that occurred in 1999 significant erosion has been predicted. This is mainly due to the fact that the initial bed level height is rather high. The erosion rate also differs for the bed level height as can be seen in Table 4.10.

A difficulty with this method is to determine when the erosion process starts. It is very difficult to tell from the available data if the surveyed waves are actually breaking. If the waves do not break then an incorrect and higher bed level has been used for the erosion predictions, resulting in an over-estimation of the erosion depth.

This method can only be used as an indication for the amount of erosion of the nearshore area during storm. The accuracy of the results cannot be tested. However, a first impression of the amount and rate is obtained.

Erosion is only calculated for one single point (MP6) on the cross-section (60m from the sea defence toe). The erosion rate and depth are not only dependent on the initial bed level height, but they also depend on the levels of the surrounding seabed. If the location of MP6 lies protected, the approaching waves are lower. If the location lies on a steep slope, a significantly larger deepening of the seabed can be expected, as well as higher waves. Furthermore wave reflection could seriously influence the results. Large long periodic waves result in more reflection that could result in higher allowable local wave heights without a required seabed decrease. These factors probably have a significant effect on the result of the calculations. More research is needed in order to improve understanding of erosion due to storms and to determine if the assumption of a constant breaker index can be justified.

4.4 Conclusions

Although little can be said about the exact quantities of erosion due to storm, the understanding has increased. It can be concluded that annual cumulative storm intensities have little effect on the volume variation of a single cross-section. Even the effect of storms on the cross-section between the groynes that is protected against longshore currents is small.

The surveyed seabed varies significantly in height, whether this is caused by storms or not. Therefore it can be doubted if the boundary conditions for sea defences stated by the National Institute of Coastal and Marine Management (RIKZ) are justified. This institute determined the boundary conditions that date back to 1995 on computations based on the most recent seabed profile available (the 1994-profile). However, if one looks at Figure 4.5 that shows the seabed variation of the cross-section 20.870 between the groynes, one can see this section significantly varies in bed level height. Therefore it is recommended to determine this parameter randomly taken into account the occurrence of bed level, instead of using the most recent available bed level.

In Chapter 6 the effects of the initial seabed level profile are shown on the crest height and probability of failure by a probabilistic analysis based on UNIBEST-TC simulations.

The hindcast method with a constant breaker index led to more understanding of the great variety of storm and also the great variety of storm effects on the seabed. In the worst case the erosion depth lies in the order of magnitude of 1.5m for the location 60m from the sea dike. Whereas the seabed that has been surveyed 2 weeks after the storm, Figure 4.8, shows that the bed level has increased several centimetres opposite to the predictions of the executed hindcast analysis.

This difference between the measurements and the predictions of the hindcast method, can be explained partly be rather fast seabed recovery after a storm. However wave reflection against the sea defence increases with the wave height. Therefore the reflection increases with storm and this could clarify the large erosion depth predicted by the hindcast method. However the exact effects of reflection are still uncertain and further research has to be carried out before it can be taken into account during the hindcast method. In the next chapter the erosion in the nearshore area is predicted with a model called UNIBEST-TC. Together with the results from the hindcast analysis and the survey data analysis an even better perception of the storm effects can be obtained.

5. UNIBEST-TC analysis

5.1 General

Another possibility to predict erosion and morphological changes due to storms is with a numerical model. A sediment transport computer model called UNIBEST-TC has been selected to predict the morphological changes in cross-shore profiles due to waves and currents.

Besides the fact that UNIBEST-TC is capable of predicting morphological changes, it can also show the effects of these seabed alterations on the local wave height. The local wave height is on its turn used to determine the sea defence crest height, by means of the failure mechanism 'wave run-up'. The sea defence height has been determined in the next chapter. Furthermore, the model can be used to examine the contribution of several parameters that are expected to determine the erosion quantity.

This chapter is structured as follows. In Paragraph 5.2 the model performance has been compared with other similar models. Next, Paragraph 5.3 treats the model characteristics along with the restrictions and assumptions. Paragraph 5.4 summarises the calibration results that are extensively explained in Appendix 11. After the calibration the contribution of several parameters on the nearshore erosion and local wave height has been discussed in Paragraph 5.5. This parameter analysis is supported by simulation results treated in Appendices 13 and 14. In Paragraph 5.6 the morphological effects on the local wave height growth have been treated in detail. Furthermore, the wave height predictions capabilities of UNIBEST-TC are compared with those of SWAN-1D in Paragraph 5.7. This has been done because the wave height prediction is of considerable importance during the probabilistic analysis treated in the next chapter. Finally this chapter is closed with a final evaluation, including a summary of conclusions and recommendations.

5.2 Model performance

For the computation of morphological changes due to cross-shore sediment transport several models are available:

- UNIBEST-TC (Delft Hydraulics, NL).
- DUROSTA (Alkyon, NL).
- COSMOR (HR Wallingford, UK).
- CROSMOR (University of Utrecht, NL).
- BEACH (University of Liverpool, UK).
- CIIRC (University of Caen, FR).

UNIBEST-TC has been used during this thesis. According to the first test reasonable amounts of erosion at the nearshore area were computed using default settings. These initial test results are described in Appendix 9. UNIBEST-TC (TC: Time-dependent Cross-shore) is a module of the program package UNIBEST-TC, which stands for UNIform BEach Sediment Transport. All modules of this package consider sediment transport along a sandy coast. During this thesis version 2.04 beta has been used. Furthermore, UNIBEST-TC is a process-based model, meaning that it is based on physical relations that are with calibrated constants. In Appendix 1 the basic sediment relations are discussed as well as the processes involved.

In the Coast-3D report [RIJN VAN ET AL., 2002] the performance during storm of all models except DUROSTA have been compared. The Egmond-site has a comparable shore accept for the absence of the sea defence. Some results of the models performance are shown in Figure 5.1. Before the UNIBEST-TC predictions can be compared with other model result the root-mean-square wave height has to be converted into a significant wave height. In the comparison shown in Figure 5.1 a ratio of 1.41 has been used.

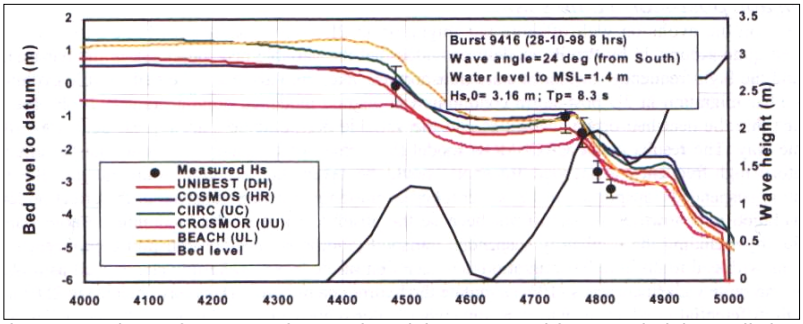

Figure 5.1: The performance of several models at Egmond for wave height predictions [RIJN VAN ET AL., 2002].

UNIBEST-TC over-predicts the measured wave height (H_s) in the surf zone slightly. However, the error will decrease if a value of 1.35 instead of 1.41 is applied for H_s/H_{rms} ratio. According to Egmond measurements the H_s/H_{rms} ratio in the surf zone is about 1.35 instead of the normal ratio of 1.41. Nevertheless the UNIBEST-TC output lies within the 0.5m error range, which is classified as 'good'.

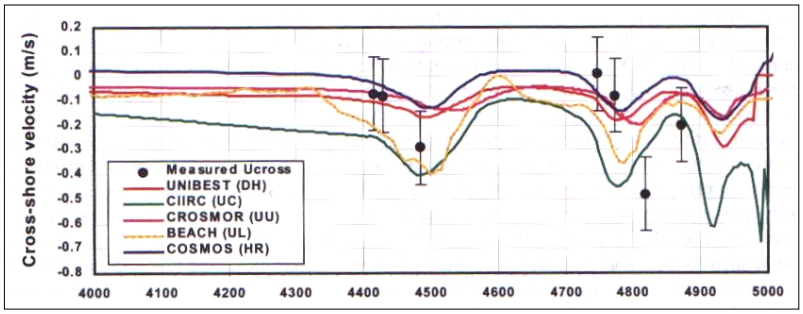

Figure 5.2: The performance of several models at Egmond for cross-shore velocity predictions [RIJN VAN ET AL., 2002].

Cross-shore velocities predicted by UNIBEST-TC are in the order of magnitude of 0 to 0.1 m/s. According to Figure 5.2 the cross-shore velocities are under-predicted. The results are classified as reasonable to good. It has been concluded that UNIBEST-TC as well as the other models can simulate bar migration reasonably well. However, prediction of beach development appears difficult. The performance of UNIBEST-TC compared to the other models is good.

One alternative model that has not been tested along with the other models is DUROSTA. This model is specially designed to predict seabed variations due to solely seaward sediment transport during severe storm conditions accompanied by high water levels. In contrary to DUROSTA is UNIBEST-TC capable of computing landward directed sediment transport during fair weather conditions. [DIJK, 2002]

Almost all sediment transport models are capable of predicting variations in seabed level and wave height with a reasonable good accuracy. In case of this thesis the responds of the relatively shallow area is of most interest during severe hydrodynamic conditions. Especially, wave and seabed predictions are examined. Whether the model will be classified as 'good' during severe conditions is still unanswered, due to the absence of the required validation data. Therefore the assumption has been made that the validation during fair weather is representative for an extreme storm event. However, it is unexpected that fair weather conditions are similar to storm conditions. Consequently, one should keep in mind that the results can differ significantly from the UNIBEST-TC prediction.

5.3 Model characteristics

UNIBEST-TC has been designed to compute cross-shore sediment transports and the resulting profile changes along any coastal profile of arbitrary shape under the combined action of waves, longshore tidal currents and wind. UNIBEST-TC takes the principal cross-shore processes such as wave asymmetry, undertow, gravity and mass-flux below wave troughs into account and can be applied on several coastal problems. [BOSBOOM ET AL., 1997]. The principles of sediment transport are treated in Appendix 1.

UNIBEST-TC uses a co-ordination system as is shown in Figure 5.3; the x-axis is perpendicular to the shoreline positive in landward direction. The z-axis is positive in upward direction and starts at the SWL (Still Water Level). Waves orientated under an angle are defined with respect to the angle with the x-axis (shore normal direction).

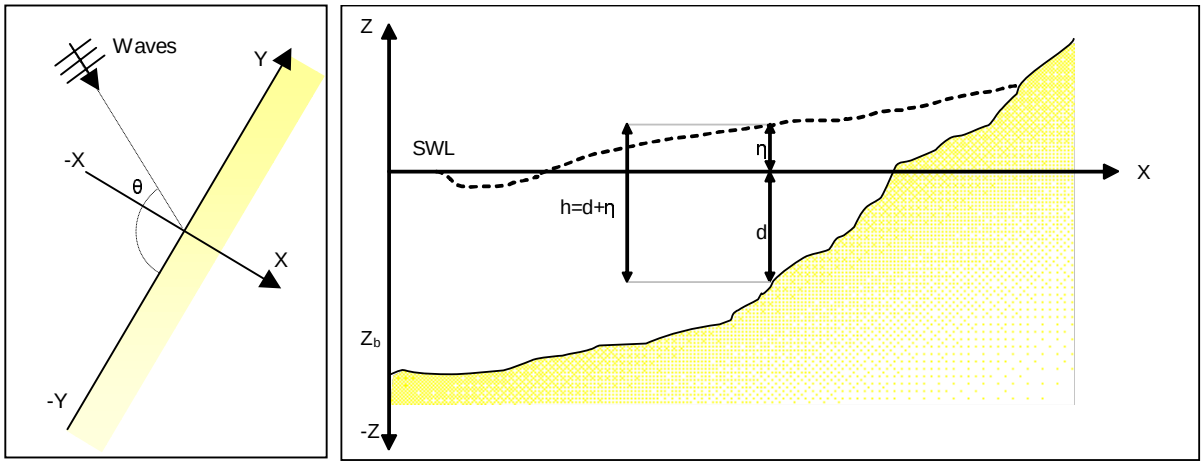

Figure 5.3: Co-ordination system in UNIBEST-TC [BOSBOOM ET AL., 1997].

Restrictions
In order to apply UNIBEST-TC, a number of hypotheses have been taken into account to incorporate the complex reality into a model:

- The coast is supposed uniform in alongshore direction.
- 3D hydrodynamic processes are not considered.
- Sand can only be transported in cross-shore direction; therefore the sand volume in the profile stays constant throughout the calculations.
- Wave reflection has not been incorporated in UNIBEST-TC.
- Setup in the shallow zone due to wind has not been incorporated in UNIBEST-TC.

Especially the first two restrictions are important. During this thesis a point of focus lies at the nearshore area. Groins cause a discontinue profile in alongshore direction. Accompanying 3D processes in the shallow zone between the groins are not incorporated in the model. Furthermore, the bathymetry in front of the Pettemer sea defence is irregular instead of uniform. According to the surveyed profiles, profile sand volumes vary annually. This annual variation cannot be computed in UNIBEST-TC because of the operative balance equations. Wave reflection takes place against the Pettemer sea defence in case of long waves (swell) and during storm wind setup is affected by the orientation and velocity of the wind. Neglecting these processes increases the error of the UNIBEST-TC output.

Next to these model restrictions some assumptions are done during this thesis in order to use UNIBEST-TC:

- No alongshore transport gradient has been considered.
- No difference in wave orientation has been considered.
- No tidal currents and variations have been considered.
- Sea-bottom profiles surveyed during fair weather conditions are used as input for storm calculations.

Whenever the wave orientation appears to be important it is recommended to include alongshore transport gradients as well, because the longshore transports induced by oblique waves are greatly affected by the transport quantities due to alongshore-tidal gradients.

Furthermore, UNIBEST-TC has been developed to study sandy coasts. However, it is possible to implement a fixed layer that represents the Pettemer sea defence. According to the manual the model cannot be applied to study the shallow surf zone (water depths less then approximately 0.5 to 1.0m) and the swash zone. During this study most attention is focused on the toe of the sea defence (RSP = 0). The seabed level near the toe is located at a depth of -0.68m + NAP (shallow surf zone). However, during storm the water depth exceeds the 1m due to a setup of several meters that occurs as a result of the storm. Therefore it is expected that the toe of the sea defence at RSP = 0 can be examined during storm conditions with UNIBEST-TC.

Time scale

According to the users manual [WALSTRA, 2000] UNIBEST-TC has been designed to study morphological profile developments on the time scale of storms (hours to days) and medium term (months to years). Therefore it is expected that UNIBEST-TC can be used for the purpose of this thesis.

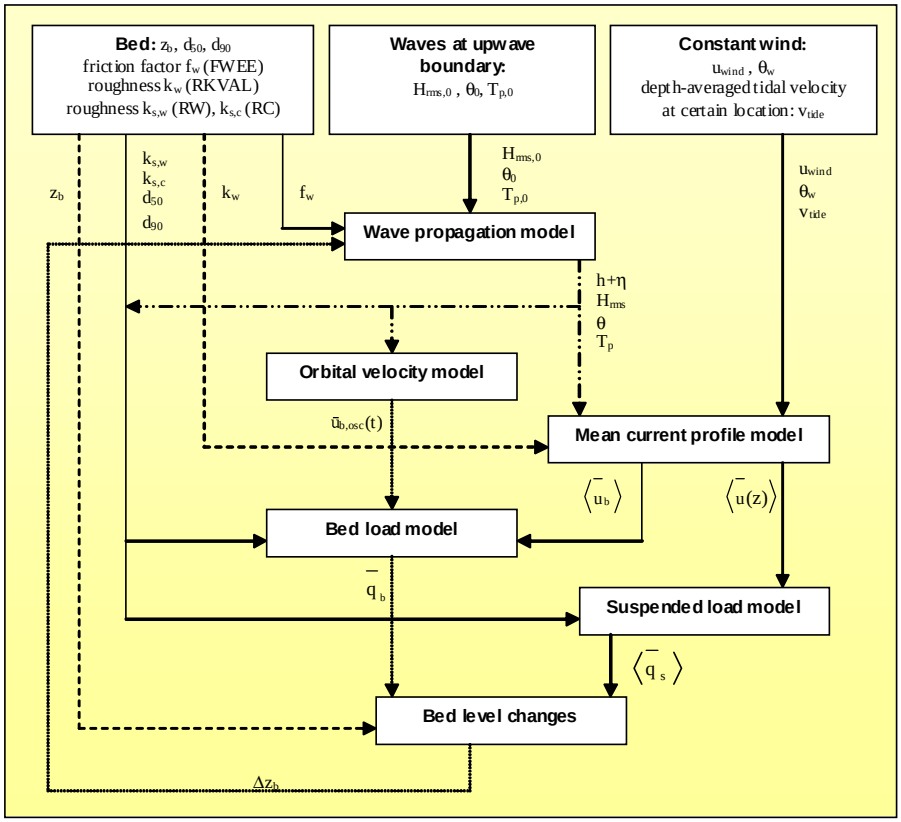

Figure 5.4: UNIBEST-TC module structure [BOSBOOM ET AL., 1997].

Model structure

UNIBEST-TC consists of 6 separate consecutive modules as is shown in Figure 5.4:

1. A wave propagation module.
2. A mean current profile module.
3. A wave orbital velocity module.
4. A bed load transport module.
5. A suspension load transport module.
6. A bed level change module.

Module definitions

The wave propagation model (ENDEC) computes the wave energy decay along a cross-shore ray taking in account the effects of shoaling, refraction and energy dissipation. The mean current profile module computes the vertical distribution of the wave-averaged mean currents in both alongshore and cross-shore direction. This module takes in account wind shear stress, wave breaking, bottom dissipation in the wave boundary layer and the free surface slope. The wave orbital velocity module calculates time series of the near-bed wave orbital velocity. These time series contain contributions due to wave asymmetry, wave group related amplitude modulation and bound long waves and are therefore representative for irregular wave groups. [BOSBOOM ET AL., 1997]

In the sediment transport module one can distinguish between the bed load and suspended load module. It is assumed that the mean current dominates the suspended load transport; the suspended sediment flux is computed as the product of the wave-averaged current and concentration profiles, which are obtained from the mean current profile and a time averaged advection-diffusion equation. Bed-load transport is computed as a function of the instantaneous bed shear stress. The near-bed velocity signals determines on the instantaneous shear stresses. Near-bed velocities are on their turn composed of the generated time-series for the near-bed wave orbital velocity plus the time averaged current velocity near the bed. [BOSBOOM ET AL., 1997]

After the computation of the transport rates along the profile, the bed level changes are computed from the depth-integrated mass balance:

$$\frac{\partial z}{\partial t} + \frac{\partial q_{bot+sus}}{\partial x} = 0 \qquad (5.1)$$

z	= Vertical water column	[m]
t	= Time step	[s]
x	= Distance along the cross-shore profile	[m]
$q_{bot+sus}$	= Bottom and suspended sediment transport rate	[m^3/sm]

5.4 Calibration

The Calibration for UNIBEST-TC has been executed solely for the module ENDEC due to the absence of sufficient calibration data. Only wave heights during storms are available for a consecutive period of one single day. Over a period of 20 minutes the wave heights have been averaged. However, the accompanying seabed profiles are measured about 6 times a year and never during heavy weather conditions.

Other measurements needed for the calibration of the other 5 modules in UNIBEST-TC are not available. In order to calibrate UNIBEST-TC more accurately the following aspects have to be measured:

- Cross-shore velocity.
- Longshore velocity.
- Near bottom sediment concentration.
- Suspended sediment concentration.

UNIBEST-TC uses a default setting for the model parameters. This default setting is shown in Figure A11.4 (Appendix 11) and has been based on an extended calibration at Egmond. Egmond is located 20km south of Petten and has a similar barred coast. Therefore it is plausible that the default setting is representative for the Petten location as well. The Petten shore differs from Egmond in two major aspects. First of all at Egmond a beach with dunes instead of a sea defence protects the shore. Second of all, the 'Pettemer polder' bank resulting in offshore breaking of high waves protecting the Petten coast, while Egmond has no protection on deep-water.

Restrictions and assumptions

In Appendix 11 the calibration method as well as the results has been described. The most important assumptions and boundary conditions are summarised:

- The surveyed seabed profile of 20 October 1999 has been used.
- Waves measured at wave buoy (MP1) located 7900m offshore from the sea defence have been used as input.
- At locations 540m, 60m and 10m wave measurements are used as validation.
- The measured vertical tide at MP3 has been used.
- The peak wave period measured at K13a (100km offshore) has been used to complete the wave data set.
- All waves have been given a similar orientation to the shore, because waves measured with an angle to the shore normal that exceeds 20 degrees will not pass the 'Pettemer polder' bank.

Results

According to the results shown in Appendix 11 Figures A11.8 to A11.22, the default parameter settings without the breaker delay result in optimal predictions. The breaker delay parameter switch (K_IJL) is set ON, according to the default settings. However, this results in an overestimation of wave heights above steep seabed slope and in the 'shallow' water zone (zone from 100m to 0m offshore of the sea defence)

The parameters that most affect the propagation of the wave height are the breaker delay parameter (K_IJL) and the gamma parameter (GAMMA). Next, the friction parameter (FWEE) and the roller parameter (BETD) have most effect. The wave angle (TETA) and the correlation factor (C_R) have practically no significant effect on the computed wave heights. However, besides the effect on the wave height prediction, most parameters affect the computed morphological changes. Consequently, different seabed profiles are the result of different parameter settings.

Based on merely measurements no conclusions about the computed morphological changes can be made due to the absence of validation data. However, it is assumed that morphological changes computed by default settings are reasonably valid, because of the similarities with the Egmond coast. The computed seabed profiles during calibration are therefore compared with seabed profiles computed by default parameter settings.

Effect of seabed variation on wave height prediction

According to the calibration the default settings with the breaker delay parameter set off have the best result. During the calibration only dynamic simulations have been examined. Dynamic runs are runs with a dynamic seabed profile (IBOD =1). It is also interesting to see the results of similar setting for a static run (IBOD = 0). At the end of Appendix 11 the figures of this comparison are shown.

The predicted wave heights have been compared for two simulations; simulation (112) is without sea-bottom movement and simulation (113) including sea-bottom movements. According to the results shown in Figure 5.5 simulation 112 predicts the waves during storm more precise. The most obvious conclusion is that the predicted seabed alterations are over-estimated, resulting in an over-estimation of the wave height.

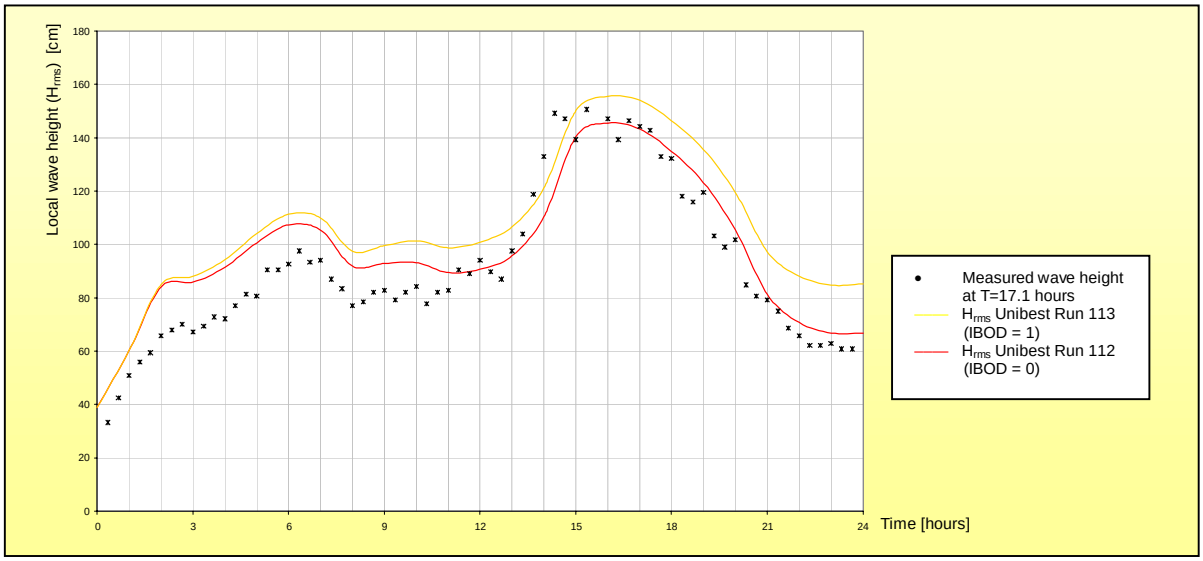

Figure 5.5: Wave heights (H_{rms}) simulated by UNIBEST-TC compared with wave heights measured at Petten during storm, at location MP7 (10m offshore).

5.5 Parameter analysis

In this paragraph the effects of several parameters are discussed, with respect to two aspects:

- Erosion depth.
- Local wave height in front of the sea defence.

To determine the level of safety and the impact of erosion dealt with in the next chapter, "probabilistic analysis' the required sea defence crest height is compared with the current crest height. The impact of erosion will be determined by means of the failure mechanism 'wave run-up'. The main parameters that contribute in the wave run-up process are the local water level in front of the sea defence (at the toe) and the local wave height. It is expected that changes in the local wave height are mainly caused by local sea-bottom decreases (erosion). Therefore the effects of both parameters are taken into account during this analysis.

The parameters that are thought to be of significant influence on the two above specified processes are listed. The effects of these parameters are examined with the sediment transport model UNIBEST-TC. The settings that were found optimal during the calibration are used. For other parameters that affect both processes into a minor extent a short description has been given at the end of this paragraph. In Appendices 13 and 14 the simulations used for this parameter analysis are described. For these simulations the bed profile surveyed in November 1999 has been used. The output has been generated for the location of the sea defence toe at x=0.

- Maximum water level.
- Deep-water wave height.
- Wave period/ wave steepness.
- Storm duration.
- Initial seabed profile.
- Grain size.
- Model accuracy.

5.5.1 Maximum water level

The maximum water level affects the erosion quantity significantly. In Appendix 14, the water level has been varied to examine the effect of the water level on the erosion quantity. However the exact erosion quantity depends on other parameters as well. The effects are illustrated in the Figures 5.6 for different deep-water wave heights.

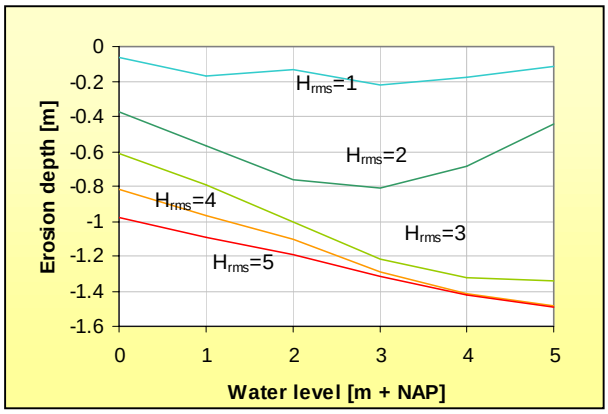

Figure 5.6: Water level versus erosion at the toe, for different deep-water wave heights after a period of 2 days.

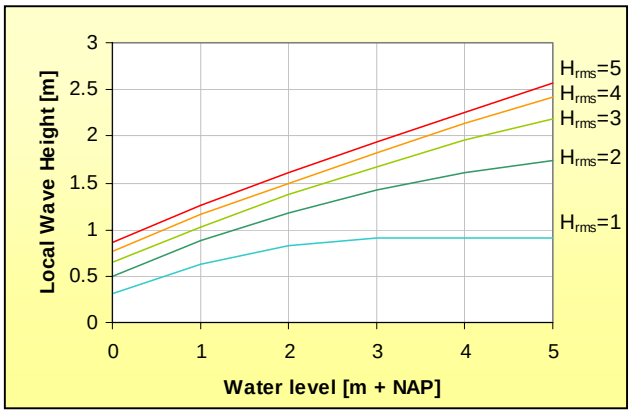

Figure 5.7: Water level versus the local wave height, for different deep-water wave heights after a period of 2 days.

During low wave conditions variation of the water level has minor effect on the erosion depth at the sea defence toe. For a deep-water wave height (H_{rms}) of 2m a parabolic relation is found, this probably has to do with the sediment transport quantities and the wave penetration on different water levels that both depend on profile characteristics as well. During severe wave conditions, the effect of the water level has decreased slightly and becomes linear. For a situation with a deep-water wave height of 5m an increase of the water level with 1m leads to an increase of 0.1m for the erosion depth.

The effect of the water level on the local wave height also depends on the deep-water wave height. In case of little waves the local wave height remains small and little wave growth occurs. Whenever a certain water level has been reached, waves stop to break. At this water level the maximum local wave height approaches the deep-water wave height. However, the deep-water wave height will never be reached because waves dissipate energy along the profile stretch.

Higher waves show a more linear growth pattern after a two-day-period of constant wave impact compared to smaller waves. Whenever, the local waves become about $^2/_3$ of the deep-water wave height, the growth rates starts to decrease.

The local wave height growth caused by nearshore erosion is shown in Figure 5.8. The growth of the local wave height is defined as the local wave height after a 2-day-period minus the initial local wave height. Figure 5.8 shows the effect of the water depth on the wave growth for different deep-water wave heights. Low water depths result in a faster growth than high water levels do. An increase of 1m in water level during severe wave conditions results in a decrease of 40mm in wave height growth.

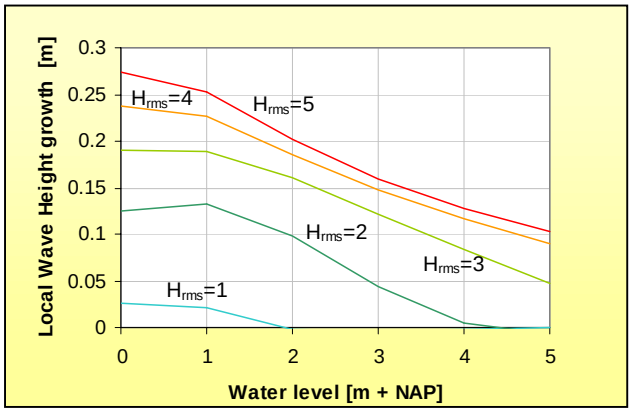

Figure 5.8: Water level versus the local wave height growth, for different deep-water wave heights after a period of 2 days.

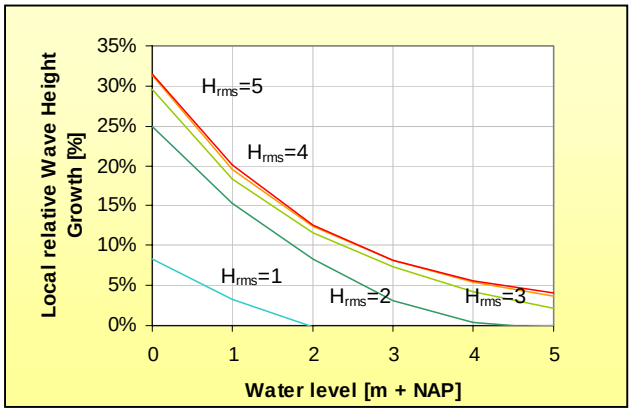

Figure 5.9: Water level versus the relative local wave height growth, for different deep-water wave heights after a period of 2 days.

The maximum local wave height growth occurs during maximum wave heights combined with minimum water levels. The maximum computed wave growth is about 0.28m (Figure 5.8). This is well below the breaker index (γ_{rms}) that varies between 0.35 and 0.42 according to theory. The breaker index can be seen as the maximum wave growth possible whenever the water level has been increased with 1m.

The relative wave height growth, shown in Figure 5.9, is characterised by a quadratic-relation for the water depth. The relative wave height growth is the absolute wave height growth divided by the initial local wave height. Whenever the water level is high the initial local wave height is also high, resulting in a reduction causing the wave height growth to reduce even further. This effect combined with the effect of high water level result in little wave growth with a quadratic-relation.

5.5.2 Deep-water wave height

The deep-water wave height affects the predicted erosion degree as well as the predicted local wave height considerably. During this analysis the root-mean-square wave height (H_{rms}) is used to characterise a set of waves. In Appendix 14 the wave height has been varied to examine the effect of the wave height on the erosion quantity. However, the exact erosion depth depends on other parameters as well.

Figure 5.10 illustrates the effects of wave height variations on the computed erosion depth at the sea defence for different water levels. Generally higher waves cause more erosion. An increase in water level contributes to this effect.

During high water levels (> 4m + NAP) the relation appears to be characterised by an s-curve. Low waves combined with high water levels cause relatively little erosion, due to relative large distance between the wave load at the surface and the erosion at the seabed. Contrary to low waves, high waves combined with high water levels cause severe erosion. High waves are often limited by the water level contrary to low waves, resulting in a different dependency for relatively high wave to the water level. High waves can increase whenever the water level is increased resulting more erosion. This explains the quadratic increase in erosion depth. However, a fixed layer brings the erosion depth even during higher wave to a stand at a depth of –1.5m

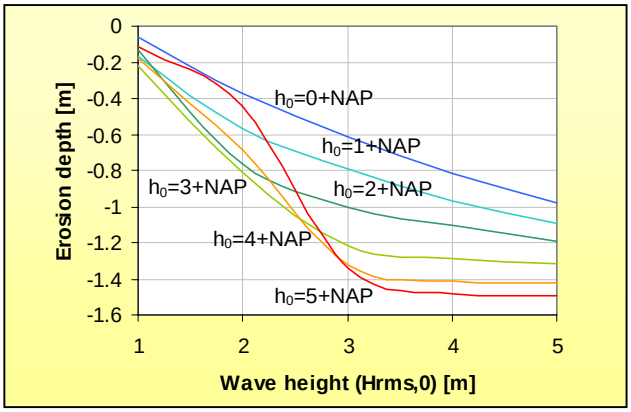

Figure 5.10: Deep-water wave height versus erosion depth, for different water levels after a period of 2 days.

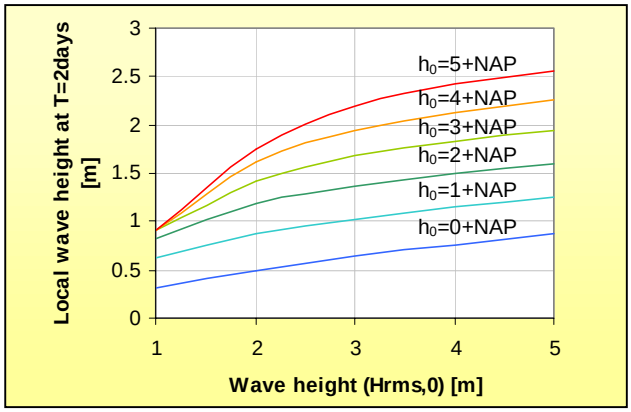

Figure 5.11: Deep-water wave height versus the local wave height, for different water levels after a period of 2 days.

Figure 5.11 shows the positive effect of an increase in deep-water wave height on the local wave height predictions. An increase of 1m in deep-water wave height causes a minimum increase of 0.2m for the local wave height. During wave breaking conditions (low water levels) the local wave height growth can reach up to values of 0.8m, which is rather large. Conclusively, variations in wave height have more affect on the erosion depth and the local wave height than water level variations do.

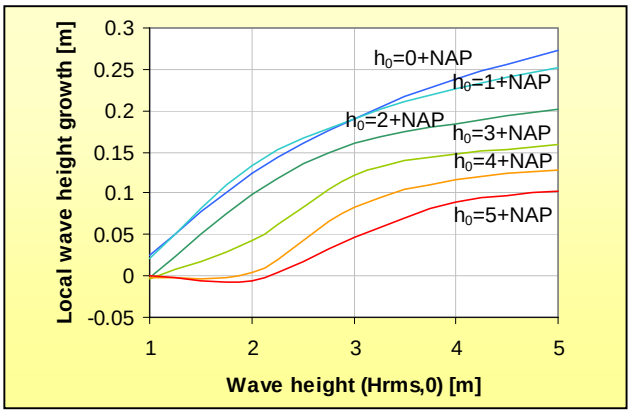

Figure 5.12: Deep-water wave height versus the local wave height growth, for different water levels after a period of 2 days.

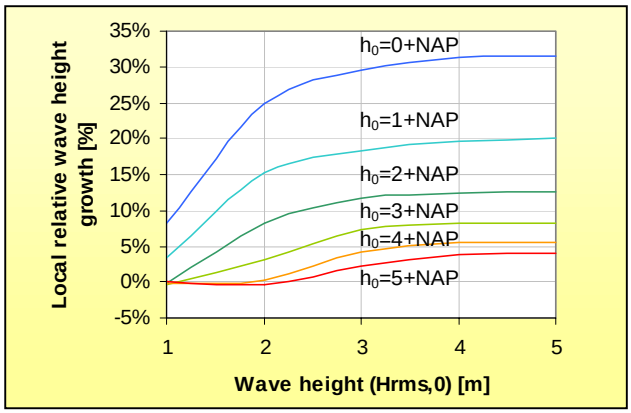

Figure 5.13: Deep-water wave height versus the local relative wave height growth, for different water levels after a period of 2 days.

The following two figures show the absolute and relative local wave height growth for a period of 2 days. Apparently high water levels accompanied by small waves cause the absolute wave growth to become negative. Generally a positive wave growth has been predicted up to a maximum of 0.27m during low water levels and high wave conditions. The negative relation for wave growth is probably caused by different sediment transport rates. However the exact cause has not been determined.

5.5.3 Wave period

The effect of a varying wave period on the erosion depth has not been examined. However, the wave period effects on the wave propagation pattern causing the local wave height to change are examined. The wave heights affect in their turn the erosion depth, as has been described previously. During this thesis the wave period has been linked to the wave height by means of a constant wave steepness parameter (s). The affects of the wave steepness parameter on the local wave height are treated in the next subsection. The affect of the wave period can be explained by means of these results.

5.5.4 Wave steepness

The wave period depends on the wave height by means of a constant deep-water wave steepness. Usage of the wave steepness is more confined, because it affects the breaker index relation as well as the 'wave run-up' process. Wave run-up is treated in the next chapter. The effects of wave steepness variation on the local wave height will be discussed.

According to the calibration the best performance is realised whenever the default value for GAMMA is applied. This means that the GAMMA value depends on the deep-water wave steepness, as is explained in Appendix 8. However, GAMMA also affects the local wave height. To examine the effects of the wave steepness on the local wave height two situations are treated. The red line in Figure 5.14 illustrates the effect of a situation with a varying the wave steepness and a constant GAMMA. The blue line (GAMMA=0) illustrates the effect of a situation that includes a dependent GAMMA. The simulations for both situations have been executed with a water level of 5m + NAP and a deep-water wave height of 5m. This analysis is further explained in Appendix 13.

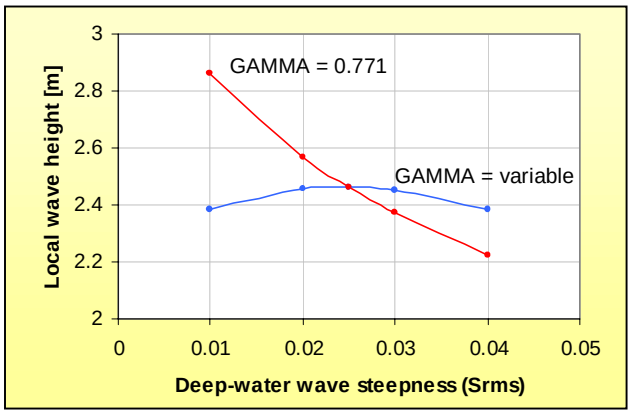

Figure 5.14: Deep-water wave steepness versus the local wave height, for a wave height of 5m and a water level of 5m + NAP.

According to Figure 5.14 the wave steepness affects the local wave height negatively. Higher wave steepness values result in waves with long wavelengths respectively high wave periods. Dissipation due to friction over the profile stretch increases if the wavelengths increase. Long profile stretches have been used during the simulation runs. The result is a local wave height decrease of 0.2m if the deep-water wave steepness has been increased with 0.01. This variation in local wave height can be reduced by shortening the profile stretch, or by lowering the FWEE parameter.

The blue line in Figure 5.14 illustrates the effect of a varying wave steepness including a dependent GAMMA parameter. The GAMMA parameter is positively affected by the wave steepness causing an increase of GAMMA whenever the wave steepness has been increased. Furthermore, the GAMMA value positively affects the local wave height. The positive GAMMA effect combined with the negative friction effect result in a relatively constant course of the blue line (relation between local wave height and deep-water wave steepness).

The positive effect of a dependent GAMMA exceeds the negative effect of increasing wave steepness up to a wave steepness of 0.02. Between a wave steepness of 0.02 to 0.03 both effects are virtually equal. While for higher wave steepness values the negative effect exceeds the positive effect.

5.5.5 Storm duration

The parameter storm duration affects local wave heights as well as the erosion depth. However, the effect mainly depends on other variables. Effects of the duration have been examined by means of constant input. Variable input probably results in different output, but this effect has been neglected. The effects caused by of storm duration on the erosion depths and local wave height, during constant wave characteristics and a constant water level, are shown in Figures 5.15 and 5.16.

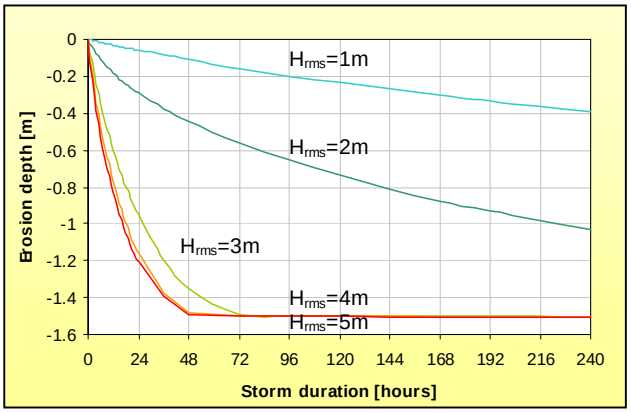

Figure 5.15: Storm duration versus erosion depth, for a varying deep-wave height and a water level of 5m + NAP.

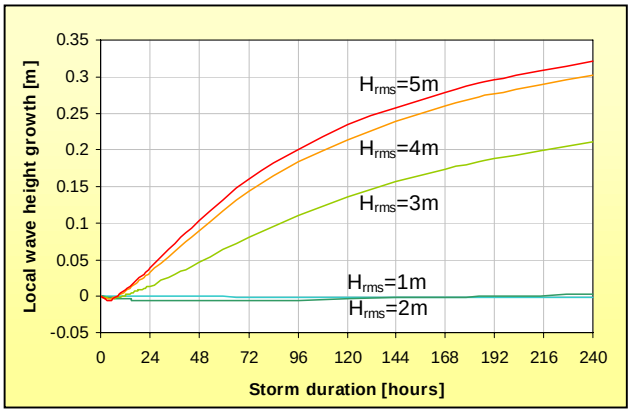

Figure 5.16: Storm duration versus the local wave height growth, for a varying wave height and a water level of 5m + NAP.

Generally the erosion depths as well as the local wave height increase if the storm duration increases. The erosion depth increases fastest during the first storm hours. The effect of the storm duration depends on the wave height as well as the water level and profile characteristics. With regard to the local wave height growth, an increase of storm duration results in almost all cases in an increase in local wave height. Apparently a few hours are needed before the wave height starts to rise; this phenomenon will be further treated in the Paragraph 5.6.

5.5.6 Initial seabed profile

The effects of the initial seabed profile on the local wave height growth are treated in this subsection. The effects on the erosion depth have not been examined. The initial seabed level has been examined for three cases listed below. The seabed profile analysis has been comprehensively described in Appendix 13.

- Profile level.
- Bar variation.
- Nearshore area.

Profile level
The effects of a 0.50m seabed level rise over the entire profile stretch results in an increase of 0.16m for the local wave height. The local wave height water depth ratio also referred to as breaker index is about 0.45, whereas the additional ratio is 0.32 ($\Delta H_{rms}/\Delta h$). According to theory the breaker index varies between, 0.35 and 0.42, hence it can be concluded that severe breaking takes place. A 0.16m wave height growth due to an increase of 0.5m water depths is a maximum growth rate.

Bar variation
Two bars are distinguished at the Petten site: The 'Pettemer polder' bank and the nearshore breaker bar. Both bars are varied in height and the combined effects have been examined. First off all, it appeared that variation in crest height of the nearshore breaker bar had most effect on the local wave height. Secondly, the wave variations were rather small compared to the variations of bar crests, in the order of magnitude of several centimetres, while the bar crest were varied in with 1m. Consequently, the level of the nearshore area is of most importance. However, variations of the bar crest height does result in significantly higher waves just in front of the nearshore area. Therefore it is expected that the bar crest height have considerable impact on the erosion speed. However, this has not been examined.

Nearshore area
Variations in the seabed level in this area, located directly in front of the sea defence, affect the local wave heights. The wave height varies in the order of magnitude of 0.25m whenever the seabed level of nearshore area has been altered with 1m. Furthermore, it is expected that whenever the initial seabed level of the nearshore area is varied this can be compared with the effects of a similar variation in water level. The effects on the erosion depth are probably slightly smaller, because whenever the water level is raised this is done over the entire profile stretch while a nearshore seabed level decrease is a local effect. Nevertheless, the water depth in the nearshore area determines the local wave height for about 80 to 90% during breaking conditions. However, the exact effects are not examined.

5.5.7 Model accuracy

According to Coast-3D report [RIJN VAN ET AL., 2002] the wave height is predicted reasonably well by UNIBEST-TC. During fair weather conditions an accuracy of about 10% with the default values has been acquired. According to the calibration results the error in the surf zone is pretty much similar to the error according to Coast-3D report. For the wave height the error is about 15 to 20%. However, the errors in the computed sediment transports are significantly higher, more or less in the order of magnitude of 50%, especially in the nearshore region. Besides the model accuracy the survey accuracy is just as important. For seabed levels the accuracy lies in the order of magnitude of about 10% to 15%, while for wave heights this is about 5% to 10%. Accept for the calibration no measurements have been taken to increase the accuracy and during the prediction capabilities of UNIBEST-TC are assumed to be adequate.

5.5.8 Grain size

The grain size of the sand in front of the sea defence will probably have a considerable effect on the erosion depth. Smaller grains have less weight and can therefore be moved easier. Another aspect that will affect the erosion depth is the bed slope. A bed of small grains has generally a gentler slope compared to steep slopes with grains, due to a difference in fall velocity. However, these effects have not been examined during this analysis.

5.5.9 Other parameters

Besides the previously discussed parameters several other parameters are, due to the complexity of the sediment transport process, of influence as well. The effects of the parameters listed below have not been taken into consideration during the determination of the local wave height are erosion depth. Most of these parameters have little influence, however some of them are considered to have little influence, sometimes based on unsatisfactory insight and know-how.

Wind characteristics

The main wind characteristics are wind speed and wind direction. The wind speed along with the wind direction and fetch length determine the wave height growth at deep water. Consequently, the maximum wave height at deep-water is determined by the prevailing meteorological conditions. Wind characteristics have significant affect on the water level setup as well. Furthermore, the wind direction mainly determines the wave direction. The wave direction on its turn affects the local wave height.

Wind characteristics are the basis for a storm; the hydrodynamic conditions are the result. However, these effects of wind speed and direction are not incorporated in the UNIBEST-TC model.

Wave orientation

Wave direction has been incorporated in UNIBEST-TC. Generally the most severe storms come from the Northwest along the Dutch Coast. For Petten this results in wave orientated almost perpendicular to the shoreline. Whenever waves approach with an angle to the shoreline, a longshore current has been generated. This wave induced longshore current combined with the longshore tidal current, generates longshore sediment transports. This longshore process becomes even more important whenever a non-uniform shoreline has been examined. However, during this thesis only cross-shore transport has been examined and the shoreline has been assumed uniform. Wave angels have therefore been neglected.

If wave angles appear to be of significant influence, it is recommended to use a three dimensional model to study the effects of longshore currents combined and cross-shore currents together.

Profile slope and sand quantity

Only the variation in height has been examined, nevertheless the slope of the profile as well as the sand quantity can also be of influence. Especially when different initial profiles are compared in UNIBEST-TC, these parameters can be of importance. The slope of the nearshore area combined with a certain profile height and sand quantity can be used as profile characteristics to compare the different profiles. All these parameters are necessary, because UNIBEST-TC considers a closed sand balance.

Groin, revetments, reflection

The effect of groins has not been taken into account, because the physical alterations are to complex to incorporate them into the UNIBEST-TC model. If the effects of groins appear to be of significance, it is recommended to use a 3D-model to simulate their effects. Other coastal protections, like revetments and anti-scour protection have not been taken into consideration. The exact effects of these protection measurements are unknown. Also the refection of waves on the sea defence have not been taken into account

5.6 Morphological effects on wave height in UNIBEST-TC

Two aspects basically determine the prediction of local wave heights:

- The water depth at the location of interest.
- The initial wave height.

Waves are limited in height by the local water depth if they exceed a certain level. The resulting wave height reduction is referred to as breaking. Shallow waters allow lower wave heights compared to deep-waters. However, local wave heights are also affected by the height of incoming waves. Whenever, these waves are small the local water depth has no effect. Consequently, waves have a similar wave height on all water depths until the water depth becomes important and breaking occurs.

In the surf zone, where wave breaking takes place, seabed level changes are expected to have significant affects on the local wave heights. In case of decreasing local seabed level and constant water levels increasing water depths are the result. Higher waves are possible on higher water depths. However, according to the results of UNIBEST-TC it appears that the local water depths have relatively little effect on the computed local wave height.

For example, the results of a simulation (run 529) with a constant water level (NAP +5m) and a constant wave height (H_{rms} = 5m) and peak period (T_p = 11.32s) have been used. In Figure 5.17 and 5.18 the effect of 3 hours of constant hydrodynamic conditions and the accompanying morphological changes have been plotted. In front of the sea defence and on top of the breaker bar erosion take place. The sand has been transported in seaward direction increasing the steepness of the outer slopes of the bar and nearshore area.

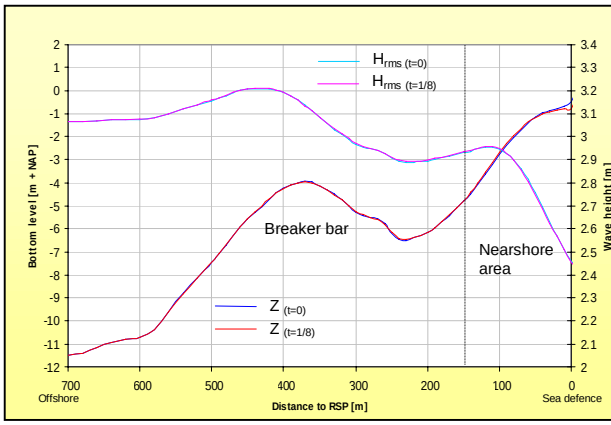

Figure 5.17: Comparison for seabed level and wave height for the initial situation (t=0) and t=1/8 day.

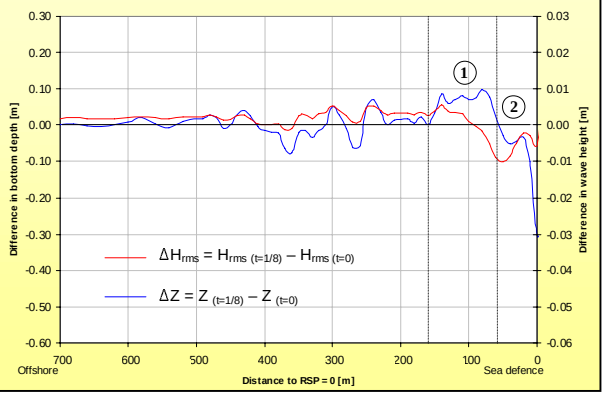

Figure 5.18: Difference between wave heights and seabed level between for t=1/8 day and t=0 days.

During this 3-hour run the wave height computed at 1000m offshore has increased with a 25mm (Figure 5.18). This increase in wave height has been caused by the reduction of the 'Pettemer polder' bank crest (3km offshore). At the crest of the second breaker bar (350m to 400m) the wave height increase reduces to nil. Nevertheless, the bar crest reduces about 0.10m in height.

In Figure 5.18 two numbers indicate the areas of sedimentation (1) and erosion (2). Sedimentation starts at 60m to 160m where it changes into erosion up to the sea defence. 100m from to the sea defence the wave height reduces compared to the initial situation with about 10mm due to the sedimentation. Over the final stretch of 60m to the sea defence only 8mm in wave height has been regained due to local erosion. Consequently, in spite of the erosion in front of the sea defence at RSP = 0 (about 0.30m) the local waves have decreased 50mm in height, due to sedimentation of the area in front (60m to 160m).

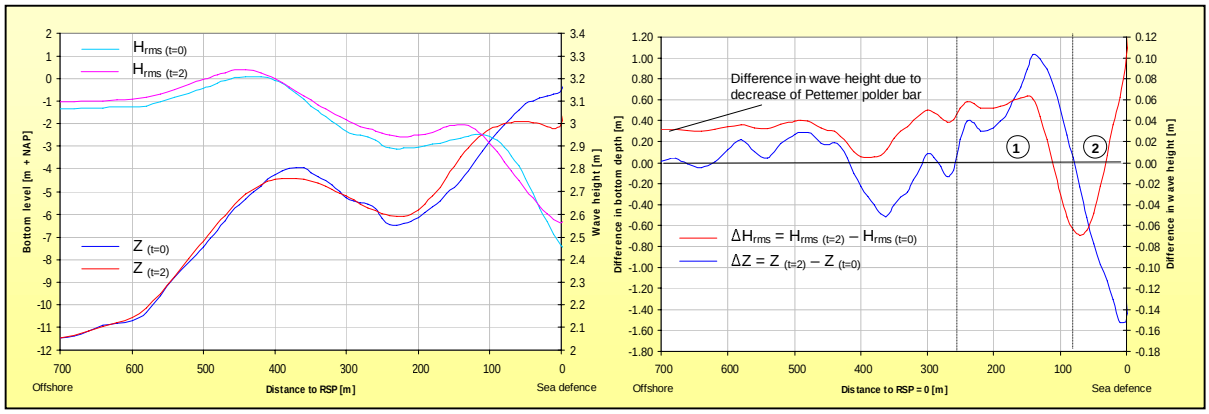

Figure 5.19: Comparison of run 129 for seabed level and wave height for the initial situation (t=0) and t=2 days.

Figure 5.20: Difference between wave heights and bed level between for t=2 days and t=0 days.

Figures 5.19 and 5.20 are similar to the Figures 5.17 and 5.18 except for the fact the period of storm conditions has been increased to 2 days (48 hours). The morphological differences have increased compared to the differences after 3 hours. First of all the 'Pettemer polder' bank has eroded further, leading to an increase of wave height at 1000m offshore to about 30mm. In front of the sea defence (fixed layer) erosion has decreased the local seabed level about 1.60m.

In Figure 5.20 the seabed level between 80m and 300m has increased due to sedimentation, which is indicated with (1), with a maximum that exceeds 1m. From 80m up to the sea defence (0m) a large volume of sand has eroded (2). Furthermore, the wave height (H_{rms}) at RSP = 0 has increased with about 0.10m. The local wave increase due to erosion has exceeded the wave height decrease due to the sedimentation of the area between 80m to 280m.

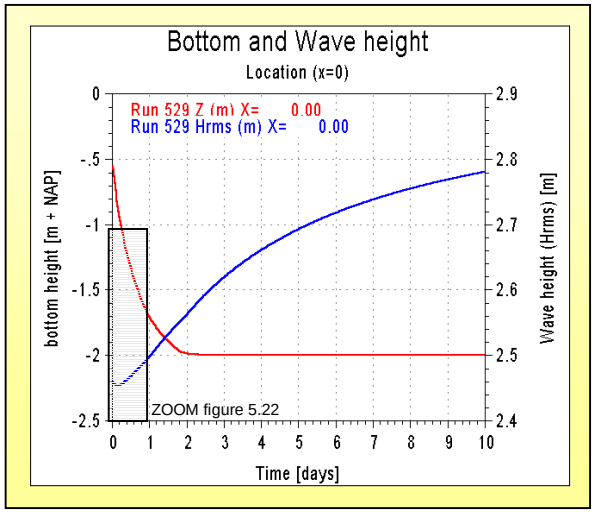

Figure 5.21: Wave height and seabed level course over a period of 10 days.

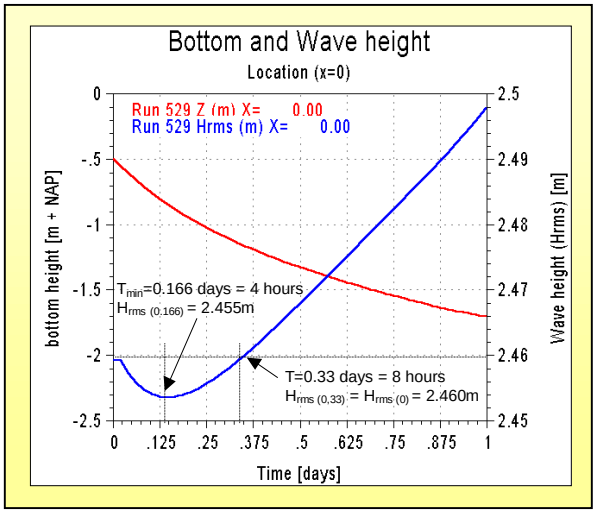

Figure 5.22: Wave height and seabed level course over a period of 2 days. (Zoom of figure 5.21)

When the erosion as well as the local wave height at x=0 are plotted in time the results shown in Figure 5.21 and 5.22 are generated. Figure 5.22 is an enlargement of Figure 5.21 for the indicated section. The initial decrease in local wave height has been compensated after 0.33 days respectively 8 hours. The initial seabed adjustments have great effects on the predicted local wave height. Due to the relatively short storm period in reality the local wave height varies little. The wave height varies in the range of centimetres while the erosion varies in the order of magnitude of 1m. These results were not expected and therefore the UNIBEST-TC computations are examined in detail.

The wave propagation model is based on wave energy (E) and wave group velocity (c_g). The product of wave energy and wave group velocity is also called Energy flux. Wave energy is a function of the wave height (H_{rms}) raised to the square. Energy flux reduction has been caused by energy dissipation (D). Two manners of energy dissipation are incorporated:

- Wave breaking dissipation (D_w).
- Bottom friction dissipation (D_f).

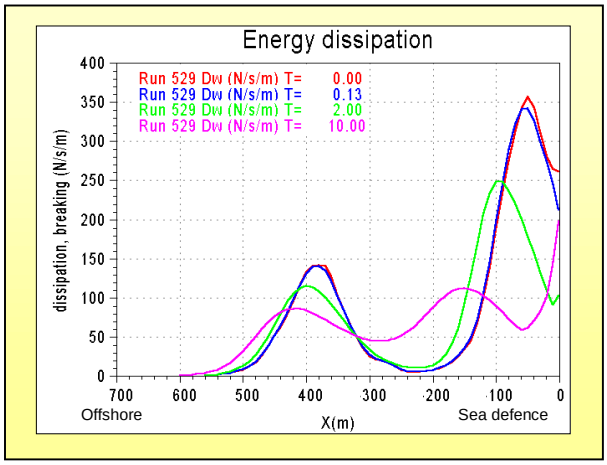

Figure 5.23: UNIBEST-TC result of dissipation due to breaking in the surf zone.

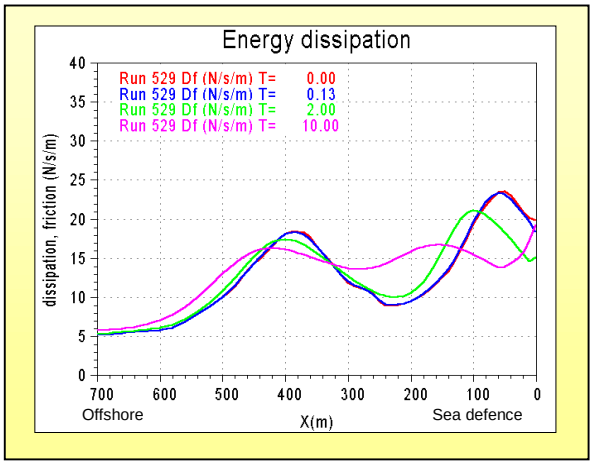

Figure 5.24: UNIBEST-TC results of dissipation due to bottom friction in the surf zone.

According Figures 5.23 and 5.24 energy dissipation due to wave breaking dominates the region from –250m to the sea defence. The share of dissipation due to friction is about 10 to 15 times smaller compared to the share of dissipation due to breaking waves. To keep the analysis simple wave friction has been neglected. The dissipation due to wave breaking has been computed, with the support of two calculations parameters; H_{max} and Q_b, respectively the maximum wave height and the share of breaking waves. The water depth determines the maximum wave height, whereas the share of breaking waves depends on the maximum wave height (H_{max}) and the local wave height (H_{rms}).

$$\text{Energy flux} = Ec_g \qquad [\text{J/ms}] \qquad (5.2)$$

$$\text{Wave Energy} = \frac{1}{8}\rho g H_{rms}^2 \qquad [\text{J/m}^2] \qquad (5.3)$$

$$\text{Dissipation due to breaking} = \frac{1}{4}\rho g \alpha \frac{1}{T_p} H_{\max}^2 Q_b \qquad [\text{J/m}^2\text{s}] \qquad (5.4)$$

E	=	Wave energy	[J/ms]
c_g	=	Wave group velocity	[m/s]
ρ	=	Water density	[kg/m^3]
g	=	Gravitation acceleration	[m/s^2]
α	=	Breaker parameter = 1	
T_p	=	Peak wave period	[s]
H_{rms}	=	Root-mean-square wave height	[m]
Q_b	=	Fraction of breaking waves	[%]
θ	=	Wave angle to the shore normal	[º]
H_{max}	=	Maximum wave height	[m]

These three equations are combined to construct the equation that determines the wave flux/ energy at a specified location *x*.

$$Ec_g \cos(\theta)\big|_{x=0} = Ec_{g,0} - \int_{x=0}^{\infty} D\partial x \qquad (5.5)$$

At the offshore boundary the wave height, direction and peak period are given. These three parameters are used to calculate the initial wave energy flux. The wave height is defined as the square root of the remaining wave energy. No additional energy has been inserted in the model (in reality, wind can increase the wave flux or energy level) resulting in an energy equation that is dependent on the offshore boundary parameters and the amount of dissipation up to the point of interest (in this case from 8000 to x).

All dissipation that has occurred offshore from the location of interest together with the initial wave energy flux determines the wave height at a specified location. However, the wave height is directly derived from the wave energy, instead of the energy flux that has been determined with dissipation. Consequently the local wave group velocity (c_g) also affects the predicted wave height.

Assuming that the wave period stays practically constant the wave group velocity depends positively on the local wavelength. The local wavelength reduces if the local water depth reduces. Consequently, the wave group velocity reduces if the water depth reduces. Whenever the local area erodes the water depth increases resulting in an increase in wave group velocity. If the wave group velocity increases and the wave energy flux remains equal this has to be compensated for by decreasing wave energy, respectively a decreasing wave height. According to Figure 5.23 the total wave dissipation reduces slightly after 0.13 days, however due to erosion the wave group velocity increases. Together both opposing processes result in a slightly lower wave height according to the UNIBEST-TC computations.

5.7 Comparison of UNIBEST-TC and SWAN-1D

Preceding the previous paragraph the UNIBEST-TC predictions are compared to SWAN-1D predictions. SWAN-1D is a computer simulation model that predicts wave propagation over a given seabed. The results of this analysis are shown in Appendix 12. Only one simulation has been checked with SWAN-1D. During this simulation al input variables were held constant according to Table 5.25.

Table 5.25: Input variables for SWAN-1D and UNIBEST-TC.

Description	UNIBEST-TC	SWAN-1D
Wave Height (H_s)	7.05m; H_{rms} = 5m	7.05m
Wave Period (T_p)	11.32s	11.32s
Wave angle (θ)	0^o	0^o
Water level (h_0)	5m + NAP	5m + NAP
Wind speed (u_{wind})	Not incorporated	0 m/s
Seabed profile (Z)	Computed	UNIBEST-TC output
Grid size	Variable from (5m to 50m)	Constant 5m

Other comments are summarised below:

- In order to compare the UNIBEST-TC output and SWAN-1D output the wave height (H_{rms}) computed in UNIBEST-TC has been changed into a Hs value that is used in SWAN-1D with the

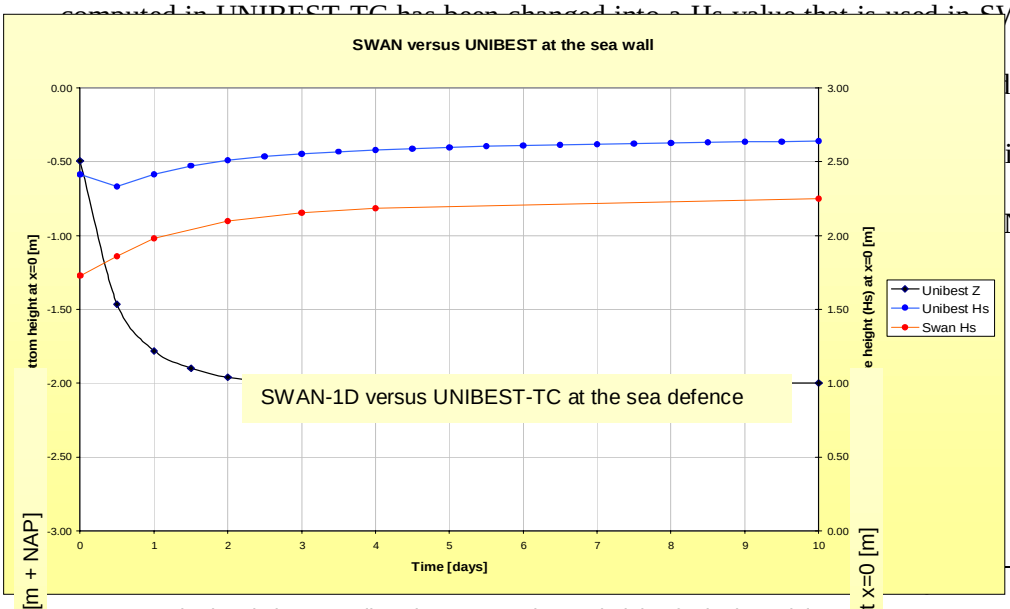

l profiles during a

ifferences are not

NIBEST-TC does

up to 20m/s are

gure 5.26: Seabed variation as well as the computed wave heights for both models at sea

According to the following Figure 5.26 that shows the results for the wave height computation over time at the toe of the sea defence (location x=0) for both models, the initial wave reduction does not occur during computations with SWAN-1D. Furthermore the predictions are about 0.40m smaller. However, qualitatively SWAN-1D predicts a wave growth similar to that of UNIBEST-TC, after the initial effect.

The difference in computed wave height is about 15%, however that is probably due to the differences between both models and the fact that SWAN-1D has not been calibrated first. Whether SWAN-1D or UNIBEST-TC predicts the wave height growth more precise cannot be answered before further examinations have been done. However the initial effect predicted by UNIBEST-TC can still be an artefact or a cold-effect, because it is not supported by SWAN-1D computations. Consequently, it is recommended to examine this effect carefully before the results are used.

5.8 Evaluation

UNIBEST-TC, a morphological process-based computer model, has been used to determine the degree of storm-erosion. However also the effects of storm-erosion on the local wave height have been examined, because in the next chapter this parameter will be used to determine the effects of storm-erosion on the probability of failure and crest height.

The performance of the UNIBEST-TC model has been compared to the performance of other morphological models during fair weather conditions. The UNIBEST-TC performance had been classified as 'good' however the error in wave height predictions in the surf zone is about 15-20% whereas the cross-shore velocities have an error of 50%. According to the calibration the seabed alterations are over-estimated as well as the local wave height predictions. However this results in a safe approach.

These errors occur due to the restrictions of UNIBEST-TC. UNIBEST-TC determines seabed alteration due to morphological processes in cross-shore direction, neglecting the longshore sediment transport. Furthermore, the hydrodynamic processes incorporated in the model are limited as a result of the following assumptions:

- The shore is supposed uniform in alongshore direction, and the sand volume remains constant.
- 3D hydrodynamic processes in the surf zone are not considered.
- Wave reflection has been neglected.

Predictions of the seabed in the surf zone have not been calibrated, due to the absence of validation data. Whenever further research is planned it is recommended to make sure that this calibration can be done to ensure 'valid' predictions including the error-range.

Nevertheless, UNIBEST-TC has been found capable of simulating storm-erosion and the accompanying wave height increase. From the parameter analysis it appeared that the deep-water wave height dominates the erosion process. An increase of the deep-water wave height always results in an increase of erosion as well as an increase in local wave height. Furthermore the water level determines the erosion degree and local wave height. The water level effects are positive during large waves, however in case of small waves, high water levels have a negative effect on the erosion.

Other parameters that have significant effect on the erosion depth or local wave height growth are the wave period or wave steepness, the storm duration, the grain size and the pre-storm seabed profile. Furthermore, the model parameters GAMMA and the breaker delay switch have significant effect on the local wave height predictions.

6. Probabilistic analysis

6.1 General

At present the evaluation of coastal structures is often based on probabilistic methods. In Chapter 2 several of these have been discussed. According to policy documents all primary coastal defence works, which includes the Pettemer sea defence, have to be maintained to a standard, which requires that the structure is able the withstand a water level with a probability of exceedance of 10^{-4} per year safely. A safe design should take into account the probability of failure, and include all parameters and failure mechanism that apply. In this thesis, however, only the 'wave run-up' failure mechanism has been taken into account. This failure mechanism is expected to show the greatest effects of storm-erosion on sea dike dimensions. Therefore the failure mechanism wave run-up qualifies for the purpose of this thesis, which is to determine the relative effects of seabed variation of the probability of failure on dikes.

It is important to realise that this method does not result in absolute probabilities of failure; however, it is possible to determine the relative effect of storm erosion on the probability of failure. Whenever the desire is present to determine the absolute probability of failure at Petten it is advised to take all known failure mechanisms into account.

At present, morphological changes during a storm event are not taken into account during the evaluation process. To determine whether these changes could be taken into account, they should be expressed in a manner that can be used during the decision-making process. A common approach is to express such changes by erosion volume. However, it is more interesting to express the effect of morphological alterations during a storm event in terms of crest height or probability of exceeding the limits of tolerance, or failure (P_f). The significance of these morphological alterations can then be directly interpreted. The probability of failure can be determined using a probabilistic approach.

A probabilistic approach is also beneficial from several other points of view. Whenever a process is examined that involves several parameters, a probabilistic method can show the significance of each parameter individually on the total probability of failure. Another benefit is that probabilistic methods are able to take uncertainties into account. The variables of interest (random variables) are characterised through a distribution function, averaged value, standard deviation and higher order moments. The following uncertainties can be taken into account:

- The inherent uncertainty due to natural fluctuations (The fitting of the measurements).
- The statistical uncertainty due to limited observations (this uncertainty decreases with the structure's lifetime and the number of observations).
- The statistical uncertainty due to slowly changing random processes (climate change, sea level rise, coastal recession).
- The model uncertainty due to model imperfections (The model does not include all physical processes that are active, due to simplifications or unknown physical processes).

6.2 Probabilistic design

In a probabilistic design, the probability of failure is determined by a limit state function. The limit state function reckons with random variables for resistance and load. In Figure 6.1 failures can actually occur during every combination of load (solicitation) (S) and resistance (R). By defining the limit state function (Z) the difference between failure and non-failure has been indicated (failure boundary). The limit state function is defined as follows:

$$Z = R - S \qquad (6.1)$$

Z>0: Safe
Z=0: Failure
Z<0: Unsafe, structure fails

The line Z=0 corresponds to the limit state of failure. In Figure 6.2, an example of a joint probability density function (JPDF) of both resistance and load has been plotted $f_{S,R}(S,R)$. In the combined SR area a chance mound exists. The contour lines or lines of equal probability density represent the mound. The limit state function has also been indicated in Figure 6.2 to show the area of failure (S>R). The sum of the probability situated in the area of failure equals the probability of failure.

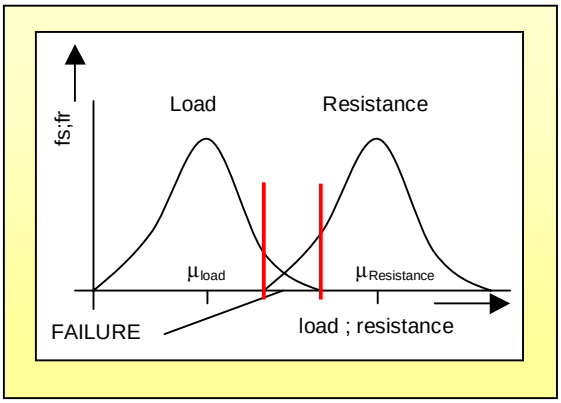

Figure 6.1: Probability density functions for load and resistance

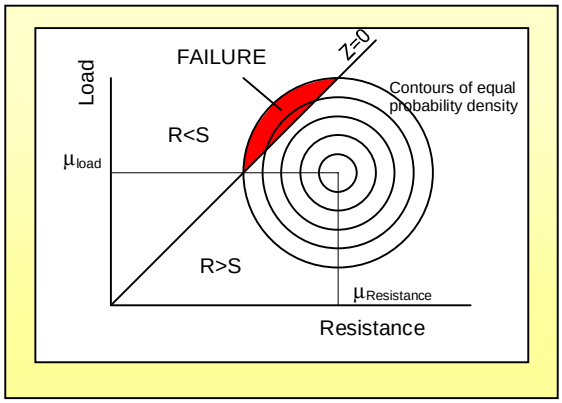

Figure 6.2: Joint probability density function diagram, combined with a limit state function (Z)

Generally the final load or resistance is constructed from a number of random variables. These random elements all have to be assessed individually, leading to a multiple dimensional problem. This could lead to a complicated disorderly format. The figures show a 2-dimensional problem, with a third dimension that represents the probability indicated with contour lines.

For politicians the probability of failure is an important factor, however for local water boards geometrical sea defence dimensions are of more interest, e.g. crest height. Whenever the probability distribution functions for all random parameters can be derived for the location at the Pettemer sea defence, the minimum crest height can easily be determined at the probability of 10^{-4} per year.

During this thesis, however, the interest is focussed on the relative probability of failure determined by only one failure mechanism instead of the absolute probability of failure. The absolute probability of failure is not necessary to determine the additional effect of storm-erosion on the probability of failure of the Pettemer sea defence.

6.3 Probabilistic methods

During the design stage of constructions it is customary to divide the used probabilistic methods into different levels. The different levels are as follows:

- Level III: Exact probabilistic approach, taking into account the probability distribution functions of all individual variables.
- Level II: Approximate probabilistic approach, that linearises the problem at a specified point (design point, the point with the highest possibility of occurrence).
- Level I: Design method that uses safety coefficients to incorporate uncertainties.

For a level II as well as a level III approach, the probability distribution function of all the random parameters involved, has to be known. [CUR 196, 1995]

6.3.1 Level III approach

The required sea defence height for a storm depends on several variables. For instance, the maximum required sea defence crest height for a specified year depends on the coincidental occurrence of the variables present for that year. An equal required sea defence crest height could be achieved by an infinite number of combinations.

required sea dike crest height ($h_{seadike}$) = f(x_1, x_2, ….., x_n)
with $h_{seadike}$ described by an undefined analytical function.

The probability that a certain level of sea defence crest height is reached or exceeded could be determined by multi-dimensional integration, if the probability density functions (PDF) of all random variables are known. The joint probability density function (JPDF) is integrated over the ‘unsafe’ region in order to acquire frequency of exceeding the limits, which accompanies it.

If e.g. the JPDF consists of 6 variables a six-fold integral has to be solved. This can be done numerical by integrating all 6 PDF's successively over the combination of parameters that result in an ‘unsafe’ situation. If the PDF of each variable is discretised by 10 steps, this would result in $(10)^6$ = 1,000.000 calculations. Considering the calculation time that UNIBEST-TC requires for each simulation would appear to make this method unattractive. Each simulation takes 1.5 minute resulting in a total simulation time of about 1000 days. Methods like for instance 'Importance Sampling' could reduce this calculation time significantly, however these methods are not considered.

Monte Carlo simulation
If the number of numerical integrations is large, a Monte Carlo simulation can be applied. By means of a random generator, random values can be generated from the actual parameter PDF. The result is a random combination of boundary conditions. For those combinations of boundary conditions the required sea defence crest height is computed with the local wave height and water level that are predicted by UNIBEST-TC. The maximum required crest height for each simulation is found during the maximum of the storm. If a sufficient number of combinations have been used (dependent on the probability of failure and accuracy) a reliable impression of the probability of failure can be determined. [CUR 190, 1997]

For a complete numerical integration, as for a Monte Carlo simulation, with sufficient simulations an exact and reliable result is achieved. However, two disadvantages appear. Firstly, the notion of the problem becomes unclear. Secondly, a large number of calculations have to be made in order to acquire an accurate result (95% reliable). Whenever the failure probability (P_f) is small, then more simulations have to be made. A probability of failure of about 10^{-4} per year is desirable; requiring a minimum of about 10^6 to 10^7 simulations (n) to be made, according to the following equation: [CUR 190, 1997]

$$n > 400\left(\frac{1}{P_f} - 1\right) \qquad (6.2)$$

6.3.2 Level II

In contrast to the standard Level III analyses, Level II provides the opportunity to take into consideration the effect of individual parameters on the variations in the probability of failure. This makes a level II analysis attractive, because additional information has been obtained.

The line of 'constant required sea defence crest height' is an unknown function described by all involved random parameters. If for instance, only two random variables (H_s and h_0) are used, the line of 'required sea defence crest height' is described by a function of Hs and h0. This function can be linearly approximated by a Taylor series from a random point (H_{s*}, h_{0*}).

$$H_{seadike}(H_s, h_0) = H_{seadike}(H_{s*}, h_{0*}) + \frac{\partial H_{seadike}}{\partial H_s}(H_s - H_{s*}) + \frac{\partial H_{seadike}}{\partial h_0}(h_0 - h_{0*}) \qquad (6.3)$$

with:	$H_{seadike}$ (H_s, h_0)	= a function of H_s and h_0	[m]
	h_0	= maximum water level	[NAP + m]
	H_s	= significant wave height	[m]
	H_{s*}, h_{0*}	= co-ordinates of design point	

The partial derivatives for h_0 and H_s are determined for the location that corresponds with the co-ordinates (H_{s*}, h_{0*}), also referred to as 'design point'. This point is also referred to as 'design point'. In the Level II analysis that has been used, the location of the design point on the line of 'constant required sea defence crest height' (Z=0 line) is the point that has a maximum probability density. The result of the linearisation is a tangent line through the design point. This tangent line can be interpreted as the approximate Z=0 line. The area above this tangent line determines the probability of failure. From the location of the design point compared to the location of the average variable values of the PDF the probably of exceeding the limits can be determined.

Since the tangent line is an approximation of the actual Z=0 line an error will occur. However, by using the design point (point of maximum probability density) the error will be minimised. All other possible tangent lines result in an increasing error.

When applying a level II analysis it is essential that all variables are described by normal distribution functions. Furthermore, all random variables have to be independent. However there are methods that be used to normalise variables (RF-algorithm) or make variables independent (Rosenblatt transformation). None of the previously mentioned criteria have been met. The random variables H_s and h_0 are dependent and h_0 is described by a non-normal distribution function. Other distribution functions can be normalised or in other words, approximated by a normal distribution function. However, the dependency between H_s and h_0 is more difficult to cope with. [CUR 190, 1997]

A model called 'PROBMOD' will be able to perform the level II computations [VOORTMAN, 2002]. This probabilistic model carries out the normalisation of non normal distribution functions as well as the entire level II computations. The result is characterised by several parameters. If only normal distributed functions are used and none of the parameters is correlated, the level II parameters are determined as follows. For the limit state function already shown, several multiple used parameters definitions are shown in the following intermezzo.

The limit state function: $Z = R - S$

The joint average: $\mu_Z = \mu_R - \mu_S$

The joint standard deviation: $\sigma_Z = \sqrt{\left(\frac{\partial Z}{\partial R}\sigma_R\right)^2 - \left(\frac{\partial Z}{\partial S}\sigma_S\right)^2} = \sqrt{\sigma_R^2 + \sigma_S^2}$

The reliability index (β): $\beta = \frac{\mu_Z}{\sigma_Z}$

The contribution of the individual stochastic parameters on the total probability:

$$\alpha_S^2 = \left(\frac{\frac{\partial Z}{\partial S}\sigma_S}{\sigma_Z}\right)^2 \cdot 100\% \qquad \alpha_R^2 = \left(\frac{\frac{\partial Z}{\partial R}\sigma_R}{\sigma_Z}\right)^2 \cdot 100\%$$

The probability of failure: $P_f = P(Z < 0) = \Phi\left(\frac{0 - \mu_Z}{\sigma_Z}\right) = \Phi(-\beta)$

Φ = the standard normal distribution function

The design point coordinates in the normalised area:

$$\mu_R^* = -\alpha_R \beta$$
$$\mu_S^* = +\alpha_S \beta$$

The design point coordinates in the RS area:

$$R^* = \mu_R + \alpha_R \beta \sigma_R$$
$$S^* = \mu_S + \alpha_S \beta \sigma_S$$

Intermezzo: Level II equations according used in the model 'PROBMOD' [VOORTMAN, 2002]

6.3.3 Level I

A Level I analysis is based on a deterministic approach. The design equations for this method have built in safety margins, or a safety factor. This usually results in a conservative, but safe approach. This level of analysis does not take into account parameter or model uncertainties with any accuracy; all possible uncertainties are combined within a set of safety factor.

6.4 Implementation

6.4.1 Method

In the previous paragraphs the theory and available probabilistic methods were discussed. The next stage is to use these methods to express the effects of morphology in terms of the probability of failure of the Pettemer sea defence. However, the situation is complicated by the use of the morphological model UNIBEST-TC. Due to this complex model the relations between the random parameters required for the design are unclear, and the relationships between the parameters are unknown. UNIBEST-TC uses several model parameters as well as input parameters to calculate morphological alterations. In turn these morphological alterations change the local computed parameters at the sea defence, which are used for the design of the sea defence.

Normally, the probability density functions of these local design parameters are used to determine the probability of failure. However, the PDF's have to be independent for a proper probabilistic analysis. Because the model generates the output parameters, they are dependent. Furthermore, due to the complexity of the model the exact dependency is unknown.

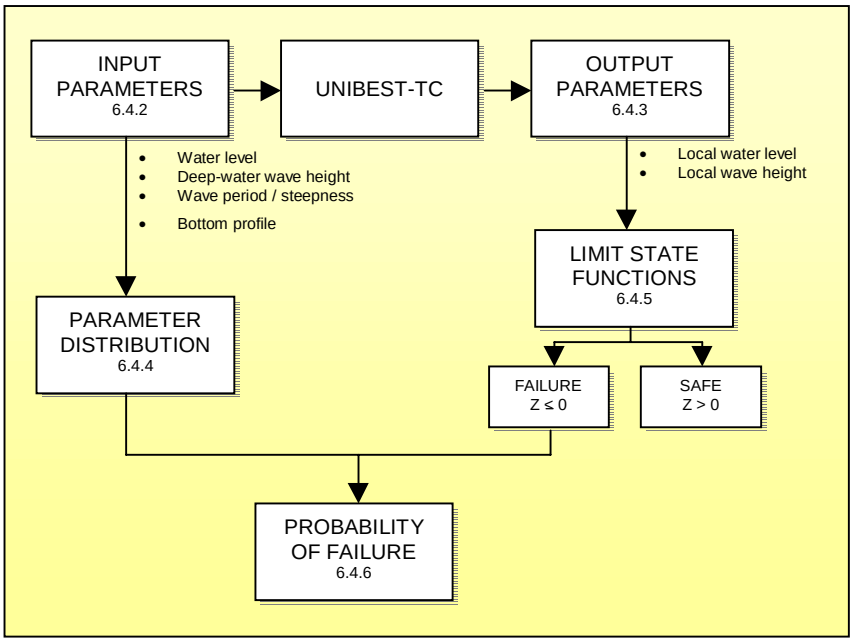

Figure 6.3: An overview of the method that has been applied to incorporate the UNIBEST-TC model results in a probabilistic analysis. The number shown in several boxes corresponds with a subparagraph for further explanation.

In Figure 6.3 the applied method has demonstrated. The random variables have been chosen as input, while the model is seen as a black box. Combinations of input variables together with constant model parameters, result in a combination of output variables that can be used in the limit state functions. The chosen limit state function, combined with the current sea defence crest height, results in two possible states: failure or safety. The joint probability that goes with the combination of input variables is used as the joint probability for the combination of output variables. The probability of failure is the sum of the probabilities of all combinations that lead to failure.

This method determines the probability of failure accurately, given that UNIBEST-TC has an accurate prediction capability, the parameter distribution is accurate and the limit state functions are valid for all possible combinations. However, predictions made by UNIBEST-TC have an error of about 20% for the local wave height. Furthermore, the limit state function has been represented by an equation that is valid for non-breaking waves. However the equation has a built in safety margin that results in an under-estimation of the probability of failure reducing the effect of neglecting breaking waves.

6.4.2 Input characteristics

To determine the wave height and water level at the sea defence toe, UNIBEST-TC has been used. Deep-water conditions have been combined with a specified seabed profile. The input conditions used for the UNIBEST-TC model simulations are as follows:

Storm characteristics
A storm can be characterised by several parameters. In UNIBEST-TC a storm can be described by water level and deep-water wave height. During a storm it is not likely that these parameters are kept constant. A storm builds up and then the weather returns to normal conditions. This process takes place over a certain amount of time. In reality a storm profile is never the same, however, it is desirable to use a standard storm profile. A standard storm profile makes it unnecessary to use a parameter that determines the storm course. During this analysis the storm profile is defined by the following parameters:

- Total storm period (T_{storm}). [hours]
- Maximum storm period (T_{max}). [hours]
- Time before storm starts (T_{start}). [hours]

In Figure 6.4 a trapezium has been used to characterise the standard storm profile, whereas in reality the storm profile shows a relatively irregular shape. Other shapes are also possible Vrijling and Bruinsma used a $\cos^2$ function to describe the storm profile. [BRUINSMA AND VRIJLING, 1980]

Simulation time: $T_{simulation} = T_{storm} + T_{start}$
Pre storm period: $T_{pre} = (T_{storm} - T_{max}) / 2$
After storm period: $T_{after} = (T_{storm} - T_{max}) / 2$

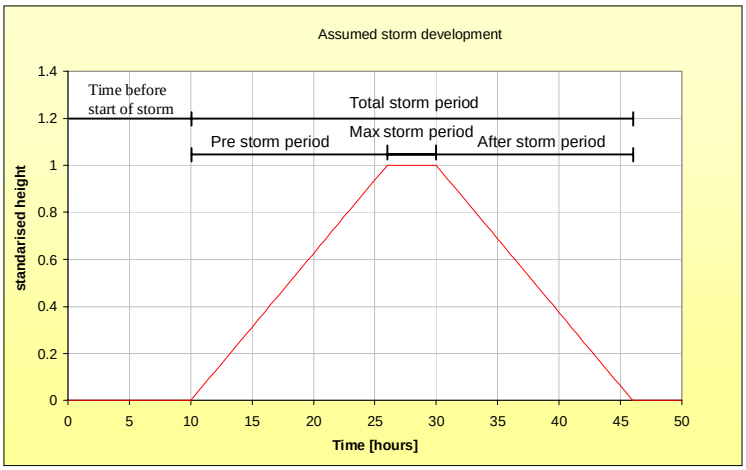

Figure 6.4: Assumed trapezoid storm profile.

The trapezium storm profile has been divided into 4 sub-function:

$S_{storm}(t) = 0;$ $t < T_{start}$
$S_{storm}(t) = (t-T_{start})/T_{pre};$ $T_{start} \leq t \leq T_{start} + T_{pre}$
$S_{storm}(t) = 1;$ $T_{start} + T_{pre} < t < T_{start} + T_{pre} + T_{max}$
$S_{storm}(t) = 1 - (t-T_{start}-T_{pre}-T_{max})/T_{after};$ $T_{start} + T_{pre} + T_{max} \leq t \leq T_{simulation}$

All other parameters depend on the storm profile. The $S_{storm}(t)$ function varies between 0 & 1.
The following fixed values are used during the probabilistic analysis:

- Total storm period (T_{storm}) = 36 [hours]
- Maximum storm period (T_{max}) = 4 [hours]
- Time before storm starts (T_{start}) = 10 [hours]

Water level characteristics

It has been assumed that two main aspects determine the water level:

- Tide (M_2)
- Storm Setup

In reality several other factors also cause variation in the water level, e.g. pressure differences and wind oscillations. The tide will be described by the M_2 component; the other components are not taken into account. Firstly, the exact timing of a super storm cannot be determined, and the probability that a storm occurs simultaneously with spring tide is also not taken into account. Secondly, multiple order tide components are of less effect on the water level. The tide is described as follows:

$$h_{tide}(t) = h_{range}/2 \sin(2\pi t/T_{tide} - T_{phase})$$

$h_{tide}(t)$ = Water level due to tidal variation [m]
h_{range} = Tidal range [m]
T_{tide} = tidal period [hours]
T_{phase} = phase shift [hours]

The storm setup is dependent on the storm characteristics. The following formulation has been used:

$$h_{setup}(t) = h_{max} * S_{storm}(t)$$

$h_{setup}(t)$ = Water level due to storm setup [m +NAP]
h_{max} = Maximum water level [m +NAP]

$$h_{water}(t) = h_{setup}(t) + h_{tide}(t)$$

Due to the possibility that spring tide and the maximum water level occur simultaneously, it is possible that a value for the water level is found that exceeds the maximum water level (h_{max}). Therefore a correction has been introduced. This correction constant equals the maximum difference between h_{max} and h_{water} for all values of h_{water} that exceed h_{max}. The function is described as follows:

$Max(h_{corr}) = h_0(t) - h_{max};$ for $h_{water}(t) > h_{max}$

The correction constant transposes the entire function to ensure that the maximum value of the water level equals the h_{max} value. Finally the water level (h_0) is described as follows:

$$h_0(t) = h_{setup}(t) + h_{tide}(t) - max(h_{corr})$$

In the following Figure 6.5 the different components as well as the functions of the water level (h_0) are shown. The maximum setup varies in height and is a random variable. The variable water level is used as input in UNIBEST-TC. The following fixed parameter settings are used:

h_{range} = 1.4 [m]
T_{tide} = 12.25 [hours]
T_{phase} = 2.5 [hours]
h_{max} = 5.0 [m] stochastic variable

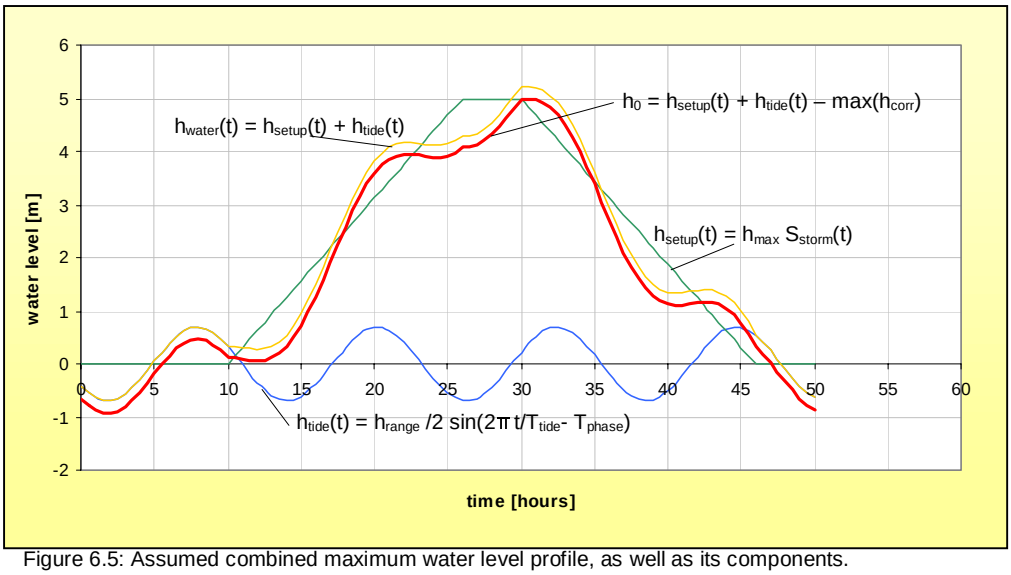

Figure 6.5: Assumed combined maximum water level profile, as well as its components.

Wave characteristics

The wave height has been assumed dependent on the $S_{storm}(t)$ parameter. The wave height will be described by two parameters:

H_s = pre storm significant wave height [m]
$H_{s,max}$ = maximum significant wave height during storm [m]

The variable wave height used as input for UNIBEST-TC has been described as follows:

$$H_{s,0}(t) = H_s + (H_{s,max} - H_s)* S_{storm}(t)$$

The results are shown in the following figure. The averaged wave height, according to the analysis of Roskam, is about H_{m0}= H_s= 1.2m. [ROSKAM, 1988] However, this is the averaged wave height during summer and winter conditions. Prior to a storm it is likely that wave height increases. Therefore a minimum wave height of H_s = 2m has been chosen. The maximum wave height is a random variable and this value will differ during the simulations. However, in the example in Figure 6.6 a value of $H_{s,max}$ = 7.05m has been used.

In UNIBEST-TC the wave height has been characterised by the root-mean-square wave height (H_{rms}) instead of the significant wave height (H_s). Both wave heights are shown in Figure 6.6.

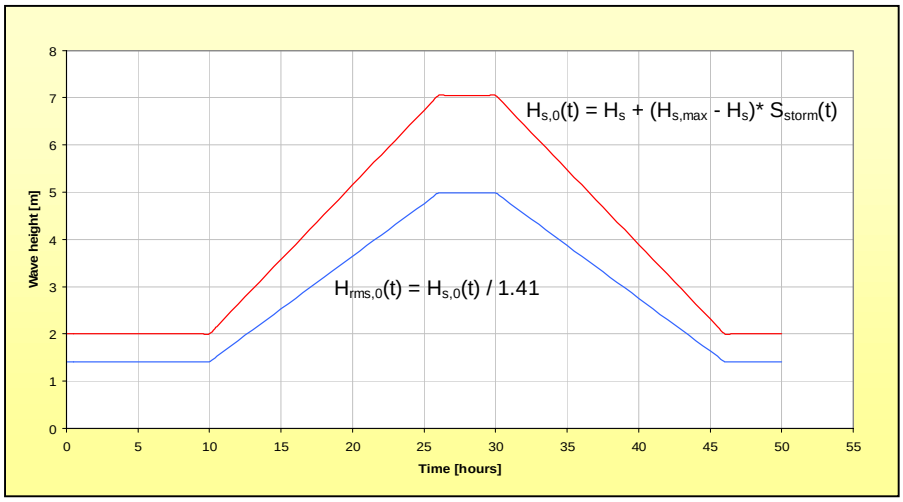

Figure 6.6: Wave height profile over the assumed period of storm.

Wave steepness and peak wave period

The wave steepness parameter (s_{rms}) has been used to link the required wave period to the variable wave height. During most of the simulations a constant wave steepness of 0.025 (2.5%) has been applied. The wave period is characterised by the peak period (T_p). This results in a peak wave period that is the square root of the wave height according to the following relation:

$$T_p = \sqrt{\frac{H_{rms}}{s_{rms}} \frac{2\pi}{g}} \qquad (6.4)$$

The peak period course in UNIBEST-TC has been shown in Figure 6.7, for a wave steepness of 0.025 and a wave height (H_{rms}) of 5m.

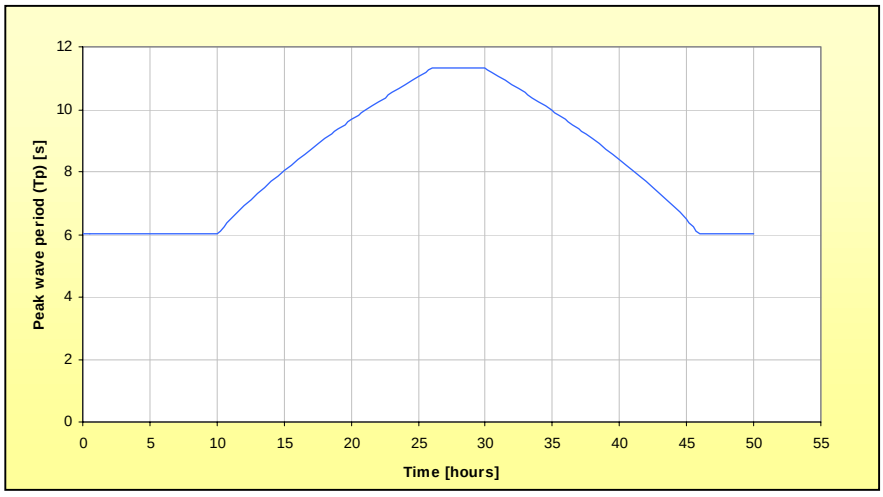

Figure 6.7 Peak wave period profile over the assumed storm period.

Seabed profile

The seabed profile used in UNIBEST-TC was surveyed in October 1999. This profile has been used during the parameter analysis in the previous Chapter and is shown in Figure A11.1 in Appendix 11.

6.4.3 Output characteristics

After the definition of the UNIBEST-TC input parameters the output parameters are discussed. Currently only two parameters are required:

- The local wave height at the toe of the sea defence (x=0).
- The local water depth at the toe of the sea defence (x=0).

Both parameters vary in time as a result of the morphological alterations and the variable input. Only the combination that results in a maximum load on the sea defence during the simulation is of interest. This maximum load has been determined by the limit state function as is described in Subparagraph 6.4.5. For each combination of input parameters the maximum load has been. Resulting in the matrices shown in Appendix 15

6.4.4 Random parameters

It is essential that accurate and credible probability distribution functions are available for all random parameters. However, it appeared to be difficult to determine a representative probability distribution for most parameters, due the absence of extreme conditions during survey periods.

The distribution functions of the random variables deserve some attention, because they will affect the final outcome of the probabilistic calculations to a large extent.

During this thesis just two random parameters have been taken into account:

- High water level.
- Deep-water wave height.

Water level distributions

The water level corresponding with the annual probability of exceeding the limits set by the government in case of the Pettemer sea defence is 10^{-4}. The water level exceedance lines have been determined by extrapolating measured historical data. The error due to the extrapolation has not been taken into account in the frequency of exceedance function.

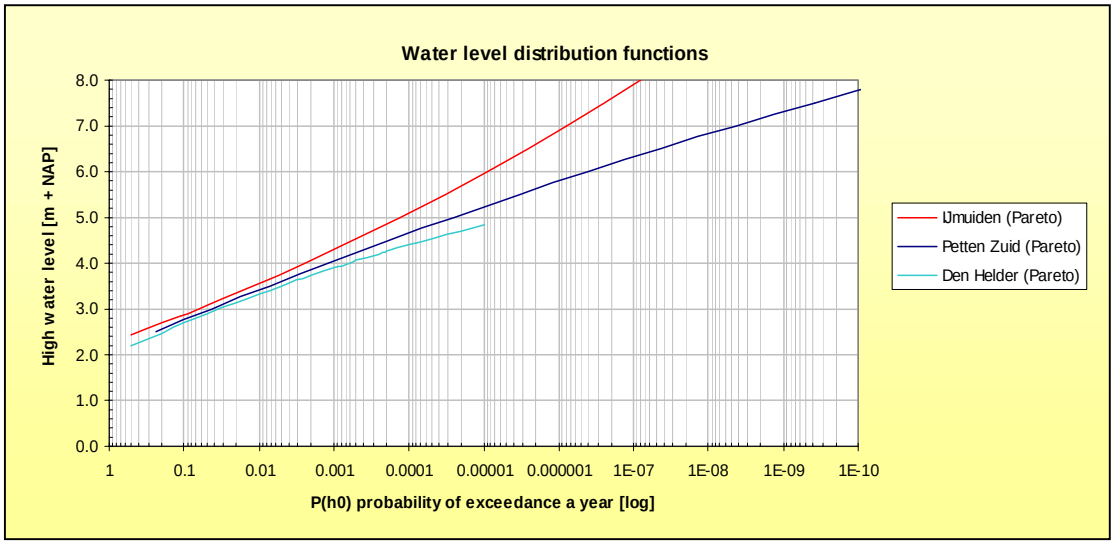

Figure 6.8: Probability of exceedance per year for the water level at IJmuiden, Petten and Den Helder.

It is possible to forecast within a given year with a reasonable accuracy, whether the storm surge level has been reached or exceeded. In Figure 6.8 the probability of exceedance line for high water levels has been plotted for three locations along the coast and these lines show that the water level height exceedance varies along the Dutch shoreline. IJmuiden and Petten are 40km from each other, but extreme high water levels occur more frequent at IJmuiden (south) than at Petten. These frequencies of occurrence (q) are determined by the following equation [PHILLIPPART, ET AL., 1995]:

$$q(x) = \frac{1}{2}\left(1+\frac{\gamma}{\sigma}(x-u)\right)^{-\frac{1}{\gamma}} = P_c \cdot f_{GPD}(x,k,\alpha,\xi) \qquad (6.5)$$

With the following values for location YM6 near IJmuiden:

Shape factor γ	= 0.03326	[-]
Scale factor σ	= 0.2722	[-]
Location factor u	= 2.42	[m]

This equation equals a Generalised Pareto Distribution (GPD) PDF whenever the frequencies are small (<0.1) under the condition that a storm is presence (P_c factor). The probability that a water level occurs while a storm is active equals the product of the conditional probability for a water level given the fact that a storm occurs and the probability that a storm occurs. [VRIJLING, 1996]

$$P(x \cap storm) = P(x \mid storm) \cdot P(storm) = P_c \cdot f_{GPD}(x,k,\alpha,\xi) \qquad (6.6)$$

The GPD with shape factor (k), scale factor (α) and location factor (ξ) is characterised by the following functions [GELDER VAN, 2000]:

Density function: $$f_{GPD}(x) = \frac{1}{\alpha}\left(1-k\left(\frac{x-\xi}{\alpha}\right)\right)^{\frac{1}{k}-1} \quad \text{if } k<0,\ x<\xi+\frac{\alpha}{k} \qquad (6.7)$$

Distribution function: $$F_{GPD}(x) = 1-\left(1-k\left(\frac{x-\xi}{\alpha}\right)\right)^{\frac{1}{k}} \quad \text{if } k<0,\ x<\xi+\frac{\alpha}{k} \qquad (6.8)$$

Quantile function: $$x(F_{GPD}) = \xi+\frac{\alpha}{k}\left(1-(1-F)^k\right) \quad \text{for } 0<F<1 \qquad (6.9)$$

Whenever the following parameters are used the PDF equals the frequency function (6.5) for small frequencies (<0.1):

$$u=\xi,\ \gamma=\frac{k}{k-1},\ \sigma=\frac{\alpha}{1-k},\ P_c=\frac{\alpha}{2} \rightarrow q(x)=\frac{1}{2}\left(1+\frac{k}{k-1}\cdot\frac{1-k}{\alpha}(x-\mu)\right)^{\frac{1-k}{k}} \qquad (6.10)$$

Vrijling and Bruinsma have described a method that determines a distribution function taking into account astronomical tide and storm surges. The distribution of extreme high water levels for locations along the Dutch shoreline is stated in [PHILLIPPART, ET AL., 1995]. The suggested probability distribution is a Pareto distribution function for yearly maximum high water levels. This Pareto distribution is only valid for water levels that exceed the u. Probabilities of lower water levels can be described by the yearly frequencies of exceedance. However, these conditions are of little interest because they are no threat.

Deep-water wave heights

The maximum deep-water wave heights exceedance depends on several factors. Firstly, all waves are generated by wind. The following factors influence the wave growth: wind speed, fetch (geometry), direction, duration and deep-water depth. However storms conditions also contribute to high water levels, resulting in a correlation between water levels and wave heights.

Extreme wave heights have severe consequences for coastal structures, therefore the frequency of an extreme wave event is of great importance. The design of civil engineering structures and risk insurance calculations rely on knowledge of the frequency of these extreme events. Estimation of these frequencies is difficult, because extreme events are by definition rare and data records are often small or incomplete. In other words: the uncertainty about the distribution analysis of wave heights is significant. [GELDER VAN AND VRIJLING, 1999]

Because wave heights depend on water levels the wave height has been divided into a water level dependent part and an independent part as follows:

$$H_{s,0} = H_{s,0}\left(h_0\right) + H_{s,0}\left(H_{HS}\right) \tag{6.11}$$

The water level dependent part has been defined according to the next equation [BRUINSMA AND VRIJLING, 1980]:

$$H_{s,0}\left(h_0\right) = a + bh_0 - c\left(d - h_0\right)^e \qquad \text{for } h < d$$

$$H_{s,0}\left(h_0\right) = a + bd + b\left(h_0 - d\right) \qquad \textit{otherwise}$$

This water level dependent part has been plotted in Figure 6.9.

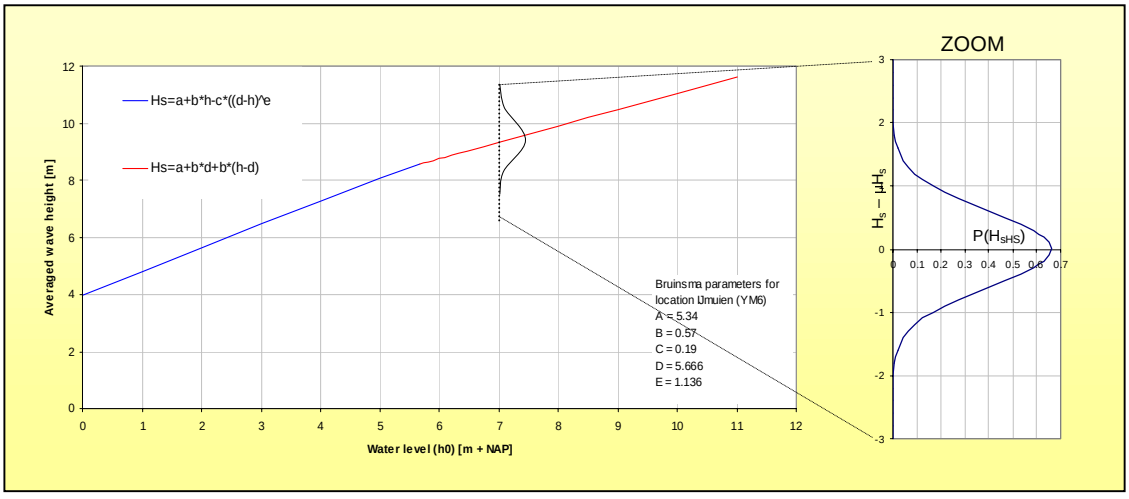

Figure 6.9: The relation between the averaged wave height and the water level according to Bruinsma and Vrijling [1980] for IJmuiden (YM6), including the normal distribution for the independent part of the wave height described by van de Graaff [1984].

The second stochastic independent part has been defined by means of a normal distribution function. The averaged and the standard deviation are also referred to as location parameter and scale parameter respectively. The normal density function has been shown below:

$$f\left(x\right) = \frac{1}{\sigma\sqrt{2\pi}} e^{-\frac{1}{2}\left(\frac{x-\mu}{\sigma}\right)^2} \tag{6.12}$$

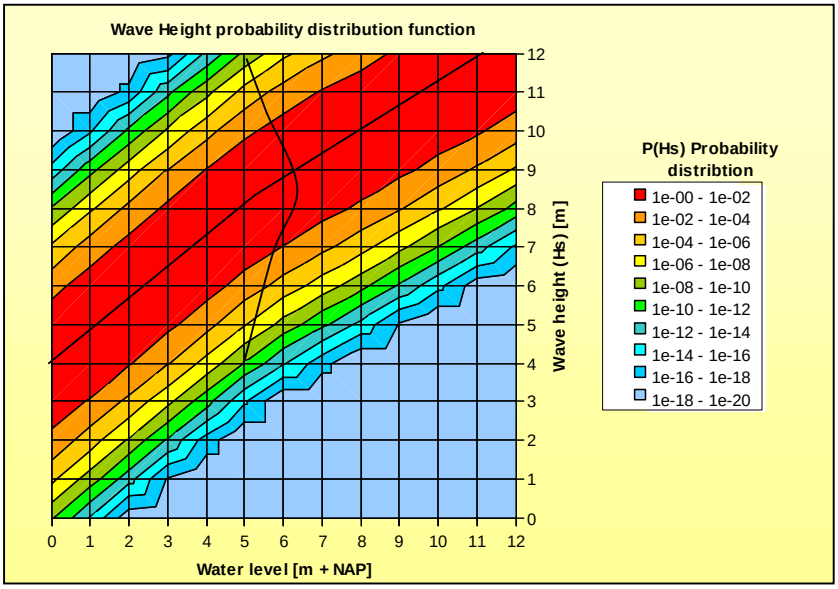

Figure 6.10: Combined wave height distribution for different water level.

The normal density function shown above has a gaussian curve mirrored around the averaged. Let *F(x)* denote the cumulative distribution function for the normal distribution with location parameter μ and scale parameter σ, let Φ denote the standard normal distribution function.

$$F(x) = \Phi[(x - \mu) / \sigma] \qquad (6.13)$$

$$F^{-1}(p) = \mu + \sigma \Phi^{-1}(p) , \qquad \text{for } 0 < p < 1 \qquad (6.14)$$

The averaged (μ) of 0.0 and a standard deviation (σ) of 0.6 have been applied [GRAAFF VAN DE, 1984]. Whenever the separate parts of the wave height function are combined, the result shown in Figure 6.10 has been generated. Figure 6.10 shows the probability of exceedance per year for the wave heights with respect to the water level. The averaged value equals the wave height determined by the Bruinsma equation, corresponding with a probability of 0.665. The probability is displayed by contour lines based on a logarithmic scale.

The wave heights probability distribution is described by two functions. The resulting probability distribution has only one drawback. Because of the use of a normal distribution for the deviation from the averaged wave height [BRUINSMA AND VRIJLING, 1980], it is possible that a negative wave height occurs. Negative wave heights are impossible and for relatively low water levels this approach is inadequate. Furthermore waves that exceed the product of the breaker index (Appendix 8) and the water depth are also not possible. Whenever it is necessary to take into account these aspects it is recommended to use a lognormal or truncated distribution.

Joint probability density function

The joint probability density function (JPDF) shows the probability of the exceedance for a combination of the both random parameters. The mutual probability density is defined as follows:

$$f(H_s, h_0) = f(h_0) \cdot f(H_s | h_0) \qquad (6.15)$$

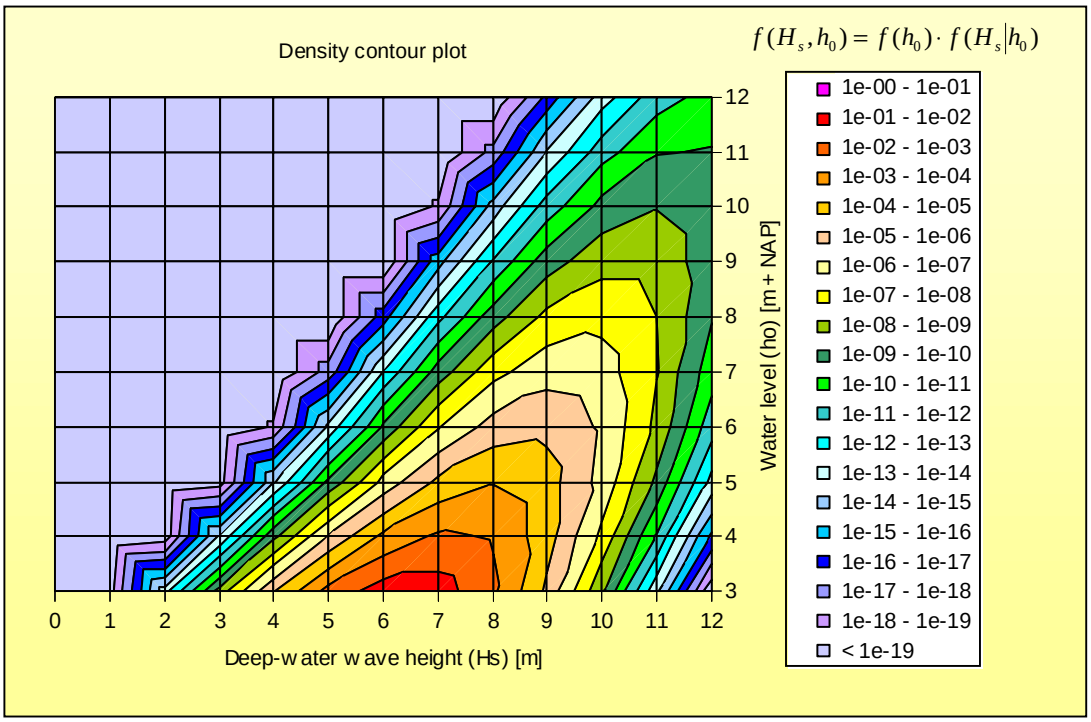

Figure 6.11: Joint probability density function for deep-water wave heights and water levels. (log scale)

In case of independent random parameters the JPDF is characterised by circular or elliptical contour lines perpendicular or parallel to the axis. However in this case the random parameters, water level and deep-water wave height, are dependent, resulting in oblique elliptical contour lines. The JPDF has been shown in Figure 6.11. The probability has been shown by contour lines that are based on a logarithmic scale. Water levels of 3m + NAP accompanied by deep-water wave heights of 6m correspond with a probability of exceedance per year between 0.1 and 0.01. This combination will be exceeded most often, according to Figure 6.11. A combination of 12m high water levels and 12m high waves will practically never occur or be exceeded.

6.4.5 Limit state functions

Limit state functions are used to determine whether failure occurs during the combination of random parameters examined. The currently used limit state function has been based on just one failure mechanism, whereas sea defences have several failure mechanisms. For a proper comprehensive probabilistic approach it is advisable to determine all failure mechanisms and develop a failure tree. However the problem has been simplified: only one single failure mechanism has been taken into account: 'wave run-up'. This is acceptable because only the relative effect of storm-erosion on the sea dike probability of failure is studied. Wave run-up is the mechanism that represents the greatest contribution of storm-erosion on the probability of failure.

The following limit state function for the failure mechanism 'wave run-up' has been applied:

$$Z = h_{crest} - h_{run-up} \quad (6.16)$$

h_{run-up}	= the required sea dike crest height based on the hydraulic conditions.	[m]
h_{crest}	= the actual crest height of the sea defence.	[m]

The limit state function exists of two parameters that both indicate a certain crest height. Whenever the actual crest height (h_{crest}) is exceeded by the required crest height based on the run-up level (h_{run-up}) failure occurs.

The actual sea defence crest height and strength are surveyed once every 5 years. The sea defence crest level is 12.95m + NAP. During this analysis the crest height is a deterministic parameter and will be kept constant. However it is possible to describe the surveyed crest height as a random variable. Measuring errors or a standard deviation due to variations in sea defence height would be taken into account if a random approach had been applied.

The required sea defence crest height equals the runup level (h_{run-up}) during this thesis and can be described by several equations. One of the most basic design equations has been used to describe the wave run-up process has been chosen:

$$h_{run-up} = h + 8H_s \tan(\alpha) \quad (6.17)$$

h	= Local water level in front of the sea dike (incl. setup and tide)	[m + NAP]
H_s	= Local significant wave height at the sea dike	[m]
Tan (α)	= Averaged slope of the sea dike	[m]
h_{run-up}	= Run-up level (equals the require crest height)	[m + NAP]

This equation is generally used to obtain a first impression. This basic equation is a non-breaking design equation, however reasonable results are still expected because a relative crest height determination is expected. A constant slope of 1:4 has been used to describe the slope steepness of the Pettemer sea defence instead of a variable slope determined by the local water level. The local wave height and water level are based on combinations of deep-water variables that have been used as input for the UNIBEST model. The limit state function is than described as follows:

$$Z = h_{crest} - \left(h_{(H_{s,0},h_0)} + 8H_{s,(H_{s,0},h_0)} \tan(\alpha) \right) \quad (6.18)$$

The design function that has been used to establish the limit state function has a built in safety margin. Consequently a significantly higher probability of failure will be computed. The over-estimation will be in the order of magnitude of a factor 10.

Furthermore, the local determined parameters are, except for the two random parameters, also dependent on the model parameters and the other input factors. In Paragraph 5.5 several parameters are examined that have a significant effect on the computed local wave height and local erosion depth. The local water level is more constant whenever the parameters are varied.

Next to the parameters dealt with in Paragraph 5.5 the following factors also effect the accuracy and the probability of failure, when computed by the method used:

- Obstacles the nearshore area.
- Sea defence strength, length and protection.
- Effect of a non-uniform coastline.
- Sea level rise.

6.4.6 Probability of failure

Finally the probability of failure can be determined. The probability of failure (P_f) equals the sum of the probabilities that result in a negative limit state. The computed failure probability can be compared with the desired failure probability, taking into account that the failure probability is over-estimated due to the built in safety margins in the limit state function.

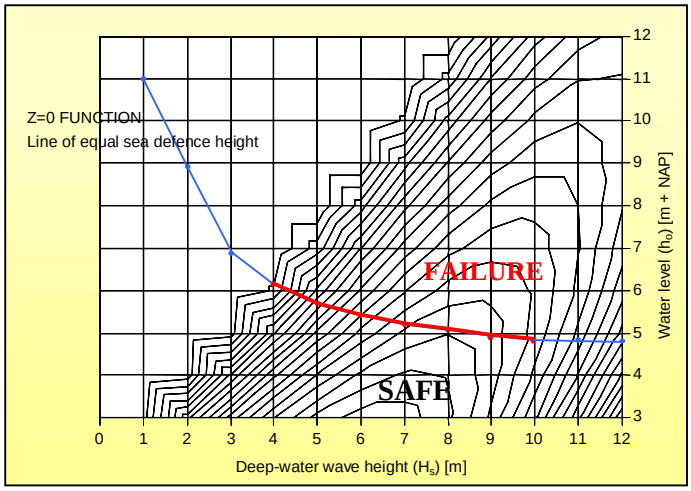

Figure 6.12: Joint probability density function combined with the limit state function (Z=0) dividing the total area into failure and safe. The blue part of the limit state function has been estimated by $8H_s\tan\alpha$, the red part is actually calculated with the previous mentioned limit state function and UNIBEST-TC calculations.

Whenever the probability distribution functions of all random parameters and the limit state functions are known the probability of failure can be determined. In Figure 6.12 the failure area (Z<0) has been shown.

6.5 Level III approach

The level III approach has been executed according to the Riemann integration [CUR 190, 1997] has been used to obtain a first impression. The actual probability of failure and the difference in probability between dynamic and non-dynamic are the main area of interest. This method integrates the density functions of all the random parameters over the area of failure, using a matrix that represents the joint probability density function of the two main random variables (water level and deep-water wave height). Each cell representing a certain combination of random parameters has a probability of exceedance. The probability of exceedance for each cell equals the product of the probability from the JPDF and the cell dimensions. Next, the cell's probability of exceedance within the area of failure can be added. The limit state function based on the UNIBEST-TC results has been used to determine the area of failure. This entire procedure is shown in the following Figure 6.13, however to assist explanation, the applied probabilities are theoretical. Furthermore the theoretical definition is shown in the following equation.

$$P_f = \iint_{z\le 0} f(r,s)\cdot dr\cdot ds = \sum_{\substack{i=1 \\ s.t.}} \sum_{\substack{j=1 \\ z\le 0}} f(r_i,s_i)\cdot \Delta r_i \cdot \Delta s_i \qquad (6.19)$$

P_f = Probability of failure.
f(r,s) = Joint probability density function for resistance and load.
r = Resistance.
s = Load.
i,j = Indices for resistance and load.

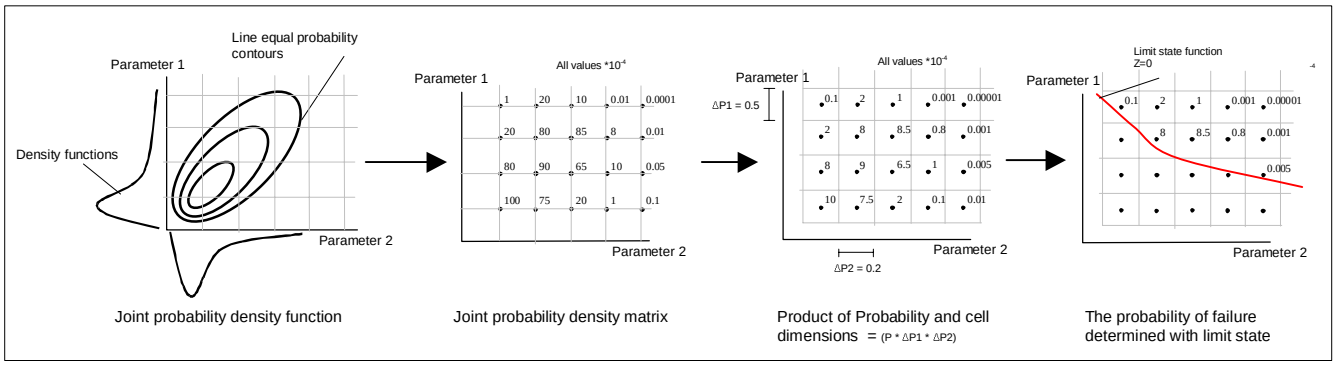

Figure 6.13: Riemann level III procedure.

Failure procedure

Sometimes the UNIBEST-TC simulation is aborted. This happens in about 5 to 10% of all simulations. The aborted simulations are easily tracked because they require less memory. Fortunately UNIBEST-TC simulations abort almost randomly, resulting in a gap surrounded by proper simulations. The gap is recovered by linear interpolation.

Matrices

Two matrices are used for the level three calculations.

- The JPDF matrix.
- The limit state matrix as a result of the UNIBEST-TC simulations.

The JPDF matrix is a matrix built by the random parameters involved. As has been shown in Figure 6.13. However, an infinite number of combinations of deep-water wave height and water level are possible, whereas a limited number of UNIBEST-TC simulations are performed. The limit state function matrix, based upon the result of UNIBEST-TC simulations, has been concentrated on the combination of random parameters with a high probability that follow from the JPDF matrix. Furthermore, the location of the limit state function (z=0) has been determined by linear interpolation with the limit state function matrix. The next set of simulations that forms another limit state matrix has been concentrated on the area just above the limit state function (the failure area). The simulation needed for the limit state function matrix has been shown in Figure 6.14. Combinations with higher water levels are also not of interest, because the probability of exceedance is really small.

Whenever the possibilities outside the UNIBEST-TC matrix are taken into account the probability increase with less than 1%.

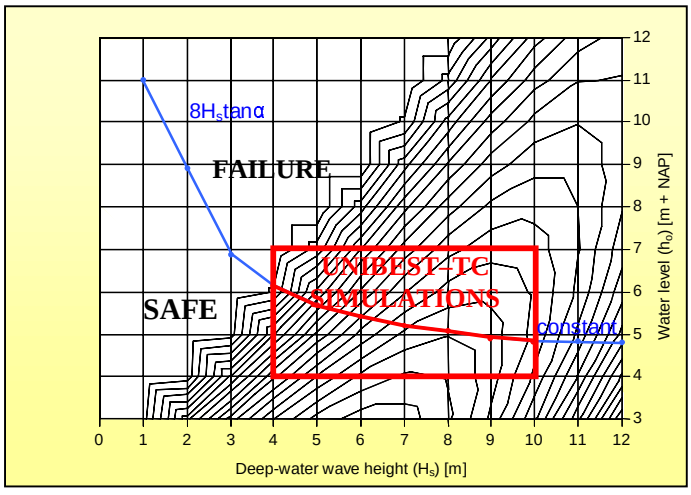

Figure 6.14: The area of UNIBEST-TC simulations has been shown in the JPDF diagram accompanied by the limit state function (z=0). The actual matrices that are computed by UNIBEST-TC and the limit state function are shown in Appendix 15.

Matrices grid

It is obvious that this type of level III method is reasonably sensitive for the applied grid of both matrices. The number of simulations made in UNIBEST-TC determines the grid size of the limit state function (Z=0) matrix. However the grid of the JPDF matrix used to determine the probability of failure can also be varied. The accuracy of the applied method increases whenever higher matrix grid resolutions are applied. The limit state function (z=0) that follows from the limit state function matrix by linear interpolation crosses a cell in the JPDF matrix, the probability of that cell contributes entirely to the probability of failure.

It is possible to increase the grid resolution without additional simulations by linear interpolation of the limit state function matrix. Linear interpolation can be justified because the limit state functions appear to show a continuous course. The JPDF matrix is based on the probability density functions and can be chosen as fine as necessary. By increasing the number of grid points the probability of failure can be determined more accurately. In table 6.15 the sensitivity has been shown for an actual set of UNIBEST-TC simulations used to construct a limit state function matrix. According to the results shown, the probability shows a convergence course whenever the resolution of the JPDF matrix has been increased. It appears, however, that an increase of resolution for the limit state function matrix hardly contributes to an increase of accuracy.

Table 6.15: Probability of failure for different grid sizes. (The grid is determined as H_s*h_0)

				Joint probability density function matrix				
Limit state function matrix			Grid	33 * 14	65*8	65*14	65*27	65*65
$\Delta H_{s,0}$	Δh_0	Grid	# Cells	462	520	910	1755	4225
0.2	0.25	33*14	462	$4.53 \cdot 10^{-5}$	$4.41 \cdot 10^{-5}$	$4.43 \cdot 10^{-5}$	$4.47 \cdot 10^{-5}$	$4.45 \cdot 10^{-5}$
0.4	0.25	17*14	238	$4.53 \cdot 10^{-5}$	$4.39 \cdot 10^{-5}$	-	-	-
0.8	0.25	9*14	126	$4.53 \cdot 10^{-5}$	-	-	-	-
1.6	0.25	5*14	70	$4.53 \cdot 10^{-5}$	-	-	-	-
0.8	0.125	9*7	63	$4.53 \cdot 10^{-5}$	-	-	-	-
1.6	0.125	5*7	35	$4.53 \cdot 10^{-5}$	-	-	-	-
6.4	0.125	2*7	14	$2.87 \cdot 10^{-5}$	-	-	-	-

The probabilities of failure determined shown in Table 6.15 are quite low. However the intension is to determine the relative contribution of storm-erosion and not the absolute. The reason for these low probabilities is found in the use of a limit state function that is only valid for non-breaking conditions as well as the fact that only one failure mechanism has been used instead of all possible failure mechanisms.

Effect of storm-erosion

The effect of morphology has been determined for the seabed of 1999. The limit state functions (Z=0) that follow from the UNIBEST-TC simulations are shown in Figure 6.16. One set of UNIBEST-TC simulations has been represented by the red line and has been based on a dynamic set of simulation, whereas the other set has been represented by the blue line and has been based on static simulations. During dynamic simulations the seabed profile can adapt to the prevailing wave conditions while during the static simulations this seabed remains constant. It is assumed that the difference between both simulations equals the effect of the storm-erosion.

The difference between both limit state lines (Z=0) is hardly visible; the effect of storm-erosion is therefore minuscule. Whenever the effect is expressed in terms of probability of failure the storm-erosion results in an increase of the probability of failure with 0.18 $*10^{-5}$ per year, this corresponds with an increase in crest level of 15mm. It can be concluded that the effects of storm-erosion can be neglected, assuming that UNIBEST-TC results in accurate output.

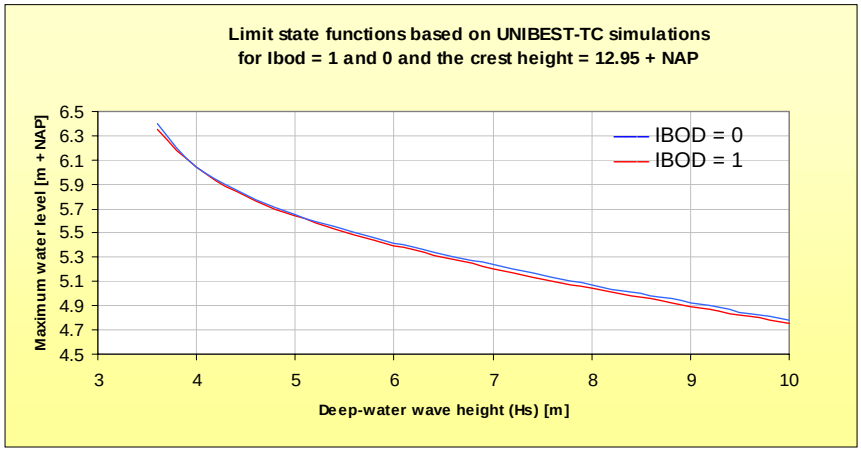

Figure 6.16: The limit state functions based on UNIBEST-TC simulation for the seabed of 1999; dynamic simulation (red) and static simulations (blue).

Whenever by a 3D model would have been used to simulated storm-erosion a different result could have been found, because the restriction in UNIBEST-TC that no sand can be lost, results in sediment relocation over the profile stretch. In a 3D model the sediment can also be relocated in longshore direction possibly resulting in local channels due to an irregular wave pattern. These locally deepened channels could significantly contribute to the wave propagation over the local profile stretch, because waves propagate more easily. The probability that such a local channel occurs increases with the longshore length of the structure.

Variation of the local wave height and local water level during a storm simulation

The computed crest height, seabed, wave height and water level variation during a dynamic simulation have been shown in Figure 6.17, compared to those of a static simulation. The run-up level has been determined along the simulation time. In this figure the run-up level variation has been indicated by the line (h_{run-up}/max(h_{run-up}). The maximum crest height determined (t=1.17 days) for a combination of deep-water wave height and water level has been used as input during the probability analysis. The increase in run-up level for a dynamic simulation has been compared with a static simulation. The red line shows the differences in the computed run-up levels. Two other lines indicate the increase in local wave height and water level due to the seabed alterations. The bed level for the location at the sea defence toe increases during low impact conditions (< 0.3 days), while the bed level decrease during severe conditions.

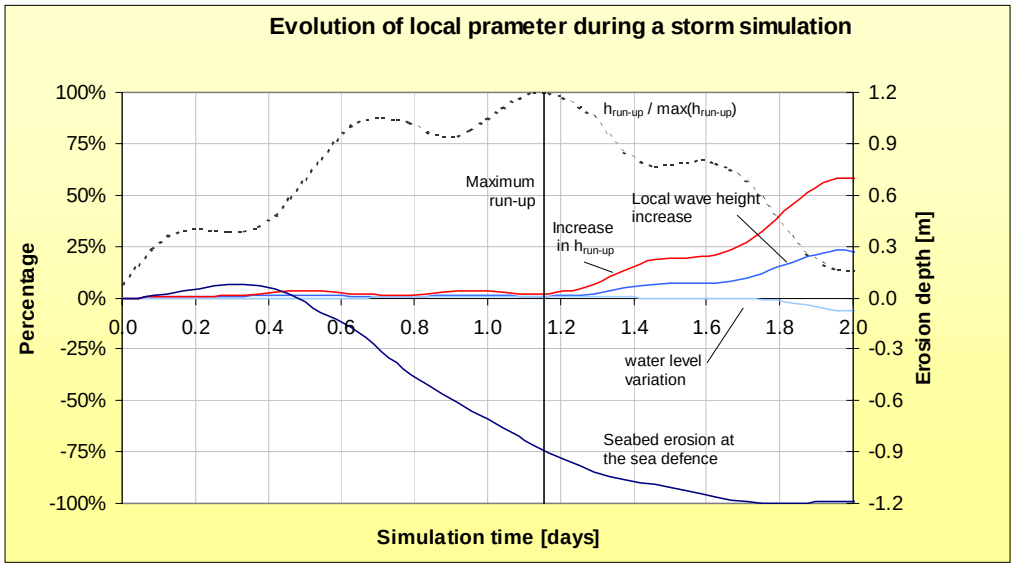

Figure 6.17: Comparison of the local parameters at the sea defence toe determined by UNIBEST-TC during a simulation of storm for a dynamic and static simulation at x=0.

Although the seabed has been eroded for 0.90m up to the storm maximum, the wave height growth as well as the water level rise is hardly visible. Only just after the maximum impact of the storm these local parameters start to vary compared to a static simulation. In Figure 6.18 the effect of the storm is shown. The sand is relocated seaward and the waves start to break further offshore (green line). At location x=0 the wave height remains reasonably constant whereas the seabed erodes significantly.

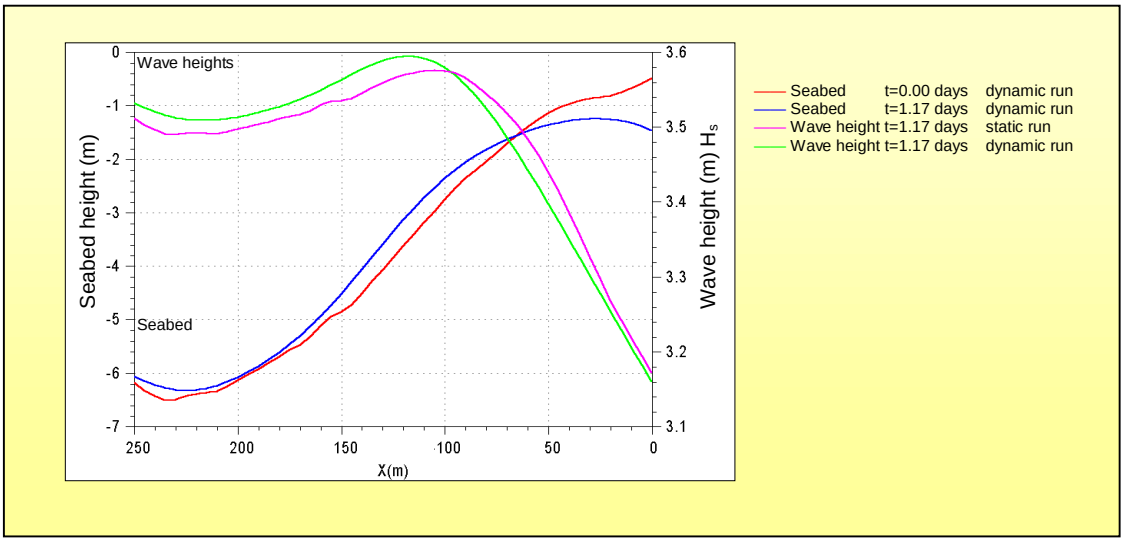

Figure 6.18: Seabed variation during a storm simulation in UNIBEST-TC. The storm is similar to the storm shown in figure 6.17.

Effect of a different initial seabed level

To show the affects of a different initial seabed level the surveyed profile of 1990 has been compared with the profile of 1999. The 1990-profile has a significantly steeper bed slope and the level of the nearshore area in front of the sea defence is situated 2 to 2.5m lower. Furthermore, the sand volume over the profile stretch (1200m) has been reduced with 870m^3/m in total. The combination of these adaptations results in a significantly greater load on the sea defence, due to the reduction of dissipation. Consequently the limit state function will be different from that computed limit state function with the surveyed seabed of 1999. The results are shown in the Figure 6.19.

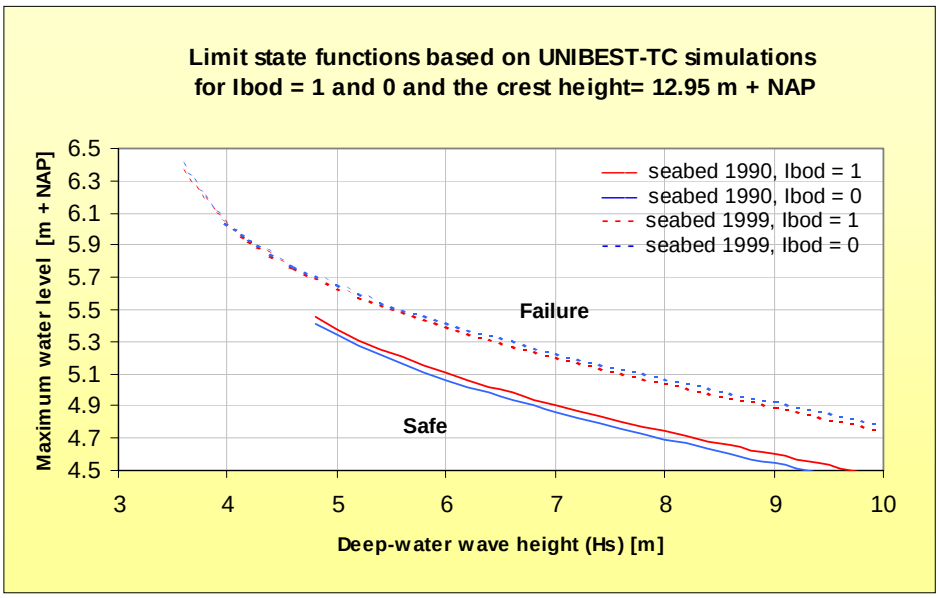

Figure 6.19: The limit state functions based on UNIBEST-TC simulation on the seabed of 1990 for dynamic (red) and static (blue) runs compared with the limit state functions of 1999 (dashed).
IBOD = 1 means a dynamic seabed during the simulation
IBOD = 0 means a fixed seabed during the simulation equal to the present evaluation methods.

The limit state function has dropped, due to the increase in load. The probability of failure has doubled to $1.11*10^{-4}$ per year (blue line) for static runs, whereas the dynamic set of simulations corresponds to a probability of failure of $9.69*10^{-5}$ per year (red line). The difference in probability of failure between the 1999 and 1990 seabed corresponds with a difference in sea defence crest height of about 0.50m. However, it is peculiar to observe that during the simulation with the 1990-seabed the limit state line rises whenever storm-erosion has been incorporated. This implies that due to the storm-erosion the situation becomes safer, whereas this is probably not the case.

To simulate the steep seabed profile of 1990 the internal friction coefficient (TANPHI) has been set to 0.3 instead of 0.1 that has been used during the simulations on the 1999 seabed. Therefore steeper steeper slopes are possible resulting in a different profile alterations combined with the different pre-storm shape this has resulted in a decrease of the load.

6.6 Evaluation

Results
During this analysis a level III approach has been used to determine the effects of storm-erosion predicted by UNIBEST-TC. According to these predictions the effects are rather small. In case of predicted erosion in the order of magnitude of one meter the increase in crest height or variation in failure probability is less than 1%. Consequently, the effects of storm-erosion can be neglected during the determination of the sea defence crest he ight.

Furthermore, two different seabed profiles have been examined. The seabed varies significantly over the years according the JARKUS data set, resulting in a large variety of profiles. Both profiles chosen differ significantly in sand volume. The 1990 seabed profile has a bed level in the nearshore area that lies about 2m deeper than the 1999 seabed profile. This differences in bed level result in a difference of 0.50m in crest height. The seabed variation due to storm-erosion remains small in both cases. However, the contribution of the storm-erosion appears to oppose for both profiles. During relatively high seabed levels the storm-erosion intensifies the storm impact, however during relatively low seabed levels the impact has been opposed by storm-erosion.

Assumptions for the probabilistic approach
The probability of failure has been expressed for an individual cross-section. In a more detailed failure analysis for a region, the length of a sea defence that encloses the region has to be incorporated. Longer sea defences have more consequences during failure in comparison to short sea defences that should result in more heavy design criteria taking into account that both structures have an equal change of failure. Furthermore the probability that a higher load occurs also increases with the length of the sea defence. Generally it can be put that the correlation between cross-sections has consequences for the strength and load requirements for different cross-section [VRIJLING, 1996].

Furthermore only one failure mechanism has been taken into account. A proper probabilistic approach should be based on the probability of failure including all involved parameters and all failure mechanisms. However, during this thesis only one failure mechanism has been taken into account namely the mechanism ‘wave run-up’.

1DV versus 2DV models
The results are acquired using a 1DV model. However a 1DV model cannot incorporate 3D processes. During storm the wave pattern is irregular. Furthermore, the direction and wind speed during the storm period often vary. Both effects cannot be taken into account. Another important assumption of a 1DV model is the fact that sand can only be relocated over the cross-shore profile stretch.

In reality sand can also be moved in longshore direction as well, resulting in the formation of local channels and bars. A 2DV model with a sufficient small grid can take into account the local seabed alterations as well as the irregular wave pattern. Whenever these processes are taken into account it could result in different conclusions. However, currently the effects of these 3D processes are unknown and therefore it is recommended to start with a study on these 3D processes before a 3D model will be used to simulate storm-erosion.

Uncertainties

As soon as an estimation of the error can be made it can be taken into account as an uncertainty. Next to the model uncertainties, the accuracy of the probabilistic method applied will be determined by other uncertainties as well. According to report van Gelder uncertainties can be divided according to Figure 6.19 [GELDER VAN, 2000]. The model uncertainties caused by UNIBEST-TC have already been discussed. However, besides the uncertainties in UNIBEST-TC the fact that only on failure mechanism has been taken into account as well as the description of the limit state function with a design function result in new uncertainties. These uncertainties can be taken into account whenever the accompanying errors are estimated.

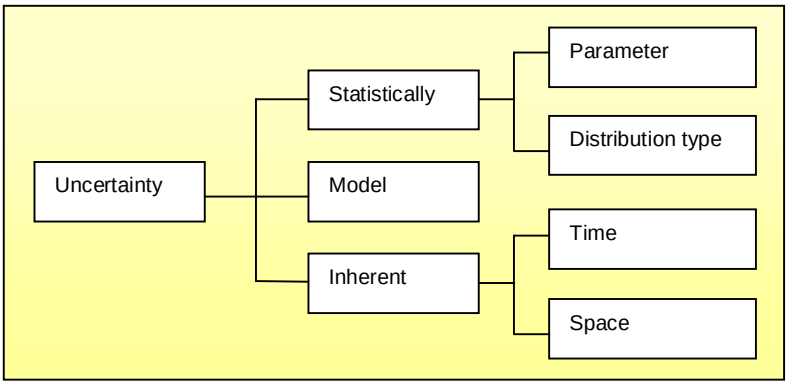

Figure 6.19: Types of uncertainty [GELDER VAN, 2000].

Furthermore statistical uncertainties are distinguished. Statistical uncertainties are split up in distribution types and parameters. During this analysis only two parameters are described randomly, for these parameters the uncertainties are taken into account, however, the uncertainties of the other involved parameters have not been taken into account. The remaining uncertainties are inherent uncertainty that have been caused by insufficient data records. Inherent uncertainties can be reduced theoretically whenever records are kept of the parameters involved for the coming centuries.

Different limit state function

The applied limit state function is generally used for a first impression. Consequently, the uncertainties are significant.

$$Z = h_{crest} - \left(h + 2H_s\right) \tag{6.20}$$

A more accurate equation has been used by the TAW to determine the height of the sea defence more exactly. The equation can also take into account complicating factors like oblique waves (γ_β), slope roughness (γ_f) and berm reduction (γ_b) by using correction factors. The basic equation is valid for the simplest case of wave approaching perpendicular onto a plain smooth slope. The correction factors are than 1. [CUR 196, 1995]

$$h_{seawall} = h + Z_{2\%} \tag{6.21}$$

$$Z_{2\%} = 1.6\gamma_b\gamma_f\gamma_\beta\xi_0 H_s \text{, with a maximum at } Z_{2\%} = 3.2\gamma_f\gamma_\beta H_s \tag{6.22}$$

$$\xi_0 = \frac{\tan(\alpha)}{\sqrt{s_0}} \tag{6.23}$$

$$s_0 = \frac{2\pi H_s}{g T_p^2} \tag{6.24}$$

Parameter definitions

$h_{seawall}$	= Distance between the SWL (Still Water Line) and the crest height	[m + NAP]
$Z_{2\%}$	= Wave run-up exceeded by 2% of the waves	[m]
H_s	= Significant wave height at the toe of the structure	[m]
γ_b	= Reduction parameter for the berm	[-]
γ_f	= Reduction parameter for the slope roughness	[-]
γ_β	= Reduction parameter for the wave angle	[-]
ξ_{op}	= Breaker parameter for wave run-up	[-]
T_p	= Wave peak period	[s]
g	= Gravitation constant	[m/s^2]
s_{op}	= Wave steepness, based on deep-water wave height and peak period	[-]
α	= Angle of the construction slope	[-]

The wave steepness (s_0) as is used in the equation is based on the significant wave height. In UNIBEST-TC the wave steepness is based on the root-mean-square wave height, which results in a more gentle wave steepness of a factor 1.41 smaller. The solution with similar simplifications as have been made for the previous limit state function results in the following limit state function:

- Slope of the Pettemer sea defence is 1:4.
- No reduction factors are applied.
- S_0 is determined by H_s instead of the H_{rms} used in UNIBEST-TC.

$$Z = h_{crest} - \left(h + 0.4 \frac{1}{\sqrt{s_{0,\,for H_s}}} H_s \right), \tag{6.25}$$

with a maximum of $Z = h_{crest} - \left(h + 3.2 H_s \right)$ (6.26)

This function has one more statistical parameter; wave steepness (s_0). If both limit state functions are compared it has been found that the whenever $s_0 = 0.04$ both function have an equal result. Wave with a lower wave steepness result in an increased load compared to steeper waves according to the latter Z-function (Equation 6.25). For both functions the water level and wave height at the toe or just in front of the sea defence is required.

During the previous examined cases a wave steepness (s_{rms}) of 0.025 has been used. For such wave steepness this more accurate equation reads:

$$Z = h_{crest} - \left(h + 2.13 H_s \right), \text{ instead of } Z = h_{crest} - \left(h + 2 H_s \right) \tag{6.27}$$

If this limit state function has been used the probability of failure will increase compared to the previously used limit state function whenever T_p or s_0 are described deterministic. However, In case they are described randomly it depends on the PDF applied.

7. Discussion

7.1 General

In this thesis the morphological alterations of the seabed have been studied as well as the importance of these alterations on the safety of sea defences. Especially the contribution of these storm induced morphological alterations on the required crest height has been examined for the sea dike at Petten. A literature study has been carried out in order to increase the understanding of the sediment transport processes involved as well as the methods for the design of a sea defence.

Data measured at Petten including storm conditions have been assessed to gain perception of the actual impact of a storm on the seabed level. This data has also been used to calibrate the morphological computer model UNIBEST-TC that on its turn have been used to determine the contribution of several parameters on the local erosion depth and the local wave height growth. Finally these simulations have been used to determine the crest level and probability of failure taking into account the failure mechanism 'wave run-up'.

This chapter discusses the research results and precedes the Chapter 8 that deals with the conclusions and recommendations.

7.2 Discussion concerning the results

Storm-erosion
Storm-erosion could not be determined by seabed surveys due to the absence of bed profiles surveys during storm. Two alternative methods have been used to assess the erosion degree. By means of a hindcast analysis the seabed level of one location in the surf zone 60m from the sea dike toe has been examined with wave data and a constant breaker index. Furthermore the seabed alterations predicted by UNIBEST-TC in a cross-section were used to determine the degree of erosion. Both methods predicted significant erosion for the section just in front of the sea defence caused by the storm. The hindcast analysis based on measured data predicts even more erosion than the UNIBEST-TC analysis does.

The hindcast analysis showed considerable difference in predicted erosion depths. This is probably caused by the difference in pre-storm seabed level as well as the fact that the breaker index does not remain constant throughout the entire period of storm.

When the surveyed profiles before and after a storm are compared only minor variations for the nearshore seabed are distinguished. These bed variations are probably small because the nearshore area immediately alters when the hydrodynamic conditions change, resulting in an under-estimation of the erosion depths.

Effects of storm-erosion

According to predictions made by UNIBEST-TC, it appears that although the local seabed erosion during a single storm is significant, the local wave height growth is rather small. This is mainly due to the seaward transportation of sand that decreases the incoming wave height. Therefore the contribution of seabed alterations due to storm remains insignificant for the determination of the crest height or probability of failure used for the design of sea defences.

One of the main reasons that local seabed erosion due to morphological alterations remains little is the fact that a period of storm is rather small, about 1 day. Whenever a longer period is examined the effects will become greater. Another aspect is the fact that UNIBEST-TC predicts a local wave height decrease before the local wave height increases over time, during relatively high wave conditions. This phenomenon has been compared with SWAN-1D computations. It appeared that SWAN immediately predicts a wave height increase. These opposing predictions could result in an under-estimation of the local wave height predictions by the UNIBEST-TC model. However, it cannot be determined which model is right, because the seabed has not been measured during storm conditions.

Another aspect that affects the reliability of the UNIBEST-TC results is the 2D approach. During this study only cross-sections have been examined, whereas 3D processes probably have a considerable impact on the bathymetry especially in shallow water. Due to the restriction in UNBEST-TC that sand can only be relocated over the cross-section. The possibility that a profile loses sand is than neglected. In reality it could be possible that channels are developed perpendicular to the shore (e.g. rip-currents) whereas these can never be predicted by UNIBEST-TC. This could result in an under-estimation of the actual storm effects. 3D models, however, have more uncertainties due to the third dimension and require a considerable longer simulation time. Whether the 3D processes that cause these irregularities are incorporated in the 3D models remains questionable too.

Parameter effects

Water depth and wave height are the main parameters that determine the hydrodynamic load that results in storm-erosion. The sediment characteristics are also of significant influence for the erosion depth, however, the effects have not been taken into account during this thesis, because variations in sand characteristics along the Holland coast are rather small.

The main parameters with respect to the crest height are again water level and wave height. However also the pre-storm seabed level in the surf zone is of significant concern. The water depths limit local waves that attack the sea defence. Up to now, only the water level has been used to characterise storm events. This simplification results in acceptable predictions, however deep-water wave heights as well as the bed level are of significance too.

To determine the probability of failure for the sea defence based on the failure mechanism 'wave run-up', model uncertainties also become of significant importance. However it remains difficult to determine the model accuracy especially during conditions that are expected to occur during extreme events. Nonetheless it is recommended to take model uncertainties into account in future research.

According to the data analysis the seabed level variations are significant, especially in the area directly in front of the Pettemer sea defence. The bed level of the area situated between the groynes varies with about 2 to 3m in height. It appears that this area contributes most to the wave load that can penetrate up to the sea defence. Variation in this region therefore leads to great variations in local wave height. To take into account these seabed variations it is recommended to use a random approach and describe the different bed profiles by the averaged level of the area between the groynes.

7.3 Reflection

Design of sea defences
According to the results of this thesis regarding erosion-effects it can be advised to neglect the effects of storm-erosion during the design of coastal defence works. Although the exact effects are still not certain, large quantities of nearshore storm-erosion predicted by UNIBEST-TC vary in the order of magnitude of 1m for the location at Petten, whereas the effects of these erosion quantities are insignificant.

The presently used design methods are therefore still valid whereas they do not take into account morphological variations during storm. However these methods do not take into account the variation of the initial seabed as well. At present, the initial seabed is determined by the most recently surveyed bed profiles. This assumption appears questionable. According to the results of these thesis the initial seabed level considerably affects the final wave impact on the sea defence.

Especially the shallow area just in front of the sea defence seems to be the most crucial region of the seabed. The water depths in this region limit the maximum wave height that is able to penetrated to the sea defence. However it appears difficult to take into account a representative seabed profile. Several studies have already been executed with little consequences. These studies did show the significant effects of the seabed level, however the methods to incorporate the seabed level into the design were not accepted.

Nowadays it is preferred to use probabilistic design methods, because these methods are also able to incorporate the uncertainties. It is recommended to take the seabed level into account by a random variable. This random variable for the seabed should than be mainly based on the level of the shallow area in front of the sea defence. The other section of the seabed is of less significance. The length of this shallow area is also of significance however the exact effects have to not been examined. The distribution function for the random variable has to be based on a sufficient survey data. Consequently, it is recommended to continue the surveys at Petten to be able to determine the distribution function for the seabed level more accurately.

The seabed appears to be event controlled (Figure 4.5) similar to water level and wave height. Thus a similar approach is recommended. It could be useful to describe the seabed by a level that corresponds to the level with a probability of exceedance of 1/10.000 a year. Whether the seabed level variation has been incorporated in the design by means of safety margins is unclear. However, for a proper probabilistic approach the safety margins limit state function without safety margins have to be applied.

Storm erosion in general
The effects of storm-erosion are only examined at Petten, where the results appear insignificant. Whether these results are valid for all other location along the Dutch shoreline is not examined. However large differences are not expected when the location is similar to the location at Petten.

The effects of storm-erosion do also depend on the pre-storm seabed level and the storm duration. During this thesis a 36-hour storm has been simulated however it could be possible that during extreme events the storm period significantly increases. A longer storm period results in a considerable greater contribution of the storm-erosion.

8. Conclusions and recommendations

8.1 General

Before this study had been executed the effects of storm-erosion were uncertain. It was expected that due to the erosion/ deepening of the area just in front of the Pettemer sea defence, the impact of a storm would be greater. The deepening of this so-called nearshore area during a storm was presumed to be initiated by a net offshore directed sediment transport. The fact that this area is situated between groynes made this presumption even more acceptable.

The additional impact due to storm-erosion was believed to be significant, because surveys showed that the level of the nearshore area considerably varied in height. The additional impact than should be caused by an increase in the local maximum wave height due to the deeper water depths as a result of storm-erosion. The local wave height growth is than about 50% of the erosion depth if the water depth limits the height of the storm waves.

To tackle the issue regarding storm-erosion and its impact on the sea defence, an inventory of the possibilities to study erosion have been made, keeping in mind the aforementioned assumption. Next, the processes involved are studied as well as their effects by means of a data analysis. To obtain a second opinion the storm-erosion process has been modelled with UNIBEST-TC. UNIBEST-TC also provides a tool to assess the effects of the parameters involved during the never measured design conditions. To determine the effect of storm-erosion regarding the sea defence, the additional impact of storm-erosion has been expressed in crest height and probability of failure.

This chapter deals with the overall conclusions. Furthermore some recommendations are made regarding future research and the use of UNIBEST-TC as well as probabilistic analysis.

8.2 Conclusions

Conclusions concerning storm-erosion
The degree of storm-erosion could not be determined by seabed surveys alone due to the absence of bed profile surveys during storm. Two alternative methods to analyse the field data, both explained in Chapter 4, have been used to assess the erosion degree. According to the first analysis, which compared annual storm intensities to variations in the annual surveyed sand volume, the annual storm intensity does not affect the annual variation in measured JARKUS profiles. Even for the seabed section between the groynes hardly any effect could have been determined.

The second approach, the hindcast analysis, predicts for a location 60m from the sea defence, a local storm-erosion depth in the order of magnitude of 0 to 1.5m. The erosion depth depends on the seabed level height and the storm intensity as well as the applied breaker index constant. These results are gathered for storms that occur relatively frequent about 1 to 0.1 times a year (Table A2.2). The reliability and accuracy of the results are difficult to determine. However a perception of the effects of storms on the local seabed has been gained.

According to the UNIBEST-TC predictions the erosion quantities are smaller than the quantities that are predicted by the hindcast analysis. However still a significant degree of erosion has been predicted. If the results of the data analysis are compared with the surveyed profiles of a few weeks later the erosion is over-estimated significantly. The most important factor that could have disturbed the hindcast analysis is the reflection of waves by the dike. Wave reflection increases when the wave height and period increase resulting in the possibility of higher waves without a seabed reduction, as had been predicted by means of the hindcast analysis.

Conclusions concerning the effects of storm-erosion
According to predictions made by UNIBEST-TC, it appears that although the local seabed erosion during a single storm is significant, the local wave height growth is rather small. Therefore the contribution of seabed alterations due to storm remains insignificant for the determination of the crest height or probability of failure used to design sea defences.

The effects of storm-erosion could become larger whenever a longer storm period would have been examined. Another aspect that has could have resulted in the minor effects, are prediction capabilities of UNIBEST-TC, because SWAN-1D predicts a greater effect of the storm-erosion according to Paragraph 5.7.

Conclusions concerning the parameters involved
Water depth and wave height are the main parameters that determine the hydrodynamic load that results in storm-erosion. The sediment characteristics are also of significant influence for the erosion depth, however, the effects have not been taken into account during this thesis, because variations in sand characteristics along the Holland coast are rather small.

The main parameters with respect to the crest height are again water level and wave height. However also the pre-storm seabed level in the surf zone is of significant concern. The water depths limit local waves that attack the sea defence. So far, only the water level has been used to characterise storm events. This simplification results in acceptable predictions, however deep-water wave heights as well as the bed level are of significance. Whenever the probability of failure has been determined, model uncertainties and the considered failure mechanisms become important too.

According to the data analysis the seabed level variations are significant, especially in the area directly in front of the Pettemer sea defence. The bed level of the area situated between the groynes varies with about 2 to 3m in height. It appears that this area contributes most to the wave load that can penetrate up to the sea defence.

Conclusions concerning the probability of failure and crest height
The crest height has been determined using the failure mechanism 'wave run-up'. Wave run-up is expected to be a reasonable indicator to show the effects of seabed alterations on the crest level. Seabed alterations are incorporated by the local wave heights that form a significant share of the wave run-up level.

The relation between the wave height alteration due to seabed variation and the run-up level has been considered with a relatively simple formulation. Therefore the probabilities of failure determined cannot be interpreted as absolute probabilities of failure. A relative comparison to determine the effect of storm-erosion, through wave- run-up, can be made with the determined probability of failure.

Whenever an absolute probability is required it is recommended to take all possible failure mechanisms into account and use a more sophisticated wave run-up formulation that is validated for breaking waves too. The wave run-up level due to breaking waves is dependent on the wave period as well as the wave height and water level. During this above-mentioned relative comparison of probability of failure the wave period has been neglected because it is not expected that the wave period will change due to alterations of the bed level.

8.3 Recommendations

Despite the uncertainties that occur due to use of UNIBEST-TC and the other assumptions that have been made it appears that the storm-erosion remains small. Therefore it is recommended to focus on the pre-storm bed profile instead of the load increase due to storm-erosion. Especially the level of the seabed just in front of the sea defence is of most significance. The large variation of bed level in this area makes it useful to describe the seabed level stochastically. It is recommended to use the averaged bed height determined by the seabed between the groins (stretch of 80m) for the location at Petten. This can only be done if a significant wide seabed is situated in front of the sea defence, which is usually the case when groins protect the sea defence.

If the number of profile surveys will increase the uncertainty of the possible seabed level will decrease. Therefore it is recommended to continue the seabed measurements at Petten. Two measuring options that could contribute into gaining perception of the seabed variation in the surf zone are given below:

- Light-sensitive measuring poles can result in continuous measurements.
- Soundings during storm at the jetty at Scheveningen.

If a more comprehensive probabilistic approach is applied to determine the probability of failure more accurately, it is recommended to incorporate more failure mechanisms and to take into account the length of the Pettemer sea defence. The length of the sea defence affects the uncertainty of the Pettemer sea defence crest height and the probability that an unfavourable combination of seabed, water level and waves exist.

Due to the relatively great uncertainties in morphological processes that take place in the surf zone it is recommended to use probabilistic tools to be able to take these uncertainties into account. Furthermore it is recommended to examine the 3D processes that are not taken into account during the analyses in order to determine whether the neglecting these processes had been appropriate.

During this thesis only cross-sections have been examined, however, 3D processes do play a significant part in the surf zone. These 3D processes are expected to generate sediment processes that have gradients in longshore as well as cross-shore direction. Therefore it is recommended to use models (Delft 3D) that are capable of simulation these 3D sediment transport processes. A probabilistic analysis of the results is than even more useful because the uncertainties increase due to the additional dimension.

References

Allersma, E., 1988. 'Analyse erosie-problematiek vooroever Hondsbossche Zeewering'. WL | Delft Hydraulics in Delft.
Augustijn, B. and Zwart, B., 1997. 'Stormkalender; chronologisch overzicht van alle stormen langs de Nederlandse kust voor het tijdvak 1990-1996'. KNMI (Koninklijk Nederlands Meteorologisch Instituut) in The Bilt.
Augustijn, B., Daan, H., Mourik, B. van, Messerschmidt and D., Zwart B., 1990. 'Stormkalender; chronologisch overzicht van alle stormen langs de Nederlandse kust voor het tijdvak 1964-1990'. KNMI (Koninklijk Nederlands Meteorologisch Instituut) in The Bil
Bakker, R., 1995. 'Verifications of the Unibest-TC model'. National Institute for Marine and Coastal Management in The Hague.
Battjes, J.A., 1974. 'Surf similarity'. Proceedings of 14th International Conference on Coastal Engineering.
Battjes, J.A. and Janssen, J.P.F.M., 1978. 'Energy loss and set-up due to breaking of random waves'. Proceedings of 16th International Conference on Coastal Engineering.
Battjes, J.A. and Stive, M.J.F., 1985. 'Calibration and verification of a dissipation model for random breaking waves'. Journ. of Geophys. Res., 90 (C5).
Bosboom J., Aarninkhof, S. G. J., Reniers, A.J.H.M., Roelvink, J.A. and Walstra, D.J., 1997. 'Unibest-TC 2.0, overview of model formulations'. WL | Delft Hydraulics in Delft.
Bruinsma, J., Vrijling, J.K., 1980. 'Hydraulic Boundary Conditions'. Symposium on Hydraulic Aspects of Coastal Structures.
Burger, M., 2001. 'Onderwateroeversuppletie Delfland'. National Institute for Marine and Coastal Management in The Hague.
Corso, D.D., 2002. 'Cross-shore profile development during storm conditions'. University of Technology Delft.
CUR 190, 1997. 'Kansen in de civiele techniek; deel 1 Probabilistisch ontwerpen in theorie'. CUR/ RWS in Gouda.
CUR 196, 1995. 'Manual on the use of Rock in Hydraulic Engineering'. CUR/ RWS in Gouda.
Dekker J., 2000. 'Inzicht in extreme golfcondities'. WL | Delft Hydraulics in Delft.
Dhyr-Nielsen, M. and Sorensen T., 1970. 'Sand transport phenomena on coasts with bars, in Proceedings of the 12th International Conference on Coastal Engineering'.
Dijk, M., 2002. 'Vergelijking Unibest-TC en Durosta'. Delft University of Technology.
Dongeren, A.R. van and Janssen T.T., 2001. 'Analysis of Low frequency Waves at Petten'. WL | Delft Hydraulics in Delft.
Gelder van P.H.A.J.M, 2000. 'Statistical Methods for Risk-based Design of Civil Structures'. Delft University of Technology.
Gelder van P.H.A.J.M and Vrijling J.K., 1999. 'On the distribution function of the maximum wave height in front of reflecting structures'. Delft University of Technology.
Graaff, J. van de, 1984. 'probabilistische methoden bij het duinontwerp, achtergronden van de TAW-leidraad ‘ duinafslag’'. CUR/ RWS in Delft.
Guillen, J., 1998. 'Shoreline evolution of the Holland coast on a decadel scale'. Delft University of Technology.
Holterman S.R., 1998. 'Golfoploophoogteberekeningen Pettemer zeewering'. National Institute for Marine and Coastal Management in The Hague.
Holthuijsen, L.H., Booij, N., Ris, R.C., Haagsma IJ.G., Kieftenburg, A.T.M.M. and Kriezi E.E., 2000. 'User manual - SWAN cycle III version 40.11'. Delft University of Technology.
Houwing, E.J., 1991. 'Analyse van de TAW-profielen, Egmond aan Zee en Katwijk aan Zee. Rapport GEOPRO 1991.019'. University of Utrecht.
Jacobse, J.J., 2000. 'Validatie van het SWAN-model voor de Pettemer zeewering'. National Institute for Marine and Coastal Management in The Hague.
Kleinhout, K., 2000. 'Hydrodynamics and morphodynamics of the Egmond field site'. Delft University of Technology, WL | Delft hydraulics in Delft.
Kok, M., Noortwijk, J.M. van, Duits, M.T., Vrouwenvelder, A.C.W.M. and Valk, C.F. de, 1998. 'Gevoeiligheidsanalyse Probabilistische Belastingmodellen en Rekentechnieken; Hoofdrapport'. Ministry of Transport, Public Works and Water Management in Lelystad.
Kroon, A., 1994. 'Suspended transport and morphodynamics of the beach and nearshore zone near Egmond, the Netherlands'. PhD thesis, dept. of Physical Geography, University of Utrecht.
Kruif, A.C. de, 2000. 'Stormdata of the Petten Field Site: 1995-2000'. National Institute for Marine and Coastal Management in The Hague.
Miche, R., 1944. 'Mouvements ondulatoires des mers en profondeur constante ou décroissante'. Annales des Ponts et Chaussées.

Nelson, R.C., 1994. 'Depth limited wave heights in very flat regions'. Coastal Engineering, 23.
Philippart, M.E. Dillingh, D., and Pwa, S.T., 1995. 'De basispeilen langs de Nederlandse kust, De ruimtelijke verdeling en overschrijdingslijnen'. National Institute for Marine and Coastal Management in The Hague.
Rijn, L.C. van, 1998. 'Principles of coastal morphology'. Aqua publications in Amsterdam.
Rijn, L.C. van, 2000. 'Hydrodynamics, sediment dynamics and morphodynamics during storm events 1998 in the nearshore zone of Egmond, The Netherlands'. WL | Delft Hydraulics, Coast 3D.
Rijn, L.C. van, Ruessink B.G. and Mulder J.P.M., 2002. 'Coast3D - Egmond'. MAST EC in Amsterdam.
Rijn, L.C. van, Walstra, D.R., Grasmeijer, B.T. and Kleinhout K., 2000. 'Hydrodynamics and morphodynamics in the surf zone of a dissipative beach'.
RIKZ, 1996. 'Hydraulische randvoorwaarden voor primaire waterkeringen'. Ministry of Transport, Public Works and Water Management in Delft.
Ronde J.G., Marle J.G.A. van, Roskam A.P. and Andorka Gal J.H., 1995. 'Golfrandvoorwaarden langs de Nederlandse kust op relatief diep water'. National Institute for Marine and Coastal Management in The Hague.
Roskam, A.P., 1988. 'Golfklimaten voor de Nederlandse kust'. Ministry of Transport, Public Works and Water Management in The Hague.
Ruessing B.G. and Jeuken M.C.J.L., 2002. 'Dunefoot Dynamics Along the Dutch Coast'. WL | delft Hydraulics in Delft.
Schiereck G.J., 2000. 'Introduction to Bed, Bank and Shore protection'. Delft University of Technology.
Sorgedrager, J.M., 2002. 'Cross-shore sediment transport on the shoreface; Behaviour analysis of UNIBEST-TC sediment transport formulations'. WL | Delft Hydraulics in Delft.
Stolk, A., 1989. 'Zandsysteem kust - een morfologische karakterisering. Kustverdediging na 1990, Technisch Rapport 1'. Dept. of Physical Geography, University of Utrecht.
TAW, 1995. 'Basisrapport Zandige Kust, behorende bij de leidraad zandige kust'. Technische Advies Commissie voor de Waterkeringen in Delft.
TAW, 1998. 'Grondslagen voor waterkeren'. Technische Advies Commissie voor de Waterkeringen in Rotterdam.
TAW, 1999. 'Leidraad Toetsen op veiligheid'. Technische Advies Commissie voor de Waterkeringen in Delft.
TAW, 2000a. 'Standaard methode schade en slachtoffers als gevolg van overstromingen'. Technische Advies Commissie voor de Waterkeringen.
TAW, 2000b. 'van Overschrijdingskans naar overstromingskans'. Technische Advies Commissie voor de Waterkeringen.
Tonis, I.E. and Veen E.J., 2001. 'Onderzoek naar een minimumprofiel bij Petten'. National Institute for Marine and Coastal Management in The Hague.
Velden, E.T.J.M. van der, 2000. 'Coastal Engineering; volume II'. Delft University of Technology.
Veuger, A.J., 2001. 'Gradients in Longshore Transport of Sediment in UNIBEST-TC'. Delft University of Technology.
Vink A.S., 2001. 'Transformation of wave spectra across the surf zone'. Delft University of Technology, National Institute for Marine and Coastal Management in Delft.
Vledder, G.Ph. Van, 2001. 'Onderzoek naar een maatgevende bodem, gebaseerd op 35 jaar jarkus-metingen'. Alkyon in Emmeloord.
Voortman, H.G., 2002. 'User manual for the Fortran library "ProbMod"'. Delft University of Technology.
Vrijling, J.K., 1996. 'Probabilistisch ontwerpen in de waterbouwkunde'. Delft University of Technology.
Walstra, D.J.R., 2000. 'Userguide for Unibest-TC'. WL | Delft Hydraulics in Delft.
Wijnberg, K.M., 1995. 'Morphologic Behaviour of a Barred Coast over a period of Decades'. University of Utrecht in Utrecht.
Wright, L.D., Boon, J.D., Kim, S.C. and List, J.H., 1991. 'Modes of cross-shore sediment transport on the shoreface of the Middle Atlantic Bight'. Marine Geology.

Appendix contents

Appendix 1: Sediment transportation

General

The Pettemer sea defence and Hondsbossche sea defence form a small part of the Dutch coastline. The future evolution of the sandy Dutch coastline is mainly affected by sediment transport patterns. At the coastline uncertainties arise both from the morphological impact due to human interference (e.g. sea defences and harbour entrances) and from the morphological impact due to climate changes, which might occur in the future, such as a rise in sea level. These morphological changes gradually alter the wave patterns and currents, hence the sediment transport paths at the shore. Even the stability of the shoreline itself can be affected.

Morphological alterations can be quick or slow, causing respectively short-term or long-term erosion. Longshore transport has been considered to contribute significantly to long-term coastal evolution, whereas cross-shore transport is considered to be responsible for short-term or seasonal morphological variations. This thesis focuses on the short-term effects of cross-shore transport due to storms, resulting in erosion in the nearshore area.

Sediment, in this case sand, can be transported by:
- Current related transport: wind-, wave-, tide- and density-driven currents.
- The oscillatory wave motion (wave-related transport), caused by the deformation of short waves (wind waves) due to changing water depths (wave asymmetry).
- Or by a combination of currents and waves.

Generally waves act as stirring mechanism, while the mean current transports the sediment.

Sediment transport process

The sediment transport process has three distinct stages:
- The stirring up of bottom material that results in suspended sediment.
- The horizontal displacement of these particles by water.
- The re-sedimentation of these particles.

The start of each stage depends on the water motion and sediment characteristics. Waves mainly loosen bottom material and stir it up, increasing the concentration of sediment, while currents mainly transport the material. Waves can also cause sediment transport and currents can stir up sediment, however these processes are secondary.

Sediment characteristics are a major factor in determining the total volume of sand transported. The diameter (D) that varies in the range of 250 to 500μm [STOLK, 1989] for the Dutch coast, and the mass density (ρ) are the most important sediment characteristics.

Types of sediment transport

The total sediment load transport has been divided into bed load transport and suspended load transport:

- Bed load transport, defined as the total load that has more or less continuous contact with the bed during transport. This includes grain particles that roll, jump and slide along the bed.
- Suspended load transport, involves that part of the total transport load that moves without continuous contact with the bed.

The suspended transport load can be determined by depth-integration of the product of sand concentration and fluid velocity from the top of the bed to the water surface.

Often suspended transport has been split up in current and wave induced transport. Current induced suspended transport includes time-averaged (mean) currents velocities (longshore currents, rip currents and undertow currents), while wave induced sediment transport includes high and low frequency oscillating fluid velocity components (orbital motion). [VELDEN VAN DER, 2000]

Basic sediment transport equation

Local sediment transport rates can be described by using the basic equation of sediment transport:

$$S = \frac{1}{T} \int_0^{h+\eta} \int_0^{T} C(z,t) \cdot u(z,t) \; dt \; dz \qquad \text{(A1.1)}$$

Where:

S	= sediment transport rate	[m^3/m]
T	= integration time	[s]
$h+\eta$	= surface level elevation, relative to the bed level	[m]
C	= instantaneous concentration of sediment	[-]
u	= instantaneous velocity	[m/s]
z	= vertical co-ordinate	[m]

Basically sediment transport is based on the velocity depth-profile and the sediment concentration depth-profile. This formulation is valid for longshore as well as cross-shore sediment transport, depending on the variables used. If u is the cross-shore component of the flow velocity, then this formulation will calculate the cross-shore transport rate, averaged over a certain period of time. [VELDEN VAN DER, 2000]

Sediment transport quantities determined with Equation A1.1 are often used to determine the erosion quantities within a specified area. These erosion quantities follow from the loss of sediment volume in a specified area over a specified period of time. This holds for situations where the density (sediment mass per volume) remains equal. However it could be possible for instance, that the density within a certain area increases, causing the sediment volume to reduce (erosion) without any transport. During this thesis the effects of sediment density variations are not taken into account.

Coastal erosion

Field experience over a significant period of time has led to the notion that storm waves cause sediment to move offshore while fair-weather waves and swell return sediment shoreward. During conditions with low non-breaking waves, onshore directed transport processes related to wave asymmetry and wave-induced streaming are dominant, usually resulting in accretion processes in shallow water (littoral zone). During high-energy conditions the beach and the littoral zone are attacked severely by incoming breaking storm-waves that usually result in erosion processes taking place.

The erosion that occurs during extreme events (storms) is related to sediment transport. Two types of erosion processes can be distinguished:

- Erosion due to mean hydrodynamic conditions.
- Erosion due to extreme hydrodynamic conditions.

Both types of erosion occur on different time scales. Generally, the impact of mean hydrodynamic conditions is seen over a large time scale (seasons, years), whereas the effects of extreme events are mostly restricted to a small time scale (hours, days).

Over the long-term, longshore transport dominates the coastal evolution. Longshore erosion can have multiple origins, as for instance the presence of a longshore gradient in wave attack. Due to an increase in longshore transport along a coastal stretch, the total volume of sand between both boundaries will decrease in time. Consequently, the cross-shore profile will shift in landward direction, resulting in erosion.

Short-term erosion takes place occasionally during less frequent extreme events, such as storm surges and hurricanes. These events primarily affect the evolution of the cross-shore profile. Compared to long-term erosion the affected region is often significantly smaller. In most cases the short-term storm event erosion is temporary since the mean hydrodynamic conditions tend to reconstruct the pre-storm profile, which principally is more or less an equilibrium profile. These short-term developments can be considered as momentary disturbances to long-term coastal development.

Even on a ‘stable’ coast without any long-term erosion, the dynamical adjustments of the cross-shore profile due to infrequent short-term extreme conditions could result in safety problems.

Cross-shore transport

Process

Cross-shore sediment transport includes offshore transport, such as that which occurs during storms, as well as onshore transport, such as that which results from mild wave activity. The cross-shore profile as it exists in nature, has been shaped by the prevailing hydrodynamic conditions. The sediment transport modifies the morphology, which in turn affects the wave propagation pattern. As a result the sediment transport rates will change.

This cycle results in a profile that agrees with the prevailing wave conditions in the sense that the cross-shore transport gradients become negligible. Finally, equilibrium between wave propagation and bottom profile would be achieved. However, in reality this equilibrium will never be reached because waves are irregular, and different waves have different accompanying equilibrium profiles. Storm conditions yield an equilibrium profile that differs from that of mild wave conditions. As extreme and moderate conditions follow each other in time, the actual profile will always be on its way to equilibrium. This is why one speaks of a ‘dynamic equilibrium’.

If fair weather profiles are compared to storm profiles, it appears that during storms greater volumes of sediment are moved offshore. Storms mainly occur during winter, while mild wave activity characterises summer. Consequently, two main equilibrium profiles are found due to the difference in seasonal waves. This can be seen in Appendix 3.

In winter the mean wave conditions are more severe than in summer, sediment is moved offshore, and the seaward slope of sand bars becomes steeper, while the slope of the nearshore becomes gentler. The offshore sand bars protect the nearshore area and, in case of Petten, the sea defence from wave attack, because waves break further offshore. Furthermore, the offshore bars protect the nearshore from severe sediment losses and also provide a temporarily storage area for eroded sediment.

In summer the mean wave height decreases, while the mean wave period increases (share of swell increases) and beach recovery begins. Sand is transported onshore and new sand bars are created along with the steepening of the nearshore.

Mean return flow (undertow)
Observation of sediment transport due to irregular waves on a beach indicates that one of the most important mechanisms under surf conditions may be the transport of sediment by the time-mean seaward directed flow near the seabed, induced by breaking waves. At the Duck site in the United States research on this subject has been executed and it has been concluded that mean flows dominate in storms and cause offshore fluxes of sediment [WRIGHT ET AL., 1991]. According to Dyhr-Nielsen and Sørensen (1970) seaward-directed return flow or undertow in the surf zone (which compensates for the shoreward directed mass flux above wave trough level) is driven by the imbalance between the vertically non-uniform wave momentum flux and the vertically uniform pressure gradient.

Cross-shore sediment transport outside the surf zone
When a satisfactory hydrodynamic description has been obtained, the sediment transport is calculated as the sum of bed load and suspended load transport.

If the near-bed wave-orbital velocity (and the bed shear stress) is larger in the onshore than in the offshore motion, a net sediment transport in the onshore direction is induced because the bed load transport is a function of the near bottom velocity.

As will be described in the following section, the cross-shore sediment transport is significantly larger in the surf zone than outside. Still, the cross-shore transport under non-breaking waves is important for the development of the coastal profile, because at a given point the waves will be non-breaking during calm conditions for a much longer time than the relative short periods of storms-induced wave-breaking.

Cross-shore sediment transport in the surf zone
The conditions in the surf zone are characterised by strong energy dissipation and production of turbulence caused by wave breaking. All mechanisms that contribute to the cross-shore sediment transport outside the surf zone are also relevant in the surf zone, but their significance is much smaller because the energy dissipation in the wave boundary layer is small compared to the energy loss due to wave breaking.

The distribution of the shear stresses together with the continuity equation gives the mean velocity profile. This velocity profile has a strong offshore-directed undertow near the bed and an onshore mean flow near the surface. The high turbulence level, due to breaking waves, affects the suspended sediment concentration profiles. The concentration distribution is much more mixed over the vertical than outside the surf zone. Nevertheless, the concentrations near the bed are the largest, and the resulting sediment transport goes offshore with the undertow.

Appendix 2: Storm events

General

This Appendix treats storm data reported by 'Rijkswaterstaat'. Over a period of 10 years the storm data is gathered and listed in Table A2.2. The table shows characteristics of individual storms. Only storms that caused a high water level are taken into account during the compilation of Table A2.2. Hence storms from the north, west or southwest are of interest. Other stormy situations that did not cause or took place during high water level are of little interest, because the sea defence is not threatened during these conditions. In Table A2.2 several main storm characteristics are listed. However, wind speed has been neglected because the accompanying hydrodynamic characteristics are of most interest.

Figure A2.1: Measuring locations along the Dutch shoreline.

At the end of this Appendix, data selected from the storm calendar gathered by Augustijn et al. is shown. [AUGUSTIJN ET AL., 1990, AGUSTIJN AND ZWART, 1997] Augustijn published a storm data set of 32-years, starting in 1964. Storms were defined as follows:

Wind has been categorized as storm when the wind force exceeds Beaufort 8. A 10-minute average is used to classify the weather data measured at several locations along the Dutch coastline.

The results that are shown at the end of this Appendix in the following graphs:

- Figure A2.3: Annual distribution of storm hours, classified by wind force.
- Figure A2.4: Summer distribution of storm hours, classified by wind force.
- Figure A2.5: Winter distribution of storm hours, classified by wind force.
- Figure A2.6: Distribution of storm percentages versus wind direction, classified by wind force over a period the period 1964-1990.
- Figure A2.7: Distribution of storm percentages versus wind direction, classified by wind force over a period the period 1964-1990, zoomed in on the heavy storm distribution.

Summer is determined as the period between 1 April and 30 September; winter is determined as the period between 1 October and 30 March.

Local effects

For this thesis the hydrodynamic conditions at Petten are of interest. Petten is located between Den Helder and IJmuiden as can be seen in Figure A2.1. Although local influences mainly determine the hydrodynamic conditions, the conditions at Den Helder and IJmuiden still give a reasonably good indication of the conditions at Petten.

Besides the already mentioned locations, Table A2.2 also describes the storm conditions over the previous decade at the location of maximum storm impact.

Storm impact

The impact of a storm depends on time, a combination of wind and wave setup and the astronomical tide. During spring tide little setup is enough to reach high water levels while much setup is needed during neap tide. Presently the water level is the only parameter that determines the storms return period. This implies that water level is the only variable that determines whether a sea defence meets the safety requirements (sea defences are designed to withstand a storm with a certain return period).

Relying on water level heights for classification purposes results in an acceptable and easy method. The water level depends on the astronomical tide and the wind/wave setup, which in their turn depend on the wind speed, fetch and storm duration. Besides the direct effect of the astronomical tide and wind conditions the local water level limits the maximum possible wave heights. In other words without high water levels it is practically impossible to reach a critical situation. It is therefore practically justified to determine the frequency of exceedance using solely the water level, instead of another or a combination of other hydrodynamic parameters.

Nevertheless it should be kept in mind that part of the wave heights is not correlated with the water depth. This share in wave height together with local bottom effects has not been incorporated and could cause an under-estimation.

Observations from storm reports that are described in Table A2.2, result in the following conclusions:

- Between the period of 1996 and 1999 no significant storms occur.
- The impact of storms varies locally, and is mainly influenced by the astronomical tide.
- The most intensive storm occurred in 1990.
- No significant influence of the storm direction on the return period can be found in this data set.
- The setup depends on the location and geometry, because it differs significantly along the Dutch shoreline.
- Storms differ a lot individually in orientation and impact.

Table A2.2: Storm data from storm reports made by 'Rijkswaterstaat'.

Date	Duration (hours)	Direction	Wave height K13a (H_s)		Location	Max setup (cm)	Water level (cm)	Return period
			Ave	Max				
29-30 Jan 2000	28	W (270°)	325	400	Max (Delfzijl)	271	381	22*/100
					Den Helder	174	227	47*/100
					IJmuiden		213	180*/100
3-4 Dec 1999	20	W	475	600	Max (Delfzijl)	253	366	33*/100
					Den Helder	168	211	81*/100
					IJmuiden		240	79*/100
6 Nov 1999	15	W → NW	575	675	Max (IJmuiden)		250	50*/100
					Den Helder	172	208	90*/100
					IJmuiden		250	50*/100
5 Feb 1999	28	NW→ NNW	475	600	Max (IJmuiden)		263	28*/100
					Den Helder	176	213	75*/100
					IJmuiden		263	28*/100
29 Oct. 1996	11	NWW → SWW	350	425	Max (Vlissingen)	150	352	42*/100
					Den Helder	133	191	190*/100
					IJmuiden		248	55*/100
29-30 Aug 1996	13	S→ NW→ SWW	375	475	Max (Vlissingen)	130	361	32*/100
					Den Helder	59	99	>1000*/100
					IJmuiden		166	>1000*/100
10 Jan 1995	19	NWW	450[1]	550[1]	Max (Delfzijl)	295	403	11*/100
					Den Helder	182	192	140*/100
					IJmuiden		220	130*/100
1-2 Jan 1995	28	NNW	575	700	Max (Vlissingen)	164	371	14*/100
					Den Helder	160	236	29*/100[2]
					IJmuiden B		273	16*/100
13-14 Mar 1994	18	NWW			Max (Delfzijl)	213	353	39*/100
					Den Helder	137	206	76*100
					IJmuiden B		184	470*/100
28 Jan 1994	20	NNW			Max (Dordrecht)		250	5*/100
					Den Helder	198	234	34*/100
					IJmuiden B		293	12*/100
19-20 Dec 1993	18	SW→ W			Max (Delfzijl)	240	350	42*/100
					Den Helder	130	211	62*/100
					IJmuiden B		274	850*/100
14-15 Nov 1993	18	W→N			Max (Vlissingen)	208	383	8*/100
					Den Helder	128	197	110*/100
					IJmuiden B		222	110*/100
21 Feb 1993	17	NW→ N			Max (Den Helder)	225	265	14*/100
					Den Helder		265	14*/100
					IJmuiden		260	35*/100
22-25 Jan 1993	80	SW→ W→ SW → NW			Max (Dordrecht)		214	30*/100 [25-01]
					Den Helder	132	210	65*/100 [22-01]
					IJmuiden		250	40*/100 [25-01]
11 Nov 1992	18	NWW			Max (Vlissingen)	135	354	30*/100
					Den Helder	85	151	55*/100
					IJmuiden		189	40*/100
20 Dec 1991	22	W			Max (Den Helder)	165	233	30*/100
					Den Helder	165	233	30*/100
					IJmuiden		239	60*/100
12 Dec 1990	16	NNW			Max (IJmuiden)		253	38*/100
					Den Helder	196	225	42*/100
					IJmuiden		253	38*/100
26 Feb – 2 Mar 1990	70	W, SW →NW			Max (Roompot)	182	360	4*/100 [27-02]
					Den Helder	215	277	11*/100 [26-02]
					IJmuiden		267	25*/100 [27-02]
25-26 Jan 1990	24	S → W			Max (Harlingen)	263	290	50*/100
					Den Helder	213	193	120*/100
					IJmuiden		170	820*/100
14 Feb 1989	14	W between SW and NW			Max (Den Helder)	205	253	20*/100
					Den Helder	205	253	20*/100
					IJmuiden		271	20*/100

[1] Measured at wave station IJmuiden.
[2] Measured during an earlier high water.

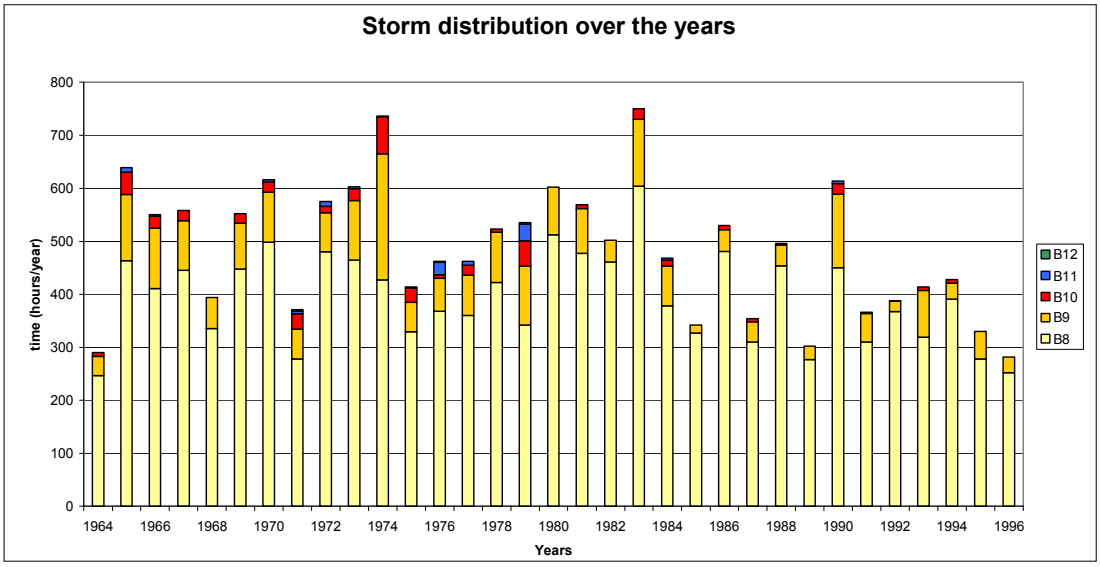

Figure A2.3: Annual distribution of storm hours, classified by wind force.

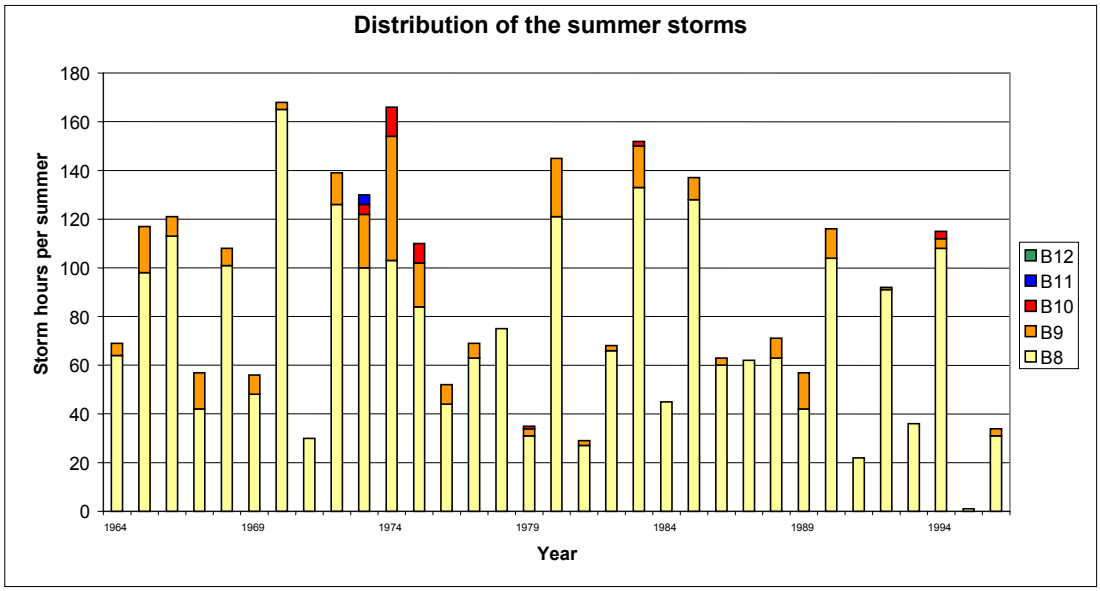

Figure A2.4: Summer distribution of storm hours, classified by wind force.

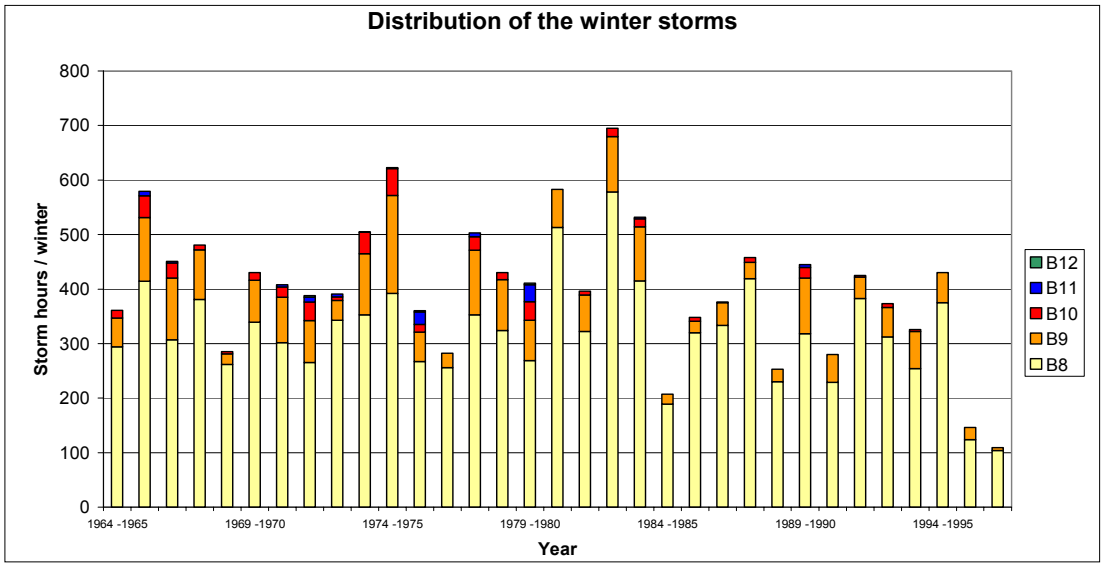

Figure A2.5: Winter distribution of storm hours, classified by wind force.

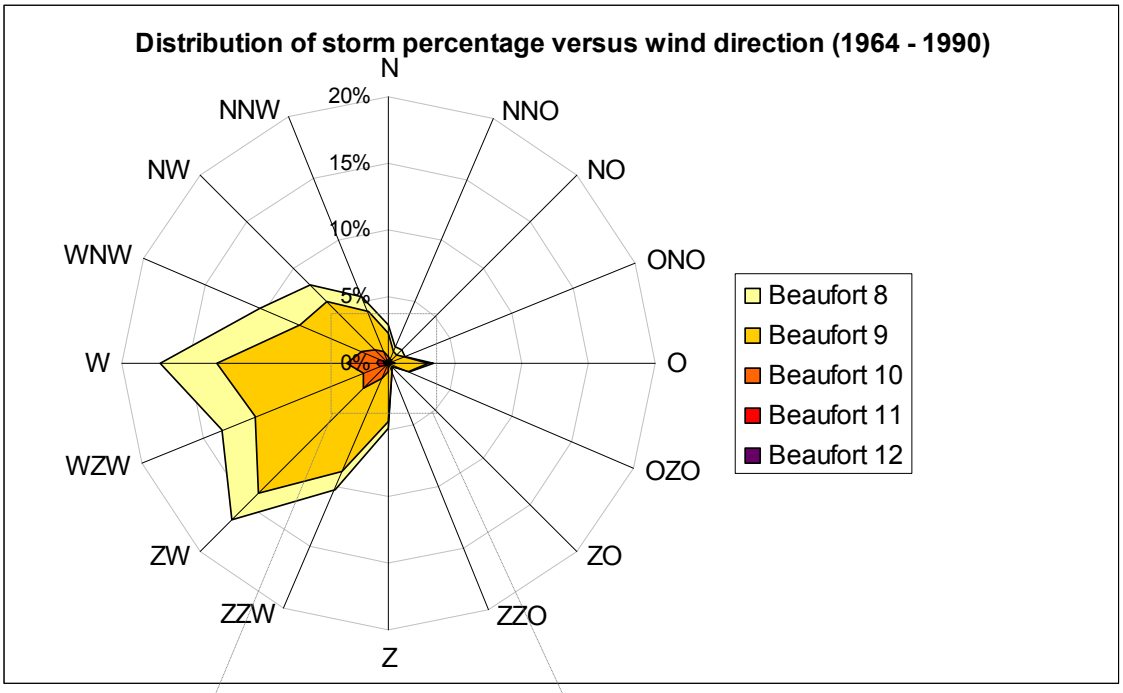

Figure A2.6: Distribution of the storm percentages versus wind direction, classified by wind force over a period the period 1964-1990.

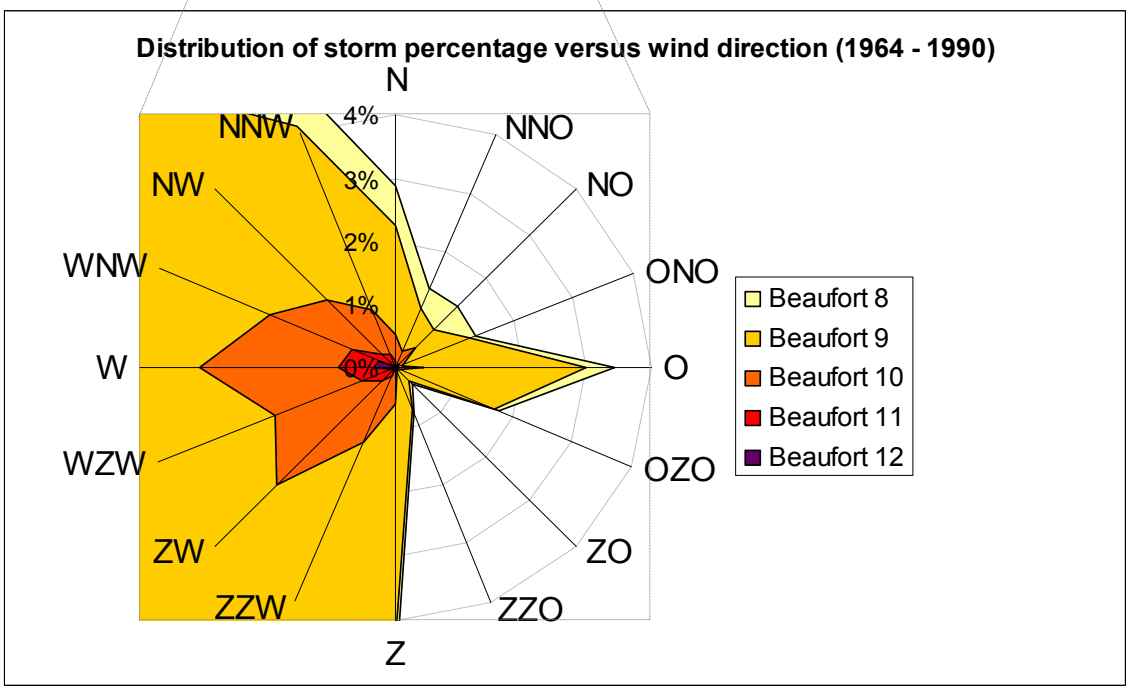

Figure A2.7: Distribution of the storm percentages versus wind direction, classified by wind force over a period the period 1964-1990; zoomed in on the heavy storm distribution.

Storm distributions by wind direction

The following years are shown:

- 1989 – 1990 (after the winter of 1990 the storm calendars stops registering the wind orientation).
- 1974 (lots of storm hours and little bottom regression).
- 1983 (lots of storm hours and almost no bottom variation).
- 1967 (lots of sedimentation along the bottom profile).
- 1968 (some regression along the bottom profile).
- 1980 (some regression along the bottom profile).

Relative storm distribution

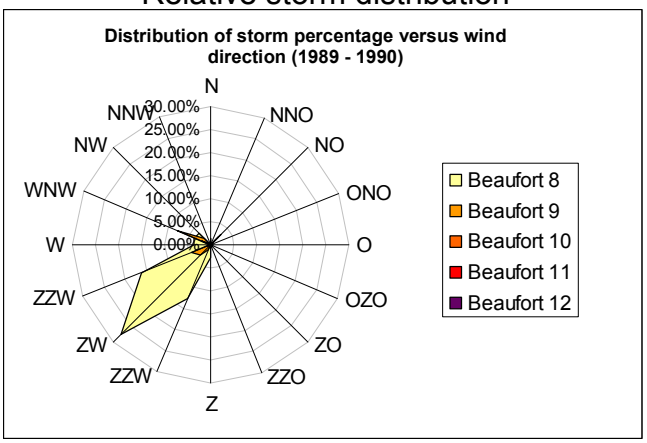

Absolute storm distribution

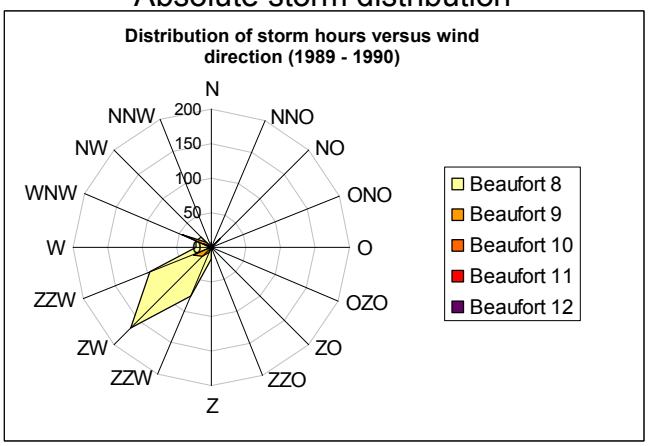

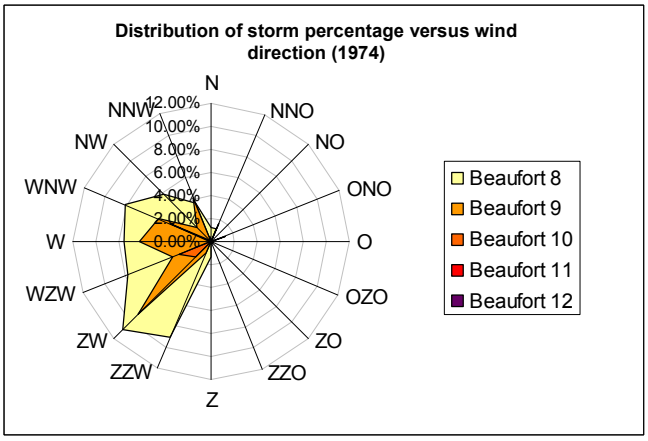

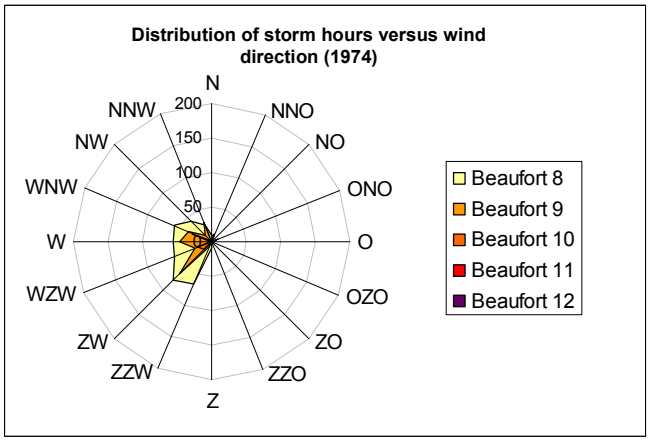

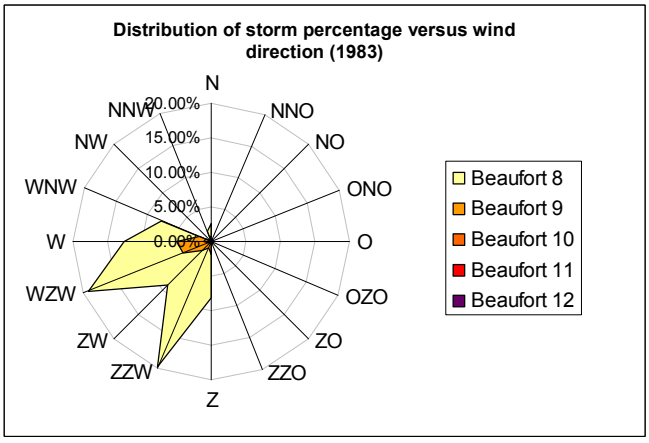

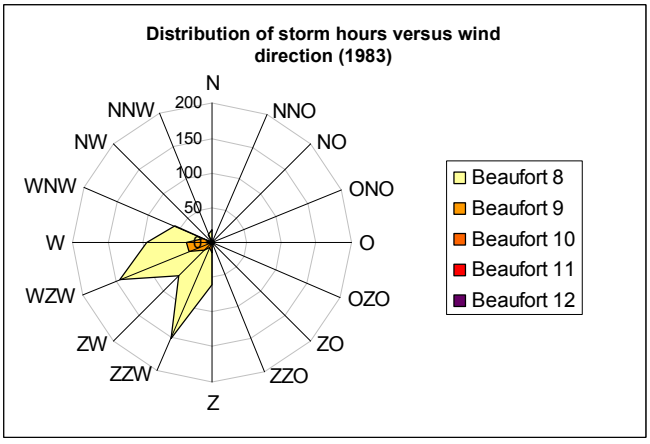

Relative storm distribution

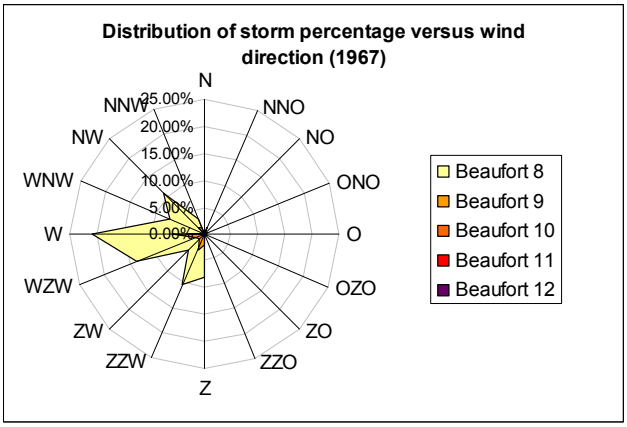

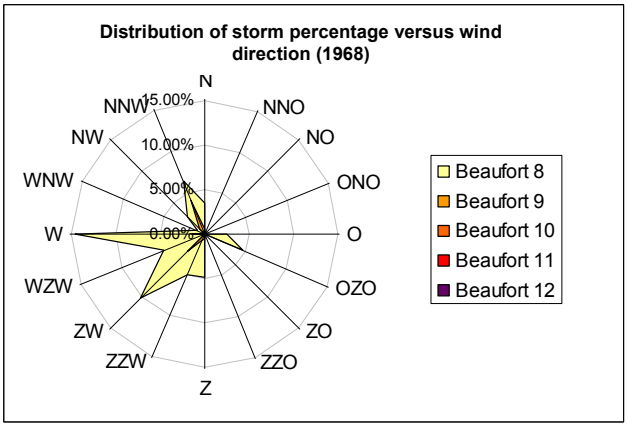

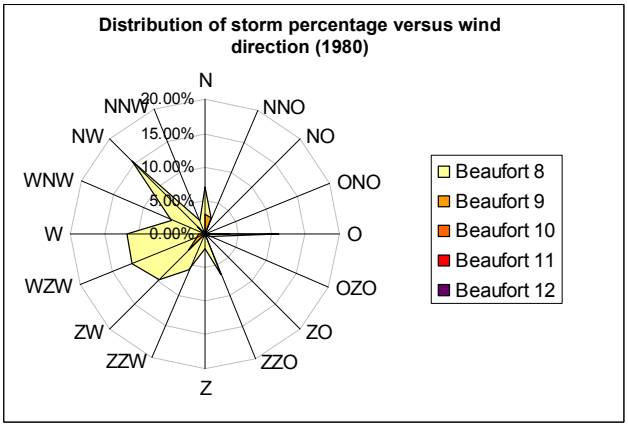

Absolute storm distribution

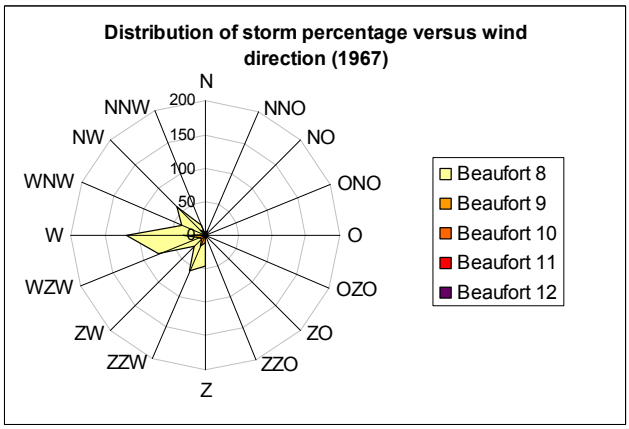

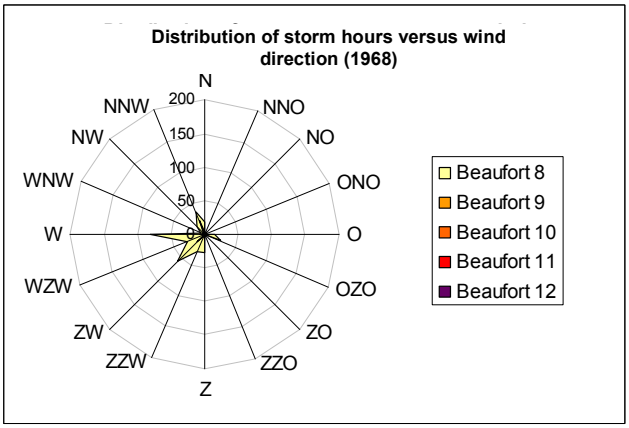

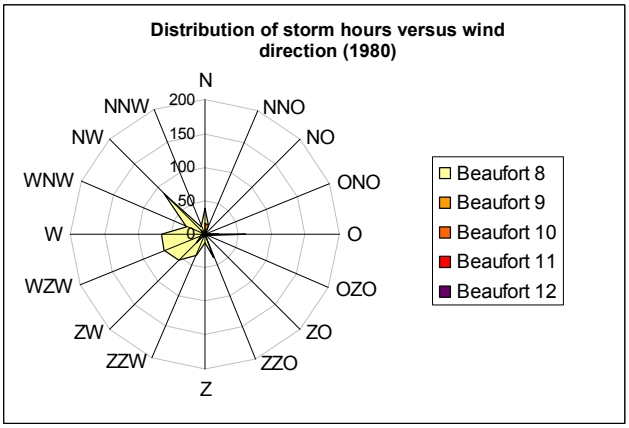

Appendix 3: Terrestrial survey data

General

The terrestrial zone also referred to as the nearshore area respectively the zone between the groynes in front of the sea defence. The following subjects are discussed in this appendix:

- Available survey data.
- Accuracy of the survey.
- Terrestrial geometry.
- Seasonal variation.

Available data

Table A3.1: Available terrestrial surveys. (Negative values are located on the sea defence)

Terrestrial survey date	Length (m)	Distance from RSP Start (m)	Finish (m)
27 November 1997	89	-12	75
7 October 1998	60	2	62
2 December 1998	77	-17	60
9 March 1999	144	-66	78
17 July 1999	119	-15	104
30 August 1999	61	-11	50
21 October 1999	118	-22	96
24 November 1999	107	-22	85
10 January 2000	81	-22	59
13 March 2000	102	-22	80
1 May 2000	107	-22	85
15 August 2000	83	-22	61
21 December 2000	104	-22	82
15 January 2001	92	-22	70
27 February 2001	76	-22	54
10 May 2001	107	-22	85
28 September 2001	79	-22	57
13 December 2001	149	-68	81

Accuracy of the available data

In the following Figure A3.2 some of the actual tracks of the survey are plotted. The axes of graph A3.1 correspond with the RD co-ordination system. The dot represents point zero, the point where the cross-section 20.830 (thick black line) crosses the RSP reference line. The plot (Figure A3.2) shows that the individual survey tracks diverge from the actual cross-section. The maximum observed divergence of the surveyed tracks is about 8m perpendicular to the cross-section. The accompanying error in seabed height depends on the bed slope as well. The bed slope of the bed in the terrestrial area is about 1/40. The maximum error due to divergence of the survey tracks is than about 20cm.

Some surveys have a high resolution with about one measured point every meter while others have a much lower resolution, about one measured point every 5 to 10m. Furthermore, the surveys are executed on foot with a rod. The estimated error is about 10 to 20%.

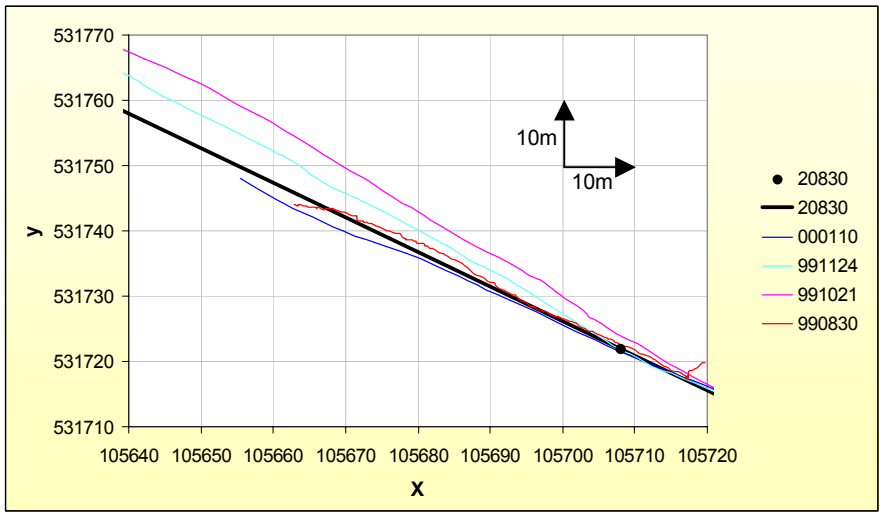

Figure A3.2: Survey tracks of cross-section 20.830.

The terrestrial geometry

Figure A3.3 illustrates the orientation and the mean dimensions of the groyne section. The surveys are executed in this section. At the Pettemer sea defence, groynes stretch out into the sea over a distance of about 80m. Within the area between the groynes that has a width of 120m, 7 rays are surveyed 15m apart. The middle line corresponds with cross-section 20.830. The blue line in Figure A3.4 corresponds with the RSP reference line. The RSP reference line has an offset 63m compared to the used reference line for the surveys (red in Figure A3.3). However, the 'nul lijn' (red line) will not be used as reference during this these. In the following graphs some of the surveyed data have been plotted.

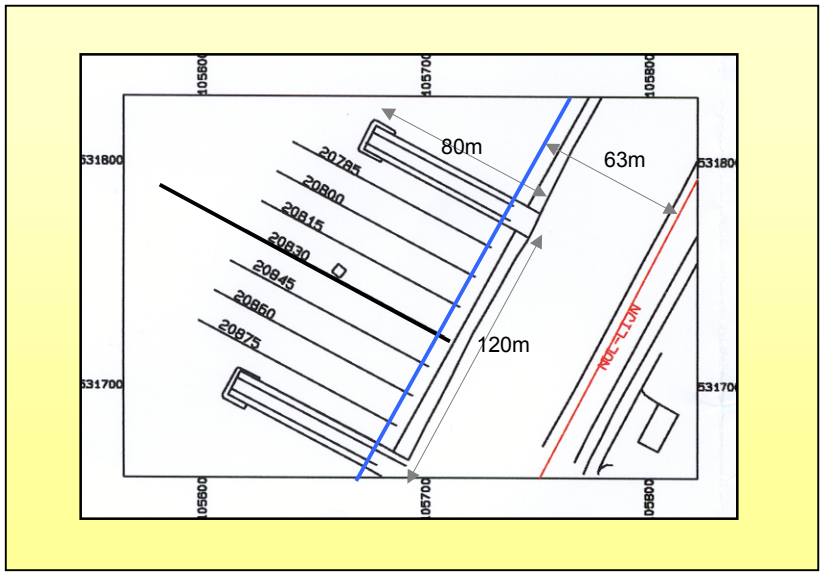

Figure A3.3: Dimensions and orientation of the groyne section.

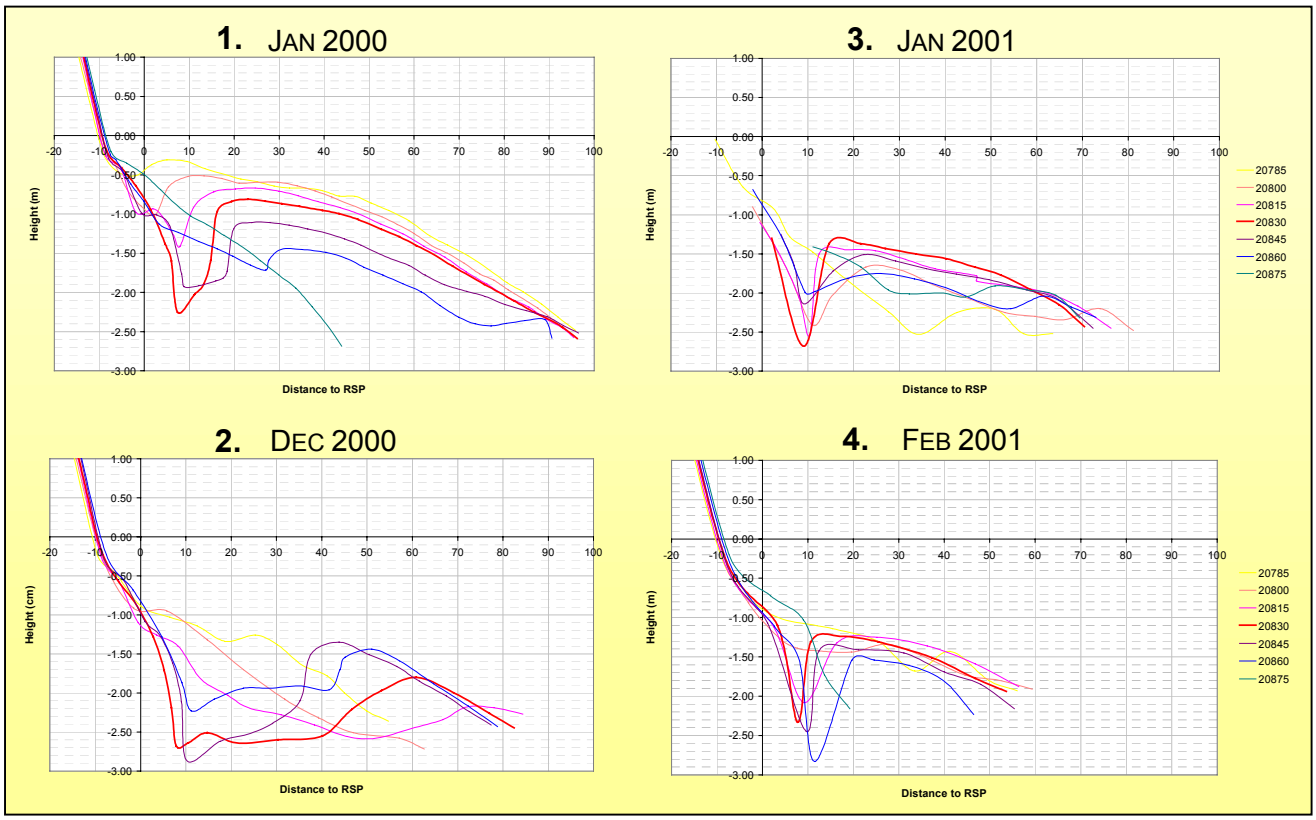

Figure A3.4: 4 Survey plots of all surveys done in the examined groyne section of cross-section 20.830.

The above Figure A3.4 shows 4 graphs that represent the geometry in the terrestrial zone. The profiles in the first graph are surveyed in January 2000; the second graph shows the survey result of 11 months later in Dec 2000. The two other graphs (Jan 2001 and Feb 2001) are from the same winter season as the Dec 2000 graph. The yellow line represents the most northern survey, the green the most southern. The red line corresponds to the cross-section 20.830 that has been further examined during this thesis.

The geometry of the terrestrial zone varies swiftly within a period of months. It can be concluded that the geometry within the groyne section adapts rapidly to the prevailing hydrodynamic conditions. The more constant hydrodynamic conditions during summertime result in a more constant overall profile. Especially the variation in longshore direction reduces during summer.

The sand volume in the terrestrial zone is difficult to determine because often the outer survey lines are missing (20.785 and 20.875) According to the surveys above, the averaged level decrease varies over a period of one year (Jan 2000 to Jan 2001) with 1 to 2 meters. The sand is possible just relocated within the cross-section or within the groyne section itself. Whether sand has been relocated or left the groyne section cannot be verified because of the incomplete data set.

In front of the dike (Distance to RSP = 10m) small troughs can be observed. These troughs only occur during winter and disappear during summer. In December 2000 the observed trough was almost 40m wide while one month later it shrank to 10m. Within a period of one month most of the trough has been filled. However, the seabed of the trough shows practically no variation in depth. To examine the physical processes involved a higher frequency of surveying is required. Nevertheless it is expected that eddies within the groyne section or some sort of scour cause the trough.

An accurate description of the groyne section can only be made properly by defining the entire groyne section three-dimensional. In general it can be concluded that the cross-section 20.830, in the middle of the groyne section, is reasonably representative for the cross-sections (A3.4-1 and A3.4-2). However, sometimes a significant under-estimation or over-estimation has been made.

Seasonal variation

To determine whether the profile between the groynes is affected by seasonal variations all available surveyed profiles of cross-section 20.830 are divided into summer and winter profiles. The data set counts 17 surveys and starts in the fall of 1998. Summer is determined as the period between (1 April and 30 September) and winter as the period between (1 October and 30 March). In Figure A3.5 the results are shown. All winter profiles are indicated with a blue colour, and the summer profiles with a red colour. The averaged summer and winter profiles (thick lines) are drawn in the graph. The difference between both averaged profiles is about 1m in for the first part, up to a distance of RSP + 40m (about 40m offshore of the sea defence toe). For the second part, up to a distance of RSP + 80m, the difference decreases to about 50 – 75cm. Therefore it seems to be justified to conclude that seasonal variation appears to be an issue in within the terrestrial zone.

Furthermore, it should be noted that the variation is significant for summer as well as winter profiles. The variable profiles even lead to situations with higher located winter profiles than summer profiles.

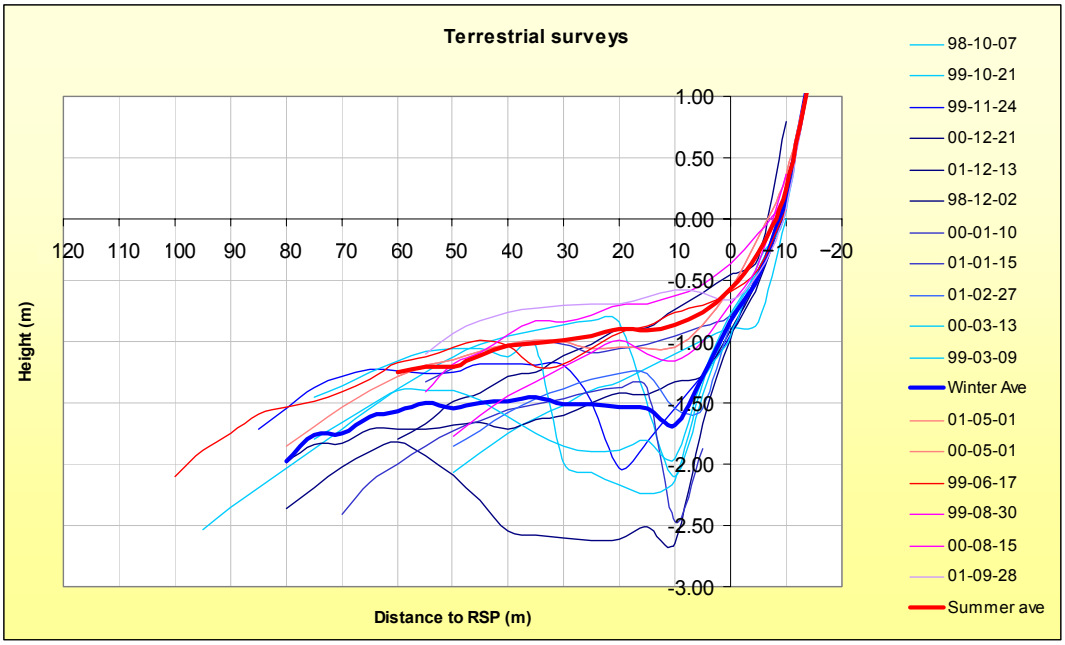

Figure A3.5: Surveyed profiles divided into summer and winter profiles (cross-section 20.830).

Appendix 4: Sounding data

General

The following subjects are discussed in this appendix:

- Available data.
- Accuracy of the survey.
- The bar (bank) and trough behaviour.
- Behaviour of the 'Pettemer polder' bank.

Available data

Table A4.1: Available soundings.

Sounding survey date	Length (m)	Distance from RSP Start (m)	Distance from RSP Finish (m)	Number of points	Ave. dist. (L/#)
10 March 1999	3442	3502	60	2638	1.30 m
18 May 1999	3397	3502	105	8480	0.40 m
7 July 1999	3469	3526	57	9289	0.37 m
13 September 1999	3440	3501	61	9664	0.36 m
20 October 1999	3360	3502	142	2002	1.68 m
15 November 1999	3367	3504	137	2102	1.60 m
24 February 2000	3442	3520	78	10169	0.34 m
6 July 2000	681	732	51	2267	0.30 m
30 November 2000	3518	3527	9	9104	0.39 m
27 February 2001	3397	3508	111	8325	0.41 m
22 May 2001	3440	3507	67	5247	0.66 m
6 July 2001	908	1036	128	1492	0.61 m
26 September 2001	3445	3509	64	6533	0.53 m
10 December 2001	3538	3549	11	5675	0.62 m

Accuracy of the available data

The soundings, surveyed by boat, appear to be reasonably accurate. Several aspects affect the error:

- Weather conditions.
- Number of different vessels used for survey.
- Survey track.
- Variation in the measured density.
- Survey equipment.

The maximum distance between actual measured tracks and the cross-shore is about 20m, as is shown in Figure A4.2. The average resolution (track distance divided by number of measured points) is between the 1.6 and 0.3m. This means that the seabed has been measured after every meter. The surveyed points are made equivalent to the actual cross-shore by plotting the surveyed track onto the cross-shore. The profile variation in longshore direction is smaller compared to the variation in cross-shore direction. Taking into account the divergence distance and the bed slope, an error-range of about 5-15cm has been determined. Furthermore other aspects, like survey equipment, weather conditions and different survey vessels increase the error. A standard deviation of 15-30cm for survey equipment including the weather conditions and a standard deviation of 10cm for different survey vessels are sufficient according to [Tönis and Veen, 2001; Houwing, 1991].

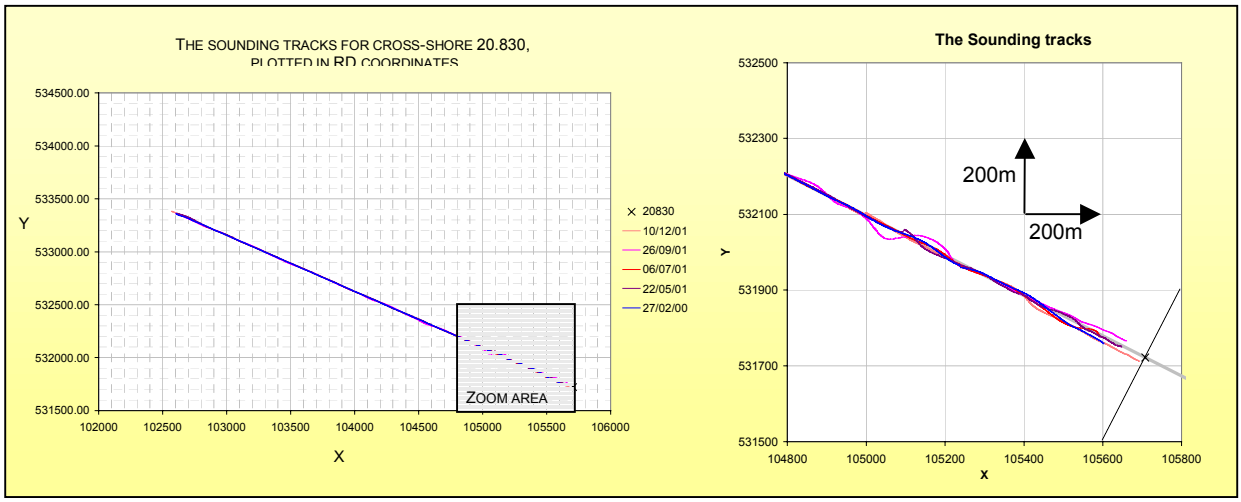

Figure A4.2: Surveyed tracks.

Seasonal behaviour of bar and trough

The system of trough and trough is situated in front of the terrestrial zone between the 100 and 500m. The location and height of the trough crest are used to examine trough migration and growth. For the trough a similar procedure has been used. The minimum seabed level has been used as reference point.

In Figure A4.3, the trough and trough data ranging from March 1999 to December 2001 are plotted. On March 1999, the trough crest is located about 400m from RSP at a height of NAP –3.8m. During a period of about 3 years it shifted landward over a distance of 50m. The crest level varies within the same period between the NAP –3.5m and –4.0m.

Most of the trough movement has occurred in the period between November 1999 and February 2000. During this winter period the trough has migrated towards the shore, whereas it is expected that troughs move seaward during winter conditions. During severe wave conditions, the share of breaking waves increases on the transport process. Breaking results in a seaward-directed undertow stimulating offshore-directed cross-shore transport. [VAN RIJN, 2002]

The depth of the trough varies within a range of a meter between the NAP –5.8m and the –6.8m. The cross-shore variation of the trough appears to be constant over the observation period.

To determine if the geometry of trough and trough system has been affected by seasonal variation, the surveyed profiles are divided into two segments; winter and summer. Summer is determined as the period between (1 April and 30 September) and winter as the period between (1 October and 30 March).

The profiles in Figure A4.4 show no obvious signs of seasonal variation. However, it is difficult to determine whether seasonal variation causes the variation in the geometry of the trough and trough system based on the limited data set.

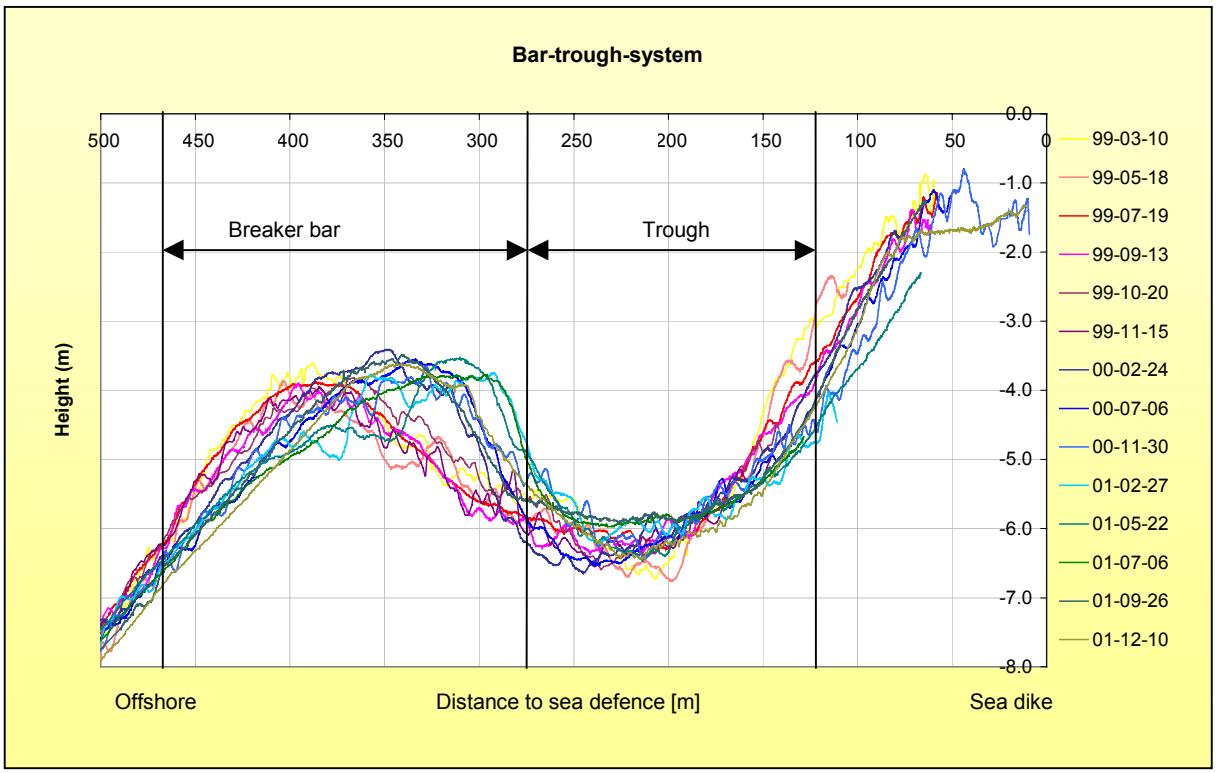

Figure A4.3: Profiles of the bar and trough surveyed at cross-section 20.830 between March 1999 and December 2001.

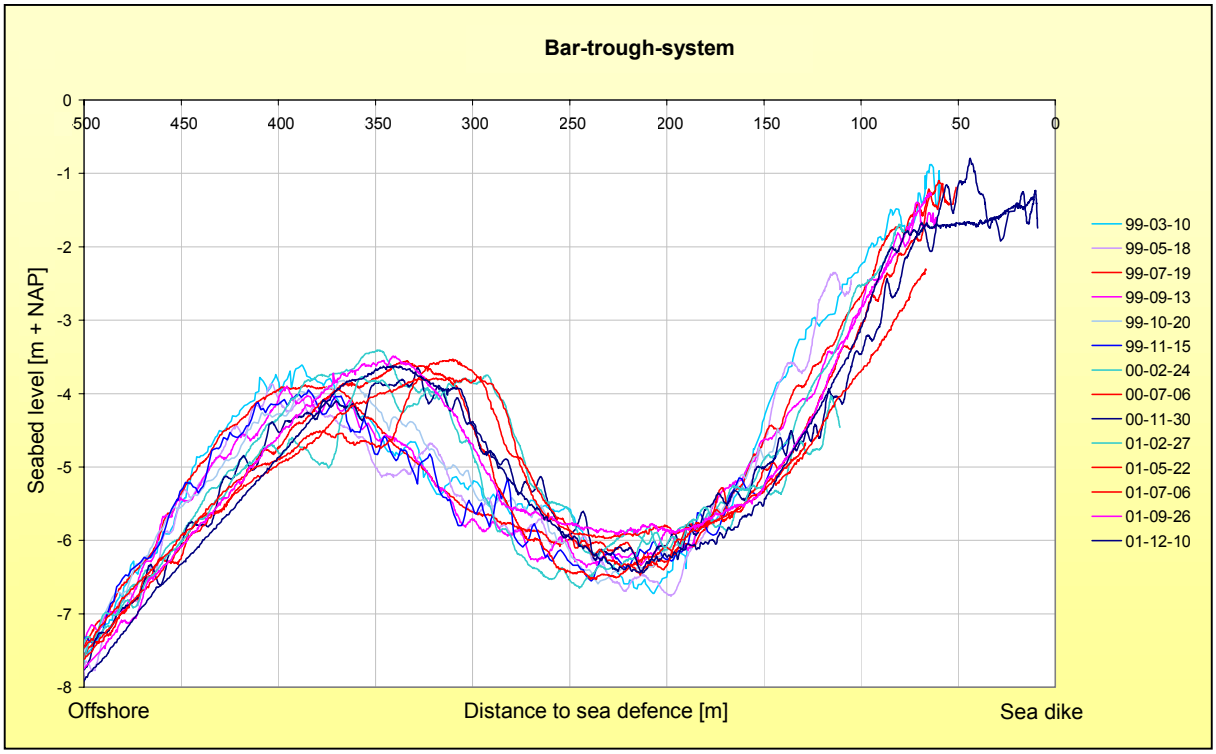

Figure A4.4: Profiles from Figure A4.3 divided in winter (coloured blue) and summer (coloured red) surveyed profiles.

The 'Pettemer polder' bank

The 'Pettemer polder' bank is located at a distance of 3km from the shore. The different surveys are shown in Figure A4.5. According to the soundings the top of the 'Pettemer polder' bank varies in the range of 1m. Possibly the variation is the result of small errors in the surveyed line. However, it is more likely that the top layer is sandy and that migrating sand waves cause the variation. A sandy crest layer can also explain the difference between the surveyed profiles that are often ribbed and sometimes smooth. The difference in profile height and shape is in that case caused by local hydrodynamic conditions.

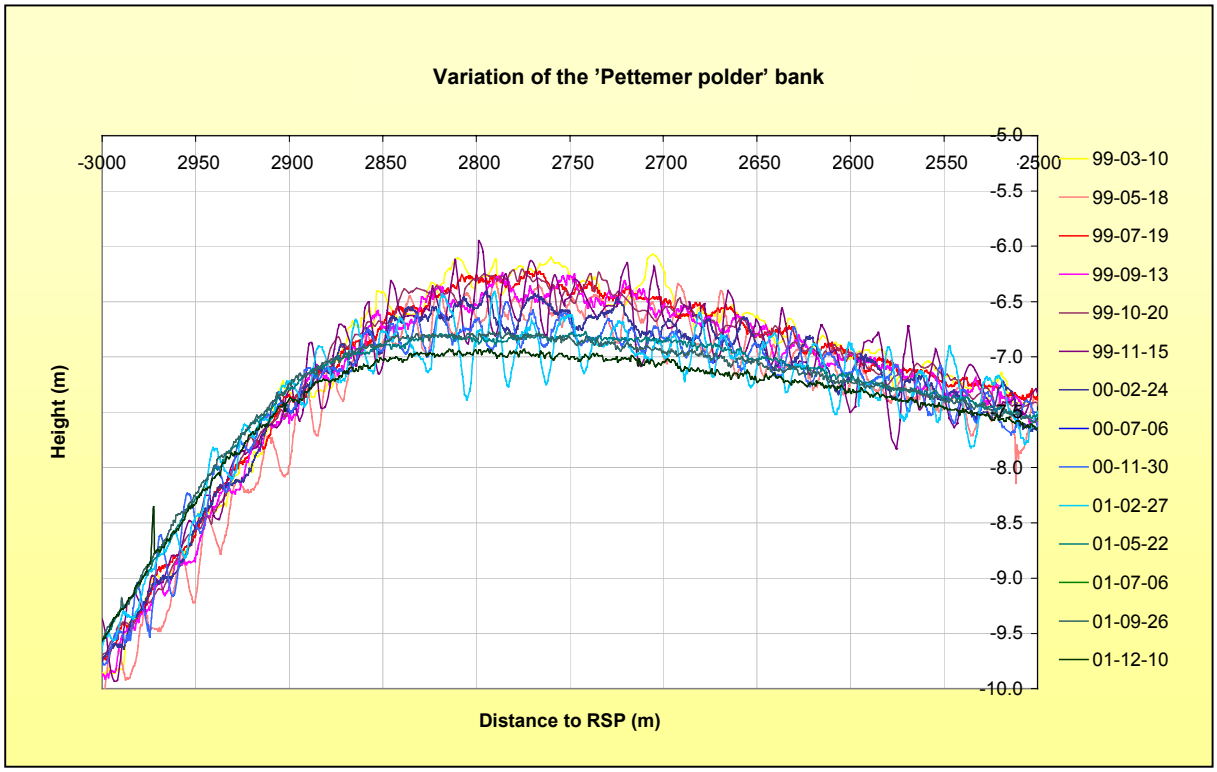

Figure A4.5: Surveyed profiles of the 'Pettemer polder' bank at cross-section 20.830.

Appendix 5: JARKUS data set

General

The following subjects will be discussed in this appendix:
Available data:

- Manipulation.
- Mean.
- Dispersion.

Trends:

- Bar and trough migration.
- Near-shore area difference.

Volume variation:

- Method.
- Averaged height variation.
- 1990 decrease in volume.

Available data

The JARKUS data set exists of seabed measurements along the sandy Dutch coastline. For this study only data from cross-section 20.830 has been used. The available profiles are listed in Table A5.1.

Table A5.1: Available JARKUS profiles for cross-section 20.830. (Negative values are on sea defence)

Terrestrial survey date			Length	Distance from RSP		Terrestrial survey date			Length	Distance from RSP	
year	height	depth	(m)	Start (m)	Finish (m)	year	height	depth	(m)	Start (m)	Finish (m)
1964		14-Jul	780	0	780	1983		07-Jul	800	0	800
1965		19-Jul	780	0	780	1984		18-Jun	810	-10	800
1966		10-Jun	870	10	880	1985		04-Jul	780	20	800
1967		10-Jul	810	-10	800	1986		26-Jun	740	40	780
1968			810	-10	800	1987		12-Aug	480	30	510
1969			800	0	800	1988		07-Sep	870	30	900
1970						1989		07-Sep	880	30	910
1971		05-Jul	810	-10	800	1990	14-Apr	24-Aug	1160	-150	1010
1972						1991		21-Jun	1030	0	1030
1973		25-Jun	800	0	800	1992		24-Jun	1020	0	1020
1974		10-Apr	800	0	800	1993		07-Sep	920	20	940
1975		10-Jul	810	-10	800	1994		01-Jul	980	20	1000
1976		24-Jun	810	-10	800	1995	30-Mar	29-Jun	1150	-150	1000
1977		24-Aug	740	60	800	1996		11-Apr	1000	0	1000
1978		06-Sep	730	50	780	1997		11-Jun	1100	0	1100
1979		21-Jun	790	-10	780	1998	19-Jul	11-Aug	1250	-150	1100
1980		13-May	760	40	800	1999	17-Apr	16-Jun	1150	-150	1000
1981		13-May	820	-20	800	2000	04-Nov	03-Jul	1150	40	1190
1982		21-Apr	810	-10	800	2001					

As is shown in Table A5.1 the survey data from 1970 and 1972 are not available. The total set counts 35 profiles that are all surveyed in the period between April and September. Before 1990 most profiles had a length of about 750 to 800m and finished at a distance of 800m offshore. After 1990 the total survey distance increases to lengths varying between the 1000 and 1200m, sometimes including the sea defence. Two dates are given; height survey dates and depth survey dates. The difference between height and depth surveys is the survey method. The height surveys for the part above the low water line are executed with an aeroplane, while the depth surveys are soundings executed by a ship. If both methods are executed in the same year, the profile consists of data from both methods.

Manipulation

Besides the difference in length, starting point and survey method the amount of surveyed points for each profile also differ. After 1986 the profiles are based on points surveyed every 10m, but before 1986 the surveyed profiles are composed of two different sets, the first set up to 300m consists of points measured every 10m and the second set consists of points measured every 20m. To make the total profiles equivalent to the first set, the part of the profiles before 1986 that is based upon the second set has been manipulated with linear interpolation. The result of all JARKUS profiles is plotted in Figure A5.2.

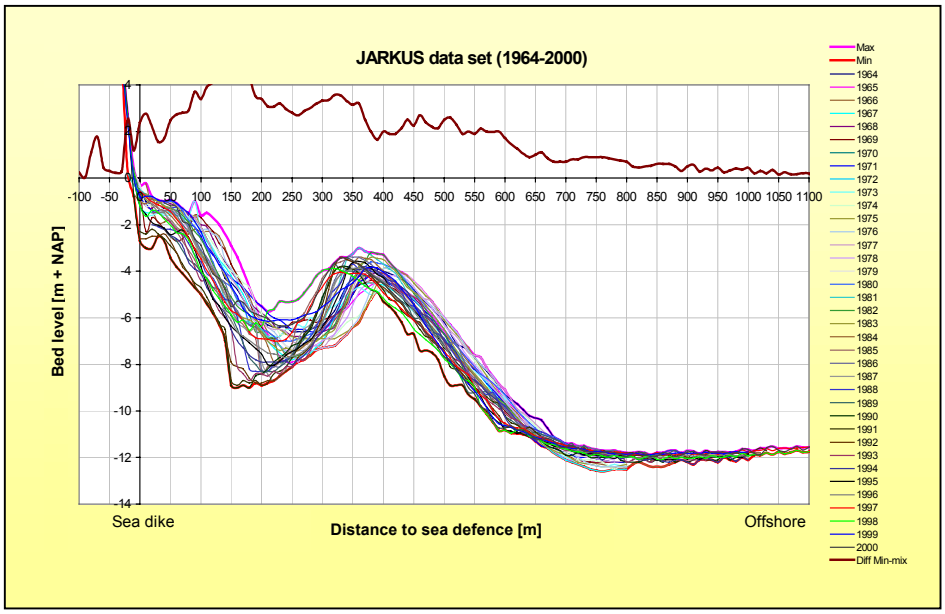

Figure A5.2: All available JARKUS profiles for cross-section 20.830.

Mean, maximum and minimum envelope profiles

The mean profile of the 35 surveyed profiles still shows the same characteristics as the single profiles do. The dynamic bar and trough system varies little over the 35-year period and therefore the mean profile as well as the maximum and minimum envelope profiles maintain the same characteristics. Generally bars migrate at a faster rate along the Holland coast, resulting in a mean profile without the clear contours of specific bars. This means that generally the mean profile is never found in reality. However, in this case the mean profile could occur in reality and is therefore a representative profile. The minimum and maximum profiles are more unlikely to occur in reality.

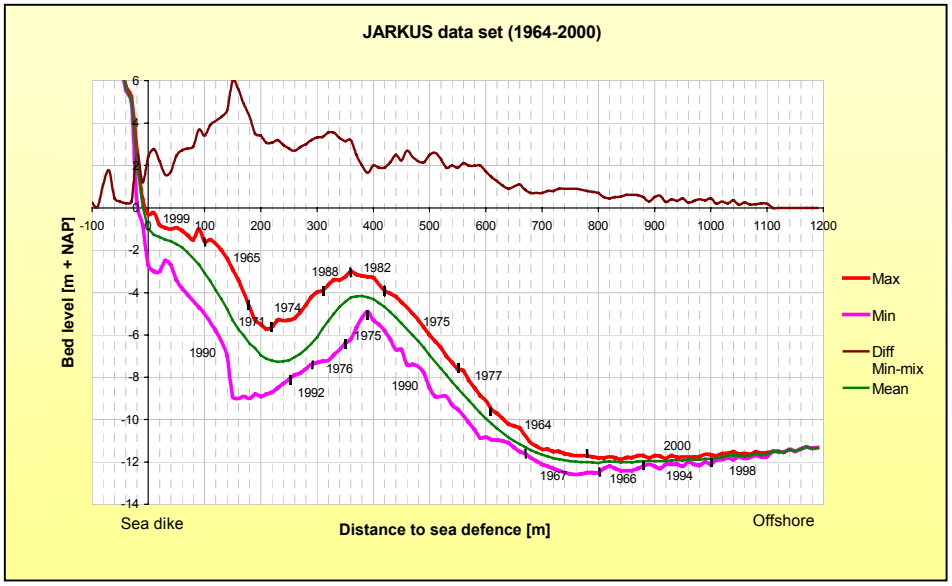

Figure A5.3: JARKUS envelope profiles for cross-section 20.830, divided by contributing year.

A first analysis of JARKUS data set considers the maximum and minimum envelope profiles, accompanied with a mean profile as is shown in Figure A5.3. The minimum and maximum envelope profiles are composed of different sections of annual profiles. The 1990 profile contributes most to the minimum envelope profile, while no specific profile dominates the maximum envelope profile.

The difference between the minimum and maximum envelope profiles is also shown in Figure A5.3 and shows the maximum variation of a specific location along the cross-section 20.830. To increase understanding of the dispersion Figure A5.4 is used.

Deviation

The deviation of the profile is determined using histograms for each location along the cross-section. Figure A5.4 shows the result. This Figure consists of two parts the upper part (diagram) shows the dispersion of the surveyed data for each location along the cross-section. The mean profile is shown below to show the level of the location along the cross-section.

The diagram combines all histograms of the location along the cross-section. The colours correspond with a specific number of profiles according to the legend that are found within the boundaries set at the y-axis. The y-axis of the diagram is divided into sections. These sections indicate the difference between the local height of the profile and the local mean profile height.

For example, at the location 50m offshore of the RSP reference line a profile is found that has a 1.0m higher seabed level as the local mean seabed level does; This profile will contribute to the number of profiles within the 0.75 to 1.25m section. Each location has a maximum of 35 profiles to divide over the sections. As the profile numbers in a section increase, the colours turn form yellow via red into dark blue.

The profile shows a normal distribution with little deviation at the tow of the bank and further offshore. The normal distribution is maintained up to the top of the bank with a slightly increased dispersion. Between the bar crest (380m) and the toe of the sea dike (0m) the deviation increases and the distribution is not characterised normally. This could be the result of the small data set (a set of only 35 items) or the normal distribution function is invalid for this section.

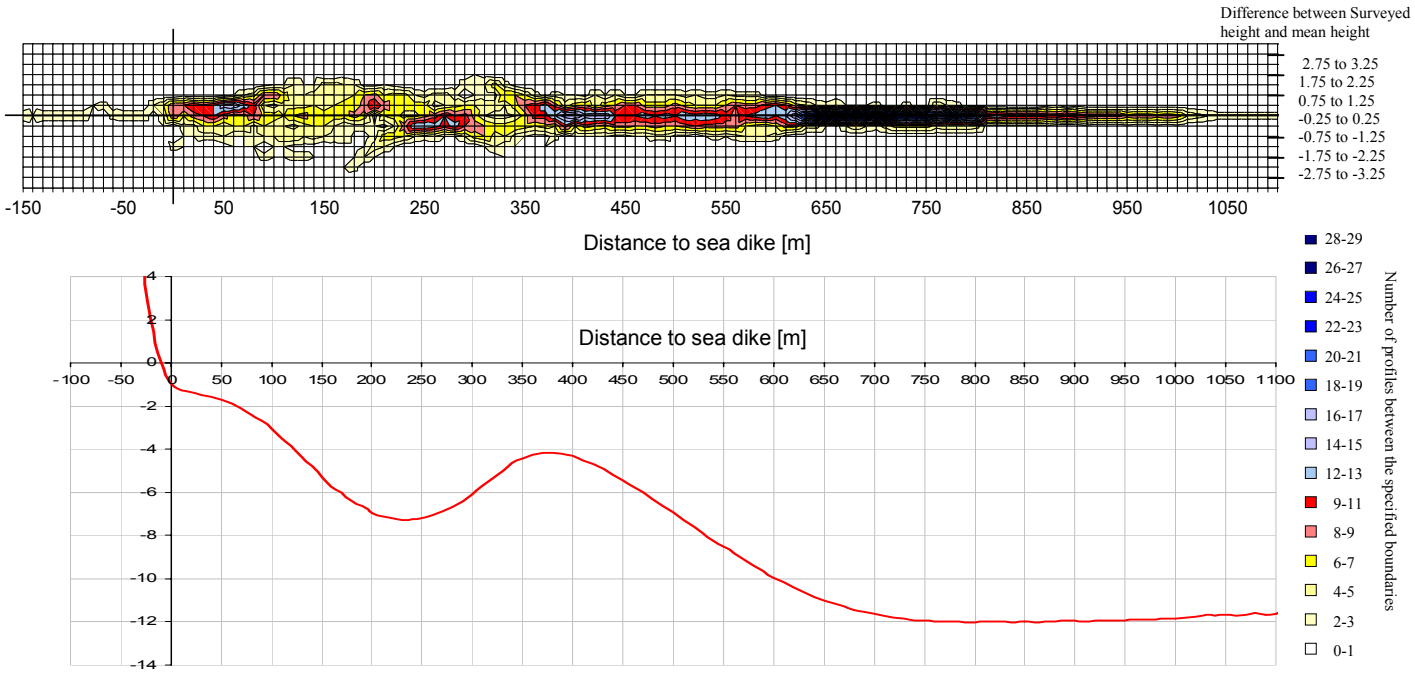

Figure A5.4: Deviation from the mean profile for the profiles surveyed at cross-section 20.830.

Variation

The difference between the minimum and maximum profile, shown in Figure A5.3, is an indication for the instability of the local profile level and corresponds with the deviation diagram. Especially the shallow area, from the toe of the sea dike to the first bar, varies significantly. Near the onshore edge of trough the variation increases up to 6m. The local increase of variation is attributed to the varying wide in cross-shore distance and the fact that the edge of the trough has a relatively steep slope. At a distance of 700 to 800m offshore the variation decreases to about 0.5 to 1.0m; the local level of the profile appears to be constant and therefore qualifies as an offshore boundary for the comparison of the sand volume.

Trends

In the previous Paragraph the JARKUS profiles were plotted onto each other, in Figure A5.5 the profiles are spread out to show the annual changes. The y-axis is only valid for the thick profile (1964), all others profiles have an offset of 1m to the previous profile.

The top and bottom of respectively the bar and trough are indicated with dots respectively squares. According to the results shown in Figure A5.5 the averaged bank migration over the total surveyed period is in shoreward direction. The trough migration shows a similar course. During an earlier period of 15 years (1975 to 1990) the trough appeared to move shoreward, while during the consecutive decade a migration in offshore direction can be observed. The bar and trough migration behaviour appears to a long-term process in the order of decades, this reduces the importance of this bar-trough behaviour on the short-term.

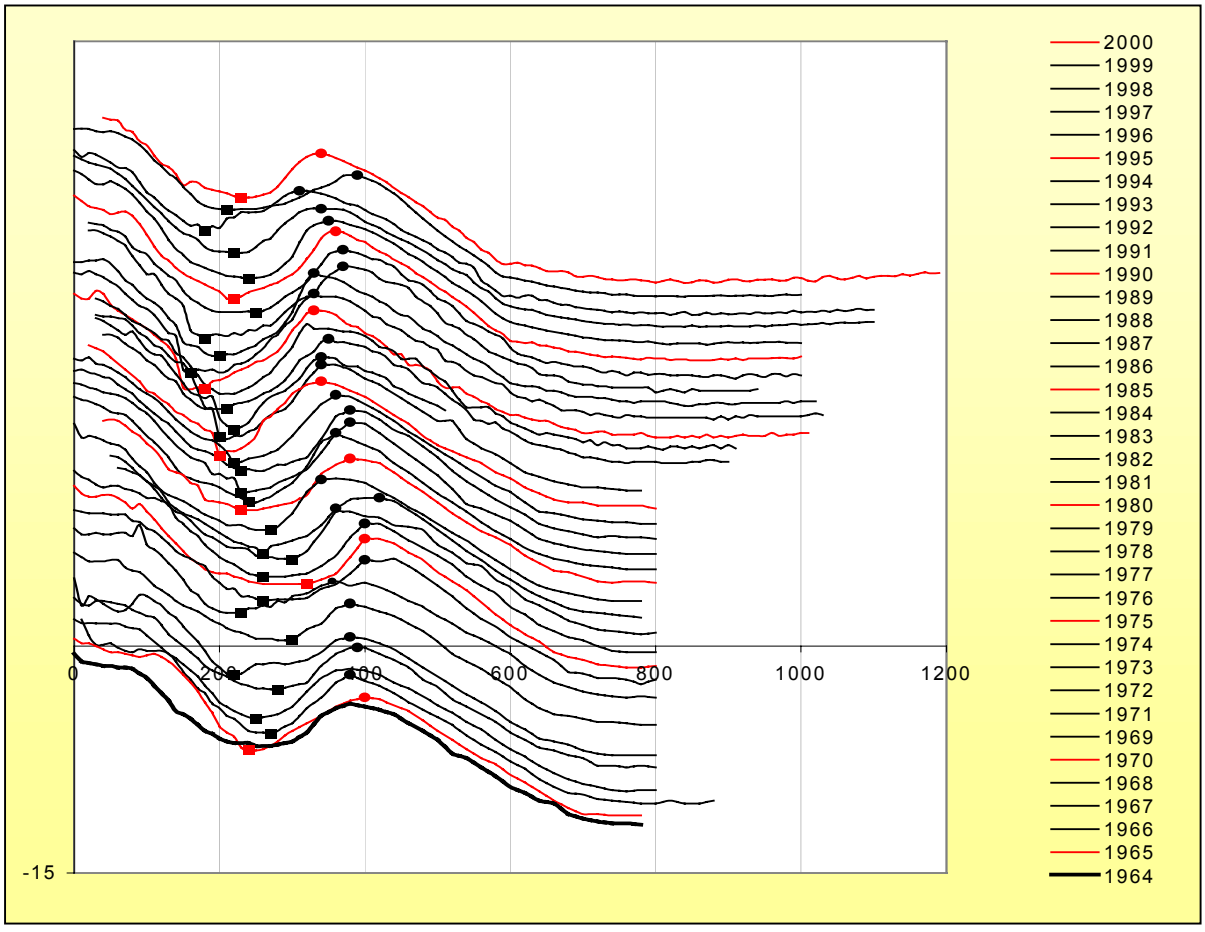

Figure A5.5: A comparison of the JARKUS profile, to determine the migration of the bar and trough, indicated with respectively dots and squares.

Another aspect that follows from A5.5 is the reduction of the amount of sand in the nearshore area. The reduction is accompanied by an increasing slope steepness that reaches a maximum in 1990. This deepening could be caused by a heavy storm that took place 4 days before the survey started. [AUGUSTIJN ET AL., 1990]

Volume variation

Sand volumes calculations are executed for different sections of the JARKUS profiles. These calculations are based on a method that approaches the volume. Because all profiles are equivalent and composed of points with an in-between distance of 10m, rectangular cells with a constant wide of 10m approach the total volume. The length of these rectangular cells is defined as the height of a profile point with respect to the NAP –14m line. The method is elucidated in Figure A5.6. In this Figure the green area is the calculated volume and the line with red dots the schematised survey profile.

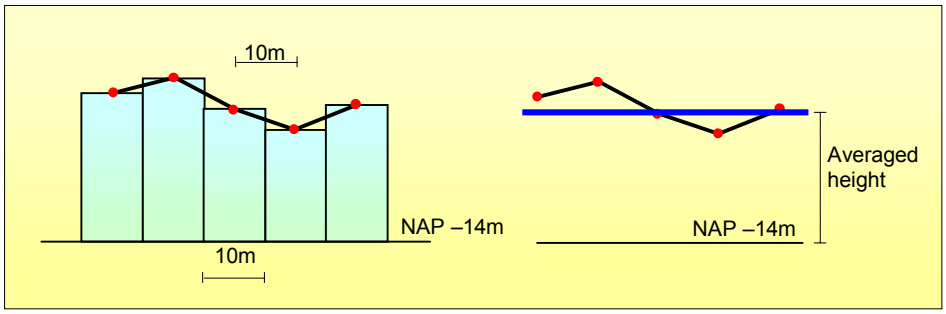

Figure A5.6: Method used to determine the profile volumes (m^3/m).

Besides the annual calculations of the sand volume over a certain distance, a comparison of the annual difference in averaged height is produced. The averaged height, the total volume divided by the total distance along the profile, is compared with the averaged height of the previous year. Before 1964 no profiles are surveyed, the difference between the profile of the 1964 and that of a previous year is therefore unknown. For now the value is set to nil. If the previous year is unavailable the difference in averaged seabed height is determined with respect to the last preceding available year.

To see if the chosen boundaries affect the outcome of the volume calculations a different onshore boundary is checked. The location of the offshore boundary is believed to have little influence on the outcome of the volume calculations because the location of the offshore boundary shows little variation in seabed level according to Figure A5.3. Between the following boundaries the sand volume is determined for all possible profiles.

Table A5.7: Boundaries used for the volume calculations.

Figure	Shoreward boundary	Seaward boundary
A5.9	60	780
A5.14	30	780
A5.10	60	380
A5.11	380	780
A5.12	60	220
A5.13	220	380

Between the 60m and 780m all-available JARKUS profiles are evaluated. The choice for both boundaries is based on two criteria;

- A maximum number of profiles.
- A maximum distance between the boundaries.

The results are found at the end of this Appendix in Figures A5.9 to A5.14. A decrease in volume and in average seabed height can be observed for the summer of 1990. The averaged height of the 1990 profile drops 0.6m compared to the previous year. The decrease in seabed height is possibly the result of the stormy conditions. Within a period of 10 years the volume seems to recovers up to its average volume.

To find the most affected region, the distance between the boundaries is split into two. A new boundary located at the averaged top of the dynamic sand bank (380m to RSP) divides the section. Both parts are shown in Figures A5.10 and A5.11. Both parts show a decrease in volume for the year 1990, only the part in front of the sand bank immediately regenerates the year after, while the onshore part starts to regenerate 4 years later. If the onshore part (between 60 and 380m) is further divided buy a boundary set at the bottom of the trough (220m); the onshore part (from 60 to 220m) seems to be solely affected by the variation.

To determine the actually changes, the profiles are shown in Figure A5.8 below. The initial profile (1986) is compared with the minimum volume profile (1990); the next profile (1991) and previous (1989) profile are added to see the annual changes. Finally the 2000 profile is added to show the results of 10-year recovery.

Figure A5.8 confirms the results based on the volume analysis. And both the slopes in offshore direction are mostly affected by the incident of 1990. The fact that these slopes are affected is understandable because the hydraulic load is absorbed at these slopes. First the outer slopes regenerate before the inner slope starts to regenerate.

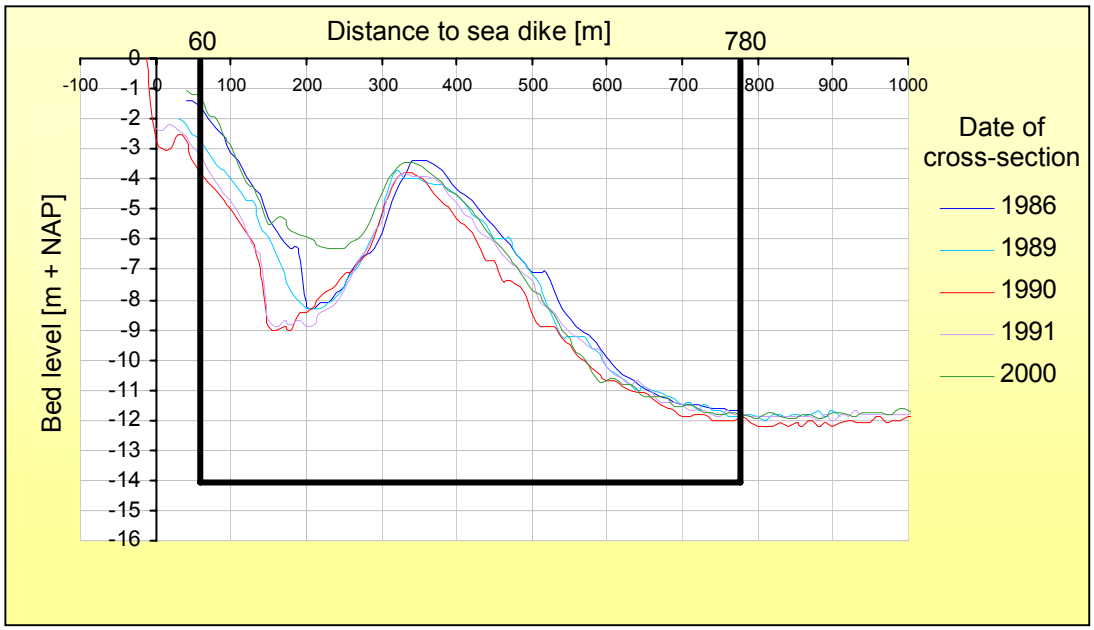

Figure A5.8: The profile variation between the set boundaries (60m, 780m and -14m + NAP).

As is mentioned before, the onshore boundary could influence the outcome of the volume calculation significantly because the seabed level varies a lot at the chosen location. A second onshore location boundary (30m) is chosen and compared with the initial results. The result of this volume calculation is found in Figure A5.14. Figure A5.14 shows practically no difference in the variation of the profile volume (m^3/m) with Figure A5.9 that had the onshore boundary set at 60m. Consequently the profile volume is hardly affected by little changes in the onshore boundary.

If cross-shore transport is solely responsible for the variations in volume, no differences in volume should be found if the offshore boundary is set at infinity (or at a distance where the seabed is not influenced by waves at all). The long-shore currents significantly exceed the cross-shore currents; long-shore transport can therefore not be neglected. According to [VAN RIJN, 2000] long shore transport determines the volume variations on the long-term currents, as are treated in the volume comparison analysis.

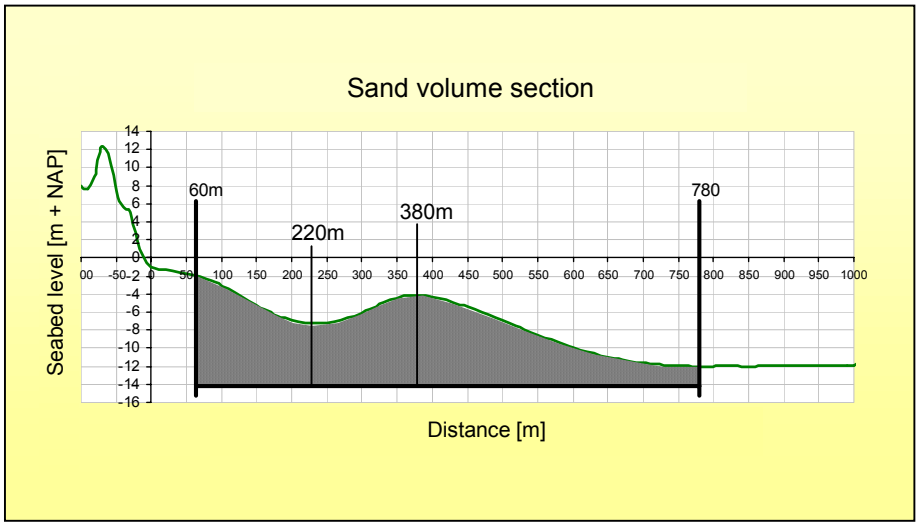

Figure A5.9: The sand volume section with boundaries (60m, 780m and –14 + NAP) and the additional boundaries used in the following analysis (220m and 380m.

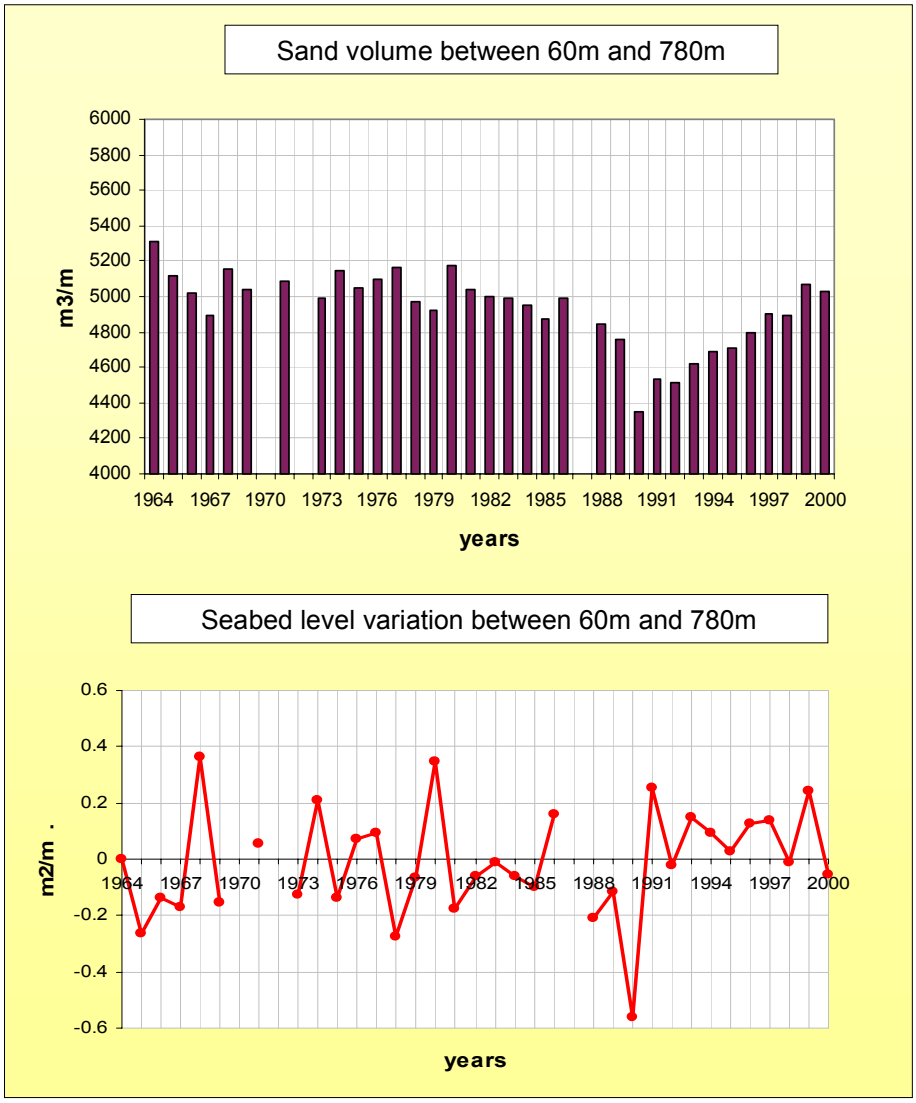

Figure A5.10: results of the volume section (60m, 780m and –14 + NAP).

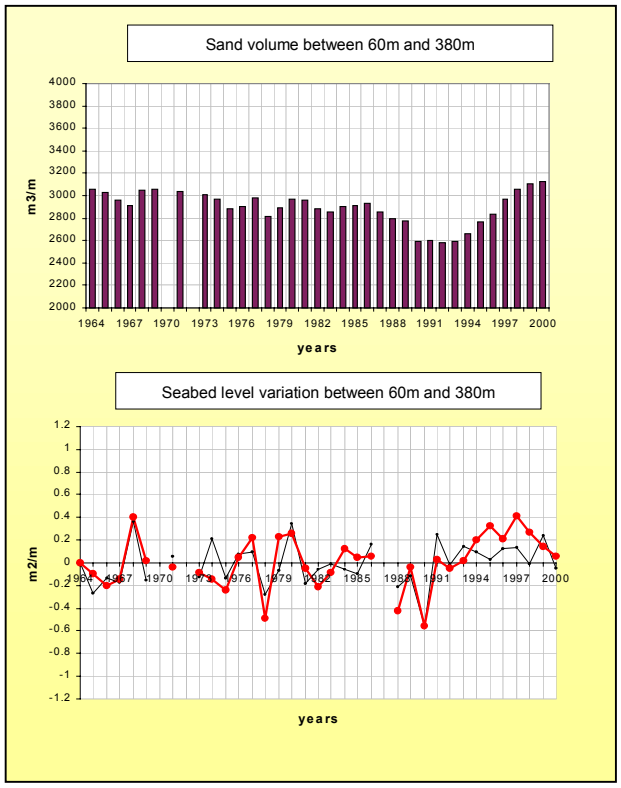

Figure A5.11: Results of the volume section (60m, 380m).

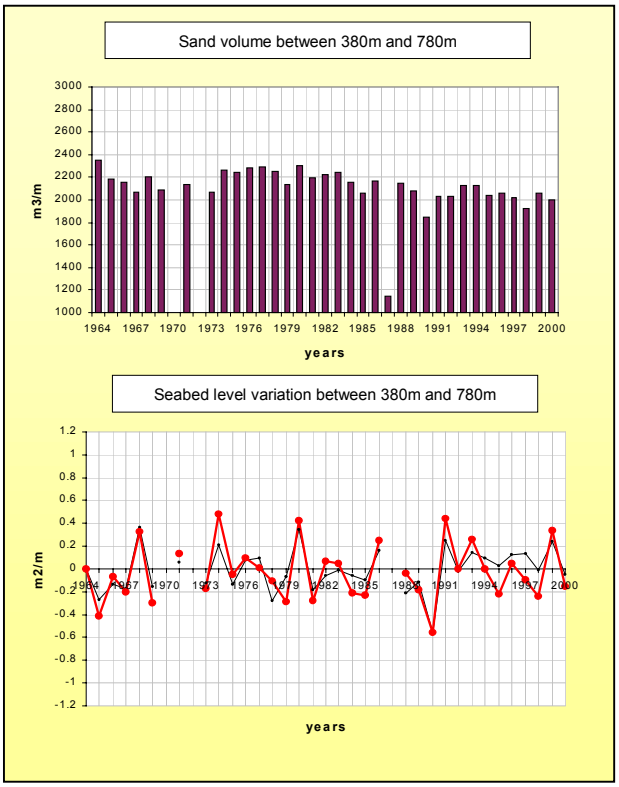

Figure A5.12: Results of the volume section (380m, 780m).

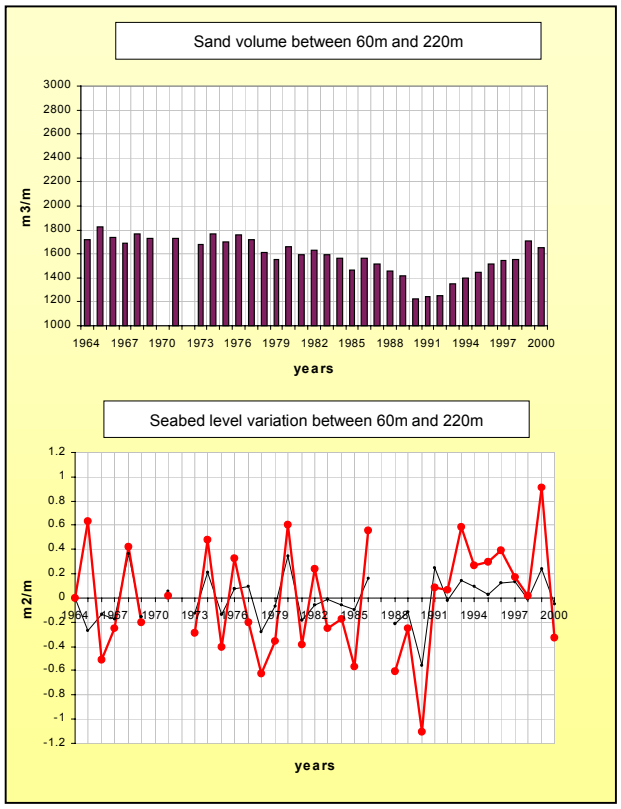

Figure A5.13: Results of the volume section (60m, 220m).

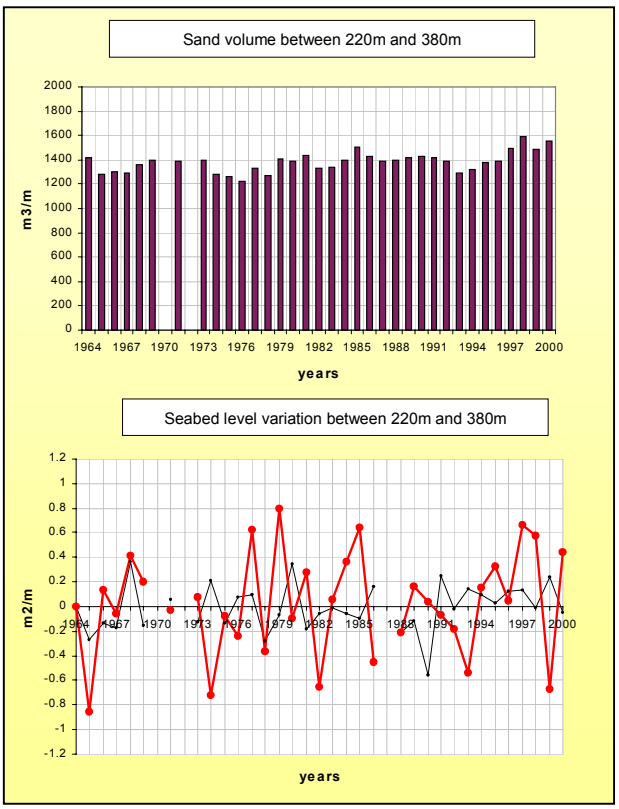

Figure A5.14: Results of the volume section (220, 380m).

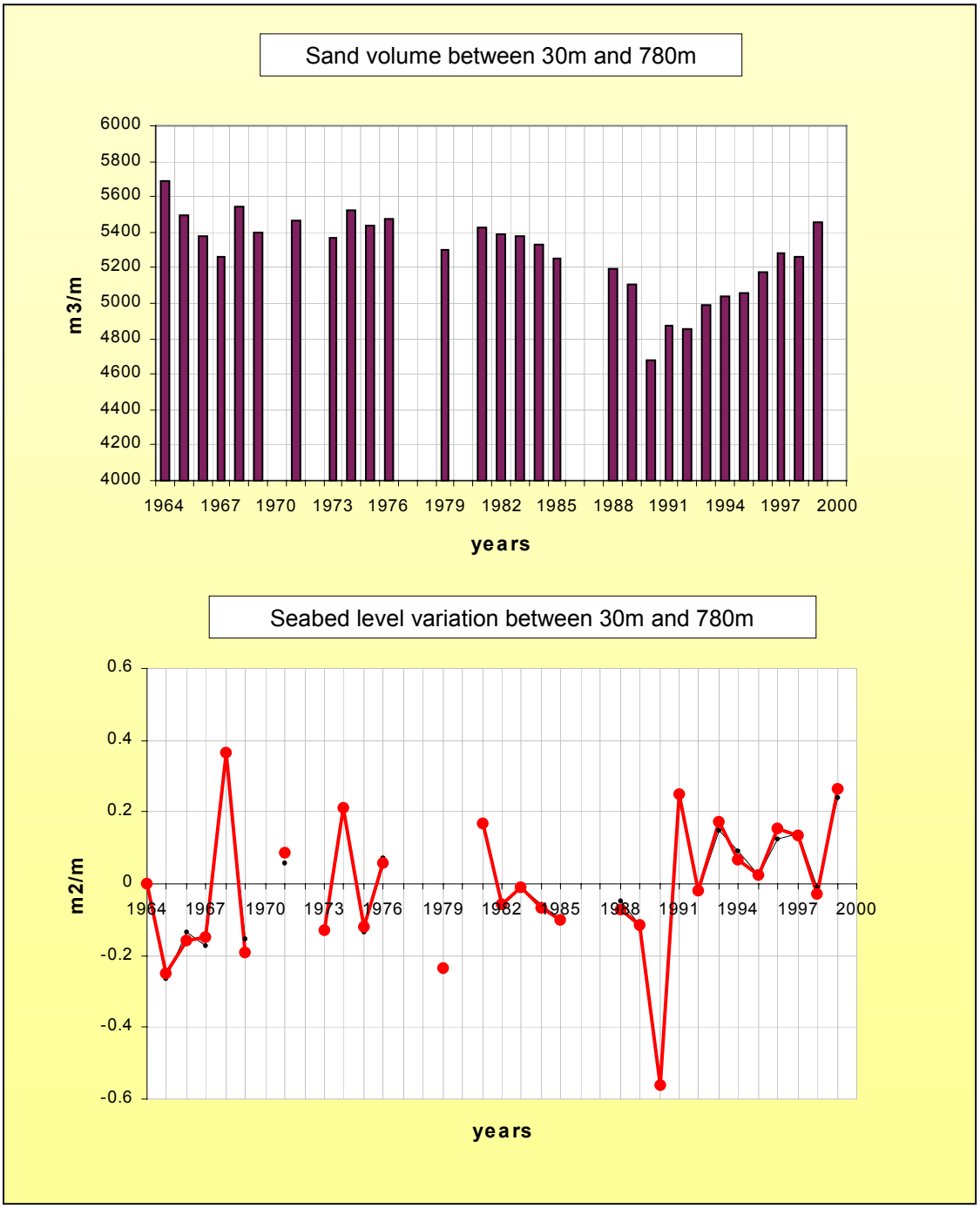

Figure A5.16: Results of the volume section (30, 780m) that has been used as reference.

Table A5.16: The manipulated gabs in the data set of the area between the groynes used in the volume comparison.

Survey data	Location of the survey points (reference point RSP)								Average
	0	10	20	30	40	50	60	70	
1964	-0.5	-1	-1.1	-1.2	-1.3	-1.3	-1.4	-1.4	-1.15
1965	-0.5	-0.8	-0.8	-1	-1.2	-1.4	-1.4	-1.5	-1.08
1966	-0.23	-0.23	-1.3	-1.9	-1.9	-1.8	-2.1	-2.3	-1.47
1967	-1.21	-1.48	-1.48	-1.49	-1.49	-1.5	-1.5	-1.7	-1.48
1968	-0.8	-1.2	-1.3	-1	-1	-1.1	-1.2	-1.3	-1.11
1969	-0.5	-2.3	-1.7	-1.9	-2.2	-2.5	-2.7	-2.6	-2.05
1970									
1971	-0.8	-1.1	-1.4	-1.4	-1.4	-1.3	-1.3	-1.8	-1.31
1972									
1973	-1.2	-1.6	-1.6	-1.5	-1.6	-1.6	-1.5	-1.5	-1.51
1974	-1	-1.1	-1.2	-1.2	-1.2	-1.3	-1.3	-1.3	-1.20
1975	-0.4	-0.9	-1.1	-1.1	-1	-1	-1.2	-1.5	-1.03
1976	-0.4	-0.8	-1	-1.3	-1.5	-1.4	-1.4	-1.6	-1.18
1977	-1.2	-1.2	-1.2	-1.2	-1.2	-1.2	-1.2	-1.3	-1.21
1978	-1.4	-1.4	-1.4	-1.4	-1.4	-1.4	-1.5	-1.8	-1.46
1979	-0.3	-1.2	-1.1	-1.2	-1.4	-1.6	-1.7	-2	-1.31
1980	-1.1	-1.1	-1.1	-1.1	-1.1	-1	-1.1	-1.4	-1.13
1981	-0.5	-0.7	-0.8	-1	-1.2	-1.5	-1.6	-1.7	-1.13
1982	-0.6	-0.7	-0.9	-1	-1.2	-1.3	-1.4	-1.6	-1.09
1983	-0.8	-0.7	-0.9	-1	-1.2	-1.3	-1.7	-2	-1.20
1984	-1	-1.1	-0.9	-1.3	-1.4	-1.6	-1.9	-2.2	-1.43
1985	-1.1	-1.1	-1.1	-1.3	-1.5	-1.9	-2.3	-2.7	-1.63
1986	-1.4	-1.4	-1.4	-1.4	-1.4	-1.4	-1.6	-2	-1.50
1987	-1.3	-1.3	-1.3	-1.3	-1.5	-1.8	-2.1	-2.4	-1.63
1988	-2.1	-2.1	-2.1	-2.1	-2.2	-2.2	-2.3	-2.4	-2.19
1989	-2	-2	-2	-2	-2.2	-2.5	-2.7	-3.1	-2.31
1990	-2.7	-3	-3	-2.5	-2.7	-3.4	-3.8	-4.1	-3.15
1991	-2.3	-2.4	-2.2	-2.4	-2.6	-2.9	-3.2	-3.7	-2.71
1992	-2.6	-2.6	-2.5	-2.5	-2.4	-2.7	-3.2	-3.8	-2.79
1993	-1.5	-1.5	-1.5	-1.5	-1.7	-1.9	-2.2	-2.5	-1.79
1994	-2	-2	-2	-2.08	-2.16	-2.45	-2.6	-2.9	-2.27
1995	-1.2	-1.56	-1.91	-2.03	-2.16	-2.43	-2.33	-2.24	-1.98
1996	-0.55	-0.78	-1.15	-1.44	-1.46	-1.25	-1.48	-1.76	-1.23
1997	-0.57	-0.8	-1.02	-1.15	-1.28	-1.43	-1.76	-2.1	-1.26
1998	-1.2	-1.65	-1.38	-1.49	-1.75	-2.01	-2.34	-2.39	-1.78
1999	-0.8	-0.78	-0.8	-0.94	-1	-0.94	-1.08	-1.3	-0.96
2000	-1.06	-1.06	-1.06	-1.06	-1.06	-1.18	-1.24	-1.85	-1.20

Appendix 6: Matching storm data with the volume changes

In this paragraph it is tried to find a correlation between the occurrence of storms and the variation in profile volume (m^3/m) between the specified boundaries (60m; 780m and NAP -14m). The results are plotted below.

At first the annual amount of storm hours is compared with variation in height of the seabed level. The results are plotted in Figures A6.1 and A6.2. As can be seen, hardly any correlation seems to exist. Both scatter diagrams show no significant relation between the amount of storm hours and decrease in seabed volume. Consequently it can be concluded that storm do not influence the sand volume between the 60m and 780m offshore of the RSP line. Another conclusion could be that the annual number of storm hours (annual storm intensity) is an improper parameter to find the influence of storm on the seabed profile.

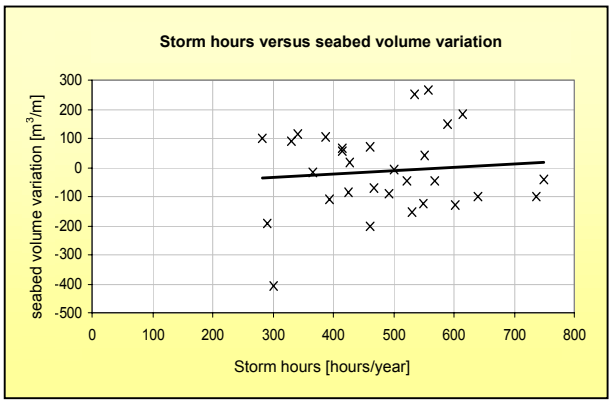

Figure A6.1: Storm hours versus annual seabed variation for section (60m to 780m).

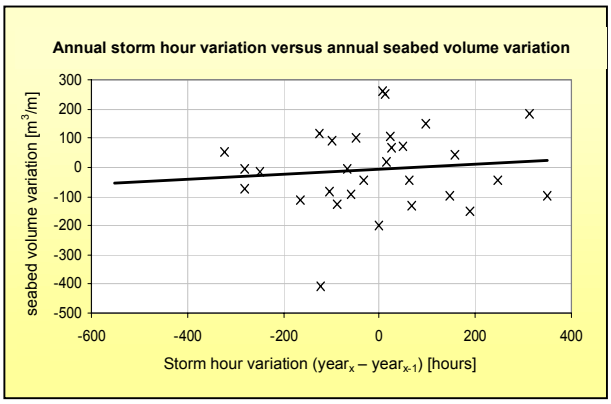

Figure A6.2: Annual storm hour variation versus annual seabed variation for section (60m to 780m).

To be sure of the fact that storm does not influence the volume of sand between the 60m and 780m offshore of RSP. The annual storm duration is split up into the duration of summer and winter storm hours. This resulted in two scatter diagrams, Figures A6.3 and A6.4. It appears that splitting up the annual storms duration does not result in a relation between storms and bed variation.

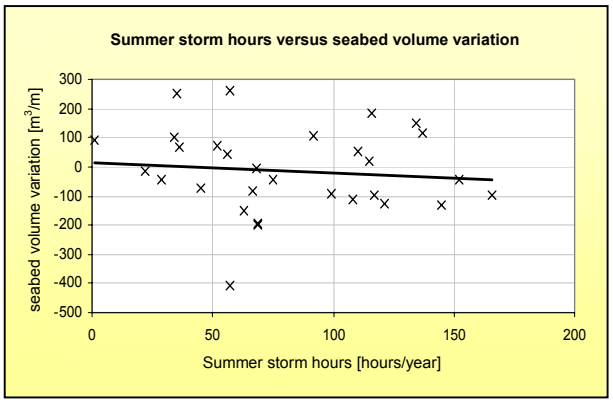

Figure A6.3: Summer storm hours versus annual seabed variation for section (60m to 780m).

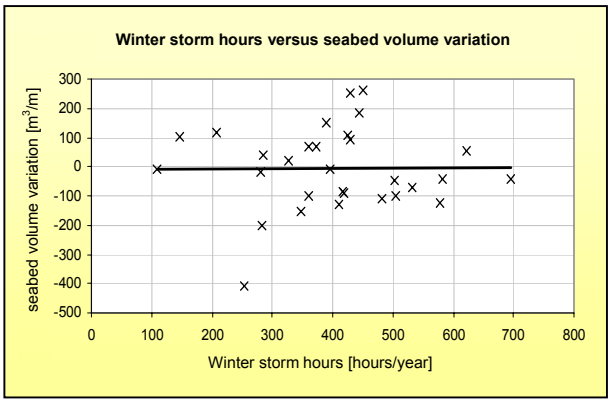

Figure A6.4: Winter storm hours versus annual seabed variation for section (60m to 780m).

The volume of the previous survey could also cause the fact that still no relation is found. The volume of a profile will be expressed as the averaged height of a profile in the following diagram if this initial bed level (or previous bed level) is relatively high it is more likely that the consecutive bed level

height decreases in height. To check this with the available data Figure A6.5 has been made. It appears that the initial seabed level does influence the variation in seabed level negatively as was expected.

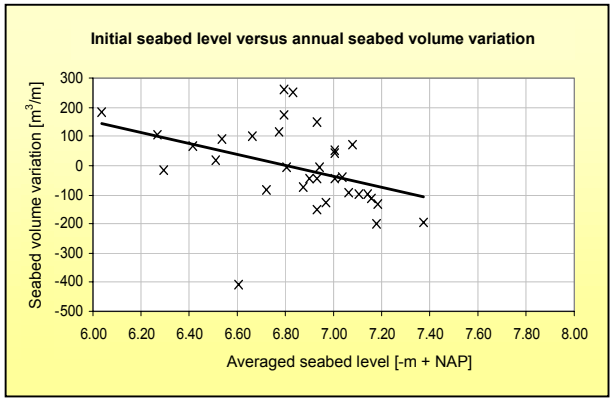

Figure A6.5: Initial seabed level versus annual seabed variation for section (60m to 780m).

The following conclusions can be drawn from this analysis:
The volume in the section between the 60m and 780m offshore of the RSP reference line is not influenced by the storm duration, but it is influenced by the sand volume of the previous year.

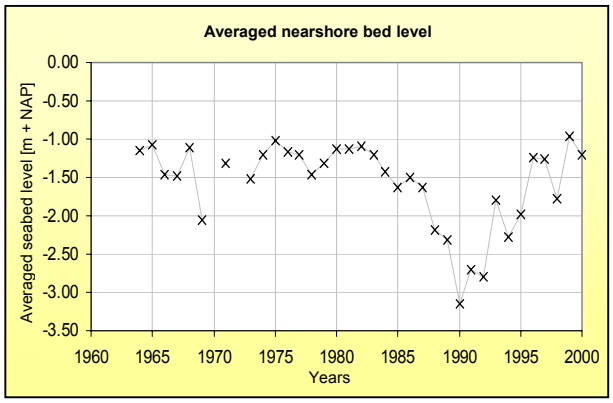

Figure A6.6: Averaged seabed level variation (0 to 80m).

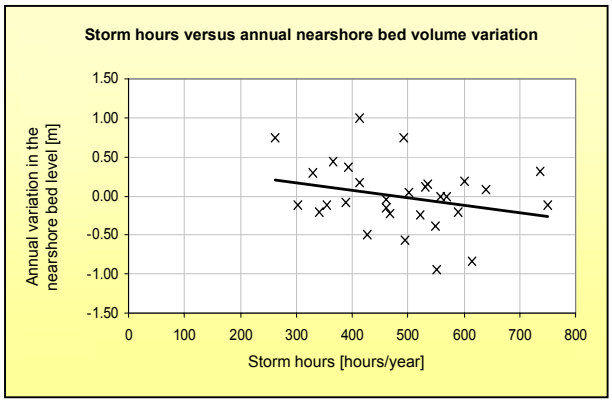

Figure A6.7: Storm hours versus annual seabed variation for section (0 to 80m).

During this thesis the point of focus lies at the area between the groynes also known as the section between the 0m and 80m offshore of the RSP line. Little can be said about this section based upon the analysis. Therefore a similar analysis is done for this section. First the volume variation of the section between the groynes is shown in Figure A6.6, to show the magnitude of the variation in annual seabed height.

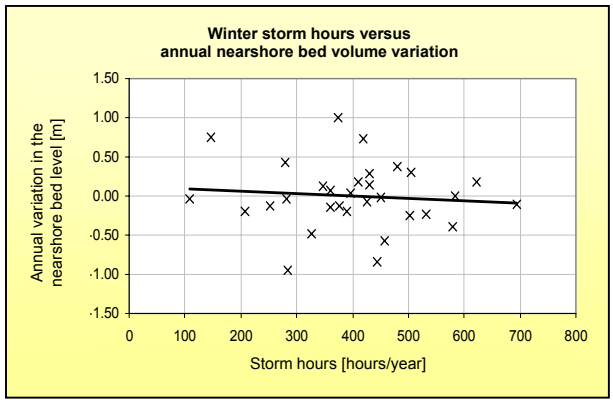

Figure A6.8: Winter storm hours versus annual seabed variation for section (0 to 80m).

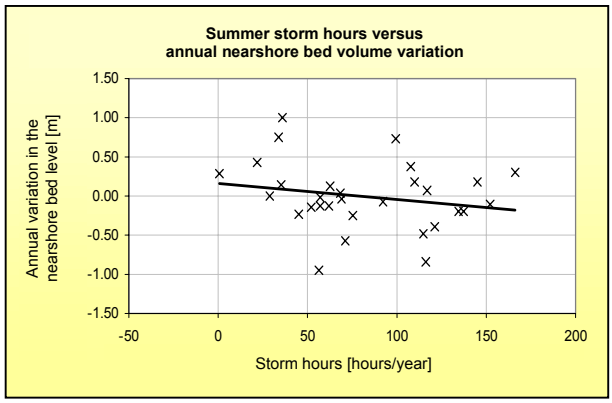

Figure A6.9: Summer storm hours versus annual seabed variation for section (0 to 80m).

The nearshore area between the groyne is often not entirely surveyed, if no manipulation is used only a few profiles can be used for the analysis therefore the most landward surveyed point is extended to the RSP line (0m). This appears rough, but according to the measurement the profile in this region is often reasonably flat. The results are shown in the next three graphs.

Again little correlation can be found in the scatter diagrams. Although it could be concluded that the annual storm duration has a minor influence on the seabed variation. The more storm hours the more seabed decrease. The split up into winter and summer storm hours shows little; accept that winter storm hours show no correlation at all.

A final examination of the influence of heavier storms is done for the near-shore region. The results are two scatter diagrams without any regularity. Therefore again it seems that storm have little influence on the annual differences in profile volume or height. The diagram shows the correlation of storms hours that exceed a Beaufort 9 wind force and the annual averaged seabed variation.

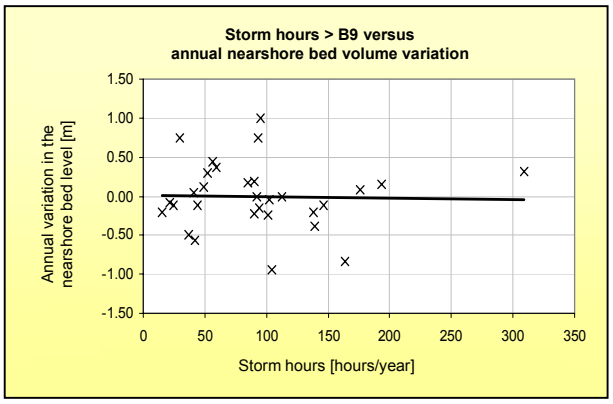

Figure A6.10: Storm hours exceeding Beaufort 9 versus annual seabed variation for section (0 to 80m).

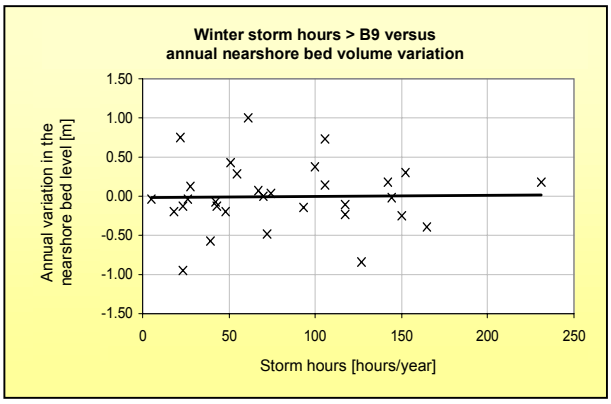

Figure A6.11: Winter storm hours exceeding Beaufort 9 versus annual seabed variation for section (0 to 80m).

After these analyses it can be concluded that the annual seabed variation is almost independent for the number of storm hours per year. If there is a correlation between storm hours and annual seabed variation is not derived from the available JARKUS data set. Still noting can be said about the influence of storms on the short-term.

Appendix 7: Measured wave data

In the following two figures the wave data measured at Petten in a period between 14 October 2000 and 9 December 2000 has been shown. The wave height at different location has been shown, from deep-water (011) up to shallow water (063). For example, the data measured at (011) are measured at MP1 7909m offshore and the data measured at (181) are measured at MP18 about 111m offshore. The wave data measured at MP6 (063) appears to follow the tidal motion. Consequently, it is expected that the wave data measured at MP6 consist of a large share of breaking or already broken waves.

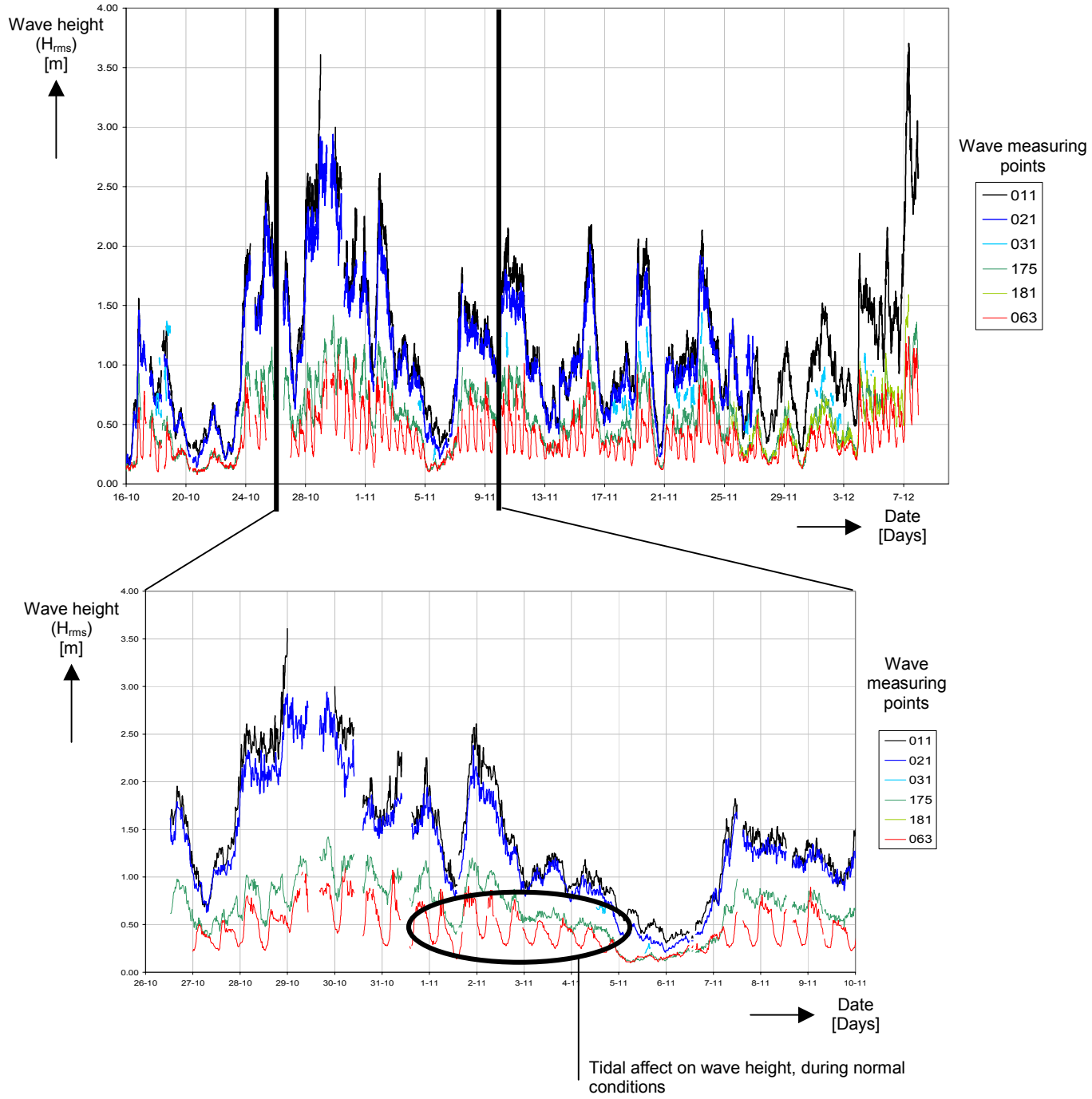

Appendix 8: Breaker index analysis

General

This appendix treats the results of the calculations with the breaker index equation. For input, several storms between 1995 and 2000 were used. The intention is to visualise the local seabed decrease during a storm using the available wave data. Since seabed profiles are not measured during storms this method could give some perception of the seabed decrease and the erosion speed.

General breaker equation

The breaker index equation is based on the assumption that waves become unstable when the wave height (H_b) exceeds the wavelength (L) by $1/7^{th}$. Miche [1944] describes the limited wave steepness for progressive, periodic waves in all water depths as follows:

$$\frac{H_b}{L} = \frac{1}{7}\tanh\left(\frac{2\pi h_b}{L}\right) \text{ or } H_b \approx \frac{0.88}{k}\tanh(kh) \qquad \text{(A8.1)}$$

For deep-water this means that waves will break or in other words dissipate energy when the wave height (H_b) exceeds $1/7^{th}$ of the wavelength (L).

In shallow water the water depth determines the propagation speed (C) and wavelength (L) instead of merely the wave period (T), which is the case for deep-water. Consequently the relation found by Miche [1944] is transformed into the following equation:

$$L = TC = T\sqrt{gd} = T\sqrt{gh_b} \qquad \text{(A8.2)}$$

$$\frac{H_b}{T\sqrt{gh_b}} = 0.142\tanh\left(\frac{2\pi h_b}{T\sqrt{gh_b}}\right) \text{ or} \qquad \text{(A8.3)}$$

$$H_b \approx \frac{0.88T\sqrt{gh_b}}{2\pi}\tanh\left(\frac{2\pi h_b}{T\sqrt{gh_b}}\right) \qquad \text{(A8.4)}$$

H_b	= Breaker wave height	[m]
L	= Wave length	[m]
T	= Wave period	[s]
g	= gravity constant	[m/s^2]
d	= water depth	[m]
C	= wave propagation speed	[m/s]
h_b	= water depth during breaking	[m]

The wave height (H_b) of breaking waves in shallow water is directly related to the water depth during breaking (h_b) and the wave period (T). The water depth and wave period are considered independent and the influence of the wave period on the maximum wave height is small.

Breaker index equation Battjes-Janssen

This equation is also known as the Battjes-Janssen equation, it is valid for shallow water and mild bed slopes. The equation below is based on sets of regular wave, meaning that all waves from a set are the same. The equation is written as follows:

$$\gamma = \frac{H}{h} \quad 0.5 < \gamma < 0.6 \tag{A8.5}$$

In reality waves sets are often irregular and the wave field is best described by a wave energy spectrum as is shown in Figure A8.1. A spectrum shows the distribution of wave energy over a range of frequencies. Although wave sets are irregular it is still customary and useful to describe a wave set by characteristic parameters. For instance, a wave set of waves with varying wave heights is described by one single value for wave height.
Two of the most common characteristic parameters to describe the wave height of an irregular set of

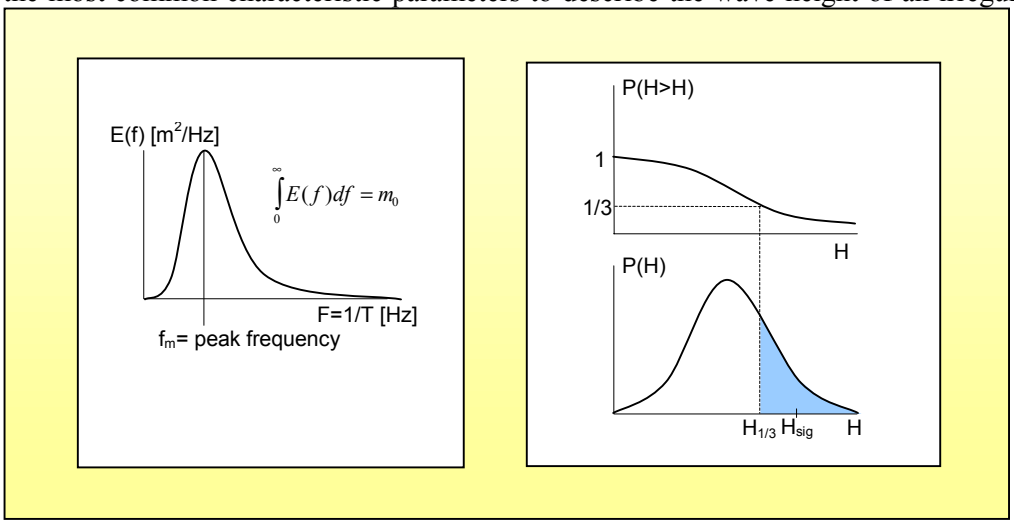

Figure A8.1: The wave energy spectrum and the significant wave height (H_s).

waves are the root-mean-square wave height (H_{rms}) and the significant wave height (H_s). Both parameters differ a factor 1.41 during non-breaking conditions [TAW, 1995]. These parameters are derived from the wave energy spectrum of an irregular wave set, as is shown in Figure A8.1, and are described as follows:

$$H_s = 4\sqrt{m_0} \tag{A8.6}$$

$$H_{rms} = 2\sqrt{2m_0} \tag{A8.7}$$

An irregular wave set contains waves with different heights consequently these waves break on different water depths. Meaning that there is an area where waves break (surf zone) instead of a breaking point, which makes it difficult to relate the breaker depth to a parameter describing an irregular wave set. Tests show that for the significant wave height (H_s) the equation constants are valid.

$$\gamma_{rms} = \frac{H_{rms}}{h_b} \quad 0.35 < \gamma_{rms} < 0.42 \qquad \text{or} \tag{A8.8}$$

$$\gamma_s = \frac{H_s}{h_b} \quad 0.5 < \gamma_s < 0.6 \tag{A8.9}$$

Seabed slope

Nelson [1983] found that seabed slopes as small as 0.01 affect the wave-breaking mechanisms sufficiently to increase the breaker index (γ) for individual waves. The components that determine the wave motion are: the bed slope (α), wave height (H), wave period (T) and gravitational force (g). Waves reflect rather than break when the bed slope is rather large. Whenever the seabed slope decreases beneath a certain value the waves become unstable and break. A common breaking criterion is described by the breaker parameter (ξ):

$$\xi = \frac{\tan\alpha}{(H / L_0)^{0.5}} < 2.3 \qquad \text{(A8.10)}$$

At the Pettemer coast the deep-water wave steepness (H_{rms}/L_0) vary between the 0.006 and the 0.029, the bed slope differs between the 1:30 and 1:40. The range of the breaker parameter is about 0.15 – 0.43. Most of the breaking waves will be of the spilling type: 'Relatively steep waves and/or a relatively flat bed; breaking occurs at a great distance offshore where the wave crest is still symmetric and accompanied by the generation of a foamy roller at the wave front while the wave through is not visibly disturbed'.

Due tot the delay of breaking, breaking takes place over a distance in the order of magnitude of one or maximum two wavelength (25m to 100m). Battjes (1974) related the γ-index to the ξ-parameter. Based on the analysis of field and flume data, the following values applied to the current situation are given:

γ=0.8 for ξ=0.2
γ=0.9 for ξ=0.4

Breaker index UNIBEST-TC

In UNIBEST-TC two sets of breaker equations are available. First of all the Battjes-Janssen equation [1978] described earlier in this appendix and secondly an equation formulated by Battjes and Stive [1985]. The Battjes-Stive equation for breaking waves takes into account the wave steepness (s_0) on deep water. The deep water wave steepness (s_0) is defined as the root-mean-square wave height on deep water ($H_{rms,0}$) divided by the peak wave length on deep water ($L_{0,p}$)

$$H_b \approx \frac{0.88}{k}\tanh\left(\frac{\gamma kh}{0.88}\right) \qquad \text{(A8.11)}$$

$$\gamma = 0.5 + 0.4\tanh(33 s_0) \quad s_0 = H_{rms,0} / L_{0,p} \qquad \text{(A8.12)}$$

In UNIBEST-TC this means that all waves in an irregular wave set that exceed the maximum local wave height determined by the breaker index shall break. Consequently, the wave set consists of broken waves with a maximum wave height determined by the local water depth and the remaining non-breaking waves.

Measured breaker indices Egmond

At Egmond, 20 kilometres south of Petten, at a similar barred coast as the Pettemer coast the relative wave height has been determined at the crest of a bar. The bed slope of the seaward flank of the bar is about 1:30. In the following Figure A8.2 the results are plotted against the deep-water steepness (H_{rms}/L_0) that shows a similar range at Petten.

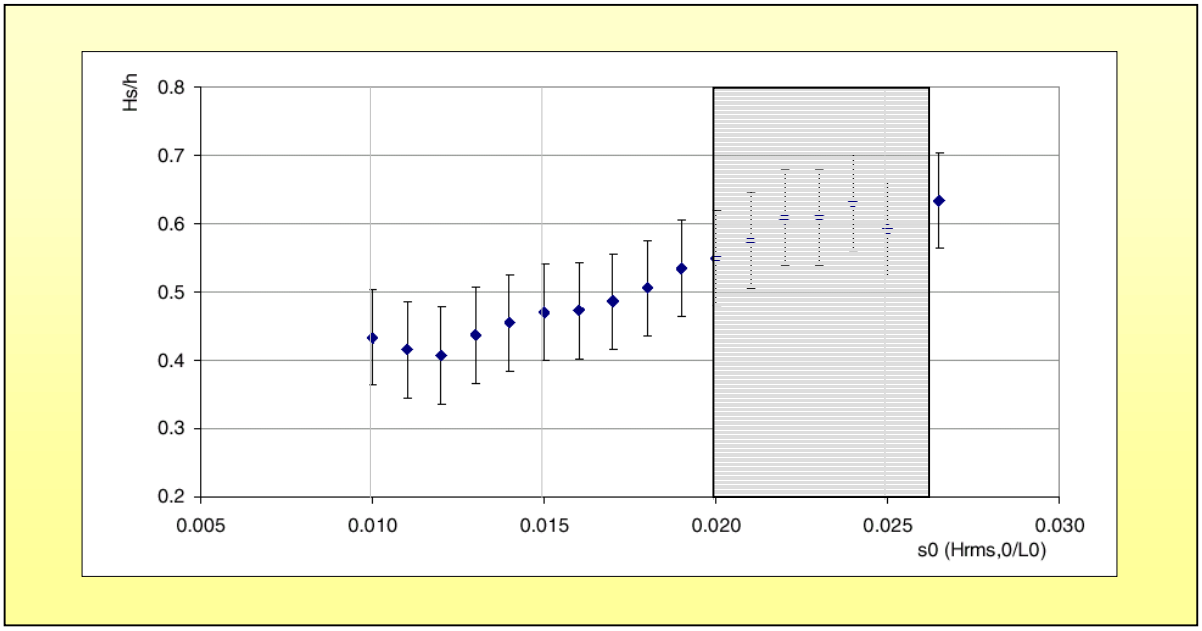

Figure A8.2: Averaged values and the (averaged) standard deviation of the maximum relative wave heights (H_s/h) as a function of the deep-water wave steepness ($H_{rms,0}/L_0$) at moment of breaking measured at Egmond. [KLEINHOUT, 2000]

According to Figure A8.2 the averaged breaker index (γ_s) varies within a range of 0.4 to 0.65 the accompanying standard deviation is about 0.075. The breaker indices derived from the ξ-parameter appears to over-estimate the measured breaker indices (H_s/h). However, these values are valid for maximum wave heights (H_{max}) instead of significant wave heights (H_s).

The wave steepness that occurred during the storm of 6 November 1999 at measuring point MP1 at Petten is indicated with the grey rectangle. The measured values for the wave steepness vary between 0.020 and 0.026, with a mean of 0.023; the accompanying breaker index varies between 0.55 and 0.65 according to the Figure A8.2.

Measured breaker indices at Terschelling

At Terschelling, a survey campaign was held from May 1994 to June 1994. Perpendicular to the barred Terschelling coastline several measuring point were operative. The obtained data had been used to calibrate the output of UNIBEST-TC. According to [BAKKER, 1995] optimal results were achieved when a constant breaker index instead of the Battjes-Stive breaker index was used in UNIBEST-TC. A conclusion was that the relation between the breaker index (γ) and the deep-water wave steepness (s_0) is weak. A constant breaker index of 0.8 describes the wave heights at locations on the outer-slope of the outer and the middle breaker bar best. In the though behind the middle breaker bar a breaker index of 0.65 has been found optimal.

Tidal effects

The local wave steepness is expected to be more important than the deep-water wave steepness at a barred coastline. The local wave steepness describes wave characteristics of waves that have penetrated the previous bars. Consequently, several high waves have been broken, while the wave period stays reasonably constant. This effect results in a local wave steepness that is smaller than the deep-water wave steepness. This effect can also be contributed to the difference in wave distribution functions. Non-breaking wave are described by a Rayleigh distribution function while breaking wave are described by a cut-off Rayleigh distribution function.

During flood the local water depths are significantly higher than during ebb. This results in a larger share of breaking wave during ebb compared to flood at a specified point behind the first breaker bar. Due to the difference in water depth, ebb and flood affect the breaker index ratio. During ebb a lower breaker index is operative compared to flood conditions.

Seabed hindcast during storms at Petten

Unfortunately, the variation of the seabed during storms is unknown. Only wave data and the water level during storms are available. To find an indication for the erosion that takes place during a single storm the maximum possible seabed height according to the breaker parameter of Battjes-Janssen is calculated. As input the following storm data is used:

Table A8.3: Characteristics of the storms used in the breaker index analysis.

Date	Max water level MP3*	Max wave height MP1* (H_S)
1 January 1995	NAP + 235 cm	575 cm
2 January 1995	NAP + 230 cm	**605 cm**
10 January 1995	NAP + 165 cm	565 cm
29 October 1996	**NAP + 215 cm**	575 cm
5 February 1999	NAP + 240 cm	575 cm
6 November 1999	NAP + 225 cm	595 cm

*MP3 and MP1 are measuring points located on the RSP line 20.830 at 7909m respectively 3434m offshore.

The graphs in Appendix 7: wave data show that during most of the storms the wave height in shallow water follows the tide. This implies that these waves are restricted by the tide and therefore restricted by the water depth/ seabed height. It is reasonable to expect that the breaker index and the water depth are able to determine the maximum seabed level height.

Method

In the following graphs (Figure A8.6 to Figure A8.11) the significant wave height (H_0) at deep water (20m), the tide and local water level at MP6 (H_s) are shown. A breaker index of 0.55 is used to calculate the column of water corresponding with wave height measured at MP6. After correcting the water column for the tide the minimum water depth with regard to NAP reference level is found. The minimum water depth is an indicator for the maximum seabed height.

The red line describes the maximum possible seabed level height that corresponds with a breaker index of 0.55. The black line is the deep-water wave height and the yellow line the tide. Both these factors determine the hydrodynamic load.

One of the basic principles is that the wave height has to be fully restricted by the water depth. However, during most storms the water depth does not limit the wave height during the entire storm period.

Breaker index variation

In the following Figure A8.4 the effect of different breaker indices is shown for the storm of 6 November 1999. The Figure shows the results of three different breaker indices including the seabed linear regression over a specified period of time. A higher breaker index results in a shift in upward direction for the calculated seabed level, as well as a smaller erosion quantity.

The fluctuations of the calculated seabed level height are the result of small variations in the local wave height and tide. It is not expected that the seabed level shows an exactly similar course during storm conditions. However, it is possible to look for trends, especially downward trends. An increased share of non-breaking waves, or load reduction could also cause the upward trends.

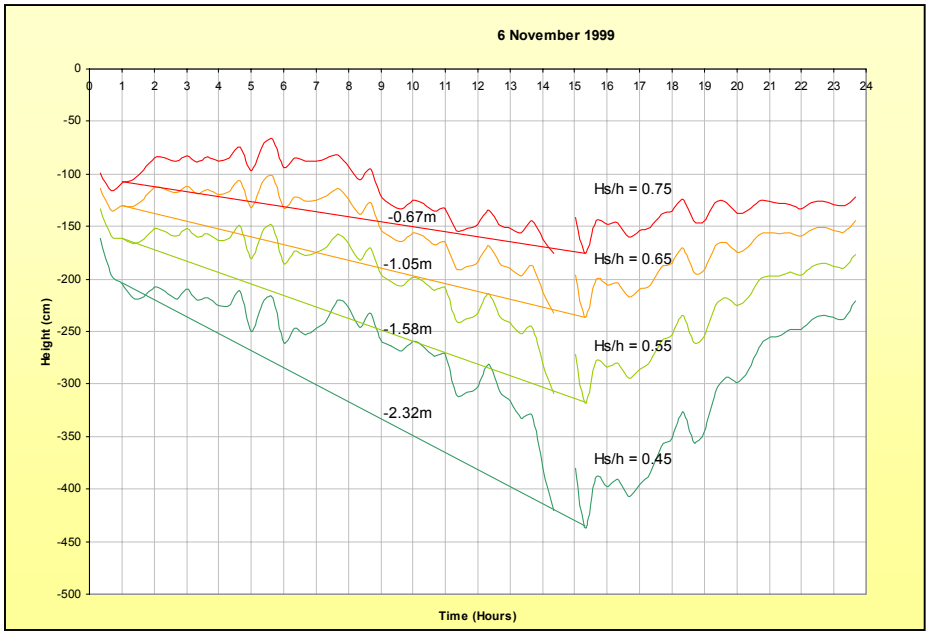

Figure A8.4: The seabed variation and erosion depth according to the hindcast analysis executed for different breaker indices (0.45, 0.55, 0.65 and 0.75).

Comments on the Figures A8.6 to A8.11

In Figure A8.5, the breaker index has also been varied to show the effect during the January storm of 1995. During the first three storms of 1995 no significant maximum seabed level decrease is seen in the graphs. This is rather strange because the water depth limits the wave height, as can be seen in the graph (the local wave height shows a similar pattern as the tide), resulting in a maximum wave load on the bed.

In every graph the measured seabed heights before and after the storm are indicated as reference. The point that represents the minimum seabed level has defined the end of a storm. It is important to note that the visualised maximum seabed height is in fact noting more than an indication that is very sensitive for the chosen breaker index, as can be seen in Figure A8.4. Another difficulty is the definition of the initiation point for erosion. The criteria where a sudden decrease in seabed profile and a wave height on deep water (H_0) that exceed the 3.5m.

In Table A8.5 the results of the analysis are shown. The erosion has been determined on a linear time scale, however it is expected that the erosion speed will decrease with the increase of depth. A parabolic function is recommended if a more realistic approach is necessary.

Table A8.5: Results of the hindcast analysis.

Date storm	Previous seabed level	Next seabed level	Start seabed level	End seabed level	Erosion amount (cm)	Erosion time (hr)	Erosion speed (cm/hr)
1 January 1995	-260 NAP	-233 NAP	-200 NAP	-250 NAP	50	10.5	4.8
2 January 1995	-260 NAP	-233 NAP	No significant erosion has been found				
10 January 1995	-260 NAP	-233 NAP	-235 NAP	-245 NAP	10	7	1.4
29 October 1996	-148 NAP	-176 NAP	-170 NAP	-210 NAP	40	7.5	5.3
5 February 1999	-168 NAP	-140 NAP	-220 NAP	-300 NAP	80	7.5	10.7
6 November 1999	-135 NAP	-124 NAP	-170 NAP	-320 NAP	150	10.5	14.3

An explanation for the practically constant course of the calculated seabed level height (red line) for the three 1995 storms is the low seabed level during that year (see previous and next seabed level). Furthermore, a small bar could have protected the measuring location, resulting in lower waves. Finally a gentle slope could have reduced the erosion speed significantly. The sediment has to be relocated on another part of the profile during cross-shore transportation.

During both 1999 storms the maximum seabed height accelerates downward during flood. A reason for this phenomenon could be that during flood the load increases (higher waves) resulting in more turbulent water. Due to more turbulent water higher transport capacities are reached acting as an accelerator for the erosion process.

The orientation of waves and wind has not been taken into account. However, both the 1999 storms are from the southwest and the 1995 storms are from the northwest. The wind direction could have a significant effect on the erosion volume. Waves from the southwest cause a current in northward direction along the shoreline, while wind and wave from the northwest cause a current in southward direction. The net sediment transport is directed northward; probably due to higher velocities. The stirring up mechanism of waves increases the sediment transportation significantly.

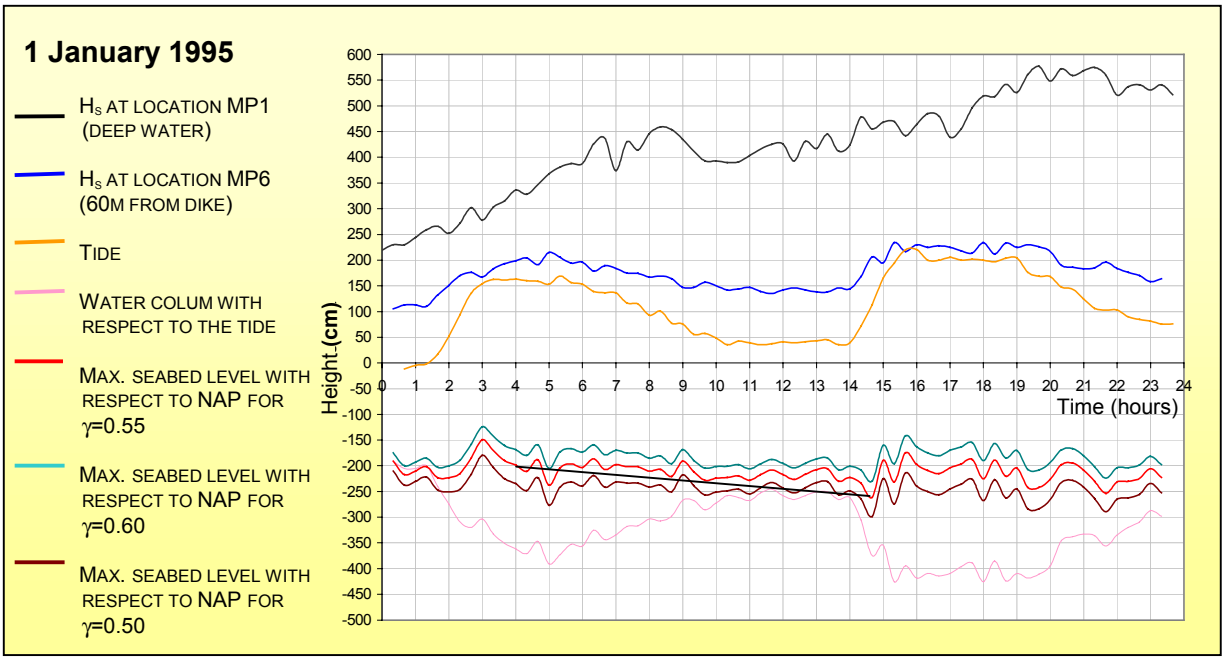

Figure A8.6: Result of the breaker index analysis on the storm of 1January 1995.

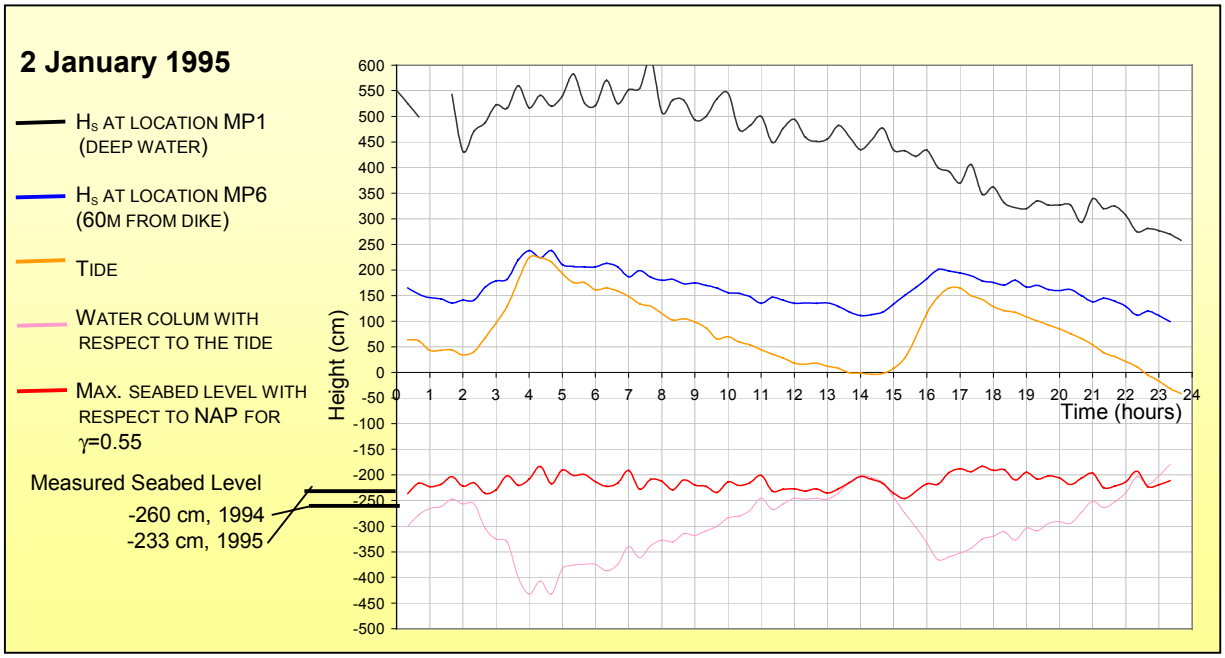

Figure A8.7: Result of the breaker index analysis on the storm of 2January 1995.

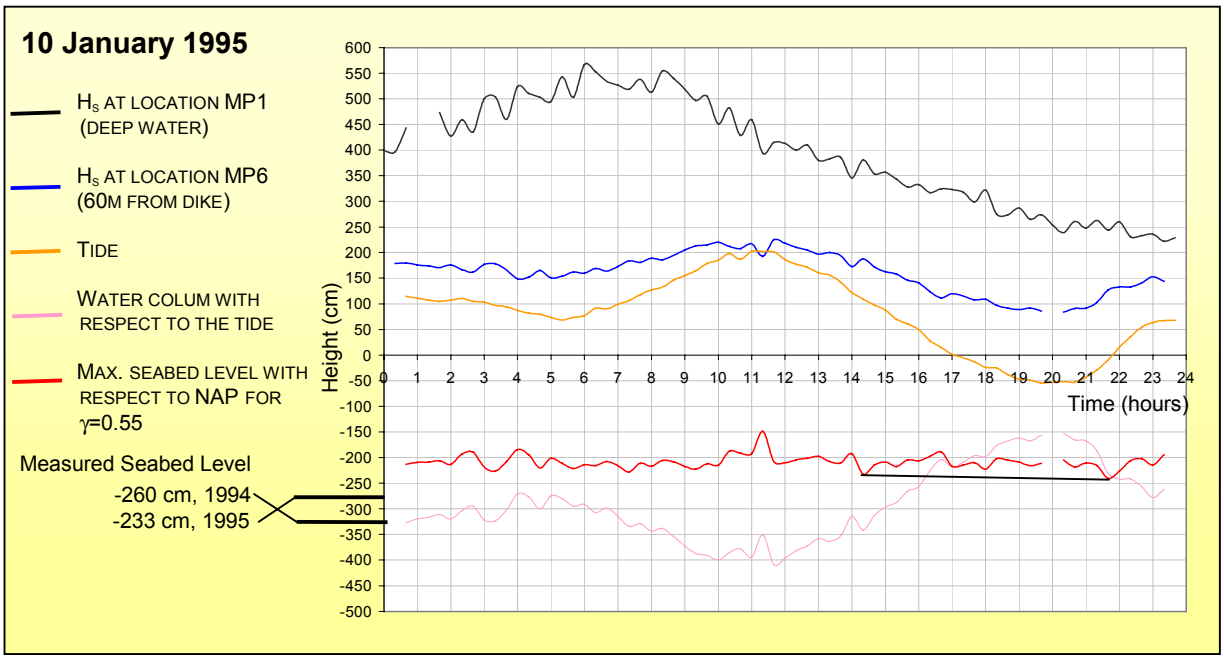

Figure A8.8: Result of the breaker index analysis on the storm of 10 January 1995.

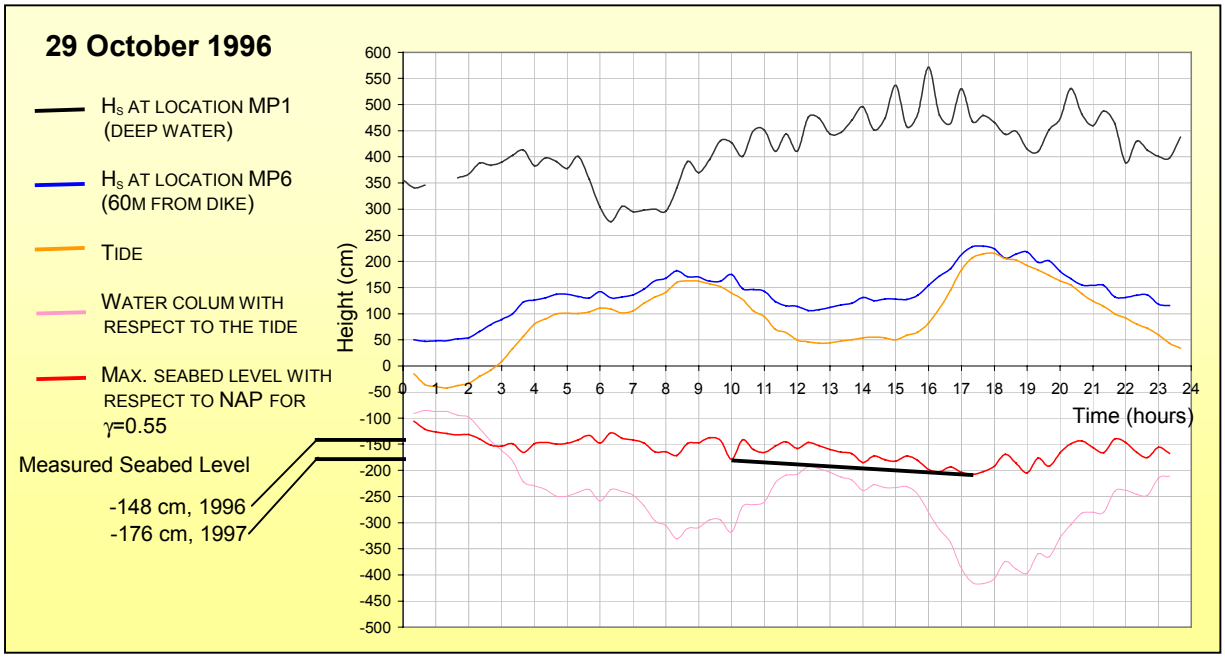

Figure A8.9: Result of the breaker index analysis on the storm of 29 October 1996.

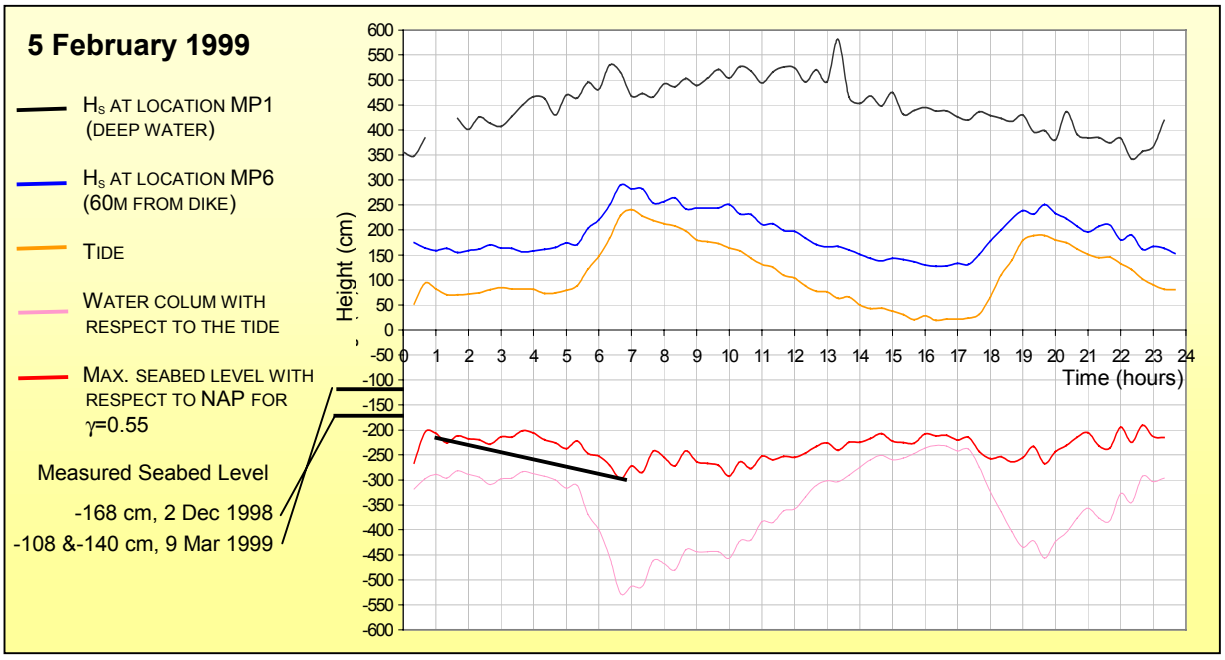

Figure A8.10: Result of the breaker index analysis on the storm of 5 February 1999.

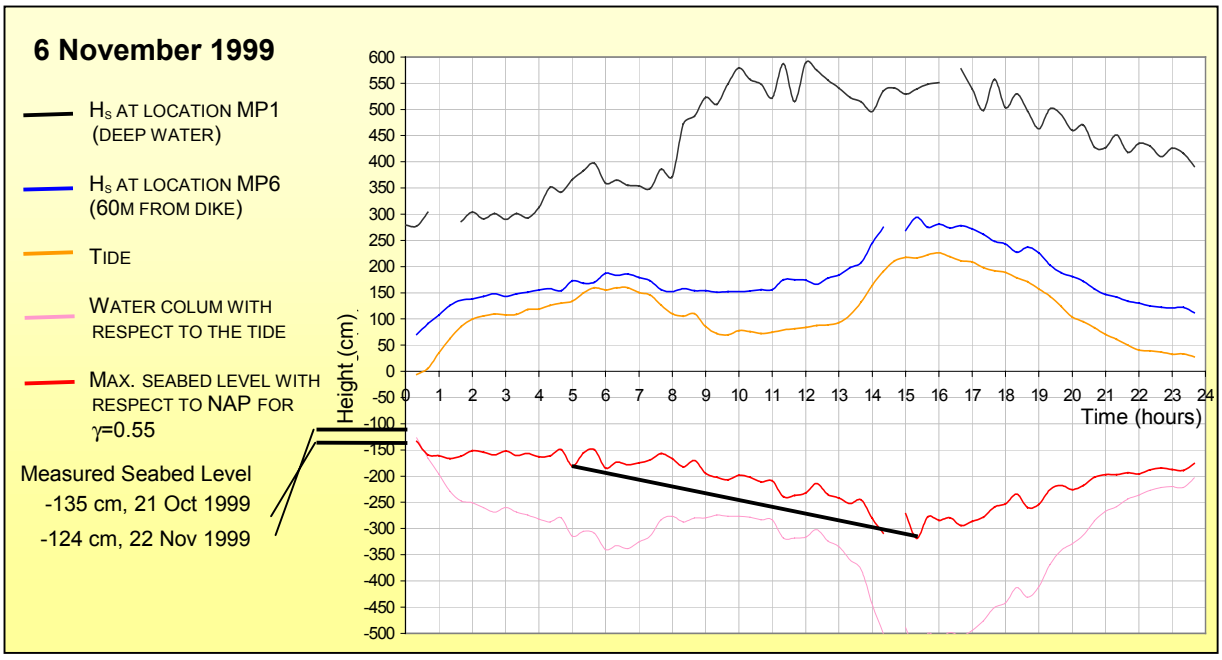

Figure A8.11: Result of the breaker index analysis on the storm of 6 November 1999.

Appendix 9: Unibest-TC parameter definition

Table A9.1: Summary of the model parameters used in UNIBEST-TC [WALSTRA, 2000].

PARAMETER	DESCRIPTION
DT	TIME STEP IN DAYS
NT	NUMBER OF TIME STEPS
TIME_ST	STARTING POINT
USTRA	TRANSPORT RATE AT THE LAST COMPUTATIONAL GRID POINT, DEFINED BY THE USER
JFR	FREQUENCY OF OUTPUT GENERATION
TDRY	RELATIVE WAVE PERIOD; A DIMENSIONLESS PARAMETER INDICATING THE NON-LINEARITY OF THE WAVE FIELD
TE_W	TEMPERATURE OF THE WATER IN °C
SALIN	SALINITY OF THE WATER IN PROMILLE
ALFAC	FACTOR FOR WAVE DISSIPATION USED IN THE EXPRESSION OF BATTJES AND JANSSEN (1978)
GAMMA	WAVE BRAKING PARAMETER, USED FOR CALIBRATION OF THE WAVE MODEL; WHEN 0, BATTJES STIVE (1986) IS USED
BETD	SLOPE OF WAVE FRONT, USED TO INFLUENCE THE ROLLER PARAMETER
FWEE	BOTTOM FRICTION FACTOR, INFLUENCES THE AMOUNT OF WAVE DISSIPATION DUE TO BOTTOM FRICTION
C_R	CORRELATION COEFFICIENT WAVE ENVELOPE AND BOUND LONG WAVES, ARRANGES SHIFT BETWEEN LONG- / SHORT WAVE ENVELOPE
K_IJL	BREAKER DELAY SWITCH (1= ON, 0= OFF)
F_LAM	NUMBER OF WAVELENGTHS OVER WHICH THE WEIGHTED DEPTH IS INTEGRATED
POW	POWER IN THE WEIGHTING FUNCTIONS
DEEP_V	SEAWARD BOUNDARY OF REDUCTION AREA
SHALL_V	SHOREWARD BOUNDARY OF REDUCTION AREA
D50	D50 GRAIN DIAMETER OF BED MATERIAL
D90	D90 GRAIN DIAMETER OF BED MATERIAL
DSS	D50 GRAIN DIAMETER OF SUSPENDED MATERIAL
DVAR	CROSS-SHORE VARYING GRAIN SIZE SWITCH
FDIA0	DIAMETER MULTIPLICATION FACTOR AT HDIA0
FDIA1	DIAMETER MULTIPLICATION FACTOR AT HDIA1
FDIA2	DIAMETER MULTIPLICATION FACTOR AT HDIA2
HDIA0	REFERENCE DEPTH FOR FDIA0 (MOST SHOREWARD)
HDIA1	REFERENCE DEPTH FOR FDIA1
HDIA2	REFERENCE DEPTH FOR FDIA2 (DEEP WATER)
IBOD	MORPHODYNAMIC SWITCH
RC	CURRENT RELATED ROUGHNESS FOR SEDIMENT TRANSPORT COMPUTATION
RW	WAVE RELATED ROUGHNESS FOR SEDIMENT TRANSPORT COMPUTATION
REMLG	FIXED BOTTOM LAYER PARAMETER
TANPH1	LOCAL ANGLE OF INTERNAL FRICTION AT LOCATION XF1
TANPH2	LOCAL ANGLE OF INTERNAL FRICTION AT LOCATION XF2
XF1	REFERENCE LOCATION FOR TANPH1 (MOST SEAWARD)
XF2	REFERENCE LOCATION FOR TANPH2 (MOST SEAWARD)
ZDRY	EXTRAPOLATION OF TRANSPORT OVER DRY PART OF PROFILE (HORIZONTAL OR VERTICAL)
FACQB	REDUCTION FACTOR FOR BREAKING WAVES

Appendix 10: UNIBEST-TC validation

General

The validation of the UNIBEST-TC model has been executed, because the prediction capabilities of UNIBEST-TC were unsure. The performance and accuracy during relatively severe conditions have been examined. The test has been executed with default settings for the model parameters. It is not expected that seabed variations will be predicted exactly. However, it is expected that that the computed erosion corresponds with the order of magnitude of the expected erosion.

In order to keep this hindcast check as realistic as possible two criteria are defined:

- A storm has to be present during the period of hindcast.
- The time between the consecutive profiles has to be minimised.

Can UNIBEST-TC simulate the seabed variation between two consecutive surveyed profiles with the use of the hydrodynamic conditions of the period in-between?

Input

The input consisted of an initial profile and the hydrodynamic conditions (wave height, period and water level) during the simulated period. The most favourable test conditions were chosen. These conditions consisted of an initial profile surveyed in October 1999. The consecutive profile had been measured in November 1999. Between both seabed surveys a reasonable severe storm was presence. The initial profile had been constructed of two different survey methods, because this is the only ways to acquire an entire seabed profile that lies partly below the water level and partly above the water level. All possible profile combinations and their in-between periods are shown in Table A10.1.

Table A10.1: All possible combinations of profiles and storms.

Sounding date	Terrestrial survey date	Time difference between surveys	Storm
	27 November 1997		
	7 October 1998		
	2 December 1998		
10 March 1999	9 March 1999	-1	No
18 May 1999	17 July 1999	29	
7 July 1999			
13 September 1999	30 August 1999	-14	
20 October 1999	**21 October 1999**	**1**	**Yes**
15 November 1999	**24 November 1999**	**9**	
	10 January 2000		
24 February 2000	13 March 2000	17	
	1 May 2000		
6 July 2000	15 August 2000	40	No
30 November 2000	21 December 2000	21	
	15 January 2001		
27 February 2001	27 February 2001	0	No
22 May 2001	10 May 2001	-12	
6 July 2001			
26 September 2001	28 September 2001	2	
10 December 2001	13 December 2001	3	

The outline of the chosen profile has been shown in Figure A10.2. The terrestrial survey part and the sounding part are shown. Furthermore, hydrodynamic conditions are required. During the winter of 1999 hydrodynamic data was only measured during severe storm conditions. Therefore wave data from station K13a, a location 100km offshore has been chosen. The location of wave station K13a has been shown in Figure A2.1 (Appendix 2). In Figure A10.3 the manipulated hydrodynamic data series have been shown for the period in-between. The original hydrodynamic data set starts at 20 October 1999 and finishes at 15 November 1999. However, waves with an orientation outside the 227 and 7 degrees were removed from the data set. This resulted in a simulated period of 14 days instead of the original 26 days. However, this should not have great effects for the computed seabed level for 15 November 1999, if the cross-shore sediment transport is dominant during this period.

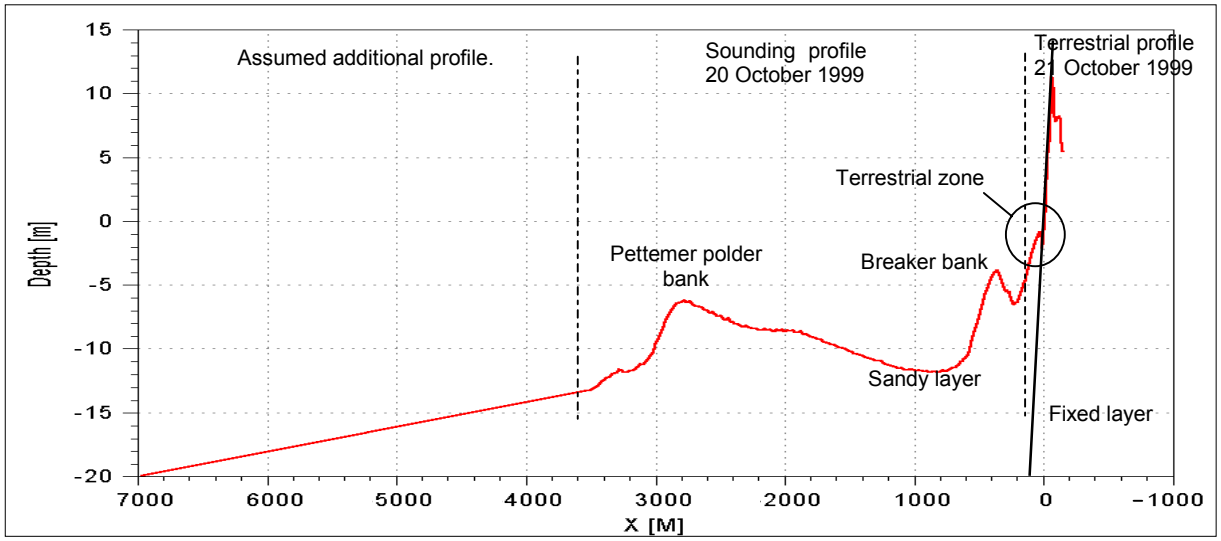

Figure A10.2: UNIBEST-TC input profile; surveyed at 20 and 21 October 1999.

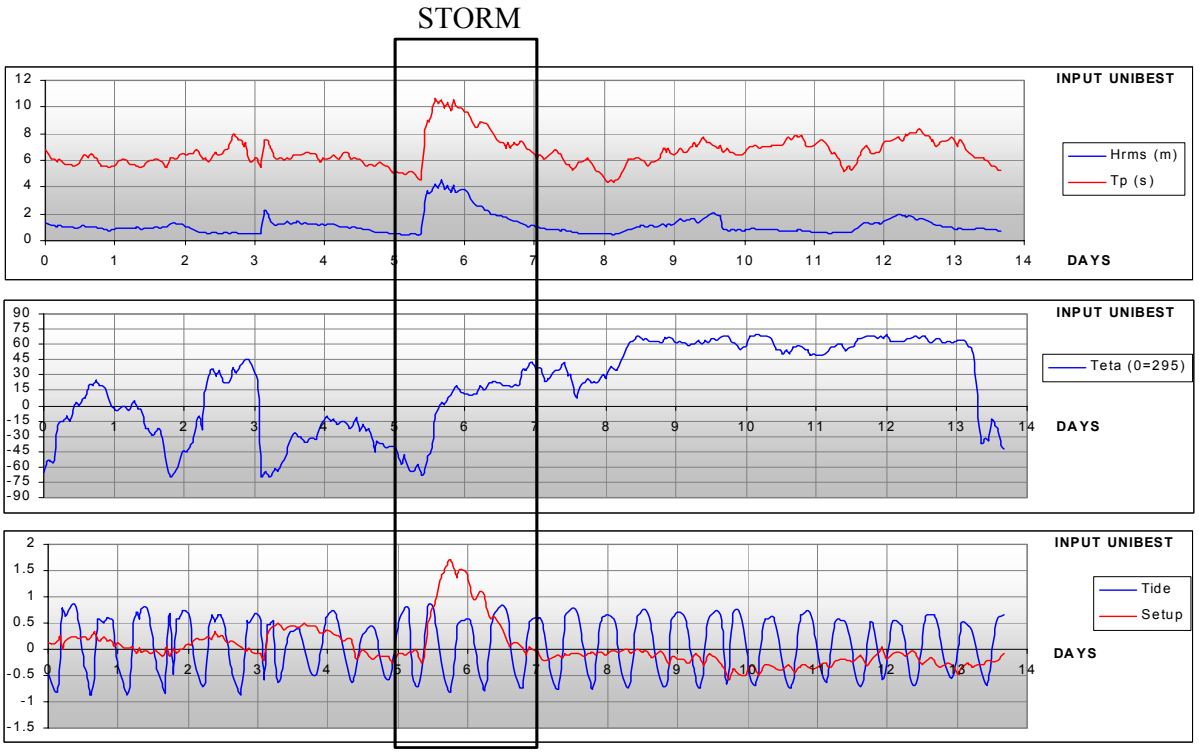

Figure A10.3: Hydrodynamic input data for UNIBEST-TC simulation.

Test results

The following graphs are the result of UNIBEST-TC simulations. For the following time steps output had been generated:

T=0	Initial profile.
T=5	Profile at the start of the storm.
T=6	Profile in the middle of the storm.
T=7	Profile directly after the storm.
T=13.56	Computed profile at the end of the simulation, corresponds with surveyed profile in November 1999.

Behaviour of the nearshore area

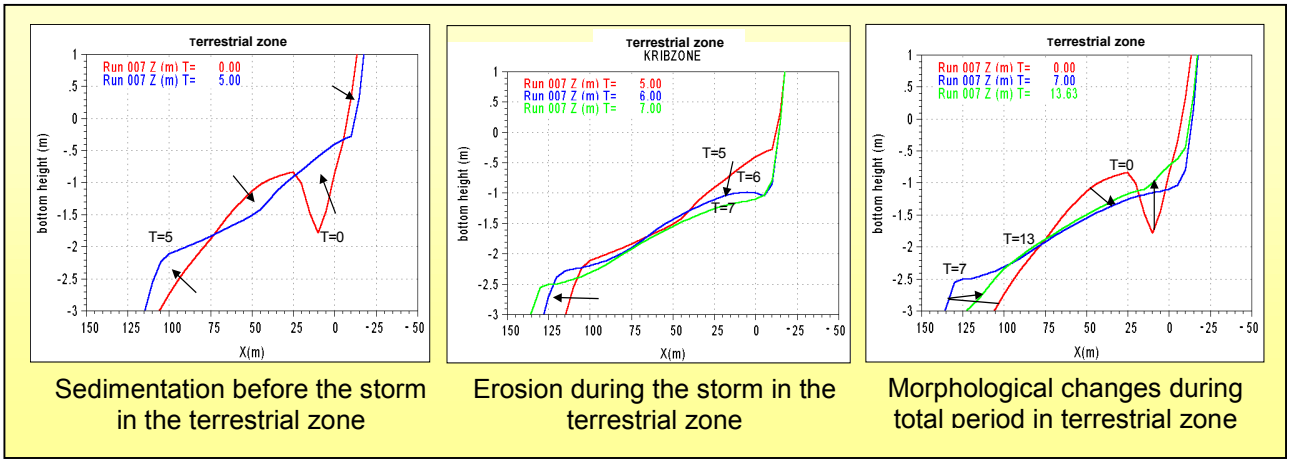

Sedimentation before the storm in the terrestrial zone

Erosion during the storm in the terrestrial zone

Morphological changes during total period in terrestrial zone

Figure A10.4: Results of an UNIBEST-TC simulation.

- Before the storm starts the hole directly in front of the dike is filled. However according the survey of November 1999 the hole increased over time. According to the processes incorporated in UNIBEST-TC the hole cannot maintain during the given circumstances.
- The bed slope becomes gentler during the storm. Directly in front of the structure the bed erodes in the order of magnitude of 70cm. Sand is transported in offshore direction.
- The final graph shows that according to UNIBEST-TC the bed profile recovers after the storm.

Comparison of the computed profile and surveyed profile

- According to Figure A10.5 UNIBEST-TC overestimates the erosion between the 100 and 0m and overestimates the sedimentation between the 100 and 160m. UNIBEST-TC probably overestimates the sediment transport quantities in offshore direction between x=0m and 200m.
- Little differences between the UNIBEST-TC profile and the survey profile can be explained by the fact that according to UNIBEST-TC no sediment leaves the profile. In reality a gradient in longshore sediment transport could be presence.
- The waves station at K13a is located 100 kilometres offshore and its wave measurements are used for input at 7 kilometres offshore. The difference between the actual waves 7 kilometres offshore of Petten K13a wave set can result in significant variation in hydrodynamic load.
- UNIBEST-TC can only compute the contribution of waves that are directed to the shore over a range of 140 degrees. In reality waves with other orientations also contribute to the profile variation.

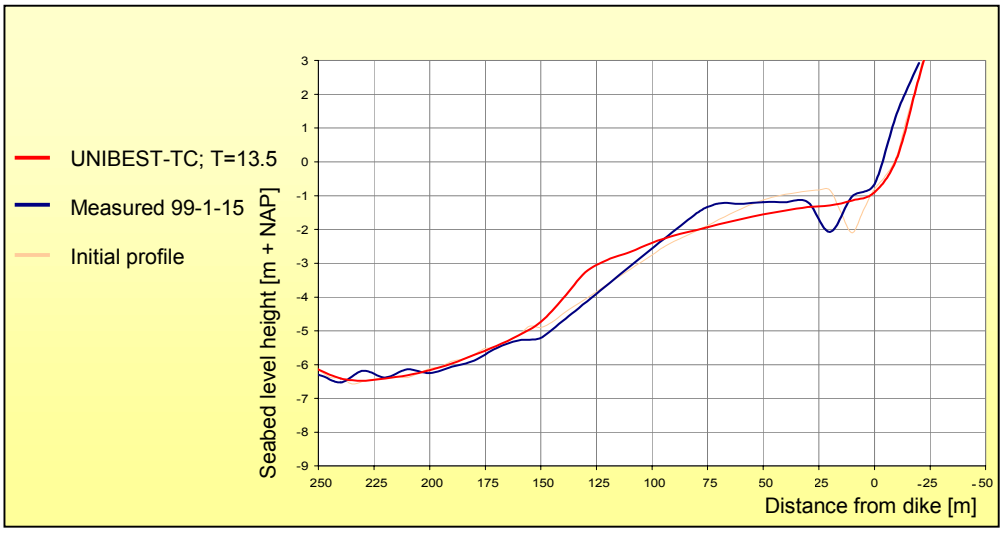

Figure A10.5: Comparison of UNIBEST-TC results and survey profile.

Observations

The maximum difference between the computed profile and the surveyed profile is about 50cm when the hole has not been taken into account. However, an error in that order of magnitude was expected, because UNIBEST-TC has not been calibrated yet. UNIBEST-TC predicts the nearshore erosion during storm and that is most important.

During this check the following adoptions have been made that probably affect the final result:

- The surveyed wave set has been reduced in size; only waves with an orientation between the –70 and +70 degrees to the shore normal have been used.
- Several 3D-processes that are present in the surf zone (zone where wave break) are not incorporated in UNIBEST-TC. For instance, wave reflection.
- The missing wave periods where completed with wave data from 100km offshore.
- Reflection related loads could be responsible for the differences because reflection has not been taken into account by UNIBEST-TC.

Appendix 11: UNIBEST-TC calibration

General

Only the wave module ENDEC can be calibrated, because no other measurements than wave measurements are available during storm conditions.

The performance of ENDEC, the wave simulation model, will be checked with measured wave data, shown in Figure A11.2. During this storm only a few wave-measuring points were operative; these locations are shown in Figure A11.1:

- MP1 located at 7900m from the sea defence.
- MP5 located at 540m from the sea defence.
- MP6 located at 60m from the sea defence.
- MP7 located at 10m from the sea defence.

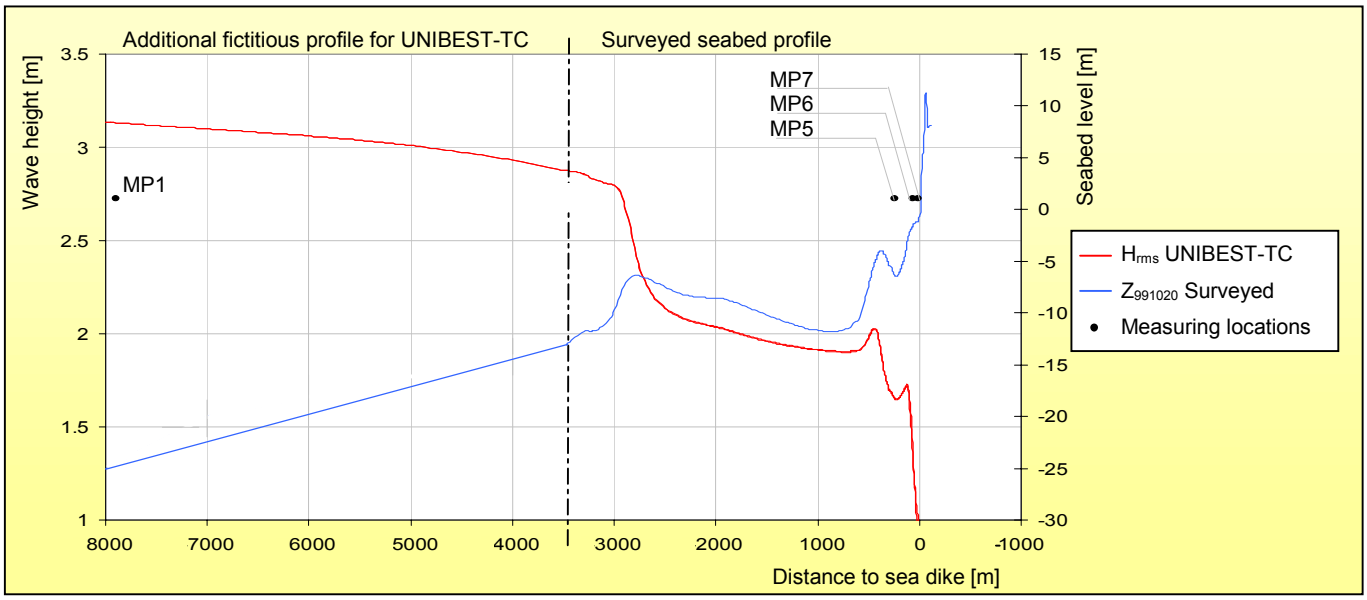

Figure A11.1: UNIBEST-TC profile and wave height development as well as the locations of the operative measuring points.

The input during calibration consists of an initial seabed profile (seabed surveyed at 20 October 1999), wave conditions split up in a root-mean-square wave height (H_{rms}), a peak wave period (T_p) and the water level. The hydraulic conditions measured at location MP1 are used as offshore boundary conditions. Data from the other three wave measuring locations in the surf zone has been used to validate the ENDEC wave-module.

The waves at MP1 are measured at a wave buoy located 8km offshore, whereas the profile has only been surveyed up to 3.5km offshore. Extending the seabed profile up to 25m under a gentle angle has filled the missing part.

In UNIBEST-TC it is possible to incorporate waves with different angles. This option has been turned down because waves with an angle that exceeds an angle of 20 degrees to the shore normal will not pass the 'Pettemer polder' bank resulting in less wave breaking offshore.

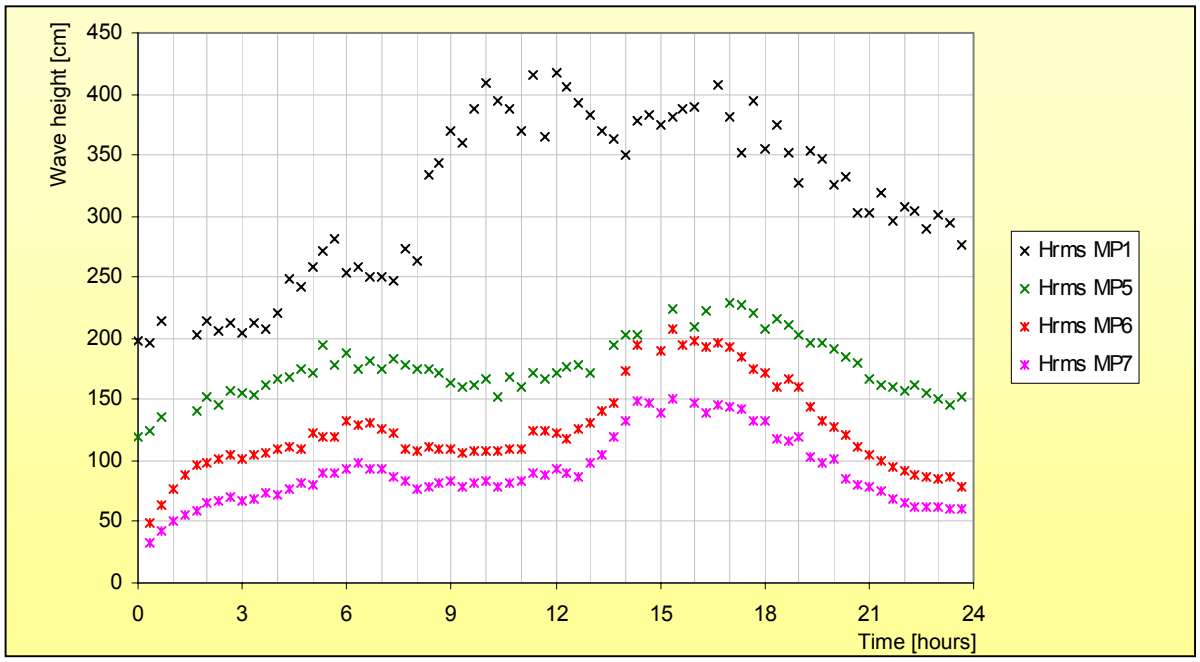

Figure A11.2: Measured wave heights (H_{rms}) at different locations along the transect 20.830, used for validation.

Input

UNIBEST-TC has been calibrated with the hydrodynamic conditions of 6 November 1999. At this day a significant storm occurred with wave heights (H_{rms}) exceeding the 4m. In Figure A11.3 the hydrodynamic conditions at the offshore boundary are plotted.

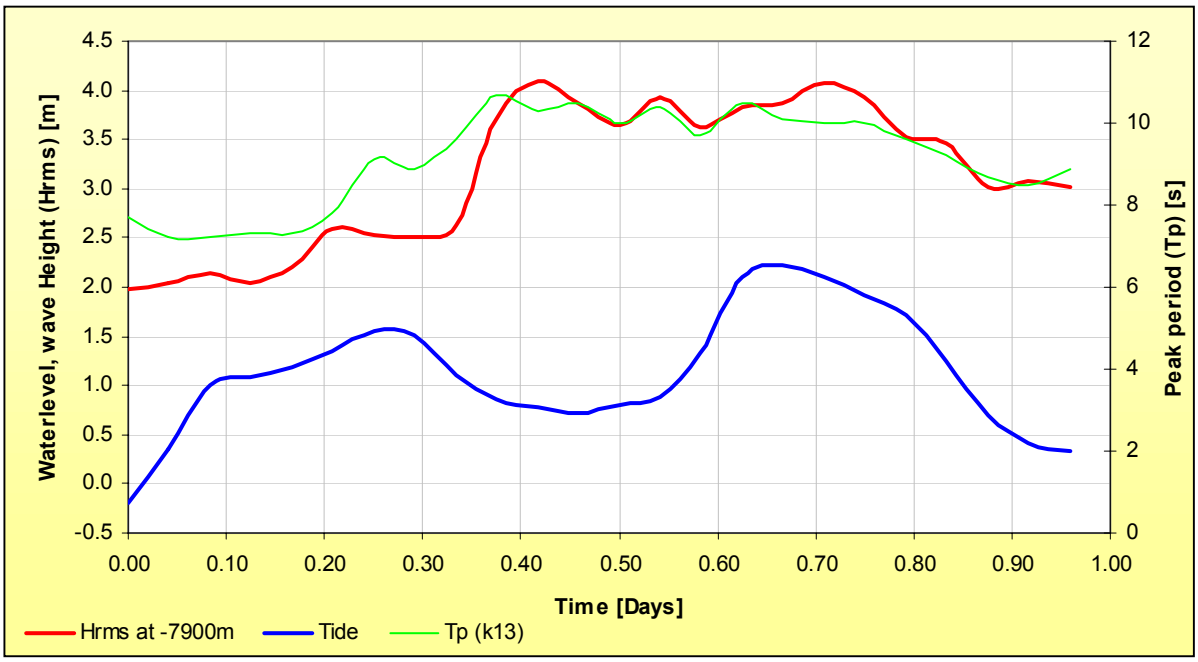

Figure A11.3: Hydraulic offshore boundary conditions used as input for the calibration of UNIBEST-TC.

The offshore wave heights and the water level (tide) have been measured at Petten. The peak period has been measured at wave station K13a, 100km offshore of MP1. However, the peak period stays reasonably constant over a distance of 100km. The surveyed water level has also been shown. The water level includes setup and tide.

Model parameters setting

The calibration has been initiated according to the UNIBEST-TC manual [WALSTRA, 2000] with recommended default parameters values. In Table A11.4 the initial parameter setting are shown. Definitions of the parameters are described in Appendix 9. In order to run UNIBEST-TC properly a grid and a time step have to be chosen.

UNIBEST-TC allows the definition of a variable grid. The grid resolution has to represent the seabed profile with sufficient accuracy. Furthermore, the grid resolution has to be capable of capturing rapid changes of wave characteristics in the surf zone. Numerical stability is dependent on the grid size in the surf zone as well as the chosen constant time step. A general guideline is to use a grid size in the order of 5 to 10m in the surf zone and in the order of 20 to 50m in the deep-water zone. The first columns display the chosen grid size. The grid has been divided into 5 regions with step sizes (Δx) varying from 50m up to10m in the surf zone. The time step (Δt) has been set to an hour ($^1/_{24}$ of a day).

Table A11.4: Initial (default) parameter settings of UNIBEST-TC.

GRID			GENERAL		WAVES		SEDIMENT		TRANSPORT	
PARAMETER	VALUE		PARAMETER	VALUE	PARAMETER	VALUE	PARAMETER	VALUE	PARAMETER	VALUE
START	-8000		DT	0.041667	ALFAC	1	D50	$2.0*10^{-4}$	IBOD	YES
END	+150		NT	24	**GAMMA**	0	D90	$3.0*10^{-4}$	RC	$1.0*10^{-2}$
	#	ΔX	TIME_ST	0	BETD	0.1	DSS	$1.7*10^{-4}$	RW	$2.0*10^{-3}$
REGIO 1	90	50	USTRA	0	FWEE	0.01	DVAR	NO	REMLG	0.1
REGIO 2	20	20	JFR	1	C_R	0.25	FDIA0		TANPH1	**0.1**
REGIO 3	100	20	TDRY	40	K_IJL	ON	FDIA1		TANPH2	0.1
REGIO 4	85	10	TE_W	10	F_LAM	2	FDIA2		XF1	500
REGIO 5	40	10	SALIN	0	POW	1	HDIA0		XF2	1200
REGIO 6					DEEP_V	-5000	HDIA1		ZDRY	HOR
REGIO 7					SHALL_V	-5000	HDIA2		FACQB	0

BOUNDARY CONDITION	SEABED PROFILE	FIXED PROFILE	TIDE ELEVATION	TIDE VELOCITY	WAVE ANGLE	WAVE HEIGHT	PEAK PERIOD	WIND VELOCITY	WIND DIRECTION
CONSTANT				0	0			0	0
991020 FROM –8000 TO 150	YES	YES							
991028.UBC			YES			YES	YES		

The default parameter setting has been applied for all parameters accept for the 'internal friction for the most shoreward bed' parameter (*TANPH1*). Instead of the default value 0.03, 0.1 has been used in order to avoid runtime errors.

During this calibration the effects of the wind speed and wind direction have not been taken into account. Furthermore, the tide velocity has been neglected and the wave angle has been held constant throughout the runs.

Calibration

The calibration has been executed according to Figure A11.5. According to the UNIBEST-TC users manual [WALSTRA, 2000] the following model parameters affect the wave output:

- ALFAC, Wave dissipation factor.
- GAMMA, wave-breaking parameter.
- BETD, roller parameter.
- TETA, wave angle boundary conditions.
- C_R, correlation coefficient.
- FWEE, friction coefficient.
- K_IJL, breaker delay switch.

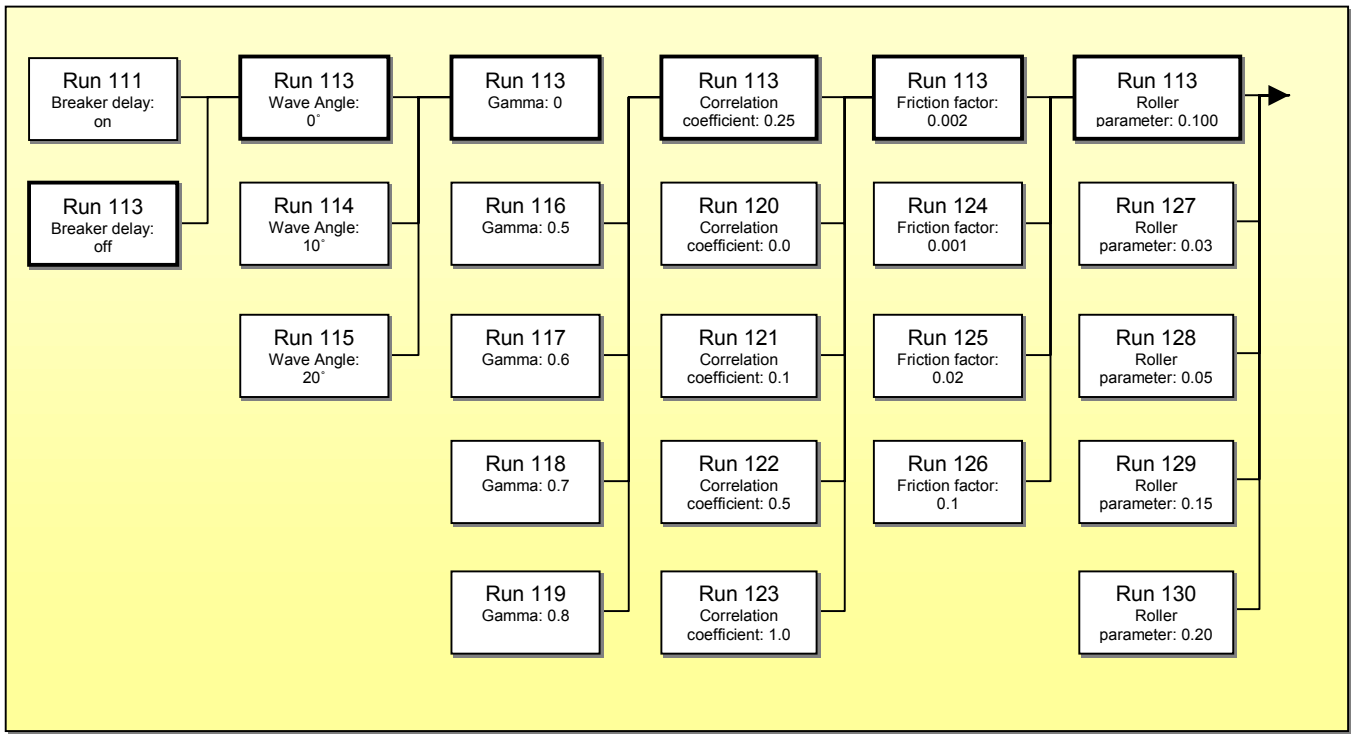

Figure A11.5: The UNIBEST-TC calibration sequence, each column represents a different parameter, whereas the rows represent the parameter variations. The thick box means this value results in the most optimal output the settings of that run are used in the next series.

Method

The run output is compared with measured data series (validation data). The calibration steps are shown in Figure A11.5, six different parameters are examined. The variation of the parameters depends mainly on the parameter range. The parameter settings that result in the best performance are used for the next parameter session, starting with the default settings. This calibration is partly done visually and partly done by with a relative root-mean-square error (RMS error).

The relative RMS error is also referred to as the Scatter Index (SI). The scatter Index varies between 0 and 1 and is an indication for the performance. Low values of the Scatter Index indicate a good model performance. However the SI can become quite high whenever the measured values are low. Whenever more points (N) have been used, the reliability improves. The SI index is determined as follows [WALSTRA, 2000]:

$$SI = \frac{\sqrt{\frac{1}{N}\sum_{i=1}^{N}\left(f_{computed,i} - f_{measured,i}\right)^2}}{\frac{1}{N}\sum_{i=1}^{N}\left(f_{measured,i}\right)} \qquad \text{(A11.1)}$$

Three point are available two check determine the run performance. The three points are located at respectively 540, 60 and 10m from the sea defence. The two closest points are off most interest, because they validate the wave heights near the sea defence. However the third (most offshore located point) is used together with the other points to examine the wave height over the profile stretch. Furthermore, an accurate wave prediction during storm situation deserves most preference. To take all these performances into account the following 5 scatter indices are computed:

1. The SI for the location 10m from the sea defence over the entire period (24 hours).
2. The SI for the location 10m from the sea defence over the period of storm (7 hours (from 13 to 20 hours).
3. The SI for the location 60m from the sea defence over the entire period (24 hours).
4. The SI for the location 10m from the sea defence over the period of storm (7 hours (from 13 to 20 hours).
5. The SI for all three locations at the maximum during the storm maximum (time = 17 hours).

Whenever the SI results are compared, the fifth, fourth and second SI deserve preference, because they are mostly affected by storm conditions. However, to ensure the run remains normal the scatter indices over the entire period are also taken into account. The scatter indices of the two most closest validation points (MP6 and MP7) are often relatively large, due to the relative small values and the relative large variations. The SI value is mainly used for a first impression, followed by a visual examination of the runs. Together the performance according to the SI value as well as the visual examination is used to determine the optimal result.

Breaker delay (K_IJL)

First of all parameters the breaker delay effect has been examined. In Figures A11.13 to A11.15 the measured wave heights as well as the UNIBEST-TC output have been shown. This parameter causes a delay in the energy dissipation process. Especially during swell conditions (waves with long wavelengths) this parameter can improve the predictions. However, during storm conditions waves with short wavelengths often prevail. Therefore, it had been expected that the default parameter setting performance could be improved by disregarding the breaker delay.

SI Value

In Figure A11.6 the results of the model performance is expressed in the SI values. The performance of the run without the breaker index (K_IJL = OFF) results in a lower SI for all cases. This means that the performance will increase if the breaker delay is turned of. The green coloured bars (1st and 3rd) are the SI values for total period; the red and orange bars (2nd and 4th) represent the SI value for the storm period. The blue bar (5th) can be interpreted as the error for the wave height over the profile stretch.

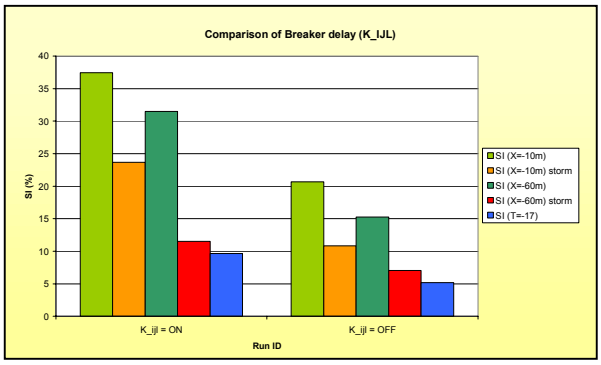

Figure A11.6: SI values for the breaker delay parameter.

Visual comment

According to the UNIBEST-TC output Figures A11.13 to A11.15 the waves are over-estimated in the nearshore area (between 0 and 100m) in case of the breaker delay, whereas without the breaker delay the prediction lies closer to the measurements. Furthermore, wave height increasing shoaling effects are also increased by the breaker delay.

Wave angle (TETA)

The orientation of the incoming wave with respect to the shore normal direction has little effect on predicted wave heights in UNIBEST-TC. In UNIBEST-TC wave heights (H_{rms}) that are used as input at the offshore boundary are multiplied by cos(θ). Waves that have an orientation that differs from the shore normal (θ =0) always have a lower wave height over the profile stretch. In reality, these oblique orientated waves generate a current in long-shore direction. However, this additional long shore current has not been taken into account during this evaluation.

Visual and SI comments

The variation in wave height is little. This can be seen in the SI-diagram (Figure A11.7) as well as the wave height plots (Figure A11.16 to A11.18). It can be concluded that the wave angle has little effect on the wave height. Larger wave angles have been neglected during the calibration, because these waves will not pass the 'Pettemer Polder' bank (3500m offshore).

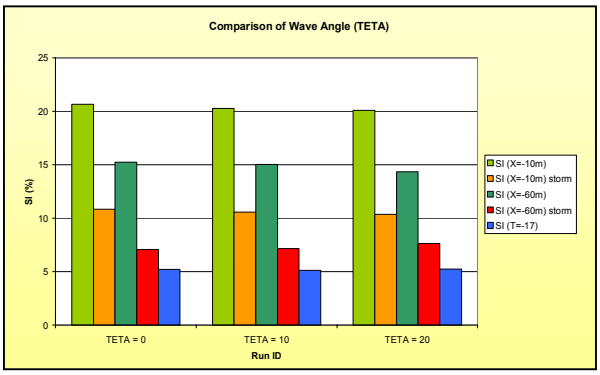

Figure A11.7: SI values for the wave angle parameter.

Larger wave angles have more effect on the computed wave height. To take waves with larger wave angles into account a 3 dimensional seabed bathymetry is recommended. The shore normal value (cos(θ) = 1) will be applied during all following UNIBEST-TC simulations.

Wave breaking parameter (ALFAC)

According to the UNIBEST-TC manual (WALSTRA, 2000) it is advised to calibrate wave heights and breaking with the breaker index (GAMMA) instead of the ALFAC value. The ALFAC parameter has therefore been held constant.

Wave breaker index (GAMMA)

This parameter has considerable effect on the wave penetration and wave heights within the surf zone. Two possibilities are optional for this parameter. First of all, a constant value can be chosen in the range of 0.5 to 0.8. Second of all, the breaker index can be made dependable on the deep-water wave steepness (s_0). The deep-water wave steepness is determined by the root-mean-square wave height (H_{rms}) and the peak wave period (T_p) at the most offshore boundary.

SI value

5 different values are examined because of the significant effect this parameter has on the wave height. According to the SI-diagram, Figure A11.8, the default value (GAMMA = 0) and a breaker index of 0.7 results in a reasonably good performance. The Gamma is 0.7 run performs best at location X=10 (1st and 2nd bar in series), while the default setting results in a optimal the best performance for the 4th and 5th bar respectively location MP6 during storm and the overall profile during storm.

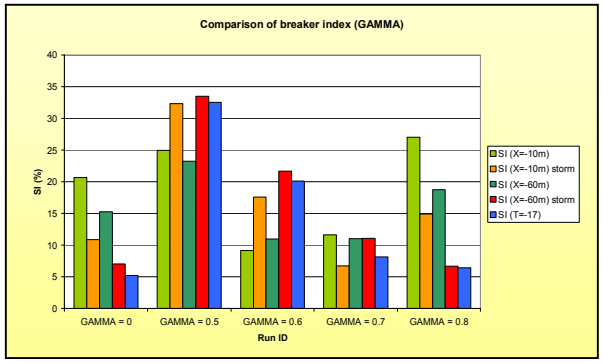

Figure A11.8: SI values for the breaker index parameter.

Visual comments
According to the SI-diagram the averaged SI value for the GAMMA = 0.7 run is slightly lower than the SI value for the default setting. Therefore these runs are carefully examined. The results are shown in A11.19 to A11.21.

According to the SI-diagram a GAMMA of 0.7 and a GAMMA of 0 result in the best performance. However, if the runs are examined a GAMMA of 0.7 results in a good performance during non-storm conditions and only at location X=10m the performance is good during storm. However, according to the overall profile and the storm profile of X=60m the default value as well as a value of 0.8 perform better.

If higher values have been used for GAMMA higher waves are possible on more shallow water. Two runs have a more or less similar outcome; GAMMA = 0 and GAMMA = 0.8. A GAMMA value of 0 implies that GAMMA depends on the deep-water wave steepness resulting in a GAMMA-value of 0.771 close to 0.8.

It appears that during storm higher values of GAMMA are necessary in order to predict the wave heights accurately. A constant value of 0.8 results in a reasonably good prediction at the location 60m offshore from the toe of the sea defence. However, at a distance of 10m offshore the wave height will be over-estimated significantly, about 30cm during the storm maximum.

A deep-water wave steepness dependent value for GAMMA results in an improved result for fair weather conditions with low waves, whereas during storm still reasonable wave heights are possible. At the toe of the sea defence the over-estimation of wave heights has decreased to about 25cm. A GAMMA-value of 0 is therefore recommended, instead of the GAMMA = 0.7.

Correlation coefficient (C_R)
This parameter is the correlation coefficient between wave envelope and bound long waves and it expresses the long and short wave interaction. This coefficient arranges the phase shift between long-wave and short wave envelope. It varies from -C_R at deep water up to C_R at the shore. A negative phase shift causes an increased offshore Table, while a positive phase-shift has the opposite effect. By using 0 for this value the long-wave effects will be eliminated.

Visual and SI comments
The effect on the wave height prediction is little according to Figures A11.22 to A11.24 and the SI diagram A11.9. The effects are found near the toe of the sea defence after the period of storm. Because of the little effect and because little research has been executed to examine this correlation coefficient, the default value has been applied.

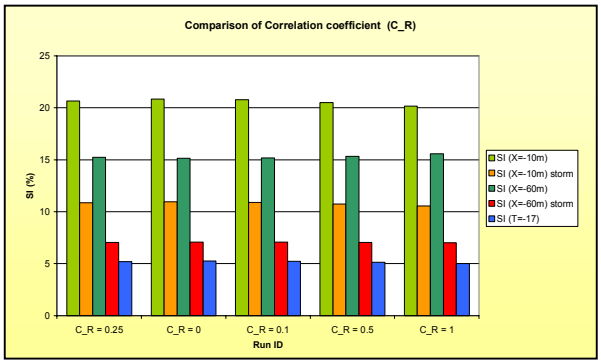

Figure A11.9: SI values for the correlation coefficient.

Friction factor (FWEE)
Two processes; 'breaking' and 'bottom friction' dissipate energy. This friction factor determines the amount of energy that is dissipated by bottom friction. The dissipation by friction is sensitive for bed forms. If waves computations are made over a relatively long distance (3 to 10km) this parameter can influence the wave height predictions significantly. Within the surf zone this parameter has little effect, as wave breaking is dominant. FWEE has been varied with values in the range of 0.001 to 0.1.

Visual and SI comments
According to Figure A11.25, A11.26 and A11.27 higher values of FWEE result in a decrease of wave heights over the entire profile. The variation in output is little, in the magnitude of several centimetres.

The variation is SI-value is also small if the performance of the FWEE = 0.1 has not been neglected. In this case the default value deserves preference.

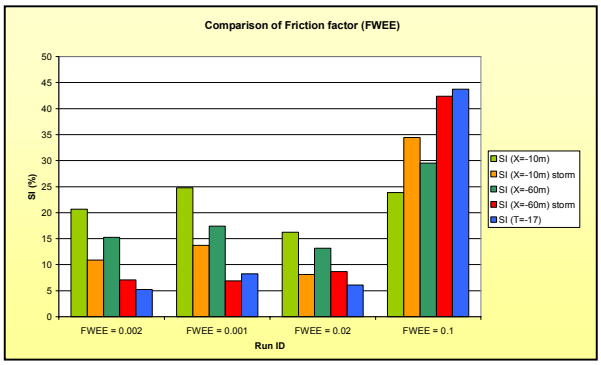

Figure A11.10: SI values for the friction factor.

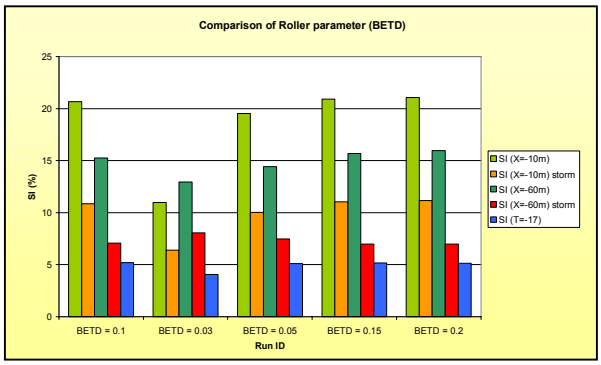

Figure A11.11: SI values for the roller parameter.

Roller parameter (BETD)

Beta (written as 'BETD' in UNIBEST-TC) is a roller parameter according Nairn et al. [1990]. The roller parameter describes the slope of the wave front and is used to determine the dissipation due to roller energy. This value has little effect on the computed wave height. However, it significantly affects the wave setup and therefore the undertow (wave induced cross-shore current).

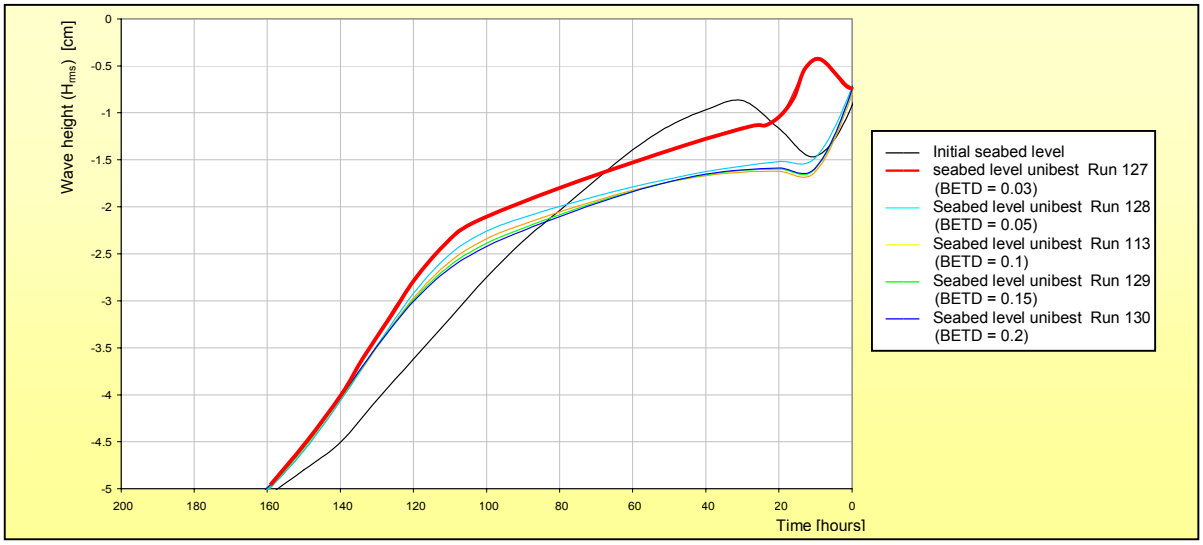

Figure A11.12: Seabed profiles simulated by UNIBEST-TC compared with initial seabed profile measured at Petten during storm.

Visual and SI comments

Several different values have been examined. According to Figures A11.28 to A11.30 a value of 0.03 results in the best performance (Figure A11.11). However, if the predicted seabed profiles are compared a significant difference occurs. The seabed increases directly in front of the toe (Figure A11.12), which is contrary to the expected changes. In the manual a minimum of 0.03 as well as 0.05 has been used, which is another reason to eliminate the results of run 127 (BETD = 0.03). If the results of this run are ignored, little variation can be observed. Therefore the default value is once more recommended.

The calibration results

According to the results of this calibration the breaker delay and gamma parameter have most effect on the predicted wave height. Simulation run 113 appears to result in the best wave height prediction taking into account all seabed variation and the measured wave heights in the surf zone. The settings of run 113 are similar to the default setting accept for two parameters:

- The TANPH1 = 0.1 instead of 0.03.
- The breaker delay module is switched off instead of on.

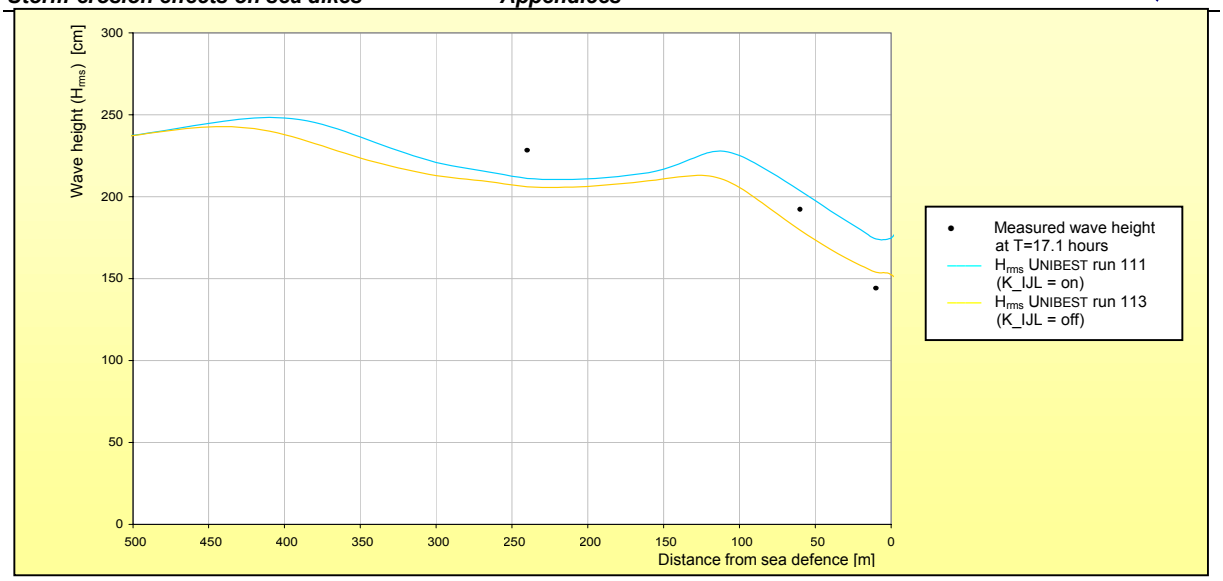

Figure A11.13: Wave heights (H_{rms}) simulated by UNIBEST-TC compared with wave heights measured at Petten during storm (t=17.1 hours).

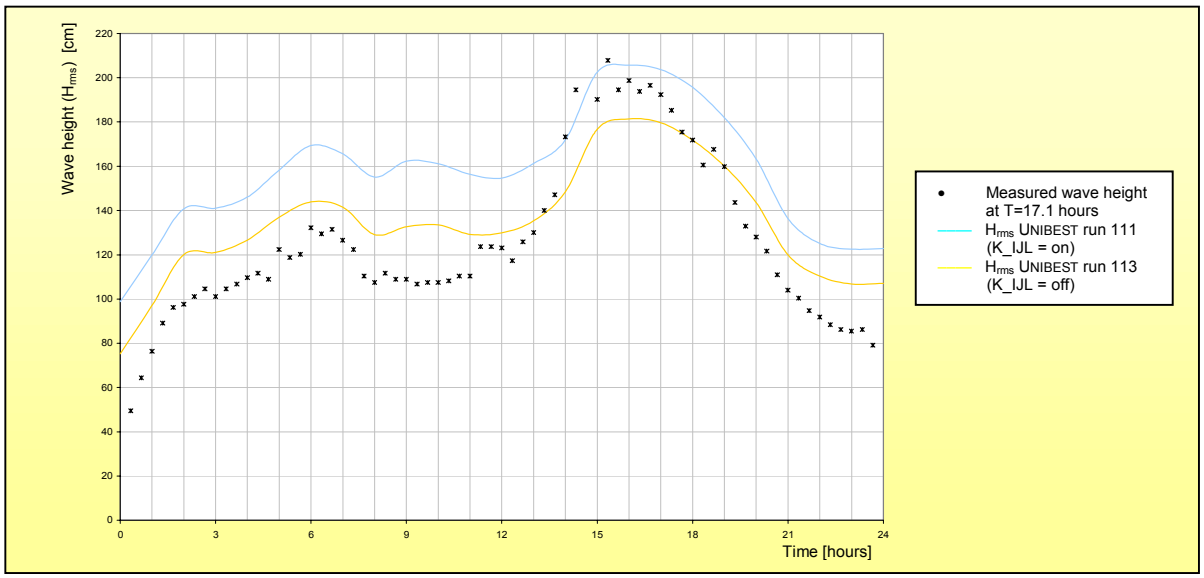

Figure A11.14: Wave heights (H_{rms}) simulated by UNIBEST-TC compared with wave heights measured at Petten during storm, at location MP6 (60m offshore).

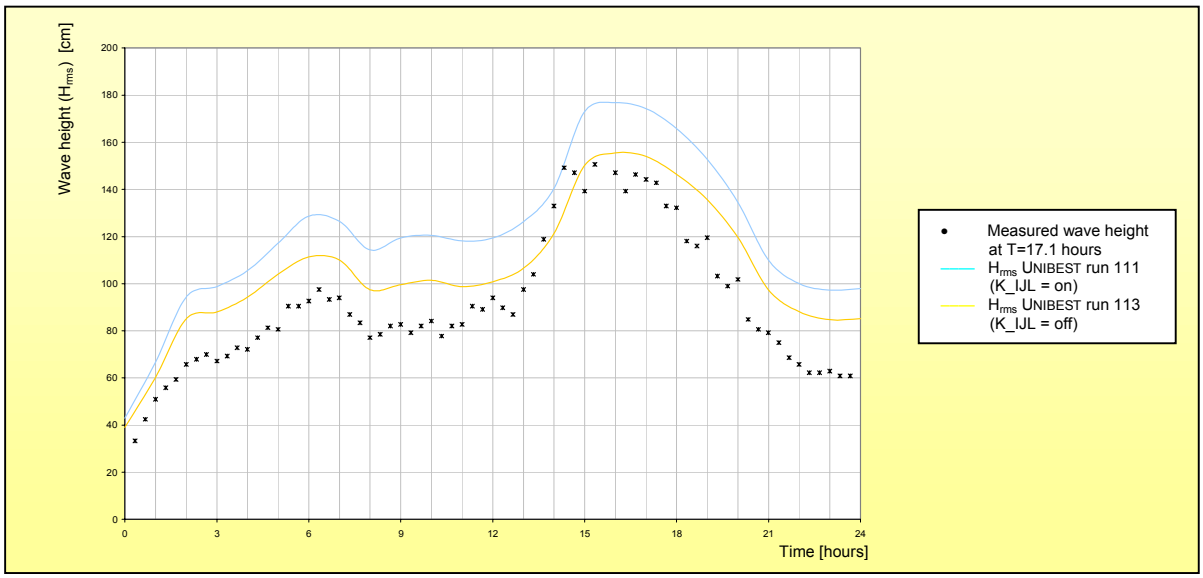

Figure A11.15: Wave heights (H_{rms}) simulated by UNIBEST-TC compared with wave heights measured at Petten during storm, at location MP7 (10m offshore).

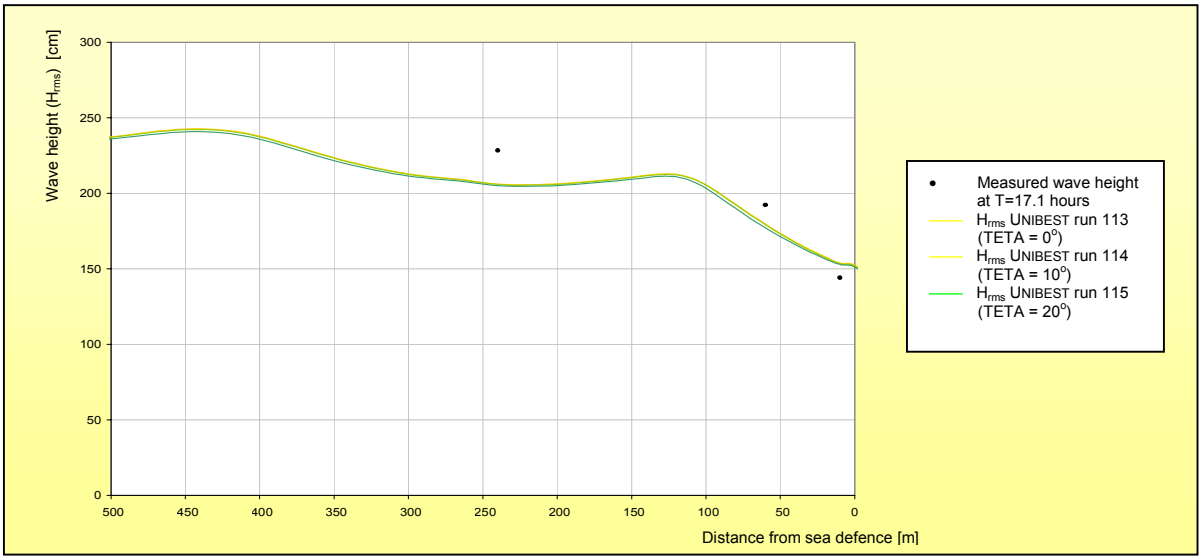

Figure A11.16: Wave heights (H_{rms}) simulated by UNIBEST-TC compared with wave heights measured at Petten during storm (t=17.1 hours).

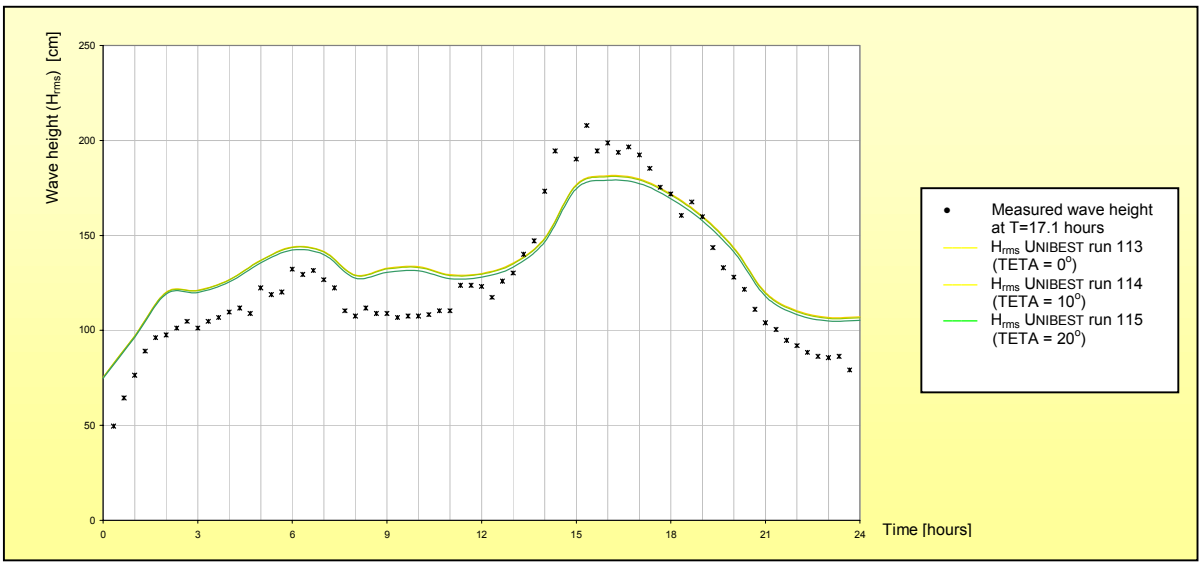

Figure A11.17: Wave heights (H_{rms}) simulated by UNIBEST-TC compared with wave heights measured at Petten during storm, at location MP6 (60m offshore).

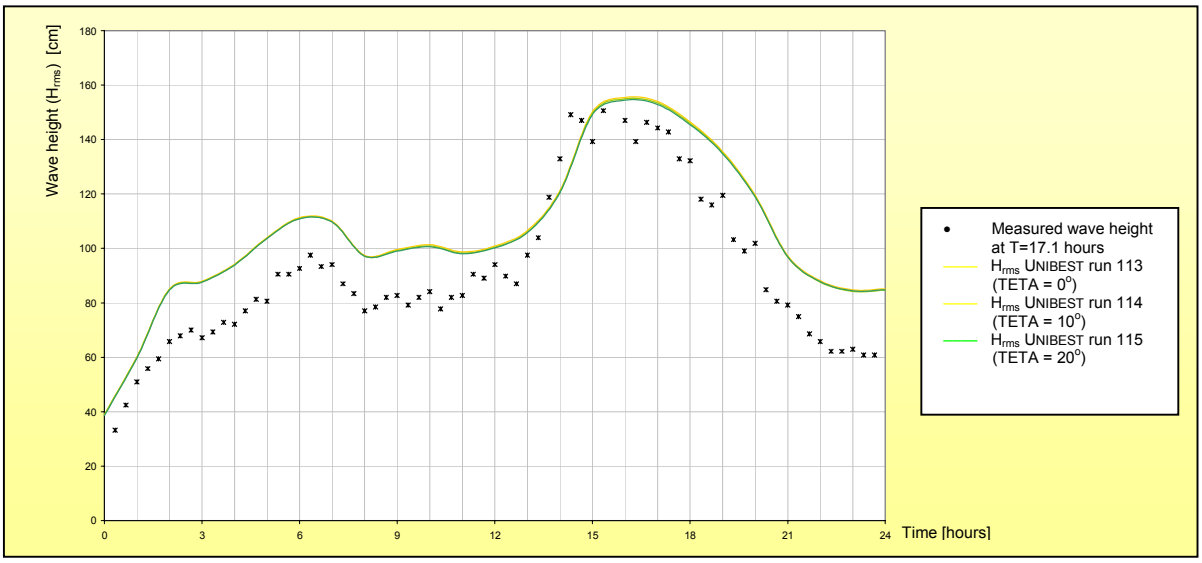

Figure A11.18: Wave heights (H_{rms}) simulated by UNIBEST-TC compared with wave heights measured at Petten during storm, at location MP7 (10m offshore).

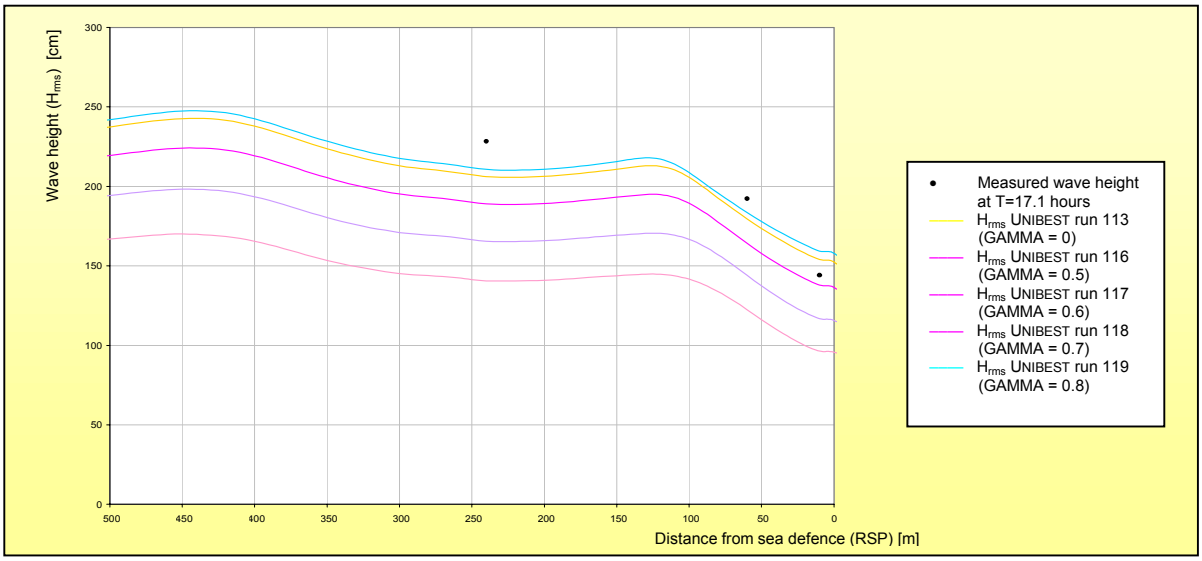

Figure A11.19: Wave heights (H_{rms}) simulated by UNIBEST-TC compared with wave heights measured at Petten during storm (t=17.1 hours).

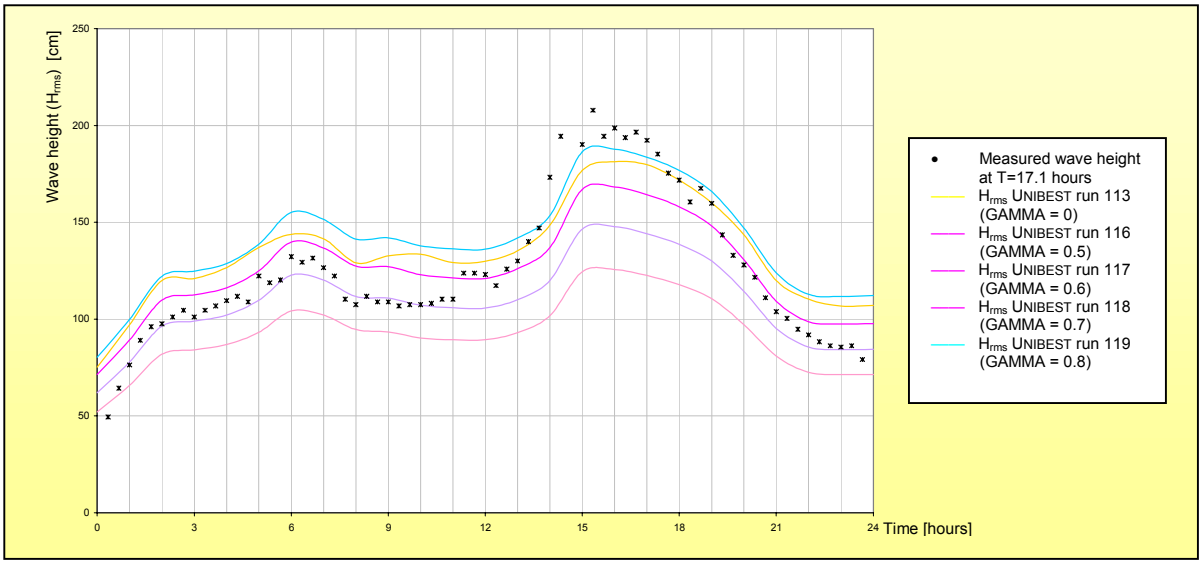

Figure A11.20: Wave heights (H_{rms}) simulated by UNIBEST-TC compared with wave heights measured at Petten during storm, at location MP6 (60m offshore).

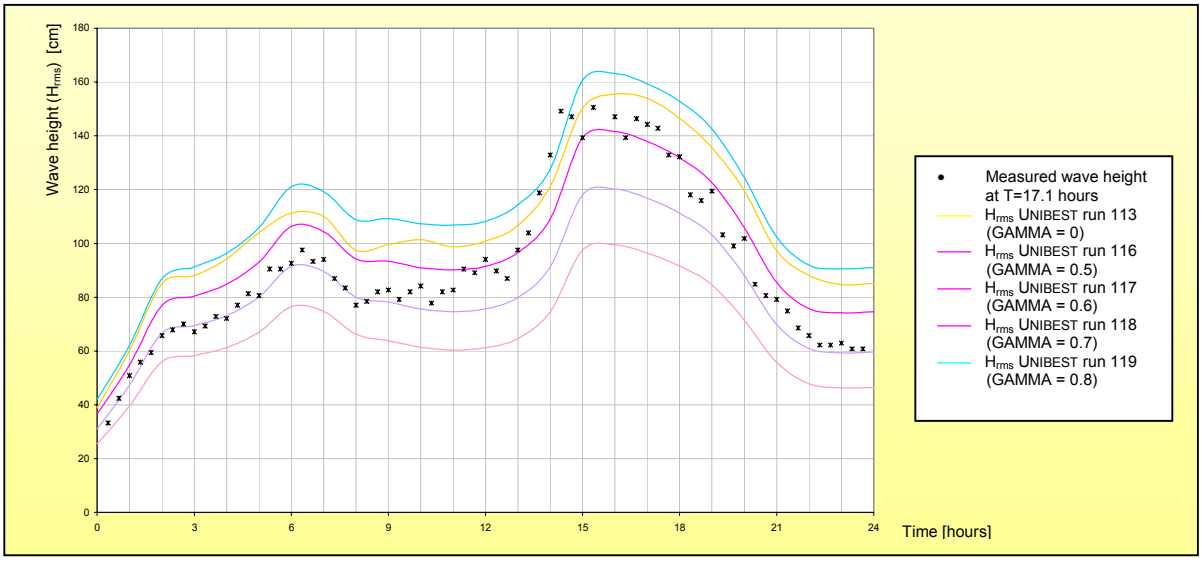

Figure A11.21: Wave heights (H_{rms}) simulated by UNIBEST-TC compared with wave heights measured at Petten during storm, at location MP7 (10m offshore).

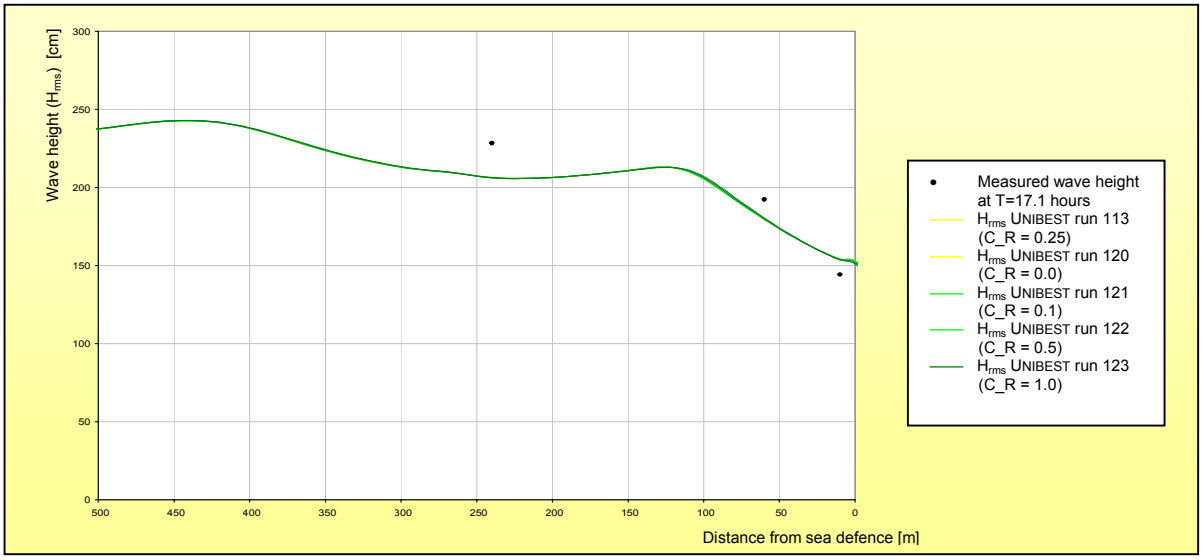

Figure A11.22: Wave heights (H_{rms}) simulated by UNIBEST-TC compared with wave heights measured at Petten during storm (t=17.1 hours).

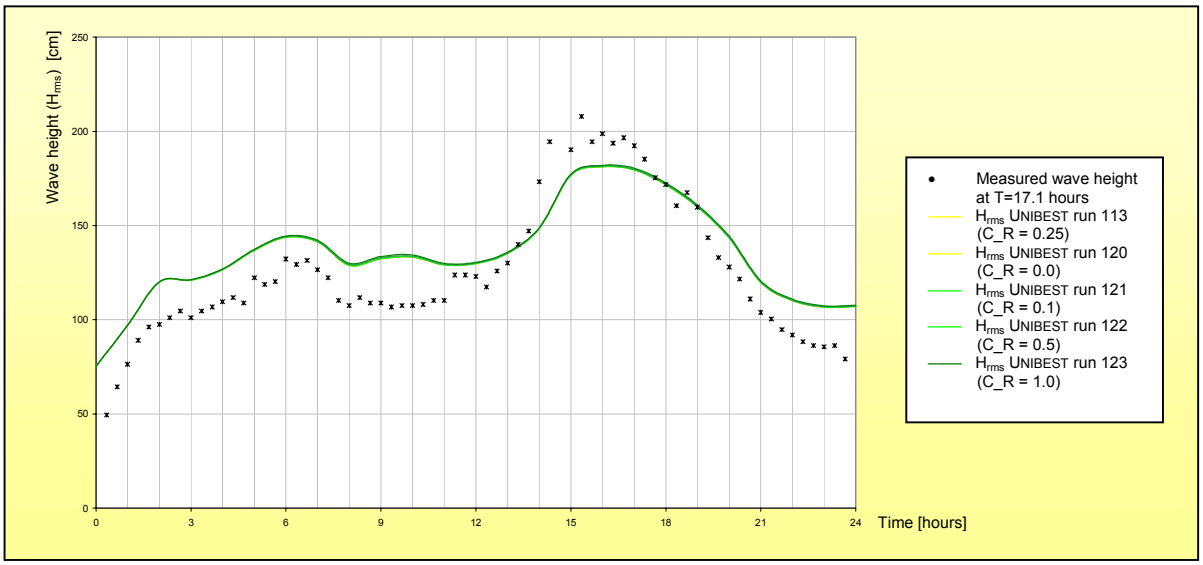

Figure A11.23: Wave heights (H_{rms}) simulated by UNIBEST-TC compared with wave heights measured at Petten during storm, at location MP6 (60m offshore).

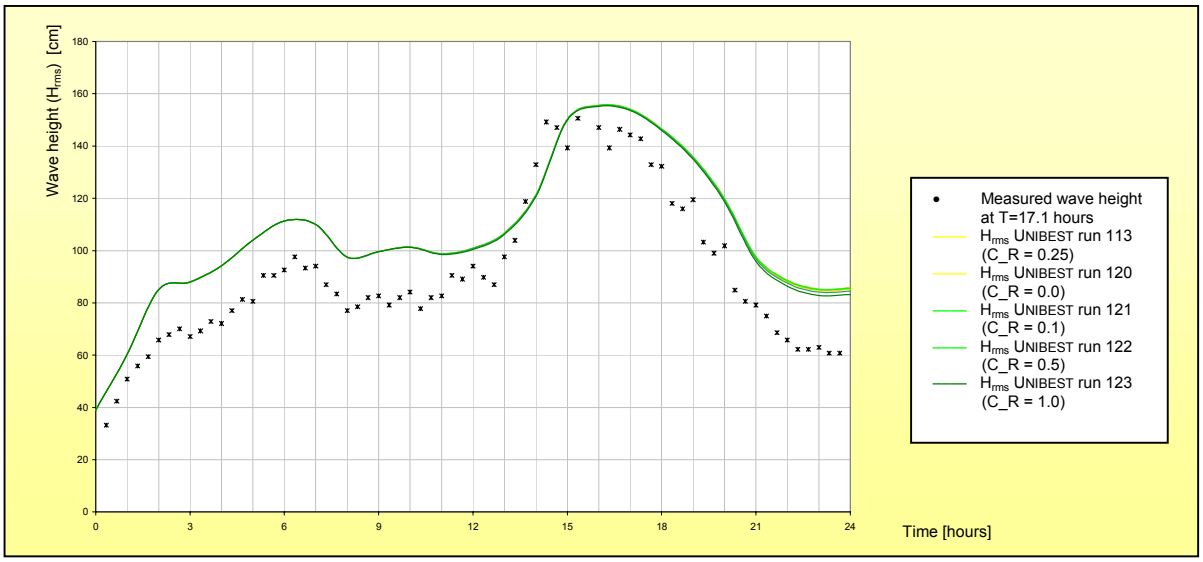

Figure A11.24: Wave heights (H_{rms}) simulated by UNIBEST-TC compared with wave heights measured at Petten during storm, at location MP7 (10m offshore).

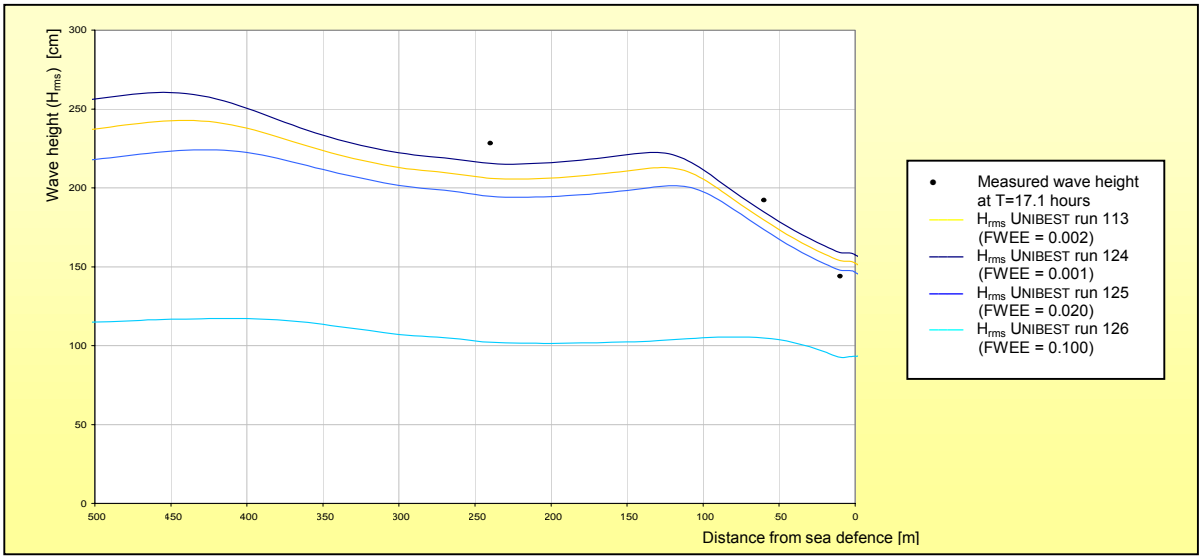

Figure A11.25: Wave heights (H_{rms}) simulated by UNIBEST-TC compared with wave heights measured at Petten during storm (t=17.1 hours).

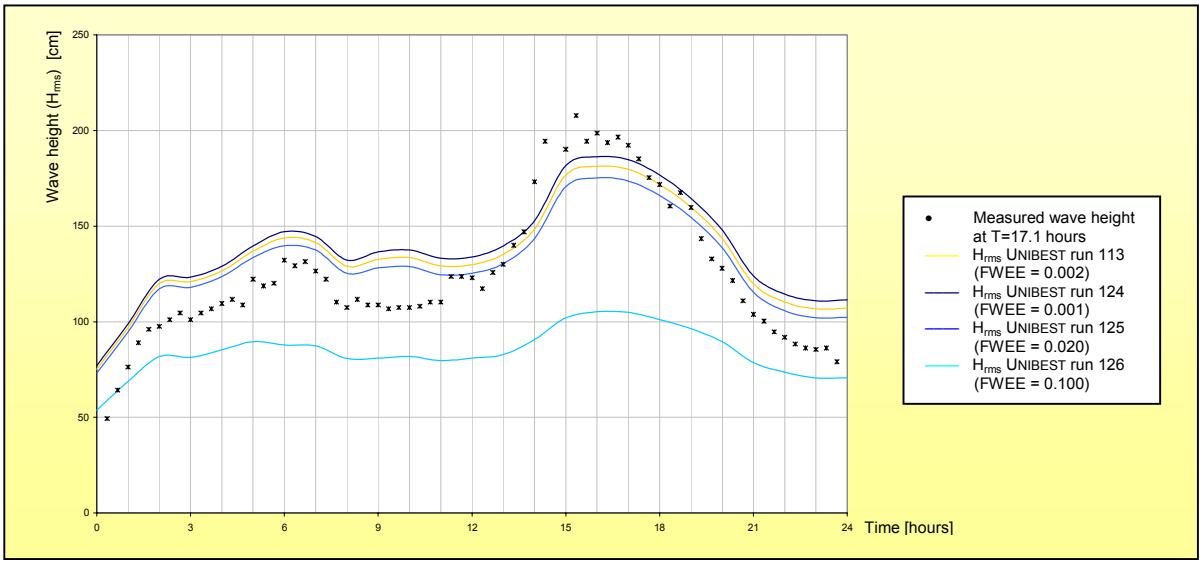

Figure A11.26: Wave heights (H_{rms}) simulated by UNIBEST-TC compared with wave heights measured at Petten during storm, at location MP6 (60m offshore).

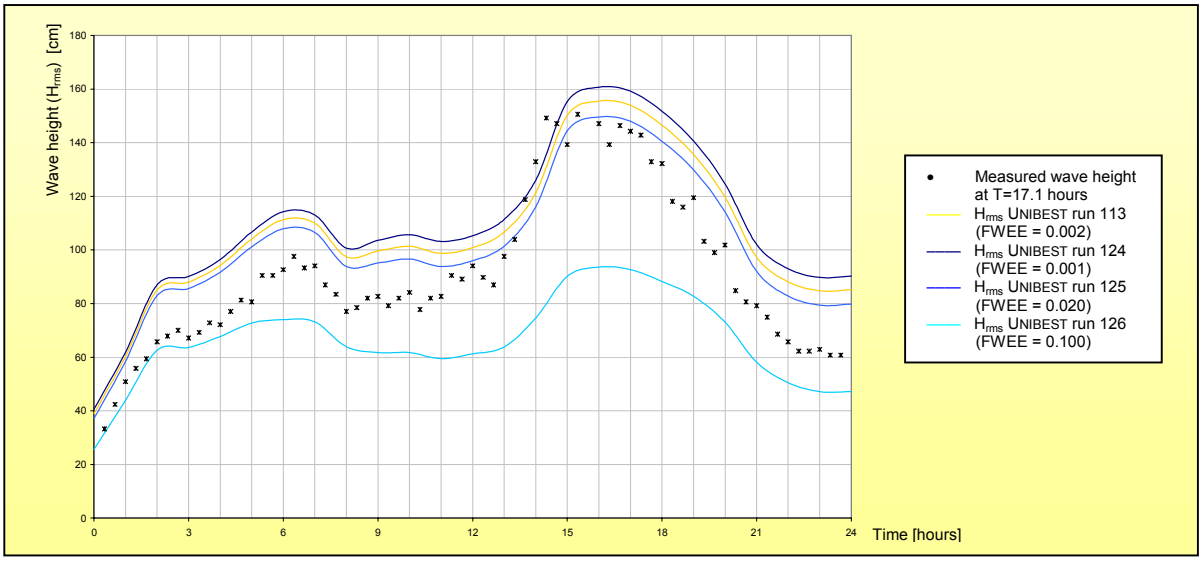

Figure A11.27: Wave heights (H_{rms}) simulated by UNIBEST-TC compared with wave heights measured at Petten during storm, at location MP7 (10m offshore).

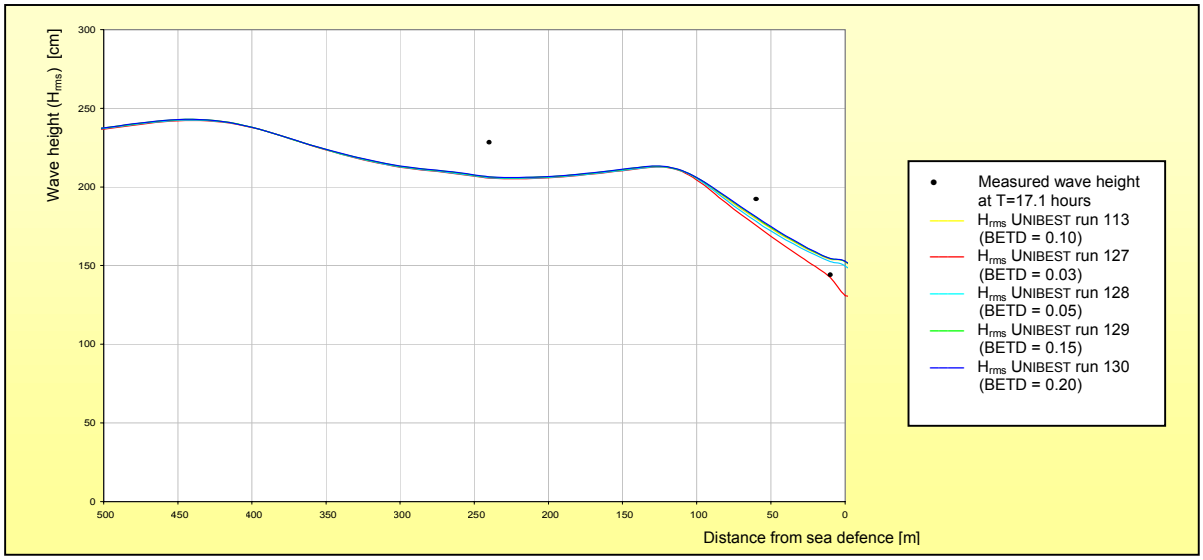

Figure A11.28: Wave heights (H_{rms}) simulated by UNIBEST-TC compared with wave heights measured at Petten during storm (t=17.1 hours).

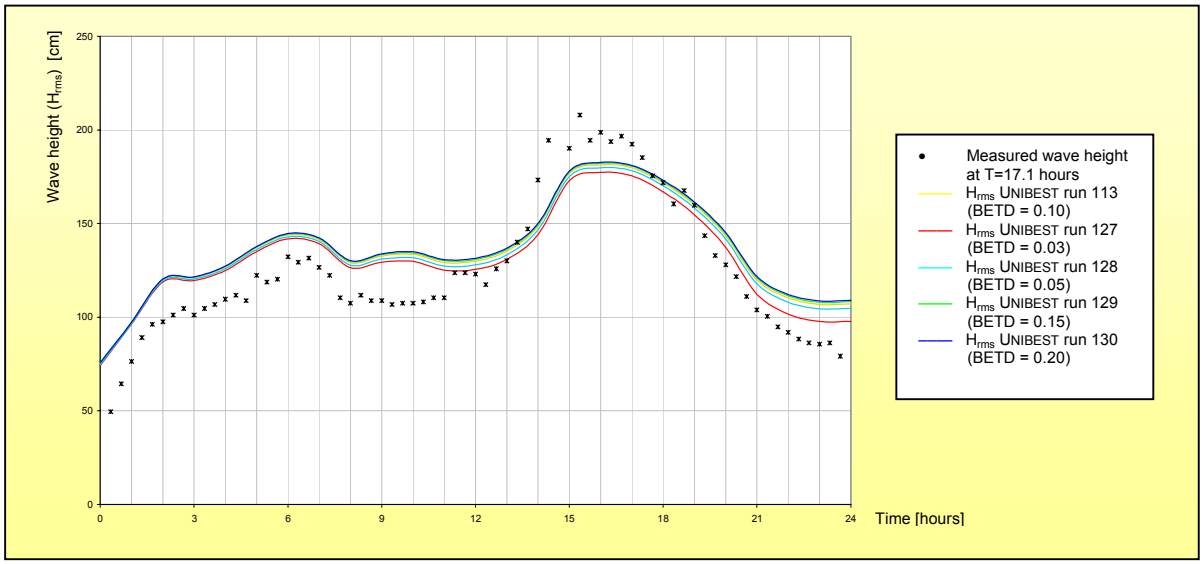

Figure A11.29: Wave heights (H_{rms}) simulated by UNIBEST-TC compared with wave heights measured at Petten during storm, at location MP6 (60m offshore).

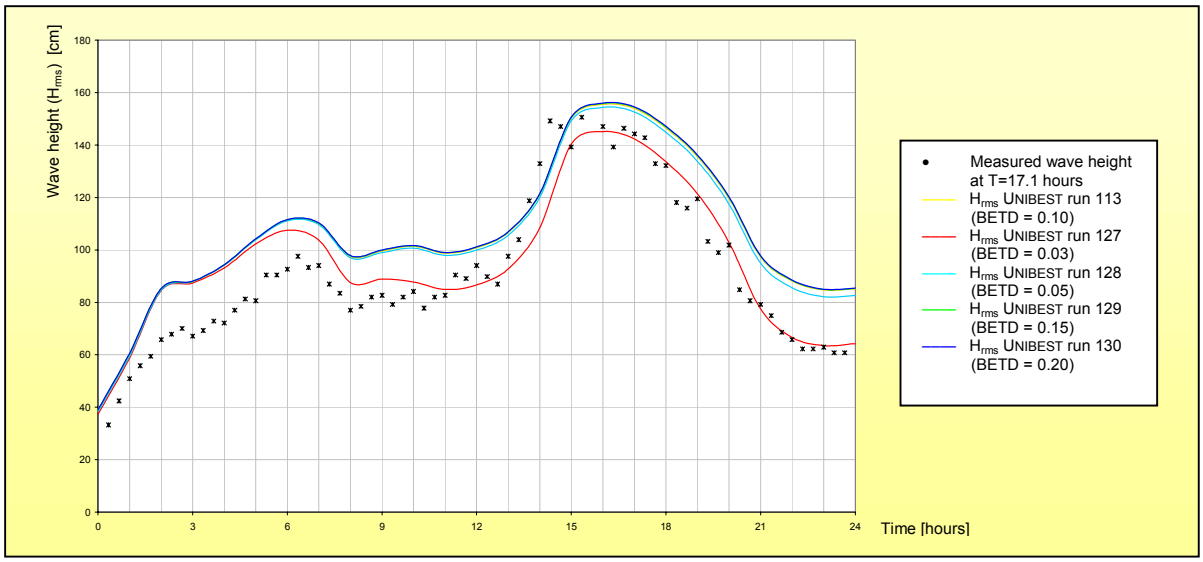

Figure A11.30: Wave heights (H_{rms}) simulated by UNIBEST-TC compared with wave heights measured at Petten during storm, at location MP7 (10m offshore).

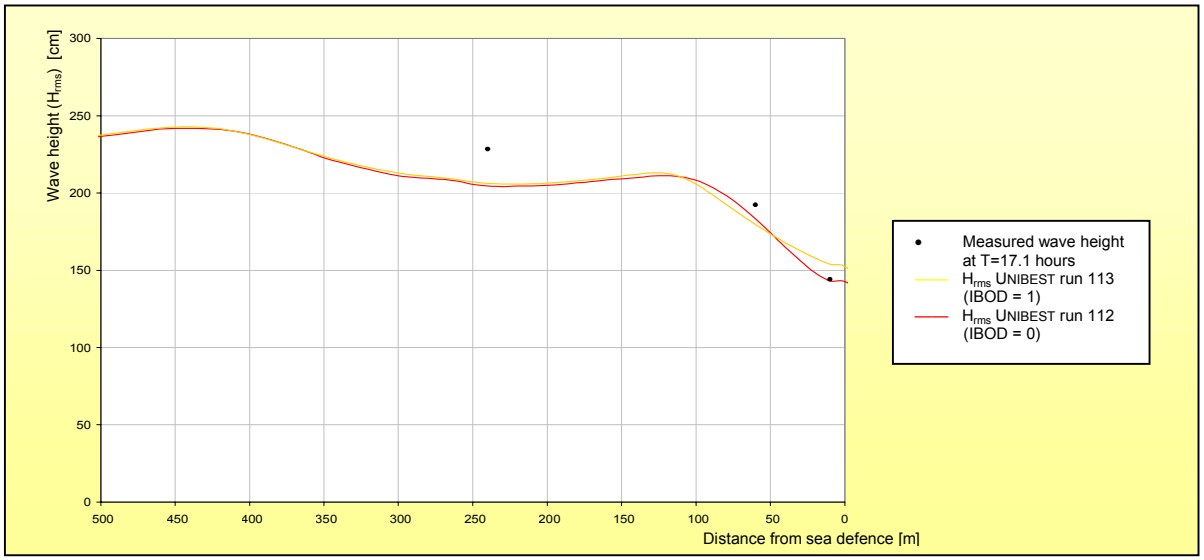

Figure A11.31: Wave heights (H_{rms}) simulated by UNIBEST-TC compared with wave heights measured at Petten during storm (t=17.1 hours).

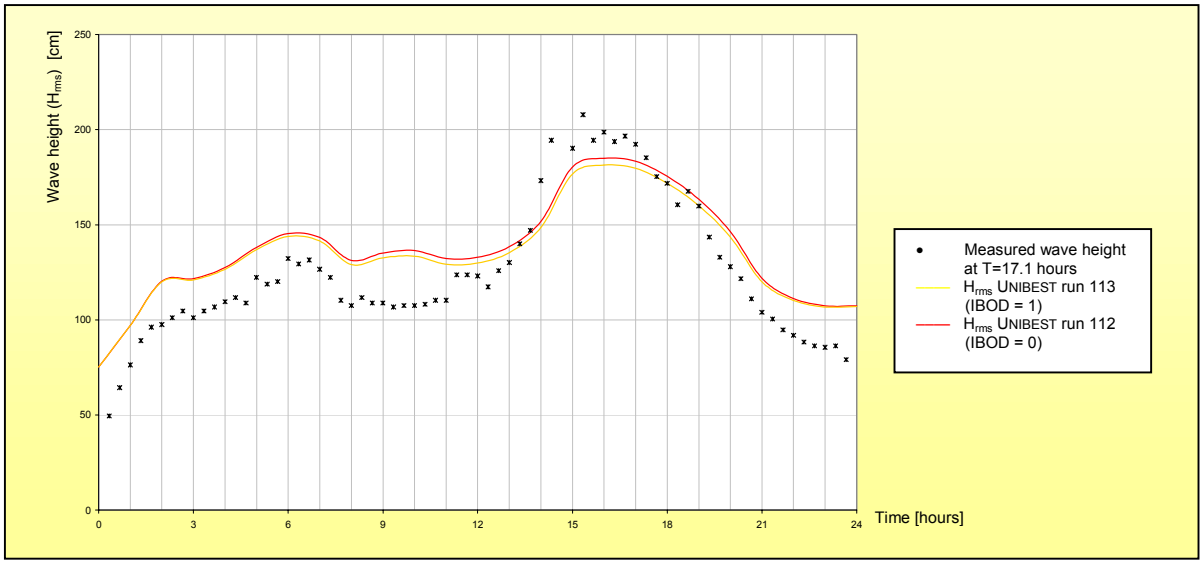

Figure A11.32: Wave heights (H_{rms}) simulated by UNIBEST-TC compared with wave heights measured at Petten during storm, at location MP6 (60m offshore).

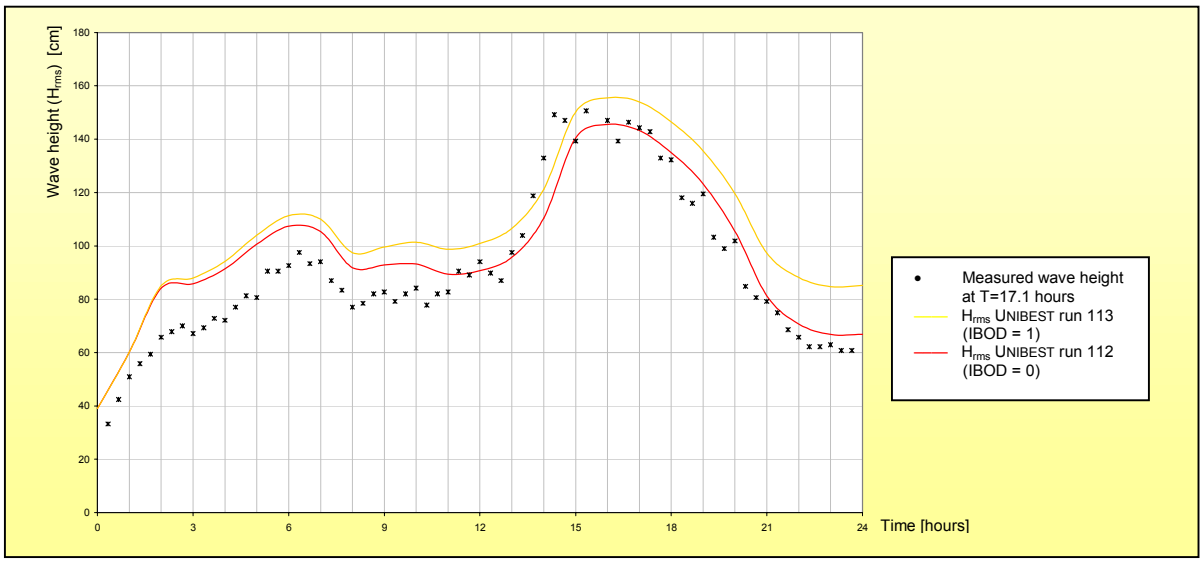

Figure A11.33: Wave heights (H_{rms}) simulated by UNIBEST-TC compared with wave heights measured at Petten during storm, at location MP7 (10m offshore).

Appendix 12: UNIBEST-TC versus SWAN-1D

General

During this thesis the morphological computer model UNIBEST-TC has been used to determine storm-erosion and the accompanying affects of local wave height variations. In the previous Appendix 11 the model has been calibrated as good as possible for the wave height. However, in Paragraph 5.5 the wave height appears to decrease slightly before an increase due to seabed decrease has been predicted. This only occurs whenever relatively high water levels have been used in the simulation.

The UNIBEST-TC wave height predictions are compared to SWAN-ID predictions. SWAN-1D is a model that predicts wave propagation on a specified bottom profile. The SWAN-1D model cannot predict seabed changes like UNIBEST-TC.

The most important differences between SWAN-1D and UNIBEST-TC:

- SWAN-1D cannot computed seabed changes.
- SWAN-1D does incorporate wind energy into the wave model.

UNIBEST-TC and SWAN-1D are two different models with different formulations for hydrodynamic processes; it is therefore unlikely that the result of both models will be exactly similar. However, it is possible to compare both results and evaluate the differences.

SWAN-1D versus UNIBEST-TC with default parameter settings

Boundary conditions

UNIBEST-TC and SWAN-1D are compared, by using the equal boundary conditions and default parameter settings for both models. The boundary conditions are shown in table A12.1.

Table A12.1: Boundary conditions for SWAN-1D and UNIBEST-TC during the entire simulation time.

Description	SWAN-1D		UNIBEST-TC	
	Parameter	Value	Parameter	Value
Wave height	H_s	7.07m	H_{rms}	5.0m
Wave period	T_p	11.32s	T_p	11.32s
Water level	h_0	NAP + 2.0m	h_0	NAP + 2.0m
Wave spectrum	Jonswap spectrum		Jonswap spectrum	
Grid size	Δx	5m	Δx	Varying 50m - 5m
Time step	No time step		Δt	0.5 hours

For the UNIBEST-TC default settings are used accept for the 'breaker parameter switch'. The breaker index switch (K_IJL = OFF) has been turned off in UNIBEST-TC because according to the calibration (APPENDIX 11) this results in a better performance.

SWAN-1D uses the significant wave height instead of the root-mean-square wave height. Both parameters differ a factor 1.41. In SWAN-1D it is possible to change the wind speed, however this option has been turned down, because UNIBEST-TC does not have this option.

In order to make it possible to compare SWAN-1D and UNIBEST-TC the root-mean-square wave height from UNIBEST-TC has been transformed into the significant wave height used in SWAN-1D. Furthermore, SWAN-1D uses the seabed profile computed by UNIBEST-TC.

Results

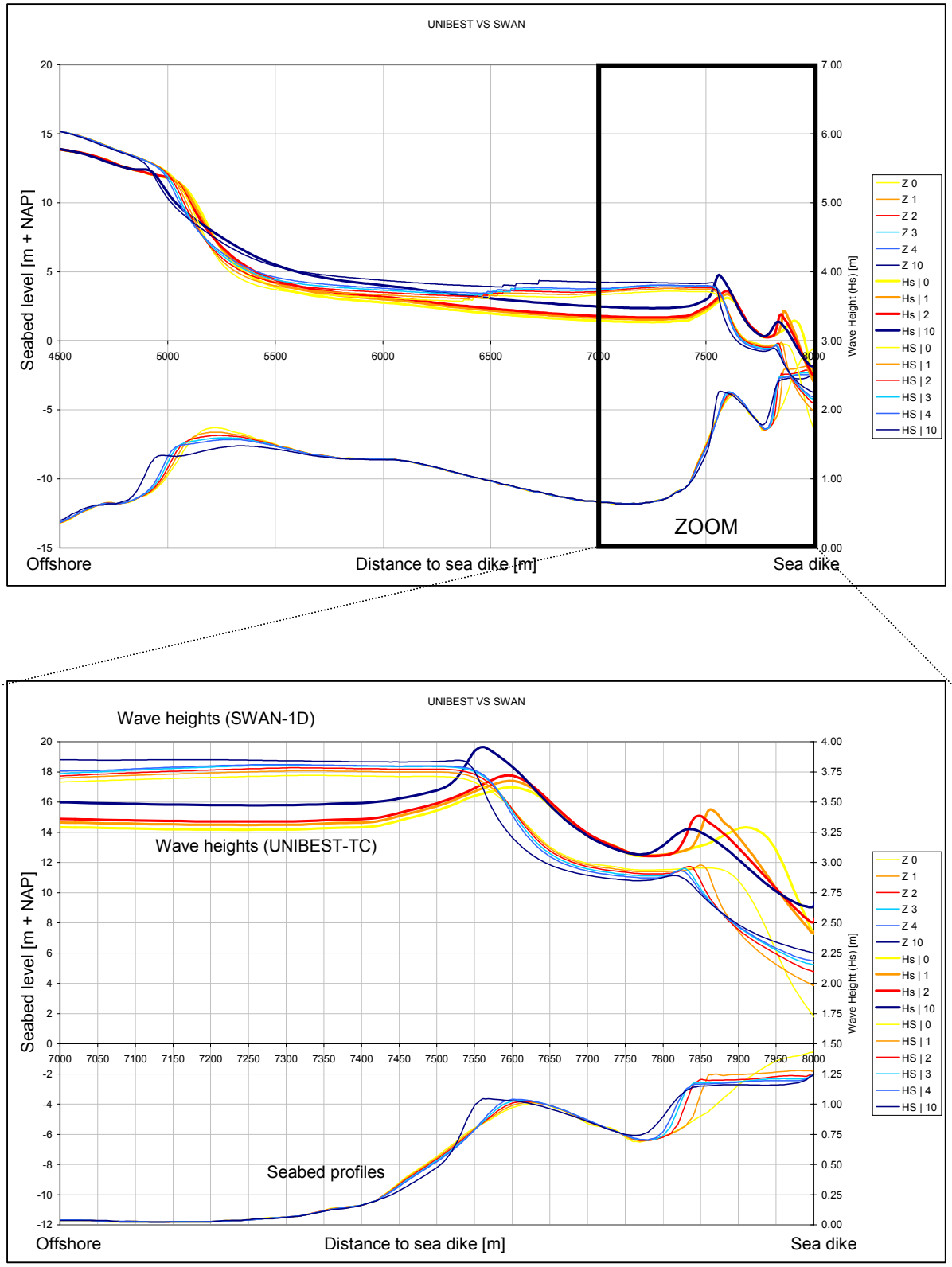

Figure A12.2: Seabed profiles, UNIBEST-TC wave heights and SWAN-1D wave heights for several time steps.

Figure A12.2 needs some explanation. Two parameters are shown; seabed profiles (Z) that are computed by UNIBEST-TC and used for SWAN-1D input, as well as significant wave heights (H_s) computed by UNIBEST-TC (thick lines) and SWAN-1D (Thin lines). The colours of the lines vary with time. For instance the yellow lines represent the conditions at 0 days, while the red lines represent the conditions after 2 simulated days of storm. The Figure composes of two graphs the first is the overall situation, while the second graph zooms in on the more interesting section.

First of all it is seen that the bottom is changed (flattened) over time. This is the reason that the wave propagation differs between the time steps.

The same colour lines that represent waves computed by SWAN-1D and UNIBEST-TC can be compared, each colour is a different situation in time. Whenever a bar is present the water depth decreases and wave breaking takes place. In figure A12.2 the SWAN-1D wave heights seem to have a greater decrease after a bar than the UNIBEST-TC waves do. It appears that the SWAN-1D model computes more dissipation due to breaking compared to UNIBEST-TC. However, on the long stretch (5500 to 7500) the wave height computed by UNIBEST-TC decrease a lot while the SWAN-1D wave heights show a small increase. UNIBEST-TC probably predicts more wave dissipation due to friction.

Another phenomenon that occurs at the breaker bar located 400m in front of the sea defence. Waves computed by UNIBEST-TC show an increase in wave height due to shoaling before they break, while SWAN-1D shows practically no shoaling at all. Furthermore, it appears that the wave heights computed by SWAN-1D at the sea defence are lower than the UNIBEST-TC waves. Another interesting aspect is the fact that the SWAN-1D waves show a continuous increase over time, while the UNIBEST-TC waves grow in time with a delay.

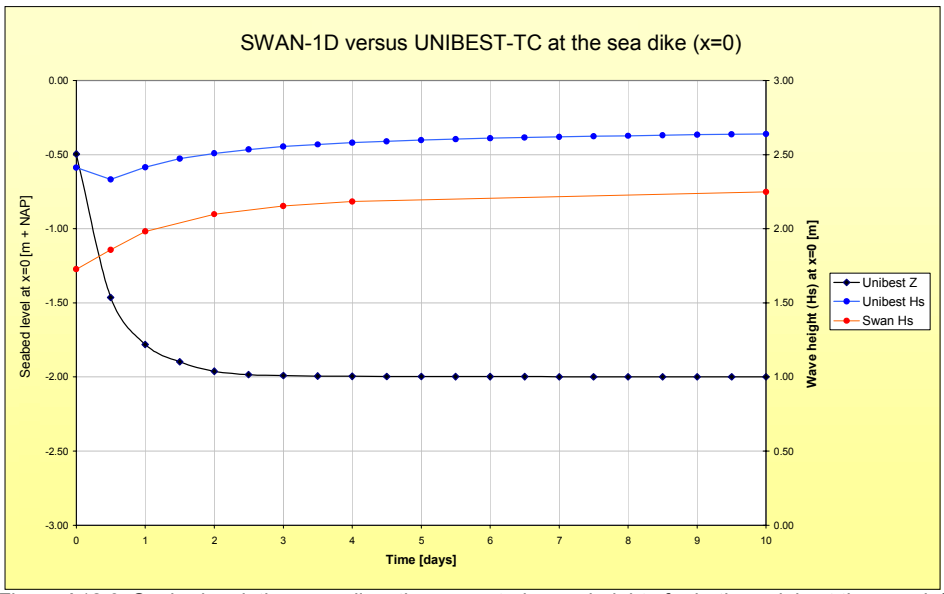

Figure A12.3: Seabed variation as well as the computed wave heights for both models at the sea defence (x=0) over time.

The following Figure A12.3 shows the predicted wave heights at the sea defence for both models as well as the seabed decrease over time. The erosion of the local seabed causes the computed increase in wave height at the sea defence. At location (x=0 or 8000 for SWAN-1D) the bottom erodes to a depth of – 2m NAP in almost two days and then stays constant. It is not the equilibrium depth that has been reached but the fixed layer that results in a constant depth over time. The SWAN-1D wave height prediction are lower than the UNIBEST-TC prediction, but according to the SWAN-1D predictions the wave height grows during the entire time, while the wave height predicted by UNIBEST-TC starts with a small decrease before it starts to increase.

Whether SWAN-1D or UNIBEST-TC predicts the proper wave growth cannot be answered. However the small decrease predicted by UNIBEST-TC should be further investigated in order to accept the UNIBEST-TC output.

The averaged difference in computed wave height is shown in Figure A12.4. Whenever the difference is negative the waves computed by SWAN-1D are lower than the waves computed by UNIBEST-TC. The following equation is used to determine the difference:

$$H_{DIFFERENCE} = \frac{(H_{SWAN} - H_{UNIBEST})}{H_{UNIBEST}} \cdot 100\% \qquad \text{(A12.1)}$$

The differences for four time steps have been incorporated (t=0, 1, 2 and 10). The maximum averaged difference in computed wave height is about 23%.

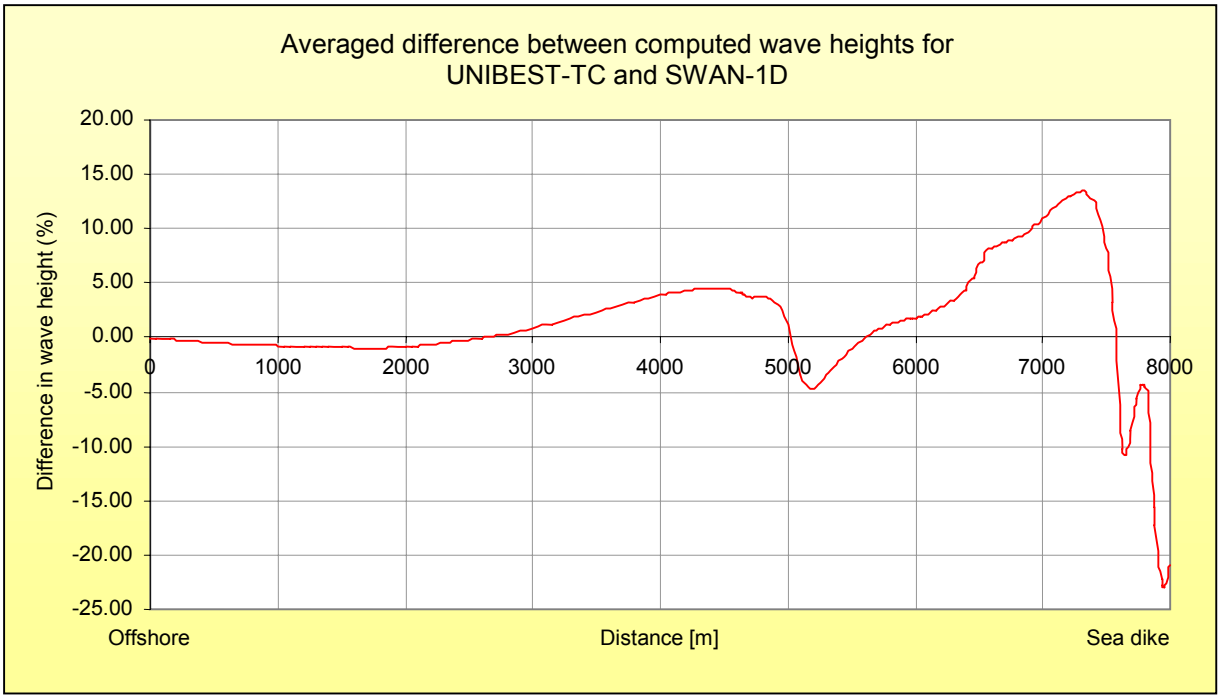

Figure A12.4: Averaged difference between SWAN-1D and UNIBEST-TC predictions over the profile stretch.

Whenever the breaker index relation has been changed into a constant relation of 0.73 (Battjes-Janssen) instead of the dependent relation (Battjes-Stive), the wave height predictions are more alike. The simulation can even be further improved by reducing the bed friction in UNIBEST-TC. However, the small wave reduction at the beginning of the simulation still stands. These alterations are shown in the next section.

SWAN-1D versus UNIBEST-TC with an equal breaker index

It appeared that the default breaker formulation in UNIBEST-TC differs from the SWAN-1D formulation. In SWAN-1D a constant wave height of 0.73 is applied and in the following simulation this is also done for the UNIBEST-TC simulation. The results are shown in Figure A12.4. As can be seen the results for SWAN-1D and UNIBEST-TC show more resemblance if an equal breaker index has been used. In the final part both wave heights are almost equal, while on deeper water before the breaker bar the difference increases.

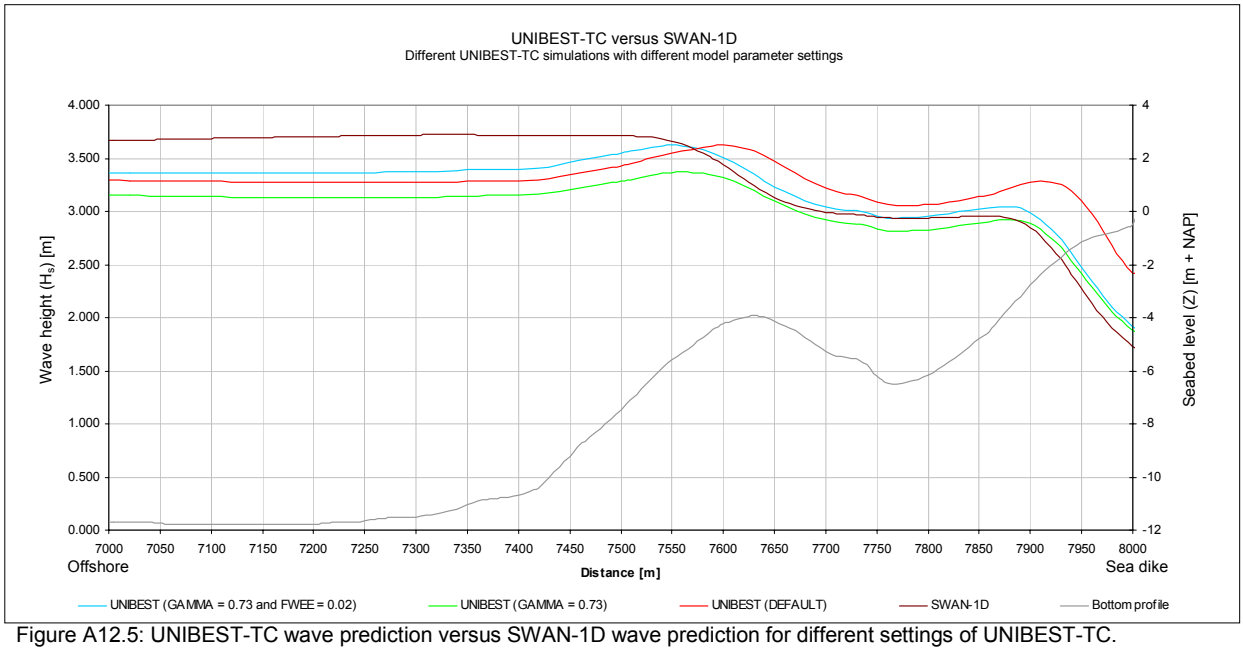

Figure A12.5: UNIBEST-TC wave prediction versus SWAN-1D wave prediction for different settings of UNIBEST-TC.

Furthermore, the bottom friction has been increased (FWEE) has been doubled to 0.02. As can be in Figure A12.5 the result is a wave propagation that approaches the SWAN-1D prediction even more. However, Figure A12.6 shows the wave height prediction by UNIBEST-TC for a constant breaker index and it still shows a small decrease at the start of the simulation.

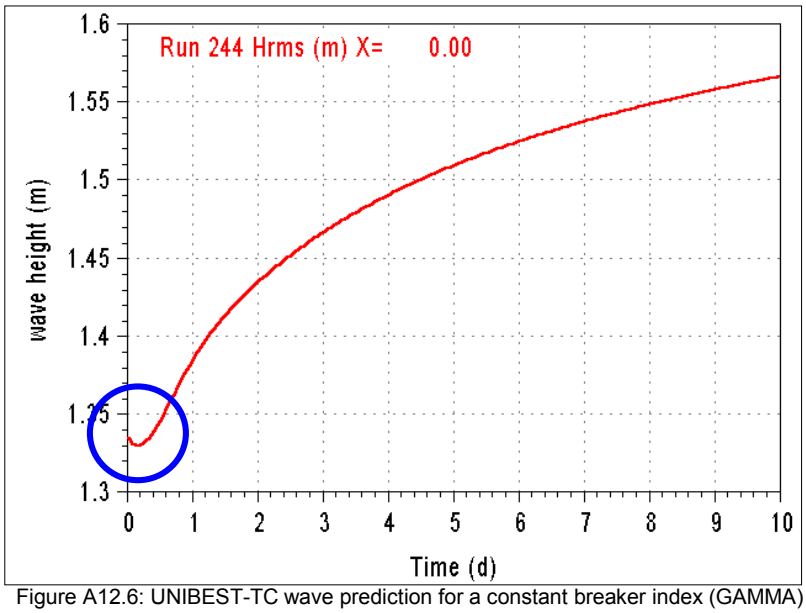

Figure A12.6: UNIBEST-TC wave prediction for a constant breaker index (GAMMA) of 0.73 over period of 10 days.

Appendix 13: Non-dynamic UNIBEST-TC analysis

General

This appendix focuses on wave propagation over different seabed profiles. Especially the influence of offshore bars and the effect of the nearshore shallow area on wave height in front of the sea defence (local wave height) have been evaluated. During this analysis only non-dynamic UNIBEST-TC runs are used. Seabed changes are not taken into account. During the analysis optimal setting for UNIBEST-TC model parameter are used according to the calibration results (Appendix 11).

Most of all, the effect of seabed height on the computed wave height at the toe of the sea defence (X=0) has been examined. The hydrodynamic boundary conditions wave height, wave period and water level have been kept constant during each run; just the seabed outlines have been varied. Three main aspects have been examined:

- The effect of the overall seabed height on the wave propagation.
- The effect of the breaker bank/bar height on the wave propagation.
- The effect of the nearshore area height (0 to 150m) on the wave propagation.

Finally, some hydrodynamic boundaries that have been kept constant have also been varied:

- Wave peak period.
- Wave height in combination with water level, seabed characteristics probably have more effect on wave propagation in low water depths. This has been examined along with the effect of breaker bars.

Effect of overall seabed height

First of all effects of the overall seabed height on the computed wave height at the sea defence have been examined. The profile surveyed in October 1999 has been used as initial profile. Three runs are compared. During all runs the following constant wave boundaries have been used:

H_{rms} = 5.00m.
T_p = 11.32s.
h_0 = NAP +5.00m.

The seabed level has been varied over the entire stretch with 50cm in height. In Figure A13.2 the results of these runs are shown. The following runs are shown:

- Run 400: initial seabed profile.
- Run 401: initial seabed profile minus 50cm.
- Run 403: initial seabed profile plus 50cm.

According to Figure A13.2 an increase of 50cm in seabed level results in a decrease in wave height (H_{rms}) of 6 to 8cm in front of the Pettemer polder bank (2800m from the sea defence). This is a wave height reduction in the order of magnitude of 1.5%. After the Pettemer polder bank the wave height reduces to 12cm. Behind the breaker bar 300m offshore from the sea defence a reduction of 12.5cm has been computed. At the sea defence (X=0) a maximum reduction of 16cm has been found.

Table A13.1: Effect of 0.5m seabed increase on the wave height, at different locations.

Location (x)	3500m to 3000m	2700m to 500m	400m to 100m	At the Sea dike (0m)
Wave height	4.4m	3.1m	2.88m	2.46m
Wave height decrease	0.07m	0.12m	0.13m	0.16m
Minimum water depth	16m	12m	10m	5.5m
Relative water depth reduction	3%	4%	5%	9%
Relative wave height reduction	1.5%	4%	4.5%	6.5%
Local H_{rms} / water depth ratio	0.28	0.26	0.29	0.45
ΔHrms / Δwater depth ratio	0.14	0.24	0.26	0.32

In Table A13.1 effects caused by an overall seabed increase have been shown. For a seabed decrease the results are similar in opposite direction. A 50cm seabed decrease results in a 16cm wave height increase (H_{rms}). About one third of the seabed variation results in wave height variations.

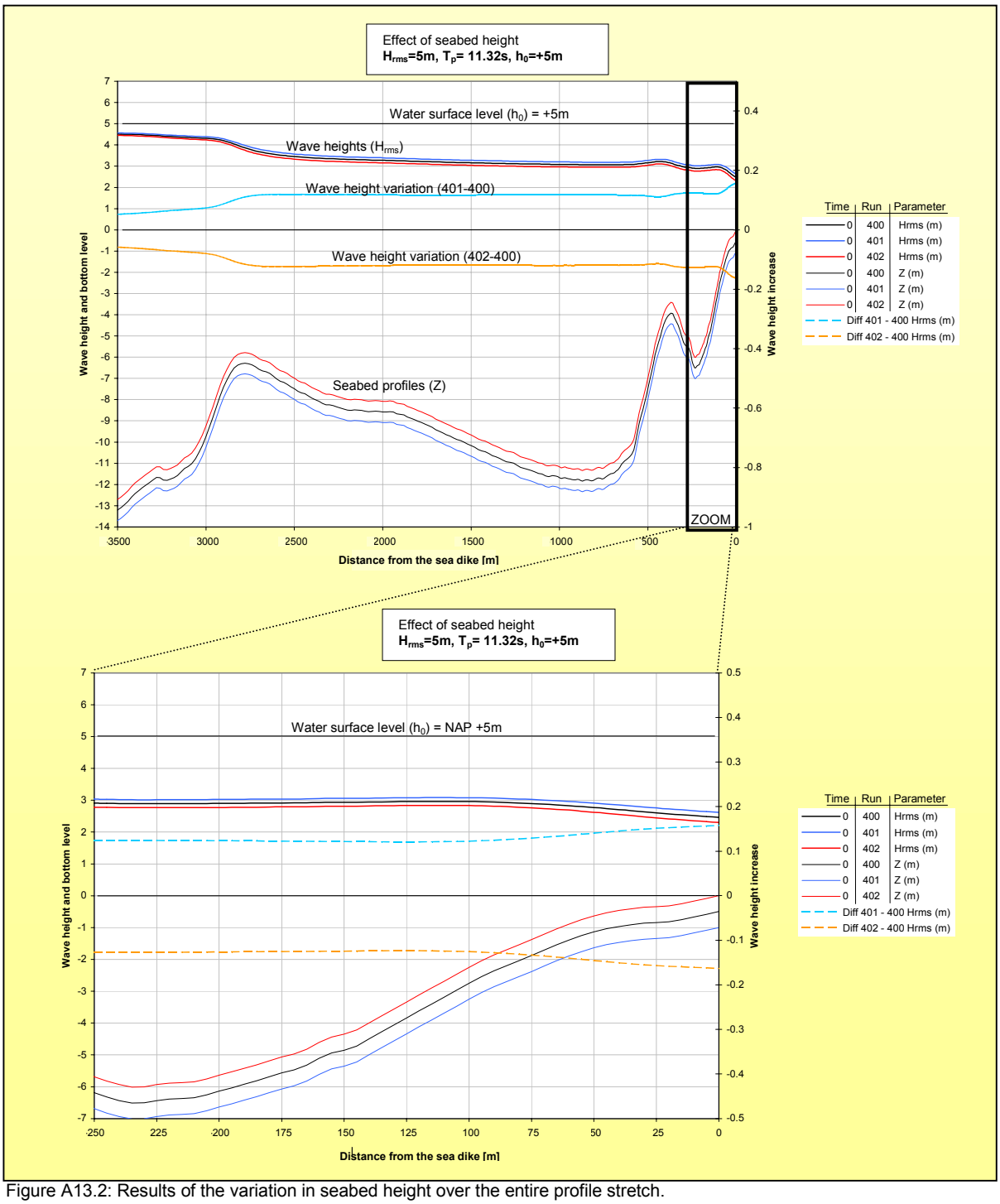

Figure A13.2: Results of the variation in seabed height over the entire profile stretch.

The relative wave height reductions as well as the relative water depth reductions are shown in Table A13.1. These are locally determined values for respectively the wave height reduction divided by the local wave height and the water depth reduction (0.5m) divided by the water depth. These relative reductions are shown because a constant increase or decrease in seabed height of 0.5m obviously has more effect on the wave height in shallow water (5.5m) than in deep water (16m). According to the results in Table A13.1 an increase in relative water depth also follows by an increase in relative wave height. This is probably due to the fact that variations have more effect in shallow water.

Finally the wave height water depth ratio is examined. This ratio is referred to as the relative wave height. During the runs a breaker index (GAMMA) of 0.771 has been used. Gamma represents the maximum wave height water depth ratio.

As can been seen in Table A13.1 the ratio between H_{rms} and the water depth meets the breaker index value. The ratio varies between 0.26 for deep and 0.45 for shallow water. These values are similar to the breaker index values for root-mean-square waves (γ_{rms}) that vary in the range of 0.35 and 0.43 [Appendix 8]. A wave height water depth ratio has also been determined for the effect of solely seabed increase (Table A13.1). This wave height water depth ratio of solely the seabed increase never meets the local ratio. Both wave height water depth ratios would have been practically equal when a straight seabed had been used. However, on account of the irregular seabed profile the wave heights are also affected by previously computed (further offshore) wave heights instead of solely by local conditions.

In a region with steep seaward facing slopes (1:100 - 1:10) the wave height water depth ratio will increase. Waves cannot adapt as quickly as the seabed profile changes.

Effect of the breaker bars on the wave propagation

This part of the analysis focuses on the affect of the breaker bar crest heights on the computed wave height at the sea defence (x=0). The seabed is characterised by two bars:

- The Pettemer polder bank (x=2800).
- The breaker bar (x=300).

During this analysis the breaker bar crests are varied in height. In Table A13.3 these variations are shown. The same hydrodynamic boundary conditions are used as in the previous section. In Figure A13.6 the results of the different runs have been shown.

Table A13.3: Breaker bar crest variations.

Run ID	Difference Pettemer polder bank ($Z_{pettemer\ polder}$)	Difference breaker bar ($Z_{breaker\ bar}$)
400	0.0m	0.0m
410	-2.0m	-1.0m
411	-1.0m	-1.0m
412	-1.0m	0.0m
413	+1.0m	0.0m
414	+1.0m	+1.0m
415	+2.0m	+1.0m
416	0.0m	-1.0m
417	0.0m	+1.0m

Figure A13.4 shows the bar crest variation effects on the computed wave height. Nevertheless, the effect is rather small, in the order of magnitude of several centimetres on a wave height of 2.46m resulting in a variation of about 4%. Another aspect is the effect of each breaker bar individually on the computed wave height. The variation at the Pettemer polder (situated 2800m from the sea defence) appear to have less affect on the computed wave height at the sea defence (x=0) compared to variations at the breaker bar (situated at 300m from the sea defence). This can be seen in Figure A13.4.

Two possible explanations can be given. First of all, the 'Pettemer polder' bank is located further offshore decreasing its effect due to distance. Secondly, the 'Pettemer polder' bank is located in deeper water. As has been explained; a variation of 50cm in water depth has less effect in deep water than in shallow water.

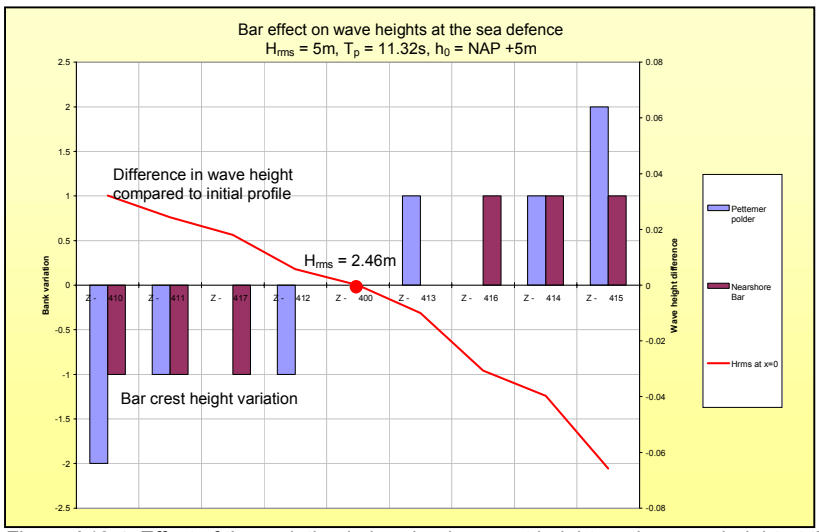

Figure A13.4: Effect of the variation in breaker bar crest height on the wave height at the sea defence.

The variations in wave height at the sea defence due to variations in breaker bar crest height are small, in the order of magnitude of 10cm. However, in Figure A13.6 it can be seen that at a distance of 250m from the sea defence the variation in wave height is 5 times larger about 50cm or (17% of H_{rms} =2.91m). Consequently, the area in front of the sea defence reduces this effect with a factor 5. Therefore it can be concluded that the height of the nearshore area is dominant for the wave height computed at the sea defence.

Executing additional runs with different wave height and water level specifications can check whether the nearshore area dominance is universal. However, only a brief check has been done. It is expected that the effect of bars will increase during more shallow water depths. Therefore, the water level has been reduced in the next set of runs. In order to keep the situation realistic the wave height as well as the wave period have been reduced while the seabed is kept constant (Table A13.3). The hydrodynamic boundary conditions are as follows:

H_{rms} = 3.00m.
T_p = 8.77s.
h_0 = NAP +1.00m.

The results are shown in Figure A13.5 and A13.7. As can be seen, the dominant position of the nearshore area has increased. The variation in wave height has reduced to 0.02m on a wave height of 0.83m; this results in a variation of 2.5%. The wave height variation at 250m offshore from the sea defence due to bar variation is about 50cm for wave heights of 1.65m. In front of the nearshore area the bar effect has been increased to 30% (50cm on H_{rms} of 1.65m) instead of 17%.

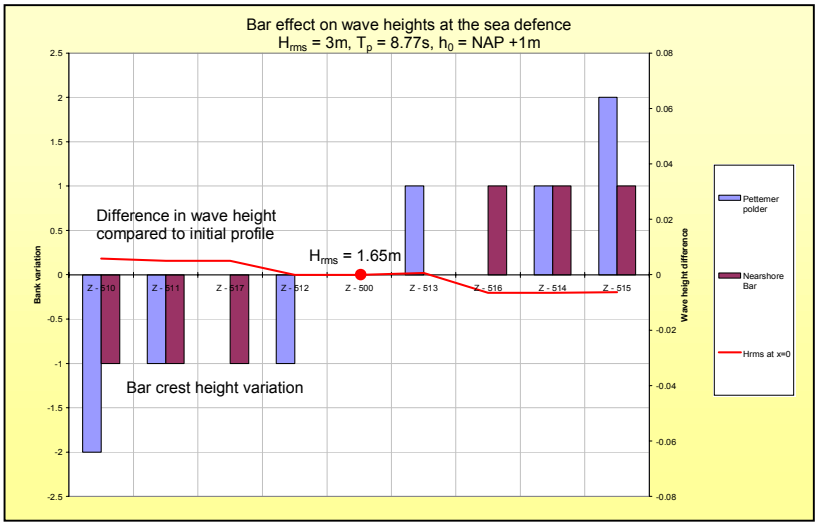

Figure A13.5: Effect of the variation in breaker bank height on the wave height at the sea defence.

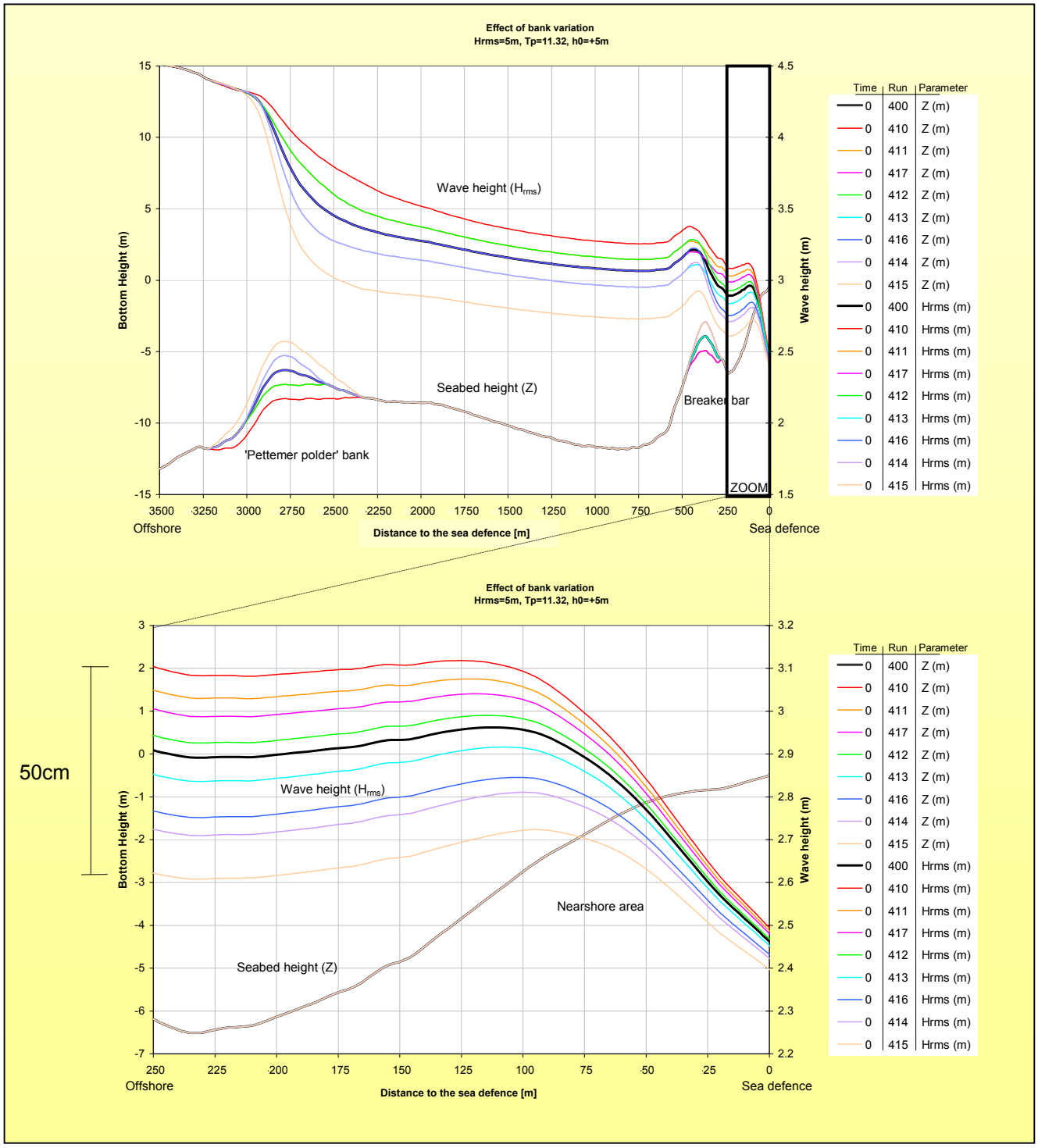

Figure A13.6: Results of breaker bar variations on the wave propagation, the run ID numbers are explained in table A13.3.

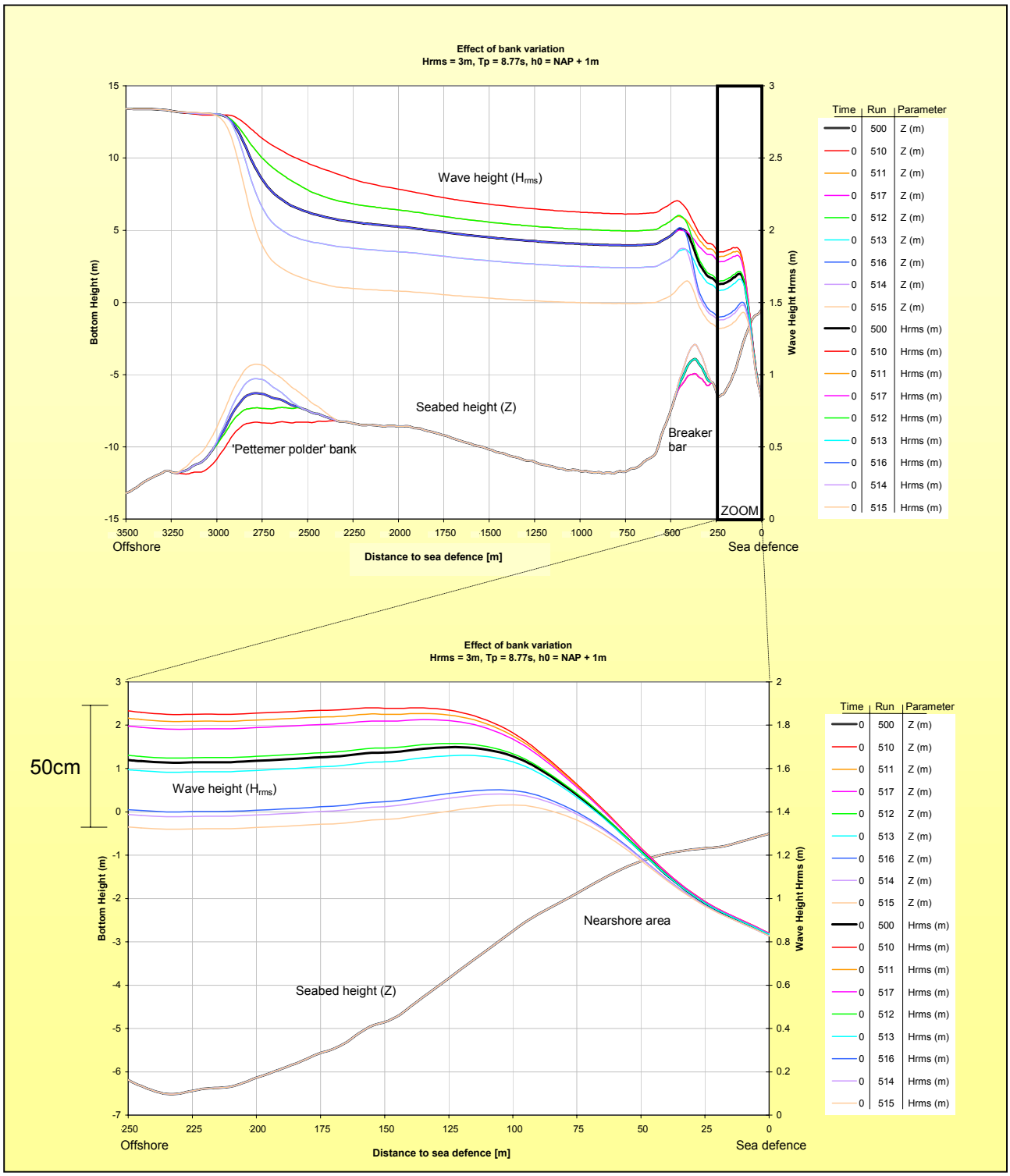

Figure A13.7: Results of breaker bar variations on the wave propagation, the run ID numbers (500 to 517) have the same characteristics as the runs that are shown in table A13.3.

Effect of the nearshore area

During the previous analysis, it has been found that the nearshore area is probably dominant for the wave height computed at the sea defence. The effects of alterations in the nearshore area height are examined during similar hydrodynamic boundary conditions as has been used before:

H_{rms} = 5.00m
T_p = 11.32s
h_0 = NAP +5.00m

The seabed profile has been kept similar to the initial profile that has been surveyed in October 1999. Only the nearshore area has been altered up to 150m from the sea defence. The following runs have been made:

- Run 400: Initial seabed profile (reference).
- Run 450: Initial seabed profile minus 2m.
- Run 451: Initial seabed profile minus 1m.
- Run 452: Initial seabed profile plus 1m.

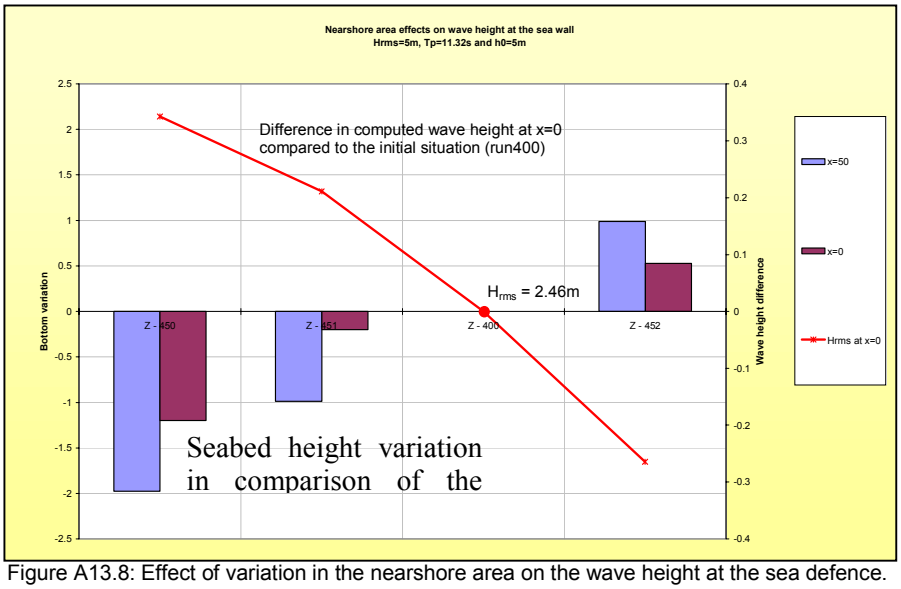

Figure A13.8: Effect of variation in the nearshore area on the wave height at the sea defence.

The results are shown in Figures A13.8 and A13.10. The nearshore area is indeed dominant, variations of a few meters in seabed height result in wave height variations of 30cm. Furthermore, a seabed increase of one meter has more effect on the wave height than a seabed decrease of one meter. Higher seabed levels or more shallow water results in more wave dissipation. As can be seen the relation is non-linear, but slightly curved. Probably due to the fact that the seabed profile with the highest levels differ most from the 'equilibrium' profile

Due to the variation of the nearshore area height the breaker index (γ_{rms}) stays practically constant, as can be seen in the final column of Figure A13.9. In this Figure the parameters are shown at the sea defence, however, shoreward variations also affect the computed wave heights. This explains why the variation in breaker index ($\Delta\gamma_{rms}$) is able to increase with 0.84 instead of a value in the order of magnitude of 0.35 and 0.45.

Table A13.9: Effect of seabed height variation in the nearshore area on the breaker index (γ_{rms}).

Seabed variation $\Delta Z_{(X=0)}$	Wave height variation $\Delta H_{rms;\,(X=0)}$	Breaker index due to variation $\Delta\gamma_{rms} = \Delta H_{rms} / \Delta Z$	Water depth $d_{(X=0)}$	Wave height $H_{rms;}$ $_{(X=0)}$	Breaker index γ_{rms}
-1.25m	+0.34	0.27	6.90m	2.80m	0.41
-0.25m	+0.21	0.84	5.90m	2.68m	0.45
+0.50m	-0.26	0.52	5.20m	2.20m	0.42

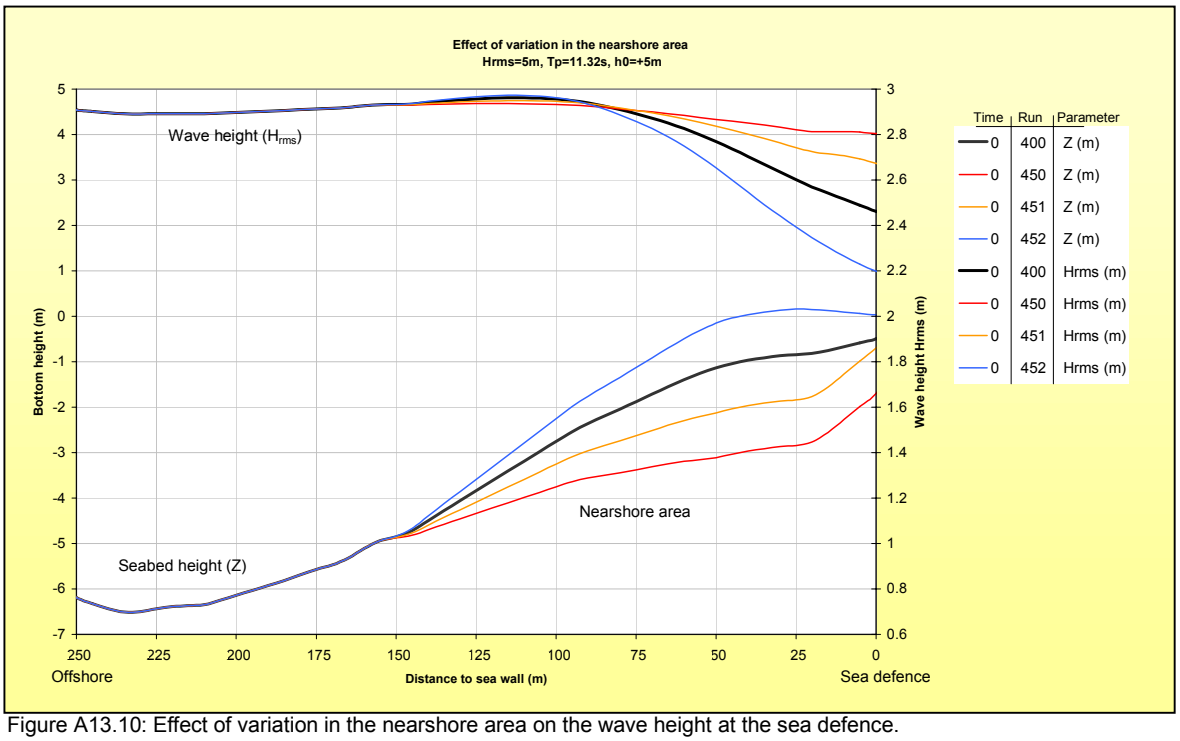

Figure A13.10: Effect of variation in the nearshore area on the wave height at the sea defence.

In Figure A13.10 it can be seen that between the 100 and 150m in front of the sea defence an increase in seabed level results in an increase in wave height. This is due to shoaling. If the water depth decreases waves become steeper and grow a few centimetres in height, before they break and loose height.

Effect of the wave period

The wave period as well as the wave height is a held constant during all previous runs. The wave peak period (T_p) has been related to the wave height due to a constant deep-water steepness (s_0). During the following runs the deep-water wave steepness has been varied between 0.01 and 0.04 with an interval of 0.01. If the wave height (H_{rms}) is maintained constant variations in wave steepness results in variations in peak wave period (T_p). Below, the equation for deep-water wave steepness is shown. The parameter (g) is the gravitation constant equal to 9.81. Table A13.11 shows the different runs including the run parameters.

$$s_0 = \frac{H_{rms,0}}{L_0} = \frac{H_{rms,0}}{\frac{g}{2\pi} T_p^2} \qquad \text{(A13.1)}$$

s_0	= Deep-water wave steepness	[-]
H_{rms}	= Root-mean-square wave height at deep-water	[m]
L_0	= Wavelength at deep water	[m]
T_p	= Peak wave period at deep-water	[s^{-1}]
g	= Gravitation constant (9.81)	[m s^{-2}]

Whenever, the wave steepness has been altered and the default value for the breaker index (GAMMA) has been chosen. The wave steepness affects the breaker index according to the following equation [BATTJES - STIVE, 1985):

$$GAMMA = \gamma = 0.5 + 0.4\tanh(33 s_0) \qquad \text{(A13.2)}$$

Furthermore, the wave period combined with the relative wave period (T_{DRY}) determines the minimum water depth for calculations purposes. UNIBEST-TC aborts its calculations when the minimum water depth (H_{MIN}) has been reached. From that point forward calculated sediment transport quantities are divided over the remaining profile. Consequently, these sediment transport quantities are not based on physical relations and the results have to be interpreted with caution. The minimum water depth for calculation purposes has been calculated according to the following equation:

$$H_{MIN} = g\left(\frac{T_p}{T_{DRY}}\right)^2 \qquad \text{(A13.3)}$$

Whenever, the water level at the sea defence (x=0) exceeds the minimum water depth the run results are trustworthy. During the runs shown in Table A13.11 a water depth that includes setup at the beginning of the sea defence (x=0) of about 5.5m has been computed. The calculations are interrupted at locations where the depths varies between the 1.36m and 2.73m, as can be seen in Table A13.11.

Table A13.11: Simulation characteristics off the used to determine the effect of the wave period.

	Hydrodynamic boundary conditions				UNIBEST-TC parameter		
Run ID	Water level (h_0)	Wave height (H_{rms})	Wave steepness (s_0)	Wave peak period (T_p)	Breaker index (GAMMA)	Minimum water depth (H_{MIN})	Relative wave period (T_{dry})
400	5.00m	+5.00m	0.025	11.32s	0.771	2.18m	24
460	5.00m	+5.00m	0.010	17.90s	0.627	1.96m	40
461	5.00m	+5.00m	0.020	12.66s	0.731	2.73m	24
462	5.00m	+5.00m	0.030	10.33s	0.803	1.82m	24
463	5.00m	+5.00m	0.040	8.95s	0.847	1.36m	24
470	5.00m	+5.00m	0.010	17.90s	0.771	1.96m	40
471	5.00m	+5.00m	0.020	12.66s	0.771	2.73m	24
472	5.00m	+5.00m	0.030	10.33s	0.771	1.82m	24
473	5.00m	+5.00m	0.040	8.95s	0.771	1.36m	24

During the first set of runs (460-463) the breaker parameter (γ) varies according to the previous equation [#A13.2]. The results are shown in Figure A13.12. Waves with a wave steepness of 0.01 or 0.04 result in a lower wave height at the sea defence compared to waves with a steepness that lies between 0.02 and 0.03. Due to the steepness dependency of the breaker parameter the wave height propagation has been manipulated. However, it appears low and high values of wave steepness respectively 0.010 and 0.040 dissipate more energy along the profile. It is possible that the steepness for these waves lies outside the UNIBEST-TC prediction range. (D.J. Walstra)

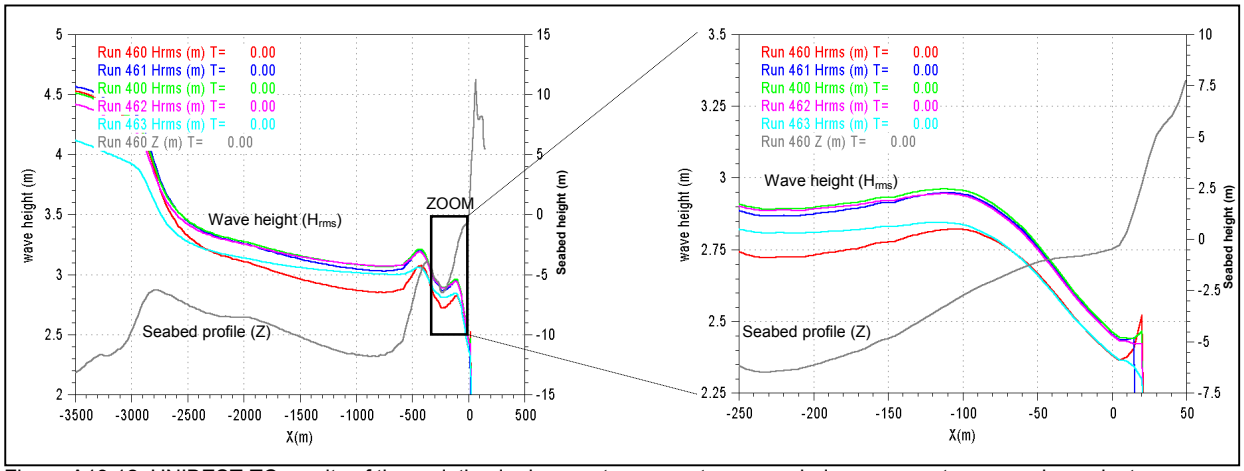

Figure A13.12: UNIBEST-TC results of the variation in deep-water wave steepness during a wave steepness dependent breaker index (GAMMA).

Constant Gamma parameter

To show the sole effect of the wave period variation, a constant breaker index of 0.771 has been used during the next set of runs (470-473). The results are shown in Figure A13.13.

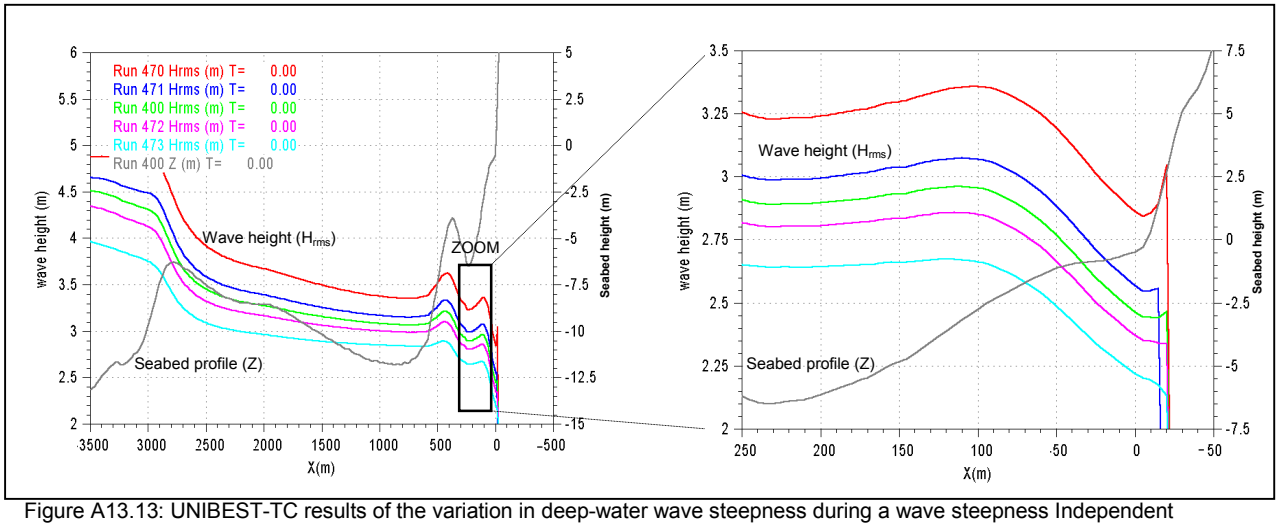

Figure A13.13: UNIBEST-TC results of the variation in deep-water wave steepness during a wave steepness Independent breaker index (GAMMA).

According to these results, waves with a steepness of 0.01 result in a wave height at the sea defence of 2.85m, while waves with a steepness of 0.04 result in a wave height at the sea defence of 2.20m. A difference of 65cm in wave height solely due to a difference in wave period can be achieved. Long waves (waves with a high wave periods) loose less energy compared to short waves. Figure A13.14 shows the energy level of waves over the profile and long waves (run 470) appear to dissipate less energy.

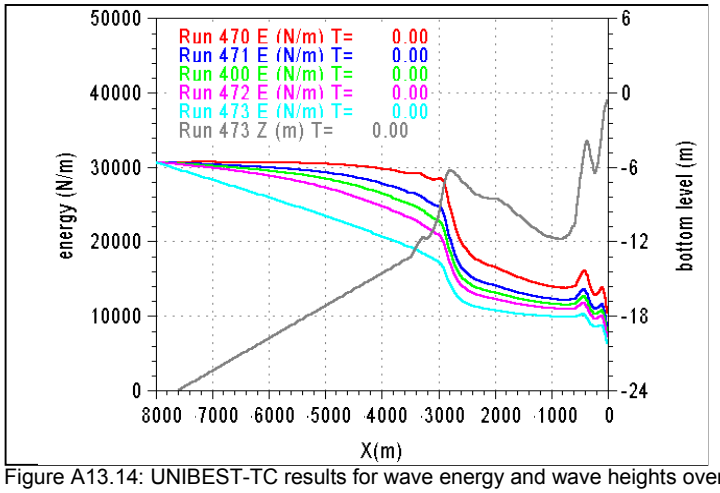

Figure A13.14: UNIBEST-TC results for wave energy and wave heights over the profile, for different wavelengths and constant wave heights at (x=8000m).

$$E = \frac{1}{8}\rho g H_{rms}^2 \qquad \text{(A13.4)}$$

The energy level (E) equals the square of the wave height (H_{rms}) multiplied by the water density (ρ) and the gravitation constant (g). The first part of the profile (between 3500m and 8000m) varies in water depth from –30m to –25m (including setup). Most of the difference in wave height has been achieved in this first part. The difference in computed wave heights and energy level can only be explained by dissipation, because no energy can been added along the run. Energy dissipation in UNIBEST-TC is solely dependent on bottom friction and wave breaking. In the following Figure (A13.15) the energy dissipation processes friction and breaking are shown.

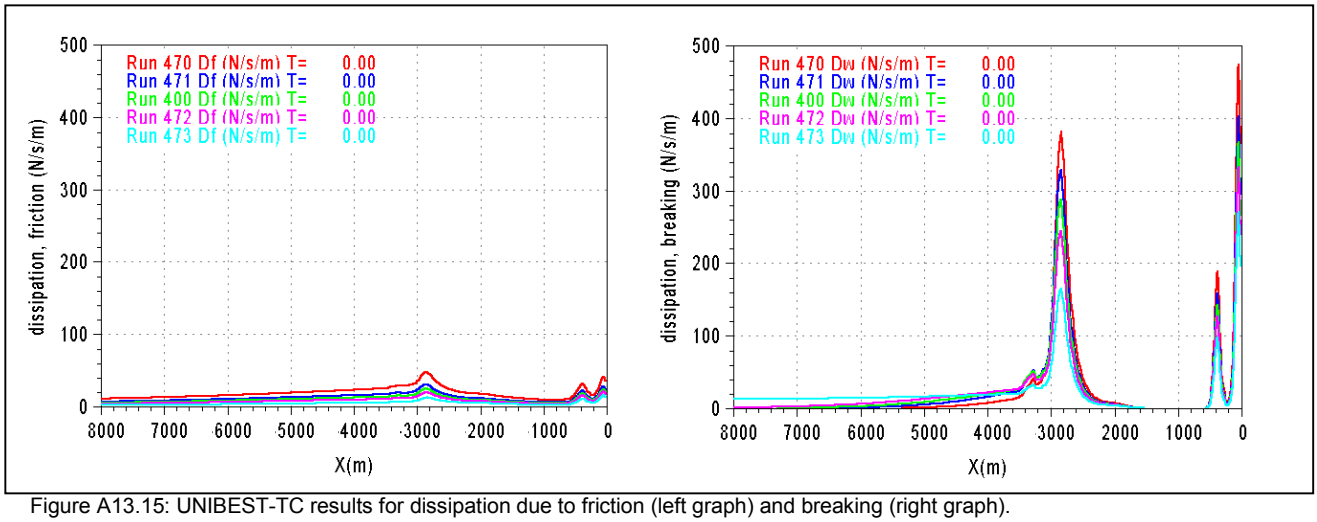

Figure A13.15: UNIBEST-TC results for dissipation due to friction (left graph) and breaking (right graph).

Long waves (run 470) loose most energy due to friction compared to short waves. During breaking long waves also dissipate more energy especially at breaker bars. However, on deep-water up to 3500m short waves (run 473) have more energy dissipation due to wave breaking. Wave breaking on deep water is solely caused by steep waves that become unstable. The long profile stretch (8km) that has been used during the runs in responsible for the fact that wave breaking on deep-water has become relatively important. This is the reason that long waves have higher energy levels at the sea defence, whereas more friction dissipation and more wave breaking dissipation at bars have been found.

The difference of 65cm due to a different wavelength becomes questionable, because the difference is the obtained during the first kilometres, where the seabed profile has been assumed. During the latter part of the profile (from 0 to 3500m) long waves encounter more dissipation. During normal conditions it is expected that long waves (high peak period) will have smaller wave heights at the sea defence than shallow waves do.

If wave period effects appear to be of significant importance, it is recommended to use a smaller profile stretch. However, a small profile stretch can also result in unrealistic sediment transport at the most offshore boundary due to wave breaking. A water depth of at least 2 times the wave height is recommended.

Appendix 14: UNIBEST-TC constant dynamic simulations

General

This appendix deals with the effects of the predicted storm-erosion by UNIBEST-TC as well as the accompanying wave height variations. The results are used in Paragraph 5.5. During this appendix the sensitivity and the effect of deep-water wave heights and water levels on the local erosion degree and local wave height at the toe of the sea defence has been examined.

Input

During this analysis the following 30 dynamic simulations have been examined. A dynamic simulation means that morphological alterations have been taken into account. However the boundary conditions have been kept constant during the entire simulation time. In the following matrix (Table A14.1) the combination of hydrodynamic boundary conditions have been shown. These simulations make it possible to examine the effect of wave height variation and water level variation.

Table A14.1: UNIBEST-TC run matrix for the constant boundary conditions.

	h_0 = 0m + NAP	h_0 = 1m + NAP	h_0 = 2m + NAP	h_0 = 3m + NAP	h_0 = 4m + NAP	h_0 = 5m + NAP
H_{rms} = 1m T_p = 5.06s	500	501	502	503	504	505
H_{rms} = 2m T_p = 7.16s	506	507	508	509	510	511
H_{rms} = 3m T_p = 8.77s	512	513	514	515	516	517
H_{rms} = 4m T_p = 10.13s	518	519	520	521	522	523
H_{rms} = 5m T_p = 11.32s	524	525	526	527	528	529

During these simulations a constant deep-water wave steepness has been used (s_0=0.025). A constant wave steepness results a wave period (T_p) that is dependent of the wave height (H_{rms}). In Table A14.2 the settings of the UNIBEST-TC model parameters have been shown. During these simulations the optimal settings according to the calibration are used. Accept for the T_{DRY} parameter that is used to determine the minimum water depth. It is necessary to vary the T_{DRY} parameter because of the wide range of possible hydrodynamic conditions that will be compared during this analysis. Whenever this minimum water is reached the calculation is aborted. The variation at the sea defence is of most interest and therefore the calculations have to be able to reach this point.

The T_{DRY} parameter varies in the range of 24 and 40. The value depends on the wave peak period (T_p) as well as the water depth at the location of the sea defence ($h_{seadefence}$). The following equation has been used to determine the acquired value:

$$T_{DRY} = \sqrt{\frac{g}{h_{seadefence}}} T_p \qquad \text{(A14.1)}$$

The water level at the sea defence is dependent on the water level and the water depth. During the simulations the water level varies between 0 and 5m + NAP. During simulations with low water depths and relatively high waves heights high T_{DRY} values are required.

The simulation time is 10 days. During some simulation severe conditions are simulated. In reality it is not likely that these conditions will continue over a period of 10 days. However, the simulations are executed to show the morphological effect of a long period of constant hydrodynamic conditions.

A time step of half an hour has been used. The minimum grid size is 10m. During the sensitivity analysis the grid size and time step have been varied. This comparison is shown at the end of this Appendix. It appears that the mentioned grid size and time step result in the most favourable situation taking into account number of errors.

Table A14.2: Parameter settings of UNIBEST-TC during the examined simulation runs.

GRID			GENERAL		WAVES		SEDIMENT		TRANSPORT	
PARAMETER	VALUE		PARAMETER	VALUE	PARAMETER	VALUE	PARAMETER	VALUE	PARAMETER	VALUE
START	-8000		DT	0.020834	ALFAC	1	D50	$2.0*10^{-4}$	IBOD	YES
END	+150		NT	480	GAMMA	0	D90	$3.0*10^{-4}$	RC	$1.0*10^{-2}$
	#	ΔX	TIME_ST	0	BETD	0.1	DSS	$1.7*10^{-4}$	RW	$2.0*10^{-3}$
REGIO 1	90	50	USTRA	0	FWEE	0.01	DVAR	NO	REMLG	0.1
REGIO 2	20	20	JFR	1	C_R	0.25	FDIA0		TANPH1	0.1
REGIO 3	20	20	**TDRY***	VARIABLE	K_IJL	OFF	FDIA1		TANPH2	0.1
REGIO 4	110	20	TE_W	10	F_LAM		FDIA2		XF1	500
REGIO 5	65	10	SALIN	0	POW		HDIA0		XF2	1200
REGIO 6					DEEP_V		HDIA1		ZDRY	HOR
REGIO 7					SHALL_V		HDIA2		FACQB	0

BOUNDARY CONDITION	SEABED PROFILE	FIXED PROFILE	TIDE ELEVATION	TIDE VELOCITY	WAVE ANGLE	WAVE HEIGHT	PEAK PERIOD	WIND VELOCITY	WIND DIRECTION
CONSTANT			VARIABLE	0	0	VAR	VAR	0	0
991020 FROM –8000 TO 150	YES	YES							

* T_{DRY} has been made variable (24 – 40), because the boundary conditions are to far apart to acquire proper results with just one parameter value.

During the simulations the modified seabed surveyed at October 1999 has been used. This seabed is shown in the following Figure A14.3. A fixed layer has been applied to simulate the sea defence. Sediment transports that are calculated by UNIBEST-TC at the location of the fixed layer cannot be reached, because no sediment is provided. Furthermore, the profile consists both bars. However, a sand bar simulates the Pettemer polder bar whereas the bar is probably more cohesive. Consequently, UNIBEST-TC predicts a decrease in height of the Pettemer polder in such a magnitude that it is not likely to occur in reality.

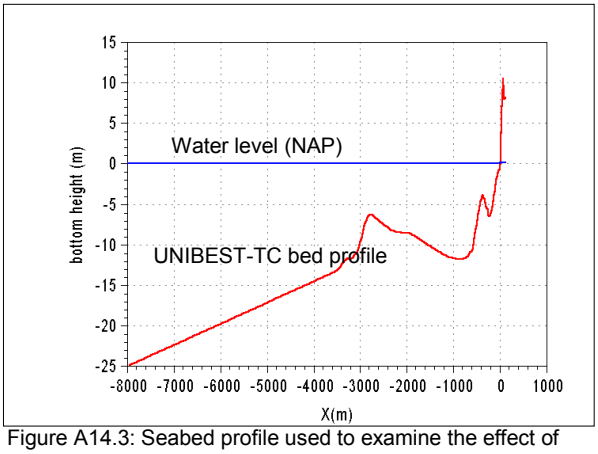

Figure A14.3: Seabed profile used to examine the effect of water level and wave height in UNIBEST-TC.

Simulation results

The evaluation of the effects of wave height variation and water level variation are done for one single point at the toe of the sea defence (X=0). The reaction at this location can be different from other points along the profile. However, this point is of special interest, because during the probabilistic analysis the results for this point are used.

UNIBEST-TC results

The following 12 graphs (Figure A14.4) show seabed levels and wave heights at location x=0. The lines in each graph represent a different simulation with a different deep-water wave height and accompanying wave period. The following combinations of wave heights and wave periods are examined:

- H_{rms} = 1m; T_p = 5.06s;
- H_{rms} = 2m; T_p = 7.16s;
- H_{rms} = 3m; T_p = 8.77s;
- H_{rms} = 4m; T_p = 10.13s;
- H_{rms} = 5m; T_p = 11.32s;

The simulations with a similar water level are combined in each graph. The upper graph of a set of two graphs shows the wave height at location x=0 for five different deep-water wave heights during the simulation time of 10 days. The lower graph shows the evolution of the bed level at location x=0 during the simulation time. The coloured lines represent the effects of one single wave height.

Observations

- Run 507 was aborted and stops at 4.5 days.
- All axes are equal and the sets are arranged by water level height.
- During high water levels, waves can increase at location x=0.
- Higher deep-water waves result in higher waves at location x=0, in spite of the constant local water depth.
- The local erosion stops at a depth of –2m +NAP due the presence of the fixed layer.
- During high water levels in the range of 3m to 5m +NAP, low waves heights (H_{rms} = 1 to 2m) hardly change due to the erosion.
- The effect of water level height on erosion appears non-linear, because during situations with low wave heights sometimes more and sometimes less erosion is found.

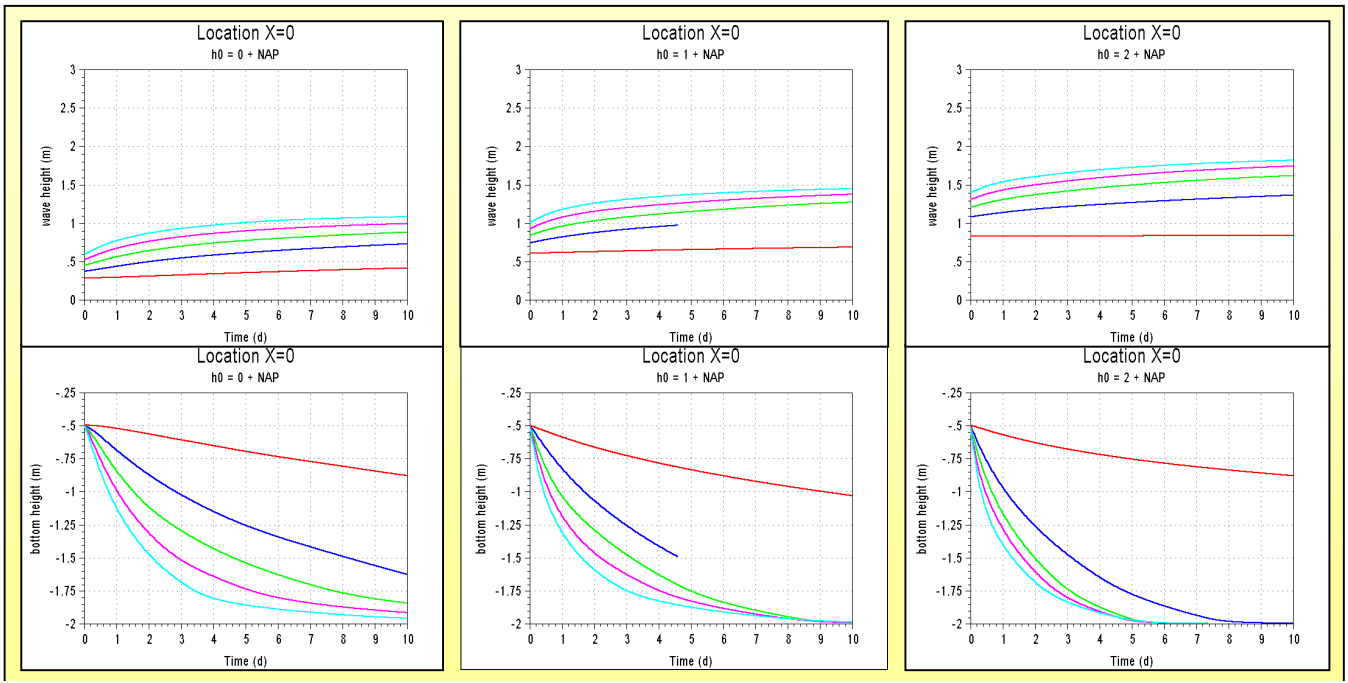

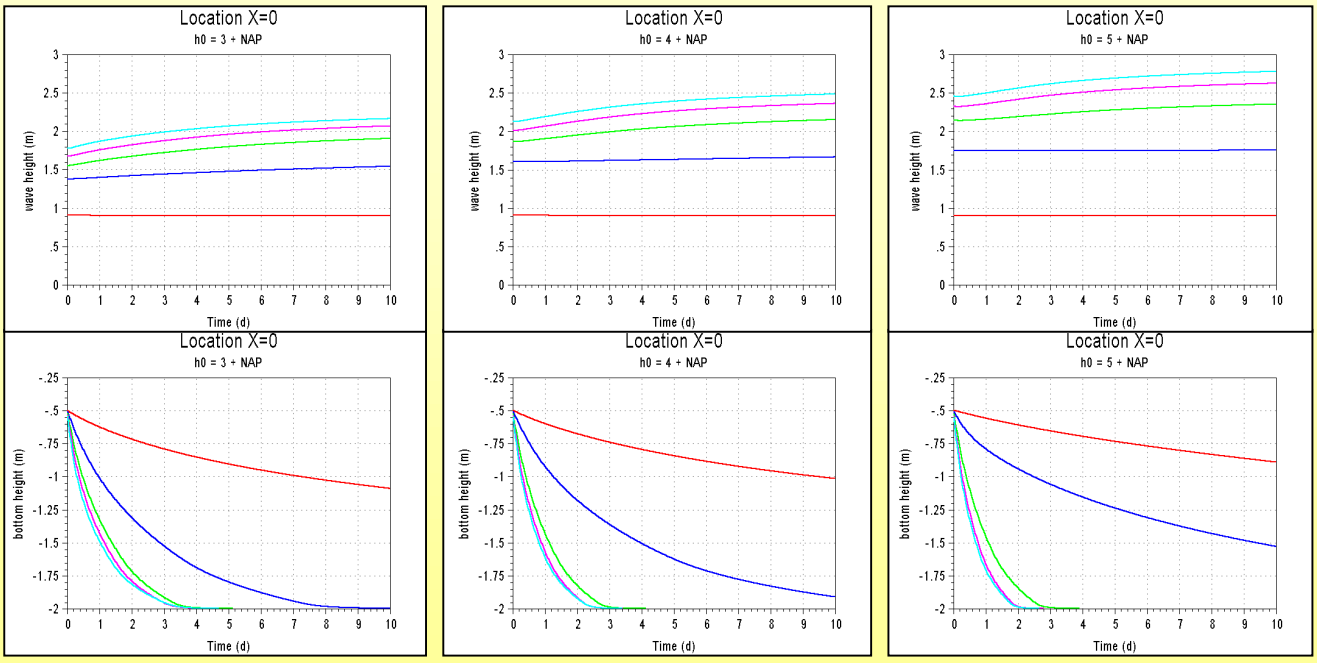

Set 4: water level = 3m + NAP | Set 5: water level = 4m + NAP | Set 6: water level = 5m + NAP

Figure A14.4: The results of the dynamic simulations with constant boundary conditions. For each simulation the bed evolution as well as the wave height evolution is shown for location (x=0) during the simulated time of 10 days.

The following legend is valid for all graphs.

- H_{rms} = 1m; T_p = 5.06s;
- H_{rms} = 2m; T_p = 7.16s;
- H_{rms} = 3m; T_p = 8.77s;
- H_{rms} = 4m; T_p = 10.13s;
- H_{rms} = 5m; T_p = 11.32s;

Combined simulation results

The results from UNIBETS-TC are combined to examine the mutual effect of both water level and deep-water wave height on local erosion and wave height growth.

Two time steps have been examined:

- T = 2 days, 48 hours.
- T = 10 days, 240 hours.

Figure A14.5 shows the combined effect of water level (x-axis) and wave height (y-axis) on the erosion depth for location x=0. The erosion depth is defined as the difference between initial seabed level and the seabed at the examined time (2 days in case of Figure A14.5). The Figure shows contour lines with an equal erosion depth. The colours in between are used to show the location of high erosion depth (purple, red) and no erosion (dark blue). The Figure is based on the output of the simulations shown in Figure A14.4. The crossing of the grid shown in this Figure represent an actual output, the lines of equal erosion height are derived by linear interpolation.

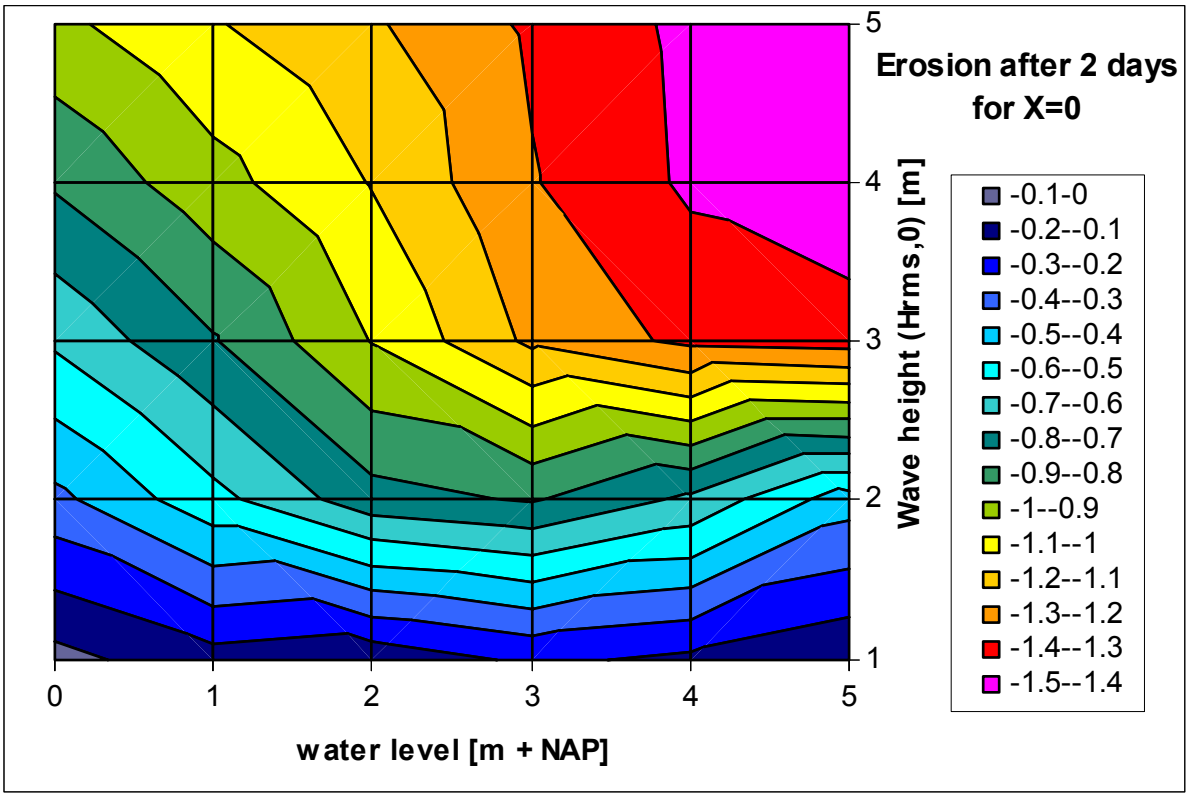

Figure A14.5: Erosion diagram for location x=0 based on the UNIBEST-TC simulations, the water level and wave height are varied along the axis.

Observation from Figure A14.5:

- Most erosion occurs during high waves accompanied by high water levels.
- Low waves practically result in no erosion, independent of the water depth.
- Variation in water depth has less effect on the local erosion depth than variations in wave height. Consequently, waves dominate the erosion process according to the UNIBEST-TC output.

Figure A14.6 shows the erosion at location x=0 after a period of 10 days. The following conclusions can be drawn:

- For almost all wave that exceed the 3m the maximum erosion depth has been reached. (the fixed layer).
- Combinations of low water levels and low wave heights as well as combinations of high water levels and high wave heights result in lower erosion depths than water levels in the range of 2 to 4m + NAP accompanied by 2m high waves.
- During low wave conditions the contours of equal erosion depth displays a zig-zag course. This zig-zag course can be related to the fact that low wave conditions can also result in accretion processes.

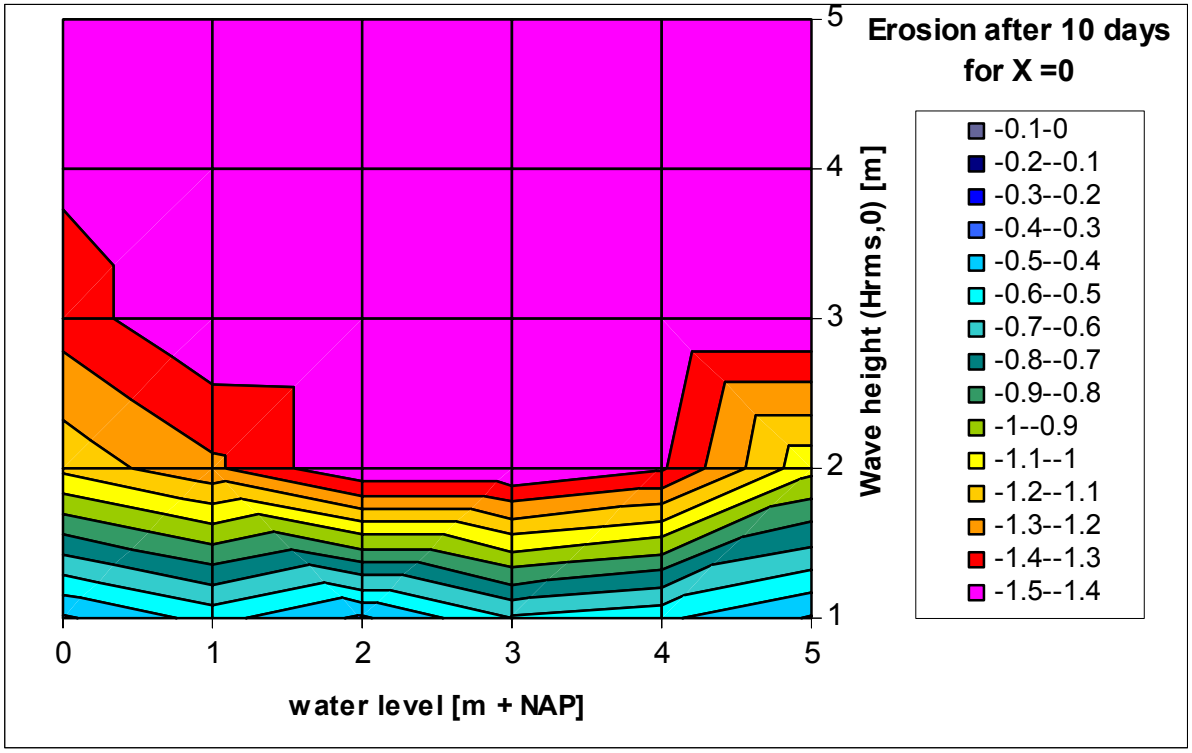

Figure A14.6: Erosion diagram for location x=0 based on the UNIBEST-TC simulations after 10 days, the water level and wave height are varied along the axis.

Another aspect of interest is the wave height growth at location x=0 due to morphological changes. Figure A14.7 shows the growth scenarios according to the UNIBEST-TC simulation.

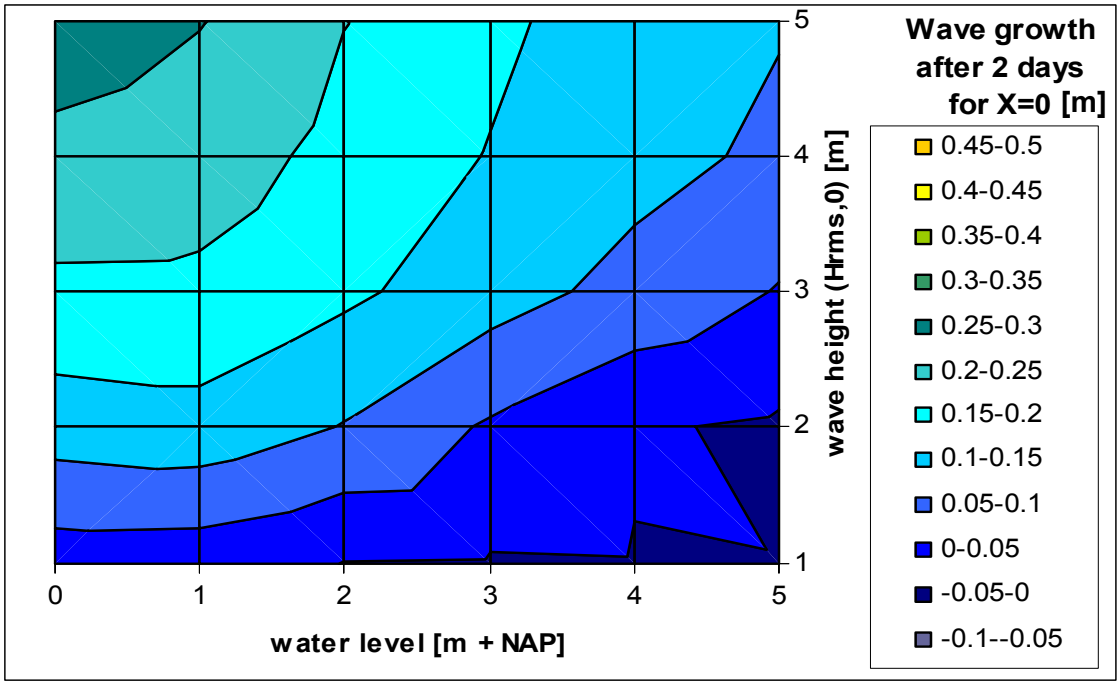

Figure A14.7: Wave height growth diagram for location x=0 based on the UNIBEST-TC simulations after 2 days, the water level and deep-water wave height are varied along the axis.

Observations Figures A14.7 and A14.8

- Maximum wave height growth occurs during low water levels and high deep-water waves
- During high water depths and low wave heights the growth contours show a strange peak. This has to do with the low grid resolution.
- Maximum wave growth happens during different conditions than maximum erosion does. However Maximum erosion does occur when maximum wave heights are present.

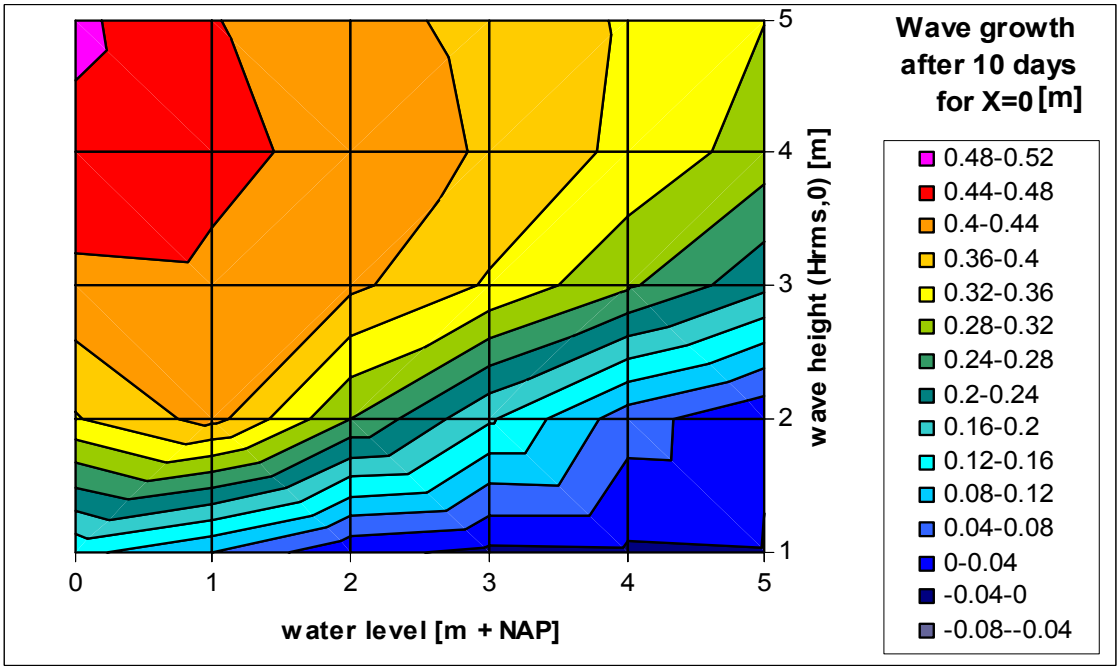

Figure A14.8: Wave height growth diagram for location x=0 based on the UNIBEST-TC simulations after 10 days, the water level and deep-water wave height are varied along the axis.

Sensitivity analysis

The sensitivity analysis compares the results of simulations with a different grid size and a different time step. A smaller grid size often results in an increase of accuracy. However, it can also result in a decrease of accuracy, especially at sea defence, in this area the sediment transport gradients are large, due to intensive wave breaking. These large gradients in sediment transport cause intensive seabed variations over the sandy profile in this area. In case of a small grid these relatively large variations result in even larger variations in seabed height. However, the sediment transport has to be divided over a smaller grid cell, consequently, larger variations can be expected.

Normally, a small grid results in a more accurate output for a part of the profile that is characterised with large variations in seabed height. However, due to the fixed layer no sediment can be stirred up, resulting in an over-capacity of possible sediment storage in the water column just in front of the sea defence. This possibility to contain additional sediment causes the large erosion quantities just in front of the sea defence.

Comparison
The two grids shown in Tables A14.9 and A14.10 are compared during two different time steps ($^1/_2$ hour and 1 hour):

A14.9: UNIBEST-TC simulation fine grid.

Number of grid cells	Grid size	Length
90	50.00	4500
120	20.00	2400
85	10.00	850
80	5.00	400
375		8150

A14.10: UNIBEST-TC simulation rough grid.

Number of grid cells	Grid size	Length
90	50.00	4500
150	20.00	3000
65	10.00	650
305		8150

The minimum grid size is used to characterise both grids. The first grid has 375 grid points and a minimum distance between two consecutive grid points of 5m at the sea defence. The second grid has 305 grid points and a minimum distance of 10 between two consecutive grid points. This comparison counts 120 simulations, 30 for each combination of grid and time step. The following Table shows the simulation settings:

A14.10: The compared simulation configurations.

Minimum Grid size [m]	Time step [hours]	Simulation ID	
		Start	End
10.00	0.020834	500	529
5.00	0.020834	600	629
5.00	0.041668	700	729
10.00	0.041668	800	829

Furthermore, all simulations have equal settings for wave height (H_{rms}) and water level (h_0). This implies that simulations with a similar run ID, like 520, 620, 720 or 820 have similar wave heights and a water levels respectively 4m and 2m + NAP.

Errors
The number of errors during a series of simulations is a reasonable good instrument to compare the performance of different settings for grid size and time step. The following Table shows the number of errors for each combination of grid size and time step. It can be seen that the 500 series corresponding with the 10m-grid size and half an hour time step has the best result. The errors show some resemblance for the series of simulations with a similar grid size. A small grid size gives an error in both cases for runs with respectively high water levels (611-711, 616-716 and 622-722). A larger grid size causes an error for both time steps during run (507-807).

A14.12: Errors that have occurred during each series of simulations.

Minimum grid size [m]	Time step [hours]	Grid size / Time step	Number of errors	Error percentage	Run ID						
10.00	0.020834	480	1	3.33%		507					
5.00	0.020834	240	5	16.67%			609	611	613	616	622
5.00	0.041668	120	3	10.00%				711		716	722
10.00	0.041668	240	2	6.67%	804	807					

The errors are probably caused by numerical instability. Whenever higher values of grid size divided by time step ($\Delta x/\Delta t$) result in fewer errors. This has to do with the numerical consistency. However a smaller time step does result in an increase of errors for a 5m grid. It appears that grid size is more important because the more errors occur whenever a small grid size has been applied, even when the ($\Delta x/\Delta t$) factor is equal. Furthermore, it is surprising that the aborted simulations during appear to occur randomly. The only explanation can be found in a different evolution of the morphology due to different grid sizes that results in unacceptable numerical conditions.

The Figures A14.13 to A14.15 show the result in wave height predictions and seabed alterations for three different scenarios:

- At location (x=0) for low water levels (0m + NAP).
- At location (x=60) offshore of the sea defence for low water levels (0m + NAP).
- At location (x=0) for high water levels (5m + NAP).

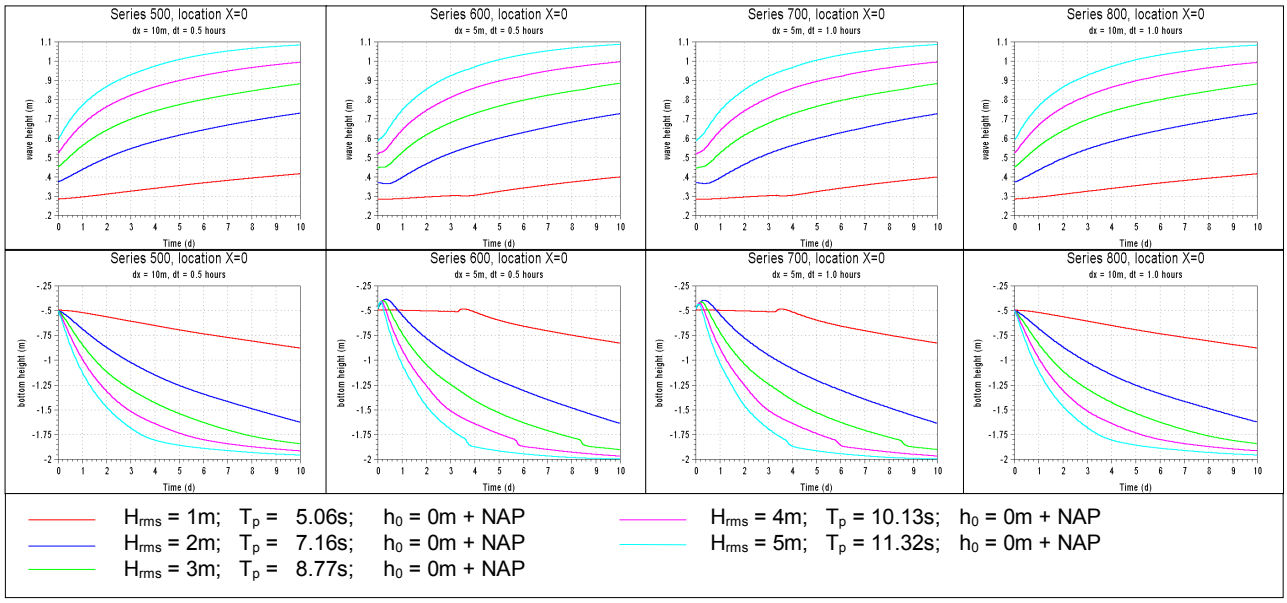

A14.13: The simulation results (location x=0) for different deep-water wave heights and different configurations. Above wave height predictions have been shown and below the seabed variations have been shown over a period of 10 days.

Observation Figure A14.13:

- Wave heights are predicted more or less similar; accept for the fact that whenever a small grid has been used the initial local wave height decrease becomes greater.
- Variation in the time step does not affect the simulation output.
- Variations in the grid size result in different seabed level predictions; larger grid sizes appear more realistic, because no strange irregularities are predicted.

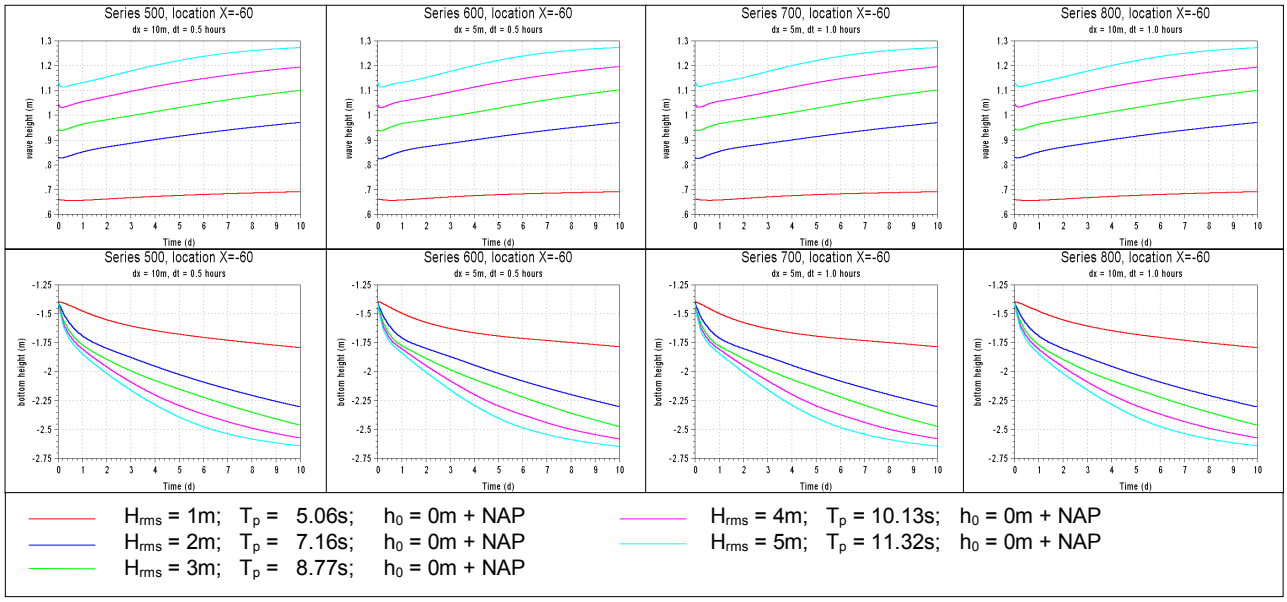

A14.14: The simulation results (location x=-60m) for different deep-water wave heights and different configurations. Above wave height predictions have been shown and below the seabed variations have been shown over a period of 10 days.

Observations Figure A14.14:

- At a distance of 60m from the sea defence toe no differences can be determined.

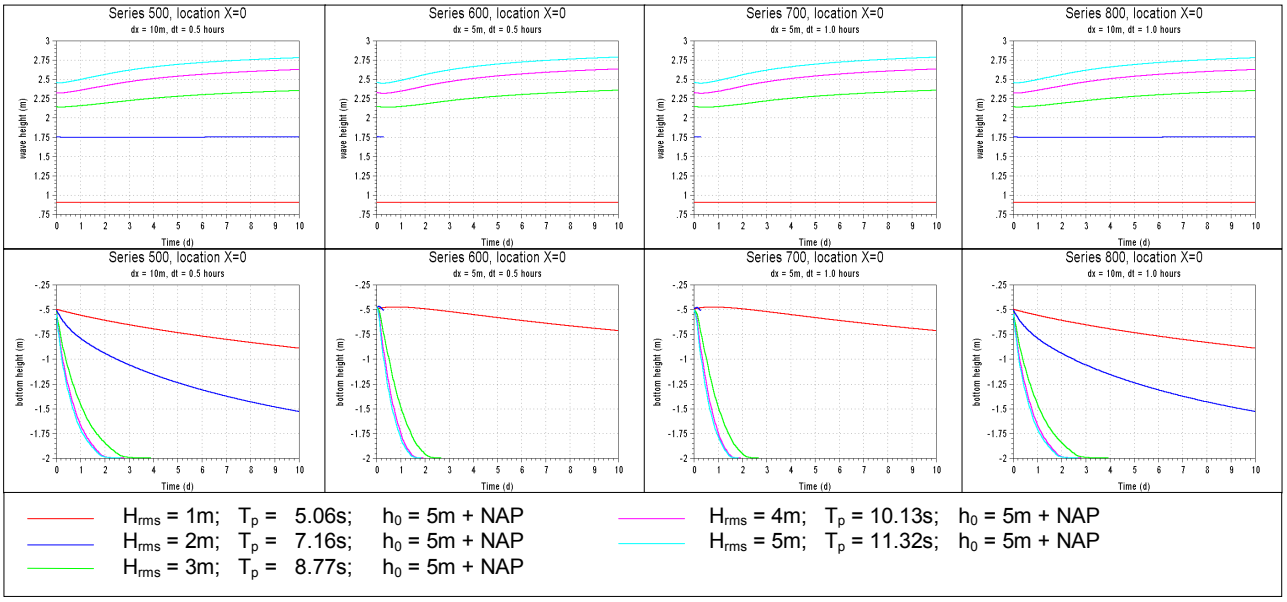

A14.15: The simulation results (location x=0) for different deep-water wave heights and different configurations. Above wave height predictions have been shown and below the seabed variations have been shown over a period of 10 days.

Observations Figure A14.15:

- The local wave height predictions are similar; accept whenever a small grid (ΔX=5m) has been used the simulation of wave height (H_{rms} =2m).
- For deep-water waves that exceed the 3m an initial decrease in the local wave height has been predicted.
- The predicted seabed levels are practically similar, during simulations with a smaller grid the erosion time decreases slightly.

Appendix 15: Probabilistic simulation results

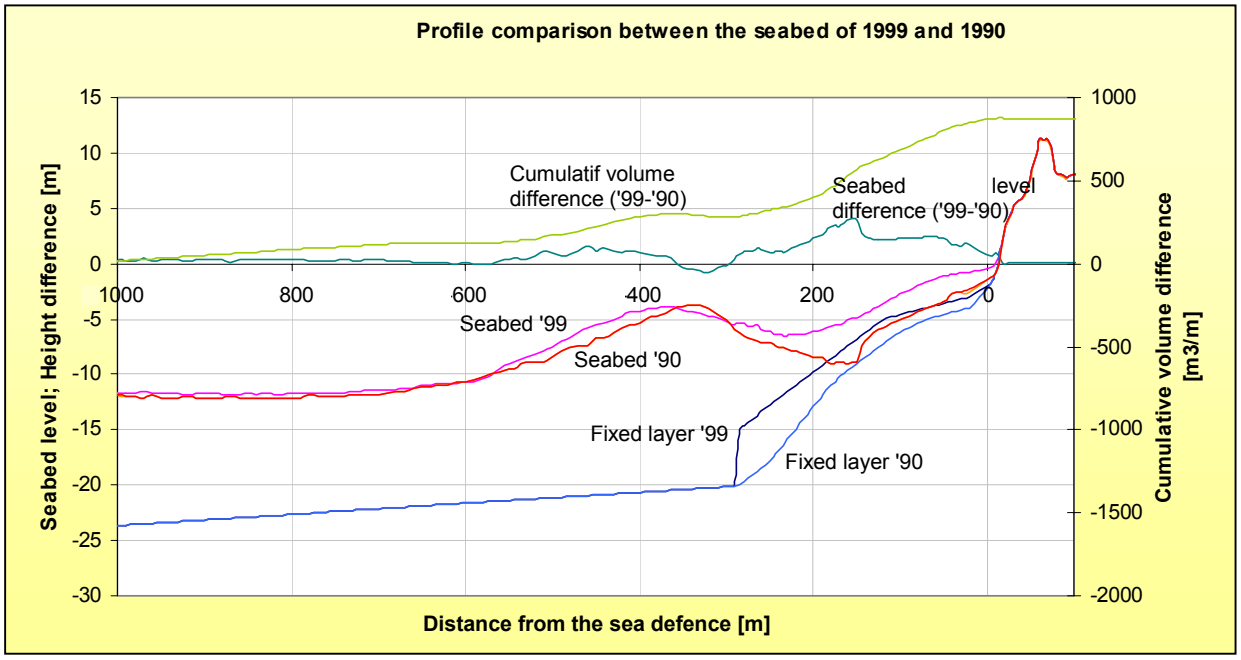

Figure A16.1: Difference between the seabed of 1990 and 1999.

Hs\ho	4.00	4.25	4.50	4.75	5.00	5.25	5.50	5.75	6.00	6.25	6.50	6.75	7.00
3.60	9.46	9.86	10.26	10.66	11.05	11.43	11.79	12.15	12.49	12.82	13.14	13.45	13.75
3.80	9.56	9.97	10.38	10.79	11.20	11.59	11.97	12.34	12.70	13.05	13.39	13.71	14.03
4.00	9.66	10.08	10.49	10.91	11.33	11.73	12.13	12.51	12.89	13.25	13.61	13.95	14.27
4.20	9.74	10.17	10.59	11.02	11.44	11.86	12.26	12.66	13.05	13.43	13.80	14.15	14.51
4.40	9.82	10.25	10.68	11.12	11.55	11.97	12.39	12.79	13.19	13.59	13.97	14.34	14.71
4.60	9.90	10.34	10.77	11.21	11.64	12.07	12.50	12.91	13.32	13.72	14.12	14.50	14.88
4.80	9.97	10.41	10.85	11.29	11.73	12.17	12.60	13.02	13.44	13.85	14.25	14.65	15.04
5.00	10.05	10.49	10.92	11.37	11.82	12.26	12.69	13.12	13.54	13.96	14.37	14.78	15.17
5.20	10.11	10.56	11.00	11.45	11.90	12.34	12.78	13.21	13.64	14.06	14.48	14.89	15.30
5.40	10.18	10.63	11.07	11.53	11.98	12.42	12.86	13.30	13.73	14.16	14.58	15.00	15.41
5.60	10.25	10.69	11.14	11.60	12.05	12.50	12.94	13.38	13.82	14.25	14.68	15.10	15.52
5.80	10.31	10.76	11.21	11.67	12.12	12.57	13.02	13.46	13.90	14.34	14.77	15.19	15.62
6.00	10.37	10.82	11.28	11.74	12.19	12.65	13.10	13.54	13.98	14.42	14.85	15.28	15.71
6.20	10.43	10.89	11.34	11.80	12.26	12.72	13.17	13.62	14.06	14.50	14.94	15.37	15.80
6.40	10.49	10.95	11.41	11.87	12.33	12.79	13.24	13.69	14.13	14.58	15.02	15.45	15.88
6.60	10.55	11.01	11.47	11.93	12.39	12.85	13.31	13.76	14.21	14.65	15.09	15.53	15.96
6.80	10.61	11.07	11.53	11.99	12.46	12.92	13.37	13.83	14.28	14.72	15.17	15.60	16.04
7.00	10.67	11.13	11.59	12.06	12.52	12.98	13.44	13.89	14.34	14.79	15.24	15.68	16.12
7.20	10.72	11.18	11.65	12.12	12.58	13.04	13.50	13.96	14.41	14.86	15.31	15.75	16.19
7.40	10.78	11.24	11.71	12.18	12.64	13.11	13.57	14.02	14.48	14.93	15.38	15.82	16.26
7.60	10.83	11.29	11.76	12.23	12.70	13.17	13.63	14.09	14.54	14.99	15.44	15.89	16.33
7.80	10.89	11.35	11.82	12.29	12.76	13.22	13.69	14.15	14.60	15.06	15.51	15.96	16.40
8.00	10.94	11.40	11.87	12.35	12.82	13.28	13.75	14.21	14.67	15.12	15.57	16.02	16.47
8.20	10.99	11.45	11.93	12.40	12.87	13.34	13.81	14.27	14.73	15.18	15.63	16.08	16.53
8.40	11.04	11.51	11.98	12.46	12.93	13.40	13.86	14.33	14.79	15.24	15.70	16.15	16.60
8.60	11.09	11.56	12.04	12.51	12.99	13.45	13.92	14.38	14.84	15.30	15.76	16.21	16.66
8.80	11.14	11.61	12.09	12.57	13.04	13.51	13.98	14.44	14.90	15.36	15.82	16.27	16.72
9.00	11.20	11.67	12.15	12.62	13.10	13.57	14.03	14.50	14.96	15.42	15.88	16.33	16.78
9.20	11.25	11.72	12.20	12.68	13.15	13.62	14.09	14.55	15.02	15.48	15.93	16.39	16.84
9.40	11.30	11.77	12.25	12.73	13.20	13.67	14.14	14.61	15.07	15.53	15.99	16.45	16.90
9.60	11.35	11.82	12.30	12.78	13.26	13.73	14.20	14.66	15.13	15.59	16.05	16.51	16.96
9.80	11.40	11.87	12.36	12.83	13.31	13.78	14.25	14.72	15.18	15.65	16.11	16.56	17.02
10.00	11.45	11.93	12.41	12.89	13.36	13.84	14.31	14.77	15.24	15.70	16.16	16.62	17.08

Figure A16.2: Results of UNIBEST-TC simulation with seabed surveyed in 1999 and IBOD=0, the table shows the maximum crest height for a combination of deep-water wave height (H_s) and water level (h_0).

Hs\ho	4	4.25	4.5	4.75	5	5.25	5.5	5.75	6	6.25	6.5	6.75	7
3.6	100	101	102	103	104	105	106	107	108	109	110	111	112
3.8	113	#N/B	115	116	117	118	119	120	121	122	123	124	125
4	126	127	128	#N/B	130	131	132	133	134	135	136	137	#N/B
4.2	#N/B	140	141	142	143	144	145	146	147	148	149	#N/B	151
4.4	152	#N/B	154	155	156	157	158	159	160	161	162	163	164
4.6	165	166	167	168	169	170	171	172	173	174	175	#N/B	177
4.8	178	179	180	181	182	183	184	#N/B	186	187	188	189	190
5	191	192	193	194	195	196	197	198	199	200	201	202	203
5.2	204	205	206	#N/B	208	209	210	211	212	213	214	215	216
5.4	217	218	219	220	221	222	223	224	225	226	227	228	229
5.6	230	231	232	233	#N/B	235	236	237	238	239	#N/B	241	242
5.8	243	244	245	246	247	#N/B	249	250	251	252	253	254	255
6	256	257	258	259	260	261	262	263	264	265	266	267	268
6.2	269	270	271	272	273	274	275	276	277	278	279	280	281
6.4	282	283	284	285	286	287	288	289	290	291	292	293	294
6.6	295	296	297	298	299	300	301	302	303	304	305	306	307
6.8	308	309	#N/B	311	312	313	314	315	316	317	318	#N/B	320
7	321	322	#N/B	324	325	326	327	328	329	330	331	332	333
7.2	334	335	336	337	338	339	340	341	342	343	344	345	#N/B
7.4	347	348	349	350	351	352	353	354	355	356	357	358	359
7.6	360	361	362	363	364	365	366	367	368	369	370	371	372
7.8	373	374	375	#N/B	377	#N/B	379	380	381	382	383	384	385
8	#N/B	387	388	389	390	#N/B	392	393	394	395	396	397	398
8.2	399	400	401	#N/B	403	404	405	406	407	408	#N/B	#N/B	411
8.4	412	413	414	415	416	417	418	419	420	421	422	423	424
8.6	425	426	427	#N/B	429	430	431	432	433	434	435	436	437
8.8	438	439	440	441	442	443	444	445	446	447	448	449	450
9	451	452	453	#N/B	455	456	457	458	459	460	461	462	463
9.2	464	465	466	467	#N/B	469	470	471	472	473	474	475	476
9.4	477	478	479	480	481	482	483	484	485	486	487	488	#N/B
9.6	490	491	492	493	#N/B	495	496	497	498	499	500	501	502
9.8	503	504	505	#N/B	507	508	509	510	511	512	513	514	515
10	516	517	518	519	520	521	522	523	524	525	526	527	#N/B

Figure A16.3: Errors that occurred during the UNIBEST-TC simulation with seabed surveyed in 1999 and IBOD=0; the red cells could not be recovered; the green cells are recovered using linear interpolation of the surrounding cells. In total 36 of the 429 simulation were aborted (8%) of which 100% could be recovered.

Hs\ho	4.00	4.25	4.50	4.75	5.00	5.25	5.50	5.75	6.00	6.25	6.50	6.75	7.00	7.25
3.60	9.50	9.90	10.28	10.67	11.06	11.43	11.79	12.14	12.48	12.81	13.13	13.44	13.73	14.02
3.80	9.61	10.02	10.41	10.81	11.21	11.60	11.97	12.33	12.69	13.04	13.37	13.70	14.01	14.32
4.00	9.71	10.12	10.53	10.94	11.34	11.74	12.13	12.51	12.88	13.24	13.59	13.94	14.27	14.58
4.20	9.80	10.22	10.63	11.05	11.46	11.87	12.27	12.66	13.05	13.42	13.79	14.14	14.49	14.83
4.40	9.89	10.31	10.73	11.15	11.57	11.98	12.39	12.79	13.19	13.58	13.96	14.33	14.69	15.04
4.60	9.97	10.39	10.81	11.24	11.67	12.09	12.51	12.91	13.32	13.71	14.10	14.49	14.86	15.23
4.80	10.05	10.47	10.90	11.33	11.76	12.19	12.61	13.02	13.43	13.84	14.23	14.62	15.01	15.38
5.00	10.12	10.55	10.98	11.41	11.85	12.28	12.70	13.12	13.54	13.95	14.36	14.76	15.15	15.54
5.20	10.19	10.62	11.05	11.49	11.93	12.36	12.79	13.22	13.64	14.06	14.47	14.87	15.27	15.67
5.40	10.26	10.70	11.13	11.57	12.01	12.45	12.88	13.31	13.73	14.15	14.57	14.98	15.39	15.79
5.60	10.33	10.76	11.20	11.64	12.08	12.52	12.96	13.39	13.82	14.24	14.66	15.08	15.49	15.90
5.80	10.39	10.83	11.27	11.71	12.16	12.60	13.04	13.47	13.90	14.33	14.75	15.17	15.59	16.00
6.00	10.46	10.89	11.33	11.78	12.23	12.67	13.11	13.55	13.98	14.41	14.84	15.26	15.68	16.10
6.20	10.52	10.96	11.40	11.85	12.30	12.74	13.19	13.62	14.06	14.49	14.92	15.35	15.77	16.19
6.40	10.58	11.02	11.47	11.92	12.37	12.81	13.26	13.70	14.13	14.57	15.00	15.43	15.86	16.28
6.60	10.64	11.08	11.53	11.98	12.43	12.88	13.32	13.77	14.21	14.64	15.08	15.51	15.94	16.36
6.80	10.70	11.14	11.59	12.04	12.49	12.94	13.39	13.84	14.28	14.72	15.15	15.59	16.01	16.44
7.00	10.75	11.20	11.65	12.10	12.56	13.01	13.46	13.90	14.35	14.79	15.22	15.66	16.09	16.52
7.20	10.81	11.26	11.71	12.16	12.62	13.07	13.52	13.97	14.41	14.85	15.29	15.73	16.16	16.60
7.40	10.86	11.31	11.77	12.22	12.68	13.13	13.58	14.03	14.48	14.92	15.36	15.80	16.24	16.67
7.60	10.92	11.37	11.82	12.28	12.74	13.19	13.64	14.09	14.54	14.99	15.43	15.87	16.31	16.74
7.80	10.97	11.42	11.88	12.34	12.80	13.25	13.70	14.15	14.60	15.05	15.49	15.93	16.37	16.81
8.00	11.02	11.47	11.93	12.39	12.85	13.31	13.76	14.22	14.66	15.11	15.56	16.00	16.44	16.88
8.20	11.08	11.53	11.99	12.45	12.91	13.37	13.82	14.27	14.72	15.17	15.62	16.06	16.50	16.94
8.40	11.13	11.58	12.04	12.50	12.96	13.42	13.88	14.33	14.78	15.23	15.68	16.12	16.57	17.01
8.60	11.18	11.63	12.10	12.56	13.02	13.48	13.94	14.39	14.84	15.29	15.74	16.19	16.63	17.07
8.80	11.23	11.68	12.15	12.61	13.07	13.53	13.99	14.45	14.90	15.35	15.80	16.25	16.69	17.13
9.00	11.28	11.73	12.20	12.67	13.13	13.59	14.05	14.50	14.96	15.41	15.86	16.31	16.75	17.19
9.20	11.33	11.79	12.25	12.72	13.18	13.64	14.10	14.56	15.01	15.47	15.92	16.36	16.81	17.25
9.40	11.38	11.84	12.31	12.77	13.23	13.70	14.16	14.61	15.07	15.52	15.97	16.42	16.87	17.31
9.60	11.43	11.89	12.36	12.82	13.29	13.75	14.21	14.67	15.12	15.58	16.03	16.48	16.93	17.37
9.80	11.48	11.94	12.41	12.87	13.34	13.80	14.26	14.72	15.18	15.63	16.09	16.54	16.98	17.43
10.00	11.53	12.00	12.46	12.93	13.39	13.86	14.32	14.78	15.23	15.69	16.14	16.59	17.04	17.49

Figure A16.4: Results of UNIBEST-TC simulation with seabed surveyed in 1999 and IBOD=1, the table shows the maximum crest height for a combination of deep-water wave height (H_s) and water level (h_0).

Hs\ho	4	4.25	4.5	4.75	5	5.25	5.5	5.75	6	6.25	6.5	6.75	7	7.25
3.6	100	101	102	103	104	105	#N/B	107	108	109	110	111	112	113
3.8	114	115	116	117	118	119	120	#N/B	122	123	#N/B	125	#N/B	127
4	128	129	130	131	132	133	134	135	136	137	138	139	140	#N/B
4.2	142	143	144	145	146	147	148	149	150	151	152	153	154	155
4.4	156	157	158	159	160	161	#N/B	163	164	165	166	167	168	169
4.6	170	171	172	173	174	175	176	177	178	179	180	181	182	183
4.8	184	185	186	187	188	189	190	191	192	193	#N/B	#N/B	196	#N/B
5	198	199	200	201	202	203	204	205	206	207	208	209	210	211
5.2	212	213	214	215	216	217	218	219	220	221	222	223	224	225
5.4	226	227	228	229	230	231	232	233	234	235	236	237	238	239
5.6	#N/B	241	242	243	244	245	246	247	248	#N/B	250	251	252	253
5.8	#N/B	#N/B	256	257	258	259	260	261	262	263	264	265	266	267
6	268	#N/B	270	271	272	273	274	275	276	277	#N/B	279	280	281
6.2	282	#N/B	284	285	286	287	288	289	290	291	292	293	294	295
6.4	296	297	#N/B	299	300	301	302	303	304	305	306	307	308	309
6.6	310	311	312	313	314	315	316	317	318	319	#N/B	321	322	323
6.8	324	325	#N/B	327	328	329	330	331	332	333	334	335	#N/B	337
7	338	339	340	341	342	343	344	345	346	347	348	349	350	351
7.2	352	353	354	355	356	357	358	359	360	361	362	363	364	365
7.4	366	367	#N/B	369	370	371	372	373	374	375	376	377	378	379
7.6	380	#N/B	382	#N/B	384	385	386	387	388	389	390	391	392	393
7.8	394	395	396	397	398	399	400	401	402	403	404	405	406	#N/B
8	408	409	410	411	412	413	414	415	416	417	418	419	420	421
8.2	422	423	424	425	426	427	428	429	430	431	432	433	#N/B	435
8.4	436	437	438	439	440	441	442	443	444	445	446	447	448	449
8.6	450	451	452	453	454	455	456	457	458	459	460	461	462	463
8.8	#N/B	465	466	#N/B	468	469	470	471	472	473	474	475	476	477
9	478	479	480	481	482	483	484	485	486	487	488	489	490	491
9.2	#N/B	493	494	495	496	497	498	499	500	501	502	503	504	505
9.4	506	507	#N/B	#N/B	510	511	512	513	514	515	516	517	518	519
9.6	520	521	522	#N/B	524	525	526	527	528	529	530	#N/B	532	533
9.8	534	535	536	#N/B	538	539	540	541	542	543	544	545	546	547
10	548	#N/B	550	551	552	553	554	555	556	557	#N/B	559	#N/B	561

Figure A16.5: Errors that occurred during the UNIBEST-TC simulation with seabed surveyed in 1999 and IBOD=1; the red cells could not be recovered; the green cells are recovered using linear interpolation of the surrounding cells. In total 36 of the 462 simulation were aborted (8%) of which 100% could be recovered.

Hs\h0	4.00	4.25	4.50	4.75	5.00	5.25	5.50	5.75	6.00	6.25	6.50	6.75	7.00
3.6	9.06	10.26	10.64	10.99	11.34	11.65	11.96	12.27	3.11	10.08	3.11	13.39	3.28
3.8	10.04	10.42	10.81	11.18	3.10	3.11	3.11	12.51	3.11	10.27	3.12	10.66	13.42
4	9.29	10.56	10.98	11.37	3.10	3.11	11.72	12.76	12.42	10.44	10.65	10.85	3.31
4.2	3.03	10.70	11.11	11.52	11.89	12.26	12.63	13.00	10.38	12.97	14.00	11.02	3.33
4.4	10.39	10.82	11.24	11.65	12.06	12.47	12.88	13.30	13.54	13.88	14.23	3.25	11.40
4.6	10.49	10.92	11.35	11.77	12.18	12.56	12.94	13.33	13.71	3.11	11.10	3.27	11.55
4.8	10.58	11.02	11.45	11.87	12.29	12.70	13.09	13.48	13.85	3.11	11.23	14.96	11.69
5	10.67	11.11	11.54	11.97	12.40	12.80	13.21	13.60	14.00	14.38	14.75	14.34	11.82
5.2	10.75	11.19	11.63	12.07	12.50	12.92	13.32	13.72	14.12	14.51	14.89	15.27	11.93
5.4	10.83	11.27	11.72	12.15	12.59	13.01	13.42	13.83	14.23	14.63	15.02	15.40	3.41
5.6	10.90	11.35	11.80	12.24	12.67	13.10	13.51	13.93	14.33	14.73	15.13	15.53	3.43
5.8	10.98	11.43	11.87	12.32	12.76	13.19	13.61	14.02	14.43	14.84	15.24	15.64	16.03
6	11.05	11.50	11.95	12.40	12.84	13.27	13.69	14.11	14.52	14.93	15.34	15.74	16.14
6.2	11.11	11.57	12.02	12.47	12.91	13.35	13.77	14.19	14.61	15.02	15.43	15.84	16.24
6.4	11.18	11.63	12.09	12.54	12.99	13.43	13.85	14.27	14.69	15.11	15.52	15.93	16.34
6.6	11.24	11.70	12.16	12.61	13.06	13.50	13.93	14.35	14.77	15.19	15.61	16.02	16.43
6.8	11.30	11.76	12.22	12.68	13.13	13.57	14.00	14.43	14.85	15.27	15.69	16.10	16.52
7	11.37	11.83	12.29	12.74	13.20	13.64	14.07	14.50	14.93	15.35	15.77	16.19	16.60
7.2	11.42	11.89	12.35	12.81	13.26	13.71	14.14	14.57	15.00	15.42	15.84	16.26	16.68
7.4	11.48	11.95	12.41	12.87	13.33	13.77	14.21	14.64	15.07	15.49	15.92	16.34	16.76
7.6	11.54	12.01	12.47	12.93	13.38	13.84	14.27	14.70	15.14	15.56	15.99	16.41	16.83
7.8	11.60	12.06	12.53	12.99	13.45	13.90	14.33	14.77	15.20	15.63	16.06	16.48	16.90
8	11.65	12.12	12.59	13.05	13.51	13.96	14.40	14.83	15.26	15.70	16.13	16.55	16.98
8.2	11.71	12.18	12.65	13.11	13.57	14.02	14.46	14.90	15.33	15.76	16.19	16.62	17.04
8.4	11.76	12.23	12.70	13.17	13.62	14.08	14.52	14.96	15.39	15.82	16.26	16.68	17.11
8.6	11.81	12.29	12.76	13.22	13.68	14.13	14.58	15.02	15.45	15.89	16.32	16.75	17.18
8.8	11.87	12.34	12.82	13.28	13.74	14.19	14.64	15.08	15.51	15.95	16.38	16.81	17.24
9	11.92	12.40	12.87	13.34	13.80	14.25	14.69	15.13	15.57	16.01	16.44	16.87	17.30
9.2	11.97	12.45	12.92	13.39	13.85	14.31	14.75	15.19	15.63	16.07	16.50	16.93	17.37
9.4	12.02	12.50	12.98	13.44	13.91	14.36	14.81	15.25	15.69	16.13	16.56	16.99	17.43
9.6	12.07	12.56	13.03	13.50	13.96	14.42	14.86	15.31	15.75	16.18	16.62	17.05	17.49
9.8	12.12	12.61	13.09	13.55	14.02	14.47	14.92	15.36	15.80	16.24	16.68	17.11	17.55
10	12.18	12.66	13.14	13.61	14.07	14.53	14.97	15.42	15.86	16.30	16.74	17.17	17.60

Figure A16.6: Results of UNIBEST-TC simulation with seabed surveyed in 1990 and IBOD=0, the table shows the maximum crest height for a combination of deep-water wave height (H_s) and water level (h_0).

Hs\h0	4.00	4.25	4.50	4.75	5.00	5.25	5.50	5.75	6.00	6.25	6.50	6.75	7.00
3.60	-	101	102	#N/B	104	#N/B	#N/B	107	-	-	-	111	-
3.80	113	#N/B	#N/B	#N/B	-	-	-	#N/B	-	-	-	-	-
4.00	-	#N/B	128	129	-	-	-	#N/B	-	-	-	-	-
4.20	-	140	141	142	#N/B	#N/B	#N/B	146	-	-	149	-	-
4.40	152	153	154	155	#N/B	#N/B	#N/B	#N/B	160	#N/B	162	-	-
4.60	165	166	167	168	169	#N/B	#N/B	#N/B	173	-	-	-	-
4.80	178	179	180	181	182	183	#N/B	185	#N/B	-	-	189	-
5.00	191	192	193	194	195	#N/B	197	#N/B	199	#N/B	201	-	-
5.20	204	205	206	207	208	209	210	211	212	213	#N/B	215	-
5.40	217	218	219	220	221	222	223	224	225	226	227	228	-
5.60	230	231	232	233	234	235	#N/B	237	238	#N/B	240	241	-
5.80	243	244	245	246	247	248	249	250	251	252	253	#N/B	255
6.00	256	257	258	259	260	261	262	#N/B	264	265	266	267	268
6.20	269	270	271	#N/B	273	274	#N/B	276	277	278	279	280	#N/B
6.40	282	283	284	285	286	287	288	289	290	291	292	293	294
6.60	295	296	297	298	299	300	301	302	303	304	305	306	307
6.80	308	309	310	#N/B	312	313	314	315	316	317	318	319	320
7.00	321	322	323	324	325	326	327	328	329	330	331	332	333
7.20	334	335	336	337	338	339	340	341	#N/B	343	344	#N/B	346
7.40	347	348	349	350	351	352	353	354	#N/B	356	357	358	359
7.60	360	361	362	363	#N/B	365	366	367	368	369	370	371	372
7.80	373	374	375	376	#N/B	378	379	380	381	382	383	384	385
8.00	386	387	388	389	390	391	392	393	#N/B	395	396	397	398
8.20	399	400	401	402	403	404	405	406	407	408	409	410	411
8.40	412	413	414	415	#N/B	417	418	419	420	421	422	#N/B	424
8.60	425	426	427	428	429	#N/B	431	432	433	434	435	436	#N/B
8.80	438	439	440	441	442	#N/B	444	445	446	447	448	449	450
9.00	451	452	453	454	455	456	457	458	459	#N/B	461	462	463
9.20	464	465	466	467	468	469	470	#N/B	472	#N/B	474	475	476
9.40	477	478	479	480	481	482	483	484	#N/B	486	487	488	489
9.60	490	491	492	493	494	495	496	497	498	499	500	501	502
9.80	503	504	505	506	507	508	509	510	511	512	513	514	515
10.00	516	517	518	519	520	521	522	#N/B	524	#N/B	526	527	528

Figure A16.7: Errors that occurred during the UNIBEST-TC simulation with seabed surveyed in 1990 and IBOD=0; the red cells could not be recovered; the green cells are recovered using linear interpolation of the surrounding cells. In total 92 of the 429 simulation were aborted (21%) of which 51 are recovered.

Hs\h0	4.00	4.25	4.50	4.75	5.00	5.25	5.50	5.75	6.00	6.25	6.50	6.75	7.00
3.60	9.01	9.42	9.81	8.76	10.56	3.11	3.11	12.21	9.83	10.02	12.48	10.40	13.60
3.80	9.99	9.56	8.64	8.89	3.10	3.11	3.11	11.80	3.11	10.21	10.41	10.60	13.94
4.00	10.12	10.52	10.91	11.30	3.10	3.11	11.64	12.00	3.11	10.38	10.58	10.79	3.32
4.20	10.24	10.65	11.06	11.45	3.10	3.11	11.81	3.11	10.31	10.53	10.75	3.25	3.33
4.40	10.35	10.77	11.18	11.59	9.47	3.11	3.11	12.33	13.47	13.81	14.15	3.26	11.33
4.60	10.45	10.87	11.29	11.71	12.11	12.51	3.11	3.11	13.64	3.11	11.03	3.28	11.48
4.80	10.54	10.97	11.39	11.81	12.23	12.64	13.02	13.41	13.78	3.11	13.75	14.88	15.23
5.00	10.62	11.06	11.49	11.91	12.33	12.74	13.14	13.53	13.92	14.30	14.68	15.05	11.74
5.20	10.70	11.14	11.57	12.01	12.43	12.85	13.25	13.65	14.04	14.44	14.82	15.20	3.41
5.40	10.78	11.22	11.66	12.09	12.52	12.95	13.35	13.76	14.16	14.55	14.94	15.33	3.42
5.60	10.85	11.30	11.74	12.18	12.61	13.03	13.45	13.86	14.26	14.66	15.06	15.45	15.84
5.80	10.92	11.37	11.81	12.25	12.69	13.12	13.54	13.95	14.36	14.76	15.16	15.56	15.95
6.00	10.99	11.44	11.89	12.33	12.77	13.20	13.62	14.04	14.45	14.86	15.26	15.67	16.06
6.20	11.06	11.51	11.96	12.40	12.84	13.28	13.70	14.12	14.54	14.95	15.36	15.76	16.16
6.40	11.12	11.57	12.02	12.47	12.92	13.35	13.78	14.20	14.62	15.03	15.44	15.85	16.26
6.60	11.18	11.64	12.09	12.54	12.98	13.42	13.85	14.27	14.69	15.11	15.53	15.94	16.35
6.80	11.24	11.70	12.15	12.60	13.05	13.49	13.92	14.35	14.77	15.19	15.61	16.02	16.44
7.00	11.30	11.76	12.21	12.67	13.11	13.56	13.99	14.42	14.84	15.27	15.69	16.10	16.52
7.20	11.36	11.81	12.27	12.73	13.18	13.62	14.06	14.49	14.91	15.34	15.76	16.18	16.60
7.40	11.41	11.87	12.33	12.79	13.24	13.69	14.12	14.55	14.98	15.41	15.83	16.25	16.67
7.60	11.47	11.93	12.39	12.85	13.30	13.75	14.18	14.62	15.05	15.47	15.90	16.32	16.74
7.80	11.52	11.98	12.45	12.90	13.36	13.81	14.24	14.68	15.11	15.54	15.97	16.39	16.81
8.00	11.57	12.04	12.50	12.96	13.42	13.87	14.30	14.74	15.17	15.60	16.03	16.46	16.88
8.20	11.62	12.09	12.56	13.02	13.47	13.92	14.36	14.80	15.23	15.67	16.10	16.52	16.95
8.40	11.67	12.14	12.61	13.07	13.53	13.98	14.42	14.86	15.29	15.73	16.16	16.59	17.01
8.60	11.73	12.19	12.66	13.12	13.58	14.04	14.48	14.92	15.35	15.79	16.22	16.65	17.08
8.80	11.78	12.24	12.72	13.18	13.64	14.09	14.53	14.97	15.41	15.85	16.28	16.71	17.14
9.00	11.82	12.30	12.77	13.23	13.69	14.15	14.59	15.03	15.47	15.90	16.34	16.77	17.20
9.20	11.87	12.35	12.82	13.28	13.74	14.20	14.64	15.08	15.52	15.96	16.40	16.83	17.26
9.40	11.92	12.40	12.87	13.33	13.80	14.25	14.70	15.14	15.58	16.02	16.45	16.89	17.32
9.60	11.97	12.45	12.92	13.39	13.85	14.30	14.75	15.19	15.63	16.07	16.51	16.94	17.38
9.80	12.02	12.50	12.97	13.44	13.90	14.36	14.80	15.25	15.69	16.13	16.56	17.00	17.43
10.00	12.07	12.55	13.02	13.49	13.95	14.41	14.85	15.30	15.74	16.18	16.62	17.06	17.49

Figure A16.8: Results of UNIBEST-TC simulation with seabed surveyed in 1990 and IBOD=1, the table shows the maximum crest height for a combination of deep-water wave height (H_s) and water level (h_0).

	4.00	4.25	4.50	4.75	5.00	5.25	5.50	5.75	6.00	6.25	6.50	6.75	7.00
3.60	0	0	0	0	0	0	0	537	0	0	0	0	542
3.80	543	0	0	0	0	0	0	0	0	0	0	0	555
4.00	#N/B	557	#N/B	559	0	0	0	0	0	0	0	0	0
4.20	569	#N/B	571	572	0	0	0	0	0	0	0	0	0
4.40	582	#N/B	584	585	0	0	0	0	590	#N/B	592	0	0
4.60	595	596	597	598	#N/B	600	0	0	603	0	0	0	0
4.80	608	609	#N/B	611	612	613	#N/B	615	#N/B	0	0	619	620
5.00	621	622	623	624	625	#N/B	#N/B	#N/B	629	#N/B	631	632	0
5.20	634	635	636	637	638	639	#N/B	641	#N/B	643	644	645	0
5.40	647	648	649	650	#N/B	652	653	654	#N/B	656	657	658	0
5.60	660	661	662	663	664	#N/B	666	667	668	669	#N/B	671	672
5.80	673	674	675	676	677	678	679	#N/B	681	682	683	684	685
6.00	686	687	688	689	690	691	692	693	694	695	696	697	#N/B
6.20	699	700	701	702	703	704	705	706	707	708	709	710	711
6.40	712	713	714	715	716	717	718	719	#N/B	721	722	723	724
6.60	725	726	727	728	729	730	731	732	733	734	735	736	737
6.80	738	739	740	741	742	743	744	745	746	747	#N/B	749	750
7.00	751	752	753	754	#N/B	756	757	758	759	760	761	762	763
7.20	764	765	766	767	768	#N/B	770	771	772	773	#N/B	775	776
7.40	777	778	779	780	781	782	783	784	785	786	787	788	#N/B
7.60	790	791	792	793	794	795	796	797	798	799	800	801	802
7.80	803	804	805	806	807	808	809	810	#N/B	812	813	814	815
8.00	816	817	818	819	820	821	822	823	824	825	826	827	828
8.20	829	830	831	832	833	834	835	836	837	838	839	840	841
8.40	842	843	844	845	846	847	848	849	850	851	852	#N/B	854
8.60	855	856	857	858	859	860	861	862	863	864	865	866	867
8.80	868	869	870	871	872	873	874	875	876	877	#N/B	879	880
9.00	881	882	883	884	885	886	887	#N/B	889	890	891	892	893
9.20	894	895	896	897	898	899	#N/B	#N/B	902	903	904	905	906
9.40	907	908	909	910	911	912	913	914	915	916	#N/B	918	919
9.60	920	921	922	923	924	925	926	927	928	929	#N/B	931	932
9.80	933	934	935	936	937	938	939	940	941	942	943	944	#N/B
10.00	946	947	948	949	950	951	952	953	954	955	#N/B	957	958

Figure A6.9: Errors that occurred during the UNIBEST-TC simulation with seabed surveyed in 1990 and IBOD=1; the red cells could not be recovered; the green cells are recovered using linear interpolation of the surrounding cells. In total 94 of the 429 simulation were aborted (22%) of which 37 could be recovered.

Appendix 16: Evolution of the Pettemer coast

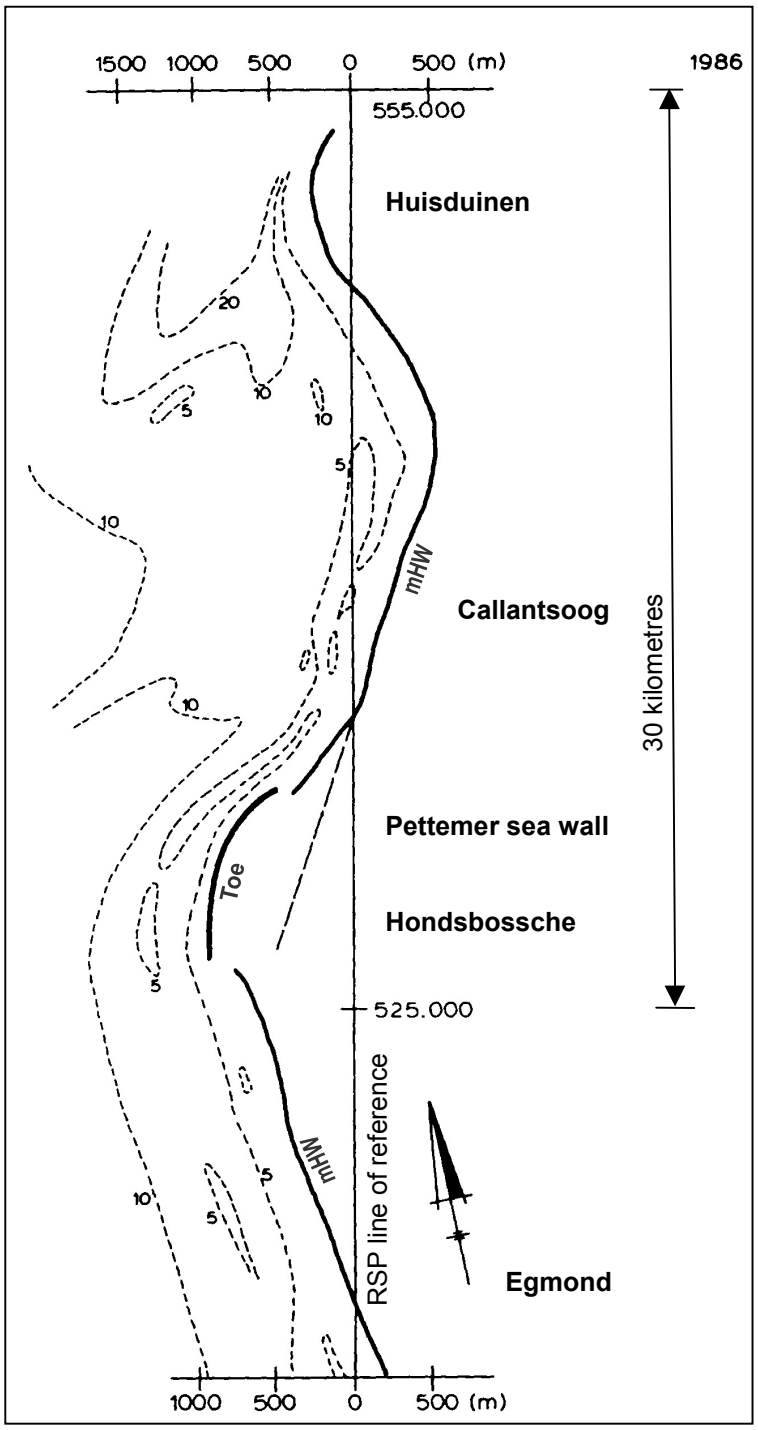

Figure A1.1: Distance between the RSP line of reference and the coastline represented by the mean High Water line (mHW) for a stretch of about 40 kilometres. The x-axis is a factor 5 smaller than the y-axis. [ALLERSMA, 1988]